Multifaceted challenges with liquid chromatography mass spectrometry determination of bioactive hormones secreted from stem cell-derived islet organoids

Dissertation for the degree of Philosophiae Doctor

by

Christine Olsen

Department of Chemistry

Faculty of Mathematics and Natural Sciences

University of Oslo

2023

Series of dissertations submitted to the
Faculty of Mathematics and Natural Sciences, University of Oslo
No. 2658

ISSN 1501-7710

Cover: UiO.
Print production: Graphic center, University of Oslo.

Table of contents

Preface

*Included in this dissertation are two published papers (**Paper I-II**) and one submitted manuscript (**Paper III**). Some additional (unpublished) work will be discussed as well. In addition, the author has contributed to three published papers [77, 106, 120], which are not included in the dissertation.*

The work presented in this dissertation has been conducted at the Department of Chemistry, University of Oslo, from 2019 to 2023 under the supervision of Prof. Elsa Lundanes and Prof. Steven Ray Wilson. Additionally, Dr. Frøydis Sved Skottvoll joined the supervisor team in June 2022 after obtaining her doctorate. I am beyond grateful for your support and guidance at each step of my journey, and for allowing me to find my way.

The Ph.D. research has been focused on developing a liquid chromatography-mass spectrometry method for determination of glucose regulatory peptides. We aimed to characterize the production and secretion of bioactive peptide hormones from stem cell-derived islets in a combined effort with the Hybrid Technology Hub (HTH) Center of Excellence at the University of Oslo and The Department of Transplantation Medicine at Oslo University hospital. Stem cell-derived islets, diabetes, and the applied methods for peptide determination are rapid developing fields of research. Therefore, to provide an updated and current state on the topics relevant to the dissertation, references were limited by choice to review articles from approx. the last five years with the addition of important papers on a broader timeline.

I would like to thank the team of HTH fronted by Dr. Hanne Scholz, and Prof. Stefan Krauss for great discussions concerning organoids and organ-on-chip. A great thanks to Dr. Aleksandra Aizenshtadt and Dr. Matias Busek for sharing their knowledge on liver organoids and organ-on-chip. Most of all, I want to express my gratitude to Dr. Shadab Abadpour and Ph.D. student Chencheng Wang for extensive collaboration and discussions concerning peptide determination and development of stem cell-derived islet organoids.

To the team at the bioanalytical chemistry (BACH) group including present and previous Bachelor, Master, and Ph.D. students: Thank you for contributing to a creative atmosphere of inspiring and impressive scientific achievements and a collaborative social environment. A special thank you to MSc. Inga Mork Aune, Master student Ilka Verner Stocker, and visiting Ph.D. student Helena

Hrušková for your work with insulin and other peptides with alternative methods. A great thanks to Ph.D. Elisa Wiborg for discussion concerning somatostatin-14 and providing feedback on the dissertation.

I want to acknowledge Ass. Prof. Hanne Røberg-Larsen and Prof. Trine Grønhaug Halvorsen for great discussion concerning LC-MS and the unpredictive behavior of insulin. I would like to thank Dr. Thomas Mikoviny technical support concerning troubleshooting of mass spectrometry instrumentation. A great thanks to engineer Inge Mikalsen for nanoLC troubleshooting and discussion concerning instrumental set-up. Thank you to Dr. Audun Skau Hansen and his students for their support with Box-Behnken optimization. I would also like to thank all co-authors for their contribution to the papers presented in this dissertation.

The current work was awarded a Young Scientist award from Analytical Science Advances at Wiley for the best lecture given by a graduate student at the 25th Norwegian Symposium in Chromatography. Thank you for noticing our work, and for all of the invited talks that followed.

I would like to express my gratitude and appreciation to my family and friends for being encouraging and supportive during this work.

To Therese and our pet bunnies, thank you for always being able to bring forth laughter and providing stability.

Christine Olsen
Oslo, June 2023

List of papers

I **On-line reduction of insulin disulfide bonds with photoinduced radical reactions, upstream to nano liquid chromatography-mass spectrometry.** Christine Olsen, Elisa Wiborg, Elsa Lundanes, Shadab Abadpour, Hanne Scholz, and Steven Ray Wilson. *Separation Science plus* 5, (2022) 220-227. https://doi.org/10.1002/sscp.202200022

II **Determination of insulin secretion from stem cell-derived islet organoids with liquid chromatography-tandem mass spectrometry.** Christine Olsen, Chencheng Wang, Shadab Abadpour, Elsa Lundanes, Audun Skau Hansen, Frøydis Sved Skottvoll, Hanne Scholz, and Steven Ray Wilson. *Journal of Chromatography B* 1215, (2023) 123577. https://doi.org/10.1016/j.jchromb.2022.123577

III **Simultaneous LC-MS determination of glucose regulatory peptides secreted by stem cell-derived islet organoids.** Christine Olsen, Chencheng Wang, Aleksandra Aizenshtadt, Shadab Abadpour, Elsa Lundanes, Frøydis Sved Skottvoll, Alexey Golovin, Mathias Busek, Stefan Krauss, Hanne Scholz, and Steven Ray Wilson. *Manuscript is currently under review at Electrophoresis and submitted to bioRxiv*. https://doi.org/10.1101/2023.06.12.544566

Summary

Stem cell-derived islet organoids (SC-islets) are emerging as potentially unlimited donor materials for type 1 diabetes patients and as models suitable to improve the understanding of human islet cell biology in disease modeling and drug screening. Determination of bioactive peptide secretion from SC-islets is dominated by immunoassays. In this work, the potential and limitations of liquid chromatography (LC) and mass spectrometry (MS) concerning bioactive peptide determination were explored. The work aimed to obtain a highly selective, sensitive, versatile, and reliable LC-MS determination of peptide secretion from SC-islets incubated off and on-chip.

In **Paper I**, the potential for development of an untargeted nano LC-MS method to examine SC-islets secretion output was assessed based on model analyte insulin. Disulfide bonds present in insulin resulted in poor fragmentation in the MS limiting unsupervised identification. Sufficient fragmentation was obtained following incorporation of an inter-chain cleavage reactor upstream to the LC-MS platform. However, the application of the developed method was not fitted for determination of bioactive peptides from SC-islets due to high detection limits and compatibility issues with sample matrices; Krebs buffer and cell medium, used for incubation of SC-islets.

In **Paper II,** a conventional LC-MS platform was tailored toward measuring insulin secreted by SC-islets with optimized LC and MS settings. The method was highly selective with suitable detection limits and quantitative properties, and was successful in determination of insulin secretion from SC-islets in Krebs buffer. However, the method showed limited compatibility with cell medium.

Therefore in **Paper III**, further optimization of LC separation led to the improved ruggedness towards cell medium and inclusion of other glucose

regulatory peptides; somatostatin-14 and glucagon. The LC-MS method could be successfully applied for determination of the peptides secreted from SC-islets in Krebs buffer. The method was also successful concerning determination of insulin secretion in cell medium from SC-islets off- and on-chip, and in complex co-culture with stem cell-derived liver organoids.

The dissertation shows that peptide determination using LC-MS requires attention to small details in method development, and provides insights into separation of bioactive peptides suitable for other applications besides SC-islets. LC-MS is shown to be a highly powerful analytical chemistry tool suitable to aid in development and characterization of complex cell models such as organoids. LC-MS and peptidomics can be used to obtain valuable information concerning islet cell biology and be a tool to improve SC-islets aimed at replacement therapy for patients with type 1 diabetes.

Sammendrag

Langerhanske øyer avledet fra stamceller (SC-øyer) kan potensielt være en ubegrenset kilde til donor materialer for pasienter med diabetes type 1. SC-øyer kan også benyttes til å forbedre forståelsen av Langerhanske øyer i sykdomsmodellering og utprøving av legemidler. Bestemmelsen av sekresjonen av hormoner fra SC-øyer domineres av immunologiske metoder. I dette arbeidet ble potensialet og begrensningene til væskekromatografi (LC) og massespektrometri (MS) utforsket for bestemmelse av hormoner. Målet var å oppnå en svært selektiv, følsom, allsidig og pålitelig LC-MS-bestemmelse av hormonsekresjon fra SC-øyer inkubert utenfor og i et mikrofluidikk system.

I **Artikkel I** ble potensialet for utvikling av en ikke-målrettet miniatyrisert LC-MS-metode for undersøkelse av sekresjon til SC-øyer vurdert basert på insulin. Disulfidbindingene i insulin var årsaken til begrenset fragmentering i MS, som videre begrenset muligheten for peptid identifikasjon. Tilstrekkelig fragmentering ble oppnådd ved å inkludere en reaktor som kan bryte disulfidbindingene i insulin mellom injeksjon og deteksjon på LC-MS-plattformen. Den utviklede metoden var ikke egnet for bestemmelse av hormoner fra SC-øyer på grunn av høye deteksjonsgrenser og kompatibilitetsproblemer med prøvematriksene; Krebs-buffer og cellemedium, som ble brukt til inkubering av SC-øyer.

I **Artikkel II** ble en konvensjonell LC-MS-plattform utviklet for å måle insulin utskilt av SC-øyer, med optimaliserte LC- og MS-innstillinger. Metoden var svært selektiv med egnede deteksjonsgrenser og kvantitative egenskaper, som medførte til at metoden var egnet for bestemmelsen av insulinsekresjon fra SC-øyer i Krebs-buffer. Metoden viste begrenset egnethet for bestemmelse av insulin i cellemedium.

Derfor ble LC-separasjonen videre optimalisert i **Artikkel III**, som bidro til forbedret robusthet for løsninger med cellemedium, og andre hormoner, somatostatin-14 og glukagon, kunne inkluderes i samme metode. LC-MS-metoden klarte å bestemme hormonene som ble utskilt av SC-øyer i Krebs-buffer. Metoden var også vellykket i bestemmelse av insulinsekresjon i cellemedium fra SC-øyer inkubert utenfor og i et mikrofluidikk system, og i komplekse løsninger samlet fra SC-øyer inkubert sammen med lever-representasjoner avledet av stamceller.

Avhandlingen viser at bestemmelse av hormoner ved bruk av LC-MS krever oppmerksomhet på små detaljer i metodeutviklingen, og gir innsikt i separasjon av hormoner som kan være egnet for andre anvendelser enn SC-øyer. Det er blitt vist at LC-MS er et svært kraftig verktøy innen analytisk kjemi som egner seg til å hjelpe i utviklingen og karakteriseringen av komplekse cellemodeller som SC-øyer. LC-MS og peptidomikk kan brukes til å skaffe verdifull informasjon om øycellebiologi og være et verktøy til å forbedre SC-øyer som er rettet mot behandling av pasienter med diabetes type 1.

Abbreviations

3D	Three dimensional
ACN	Acetonitrile
BB	Box-Behnken
BSA	Bovine serum albumin
CHGA	Chromogranin A
CID	Collision-induced dissociation
CLIA	Chemiluminescence immunoassay
DDA	Data dependent acquisition
DFA	Difluoroacetic acid
DMSO	Dimethyl sulfoxide
ECM	Extracellular matrix
ELISA	Enzyme-linked immunosorbent assay
ESI	Electrospray ionization
FA	Formic acid
GSIS	Glucose stimulated insulin secretion
HCD	Higher energy collision dissociation
hESCs	Human embryonic stem cells
HESI	Heated electrospray ionization
HR	High resolution

id	Inner diameter
IPA	Isopropanol
iPSCs	Induced pluripotent stem cells
Islets	Islets of Langerhans
LC	Liquid chromatography
MALDI	Matrix-assisted laser desorption/ionization
MEM NEAA	Minimum essential medium non-essential amino acids
MeOH	Methanol
MP	Mobile phase
MRM	Multiple reaction monitoring
MS	Mass spectrometry
MS/MS	Tandem mass spectrometry
m/z	Mass-to-charge ratio
OoC	Organ-on-chip
PEEK	Polyether ether ketone
PRM	Parallel reaction monitoring
PTMs	Post-translational modifications
RF	Radio frequency
RIA	Radioimmunoassay
RP	Reversed phase

RSD	Relative standard deviation
SC-islet	Stem cell-derived islet organoid
SC-liver	Stem cell-derived liver organoids
SP	Stationary phase
SPPs	Superficially porous silica particles
SRM	Selected reaction monitoring
T1D	Type 1 diabetes
T2D	Type 2 diabetes
TFA	Trifluoroacetic acid
t_R	Retention time
Q	Quadrupole
QC	Quality control
QqQ	Triple quadrupole

1 Introduction

1.1 Diabetes and advanced tissue engineering

Diabetes is a worldwide epidemic with an estimated prevalence of 10.5% in individuals between 20 and 79 years old in 2021 [1]. The estimated occurrence of type 1 diabetes (T1D) was about 8.4 million individuals, where 1.5 million individuals were under 20 years old [2].

Diabetes is a metabolic disorder in the pancreas characterized by impaired regulation of blood glucose levels. The glucose regulatory hormones are produced in the islets of Langerhans (will be referred to as islets), which are clusters of endocrine cells in the pancreas consisting mainly of insulin-producing β-cells (50-60% of the cells), glucagon-producing α-cells (30-40%), and somatostatin-14-producing δ-cells (5-10%) [3, 4]. The β-cells secrete insulin in response to high blood glucose as insulin stimulates receptor-mediated glucose transport from the bloodstream into insulin-sensitive cells and promotes glycogen synthesis from glucose in the liver (**Figure 1**) [5, 6]. If the blood glucose level is low, the α-cells respond with secretion of glucagon, which stimulates hepatic glucose output into the blood through the degradation of glycogen into glucose (glycogenolysis) and the synthesis of glucose from non-carbohydrate substrates e.g. pyruvate (gluconeogenesis), **Figure 1** [7, 8].

Somatostatin-14 is considered a paracrine inhibitor of both insulin and glucagon secretion [4, 9]. Urocortin-3 is another hormone produced in both α- and β-cells in human islets with debated effects on insulin and somatostatin-14 secretion [10, 11]. Endogenous insulin, somatostatin-14, glucagon, and urocortin-3 are produced in their specific cells as larger prohormones, which are enzymatically cleaved into the bioactive peptides (i.e. prohormone processing), stored, and ready to be secreted from the secretory granules [12-14].

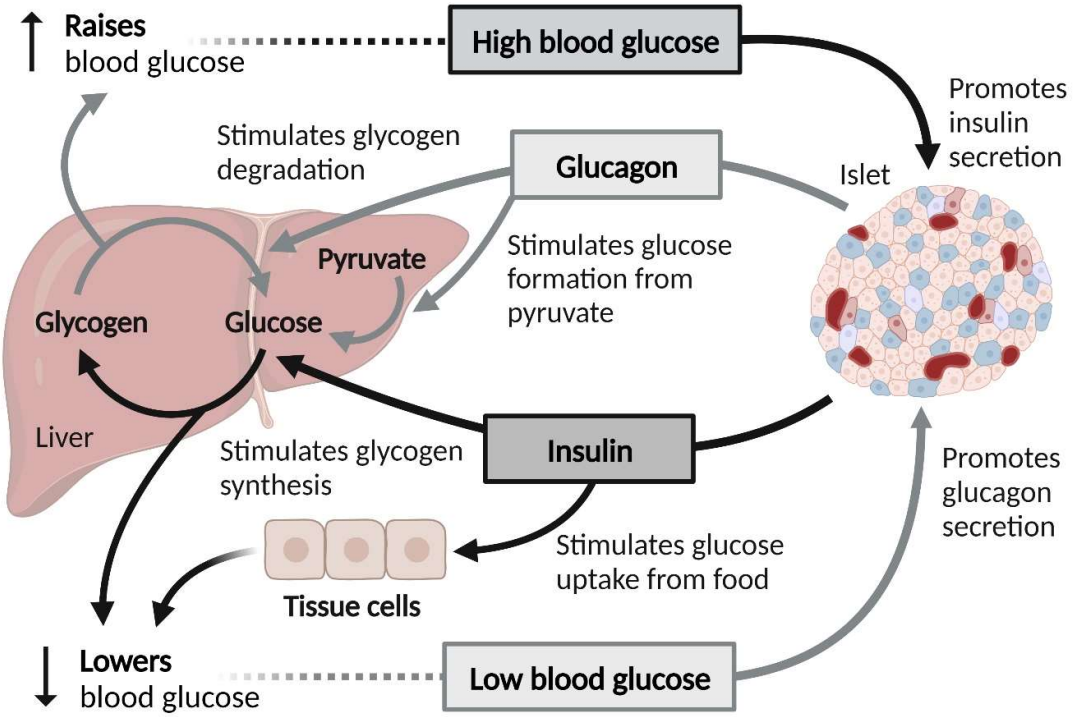

Figure 1: Schematic diagram showing islets' response to high and low blood glucose with secretion of insulin and glucagon, respectively. Insulin stimulates the uptake of glucose in tissue and stimulates the synthesis of glycogen in the liver, consequently reducing blood glucose levels [6]. Secretion of glucagon stimulates the degradation of glycogen to glucose and the formation of glucose from pyruvate, consequently increasing blood glucose [8]. Adapted from Regulation of blood glucose, by BioRender.com [15].

Both T1D and type 2 diabetes (T2D) lead to impaired regulation of blood glucose (**Figure 2**). In the case of T1D, the insulin-producing β-cells have been destroyed in an immune response mediated by various stressors (e.g. inflammation and endoplasmic reticulum stress) [16, 17], while in T2D, insufficient insulin secretion to maintain blood glucose regulation is a result of a dysfunction in the beta cells in combination with insulin resistance [18, 19]. A dysfunction in the α-cells and the secretion of glucagon may also be connected to diabetes [20, 21]. The role of the δ-cells and somatostatin-14 is also not yet fully understood [4]. Urocortin-3 has been shown to be down-regulated in β-cells from donors with T1D or T2D, therefore it would also be beneficial to study urocortin-3 in disease modeling [10]. There are also other

signaling pathways involved in the dysfunction of the islets that need further investigation [22].

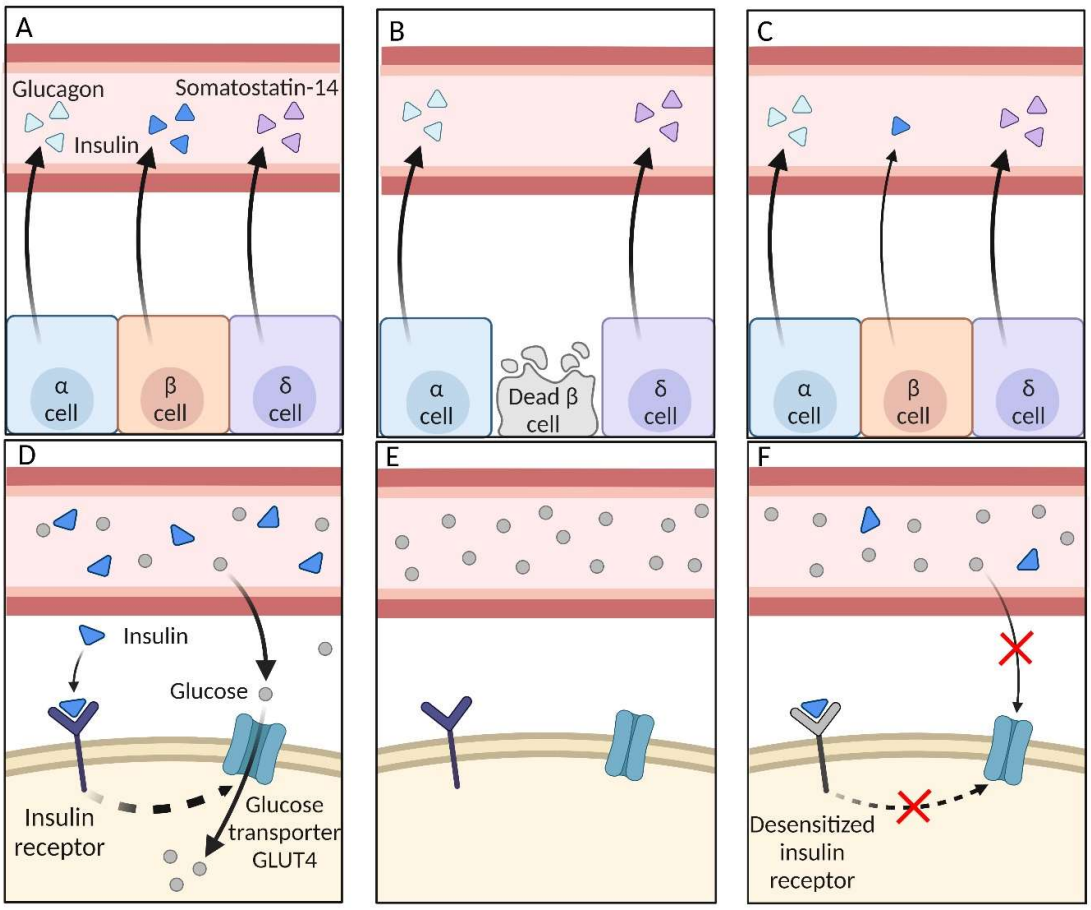

Figure 2: Schematic comparison of hormone secretion and glucose transport into insulin-sensitive cells by glucose transporter GLUT4 in healthy individuals and the case of T1D and T2D [23]. (**A**) In healthy individuals, islets secrete glucagon, insulin, and somatostatin-14 into bloodstream. (**B**) In the case of T1D, there is no insulin secretion following the destruction of the β-cells. (**C**) In the case of T2D, there is insufficient insulin secretion to uphold functional requirements. (**D**) Glucose transport from bloodstream is stimulated by insulin in healthy individuals. (**E**) No glucose transport in individuals with T1D due to lack of insulin. (**F**) Impaired glucose transport due to insulin resistance in individuals with T2D. Adapted from Immune response in type I diabetes and Type I vs. type II diabetes, by BioRender.com [15].

Since the discovery of insulin in 1921 [24], exogenous insulin therapy has been employed in the treatment of diabetes [25, 26]. However, exogenous insulin therapy does not manage to mimic the precise regulation of blood glucose achieved by endogenous insulin, leading to incidences of hypoglycemia and hyperglycemia [27, 28]. Even with the improvement in automated insulin

delivery systems, there are still various complications associated with long-term diabetes (e.g. severe hypoglycemia, hyperglycemia unawareness, diabetic kidney disease, and cardiovascular disease) [29, 30]. Glucagon emergency kits for treatment of hypoglycemia and combination treatments using insulin and glucagon have been explored [31, 32]. However, the instability of human glucagon and added complexity to the patient treatment plan are bottlenecks for applying glucagon in treatment of diabetes [32]. For patients with life-threatening diabetic complications, cell replacement therapy by transplantation of solid pancreas [29], or isolated islets are successful alternatives to exogenous insulin therapy [33-35]. Islet transplantation is preferred as it is a less-invasive procedure compared to pancreas transplantation [36]. However, widespread implementation is limited by the scarcity of donor organs and the use of immunosuppressive medications [37, 38].

The potential of islet transplantation has drastically improved with the emergence of human embryonic stem cells (hESCs) [39], the successful reprogramming of human somatic cells to generate induced pluripotent stem cells (iPSCs) [40, 41], and the generation of organoids [42]. Organoids are *in vitro* laboratory-grown three-dimensional (3D) tissue generated from e.g. hESCs and iPSCs to recapitulate architecture and function of native tissue [43, 44].

The development of stem cell-derived islet organoids (SC-islets) has focused on protocols for generation of β-cell enriched population (**Figure 3**) [45-47] and generation of islets consisting of multiple cell types found in native islets e.g. α-, β-, and δ-cells [48, 49]. Efforts are also put towards obtaining functionally mature β-cells (stage 7 in **Figure 3**) *in vivo* [48] and *in vitro* [50]. An ongoing debate in the field concerning the SC-islets for replacement therapy, is whether or not the SC-islets should have a similar cell composition

as native islets or if there should be an enriched β-cell population [51]. Patient-derived iPSC have also been used to study mechanisms of diabetes [52, 53].

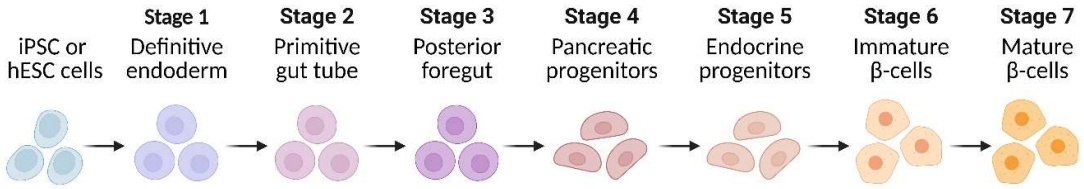

Figure 3: The development stages when iPSC or HESCs are differentiated into mature β-cells [47]. Adapted from Pancreatic β-cell Markers During Differentiation, by BioRender.com [15].

The field has made remarkable progress having reached the important milestone of having the first-in-human trials using SC-islets in replacement therapy in T1D patients [32]. An ongoing clinical trial by Vertex Pharmaceuticals showed that transplantation of a fully differentiated insulin-producing islet based on embryonic stem cells (VX-880) into the portal vein could free one T1D patient from relying on exogenous insulin on a short-term basis (90 days) [54, 55]. However, whether exogenous insulin independence can be maintained over a longer time and be repeated in other patients is currently under evaluation. In another clinical trial by ViaCyte (now acquired by Vertex Pharmaceuticals) applied a macroencapsulation device for implantation of differentiated stem cell-derived pancreatic endoderm cells (PEC-01) to obtain meal-regulated insulin secretion in T1D patients following *in vivo* maturation into functional endocrine islet tissue, however, therapeutic levels of insulin were not confirmed [56, 57].

The human SC-islets can be applied, in addition to replacement therapy, in disease modeling and drug screening to further improve the understanding of human islet cell biology and diabetes in a manner more accurately than the previously applied animal models [51, 58, 59]. SC-islets prepared from hESCs were studied concerning secretion of insulin in **Paper II** and for multiple peptides; insulin, somatostatin-14, glucagon, and urocortin-3 in **Paper III**.

Alongside the development of organoids and stem cell technology, microfluidic devices has emerged as alternative tools for culturing and monitoring of cells and organoids [60].

1.1.1 Stem cell-derived islet organoids and organ-on-chip

Commonly, organoids have been grown in static systems, meaning there is no movement in the cell medium except for when the medium is exchanged. The development of organ-on-chip (OoC) technology, where living organoids are cultured with controlled dynamic fluid flow, has made it possible to improve the recapitulation of organ functions *in vitro* [61]. In both static systems (e.g. Petri-dishes, well-plates, or vials) and on-chip devices, the organoids are embedded on or within extracellular matrix (ECM, which is a biological scaffold material) or without ECM in cell medium suspension [62, 63]. It has been shown that SC-islets grown under perfusion on an SC-islet-on-chip device have improved cell viability and glucose-stimulated insulin secretion in long-term culture compared to a static culture system [64].

Another feature improved with OoC models is the potential to co-culture multiple organoids to study organ cross-talk e.g. healthy and induced disease state [59, 61]. The co-culture of stem cell-derived liver organoids (SC-liver) and SC-islets has been successfully employed in organs-on-chip system to examine the dynamics of insulin secretion in islets and glucose uptake in liver [65]. Stem cell-derived organoids is a highly versatile cell model suitable for investigation in various devices (summarized in **Figure 4**).

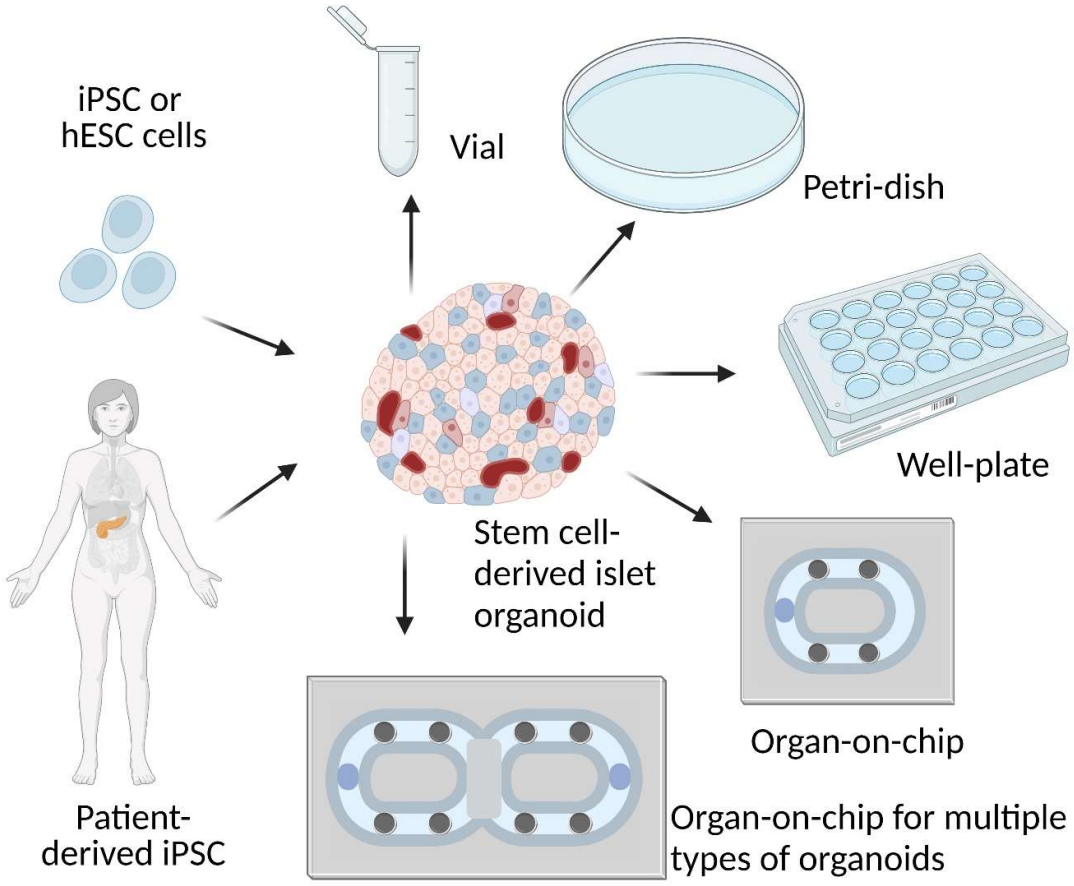

Figure 4: Stem cell-derived islet organoids can be made from iPSC, hESC, and patient-derived iPSC, and be studied in static systems (vials, Petri-dishes, and well-plates), but also in organ-on-chip platforms alone or with other types of organoids. Created with BioRender.com [15].

OoC systems has increased the possibility of enabling high-throughput analysis of secreted hormones from SC-islets. Characterization of hormone production and secretion in SC-islets off- or on-chip are dominated by immunoassays e.g. enzyme-linked immunosorbent assay (ELISA), radioimmunoassay (RIA), and chemiluminescence immunoassay (CLIA) [66-68]. These immunoassays require traditional sampling and liquid handling, is dependent on the formation of antibody-antigen complex, and have limited abilities for determination of multiple analytes in a single assay [67-69]. When applying immunoassays for characterization of hormone secretion in SC-islets, the studies are often limited to one or two analytes using specific kits: insulin [47, 64, 65], insulin and proinsulin [46], insulin and glucagon [45], c-peptide

[53], c-peptide and proinsulin [50, 52], or c-peptide and glucagon [48]. Immunoassays for glucagon and somatostatin-14 are applied to a smaller extent due to reduced availability, insufficient sensitivity, and specificity issues due to cross-activity with similar peptides [70-72]. Immunoassays do not have absolute comparability of results obtained using various kits from different producers and are vulnerable to changes in performance depending on the production of the antibodies [73, 74].

There are still several questions concerning what affects secretion in human islets in a healthy state (e.g. how insulin secretion is affected by glucagon and somatostatin-14), during development of metabolic diseases (e.g. diabetes, obesity, and non-alcoholic fatty lover disease), and following treatment of the mentioned diseases [4, 9, 68, 70, 75]. To further close the knowledge gap in understanding islet cell biology and changes in islets related to diseases, the development of methods towards simultaneous determination of several secretion products would be beneficial. A question of particular importance is deciding whether SC-islets with cell composition similar to native islets or with an enriched β-cell population is ideal in replacement therapy of T1D.

Biosensors (i.e. a device obtaining selective interaction with the target analyte using a biorecognition molecule) for determination of hormone secretion on-chip are alternatives to immunoassays [76]. However, obtaining determination of multiple analytes (e.g. insulin, somatostatin-14, and glucagon) in the same sample with sufficient detection limits without being affected by cross-reactivity remains a challenge [67, 68, 76]. Mass spectrometry (MS) detection is a powerful alternative to immunoassays and biosensors suitable for simultaneous determination of multiple peptides [77]. The determination with MS is based on the specific amino acid sequence of the peptides, rather than depending on selective interaction between biorecognition molecules and target peptides which is the basis of biosensors and immunoassays [67, 78].

1.2 Mass spectrometry in peptidomics

MS has evolved since its inception into a powerful analytical technique for determination of chemical and biological species, applied in e.g. metabolomics and proteomics, and recently to study organoids, and to be coupled to microfluidic chips [77, 79-82]. Peptides, like proteins, are chains of two or more amino carboxylic acids covalently bonded from the carbonyl carbon of one acid to the nitrogen atom of another [83]. The field is not in agreement concerning the limit between peptides and proteins, whether it be limited by size [84], or the number of amino acid residues [85]. However, according to a previous IUPAC definition, proteins were defined as polypeptides larger than 10000 g/mol (10 kDa) [86], which will be used as the defining limit between peptides and proteins in this dissertation.

Peptidomics is the study of endogenous peptides, which are produced in the tissue following e.g. proteolytic cleavage of larger precursor proteins [87, 88]. To ensure that the endogenous peptide is measured and identified, rather than the precursor protein or a similar by-product from the same precursor, peptides are determined in their native state. Therefore, a challenge in peptidomics is the heterogeneity in peptide sizes (from 200 Da to 10 kDa), large differences in the peptide structures (various post-translational modifications, PTMs, e.g. disulfide bonds between cysteine residues), the possibility of multiple charge states of each peptide, and endogenous peptides are often low abundant (**Figure 5)** [88, 89].

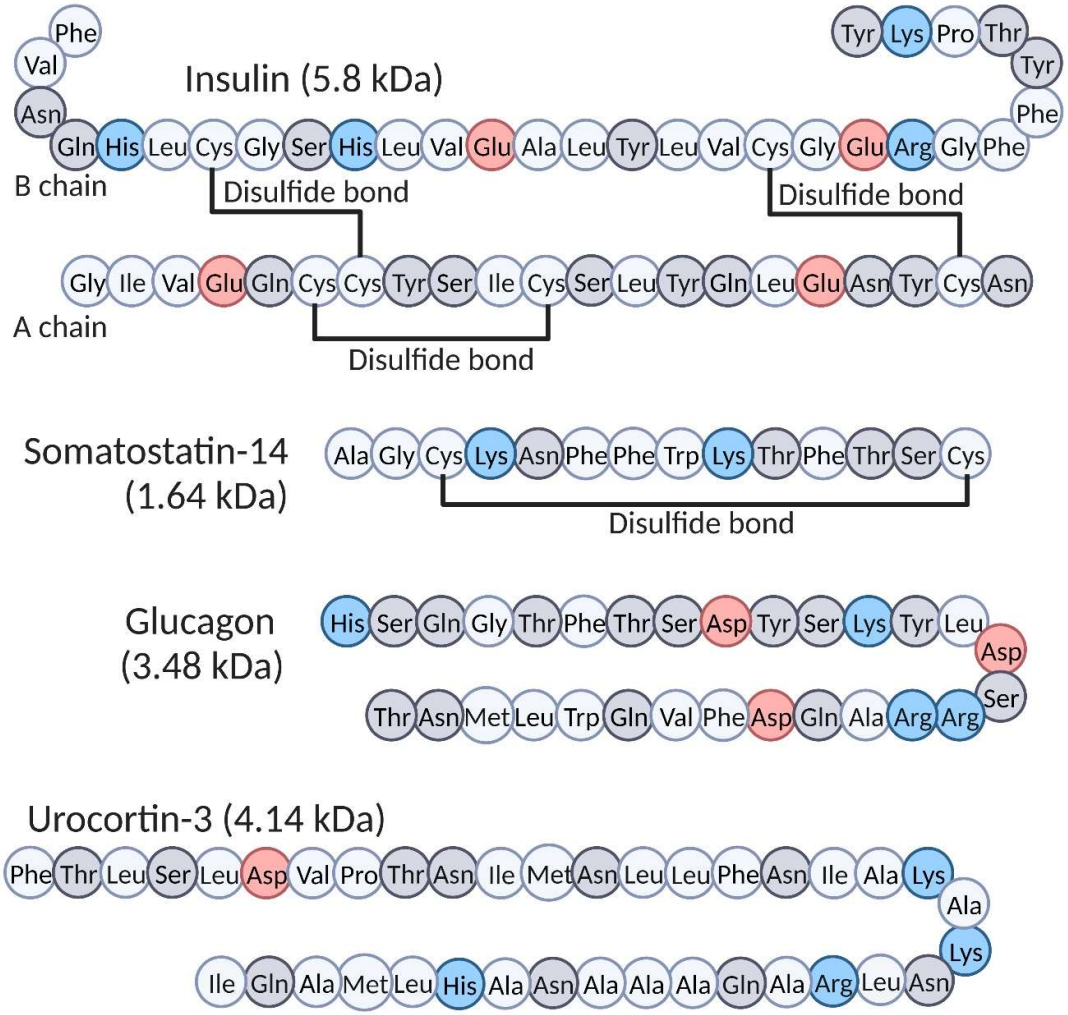

Figure 5: The heterogeneity of peptides visualized with the bioactive hormones of human origin studied in **Paper I-III**: Insulin, somatostatin-14, glucagon, and urocortin-3, ranging from 1.6 to 5.8 kDa with and without disulfide bonds. The single amino acid residues of the peptides are marked according to the following characteristics; non-polar (white), uncharged polar (grey), acidic (red), and basic (blue). Created with BioRender.com [15].

1.2.1 Mass spectrometry configurations and acquisition modes

Mass spectrometers consist of an ion source, one or more mass analyzers, and a detector, **Figure 6**. The technique is based on separation of ions under high-vacuum (low pressure) depending on their mass-to-charge ratio (*m/z*). For MS analysis of peptides, the most commonly applied ion sources are electrospray ionization (ESI) and matrix-assisted laser desorption/ionization (MALDI) [84]. ESI and MALDI provide a soft ionization technique to generate

protonated or deprotonated peptides in gas phase ($[M+nH]^{n+}$ or $[M+nH]^{n-}$, respectively), without loss of structural information due to limited fragmentation occurring in the source. The charge state of the generated ions depends on the number of basic or acidic amino acid residues in the peptides and other possible protonation/deprotonation sites.

There is a wide variety of mass analyzers available with different characteristics concerning e.g. mass accuracy, scanning speed, and sensitivity [90]. In peptide determination, it is common to apply two or more mass analyzers coupled in series (tandem mass spectrometry, MS/MS) for determination of selected peptides (i.e. targeted peptidomics) or attempt to determine all of the peptides present in the sample (i.e. untargeted peptidomics) [84].

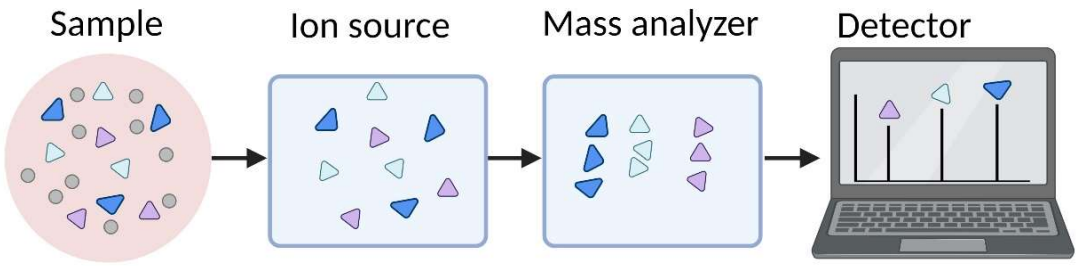

Figure 6: Schematic overview of the components in a MS, where ions of the sample components are created in the ion source, separated in the mass analyzer, and subsequently detected in the detector. Created with Biorender.com [15].

Triple quadrupole (QqQ)-MS operated in selected reaction monitoring (SRM) mode is considered to be well suited for determination of multiple low abundant peptides in complex matrices [84]. In SRM-mode, Q1 selects the target precursor ion based on a user-defined *m/z*, q2 operates as a collision cell inducing fragmentation of the selected precursor ion in collision with an inert gas (usually argon or nitrogen), and Q3 selects a target product ion based on a user-defined *m/z* (**Figure 7A**) [91]. The precursor and product ion pair can be referred to as an SRM transition, and it is common to apply at least two

transitions per target peptide to strengthen the identification and specificity of the assay (i.e. quantifier and qualifier transition). An SRM assay consisting of multiple transitions is termed multiple reaction monitoring (MRM). Determination of multiple analytes can easily be facilitated in a MRM method by applying transitions representing different peptides. The selection of ions in both Q1 and Q3 reduces the background noise to increase the sensitivity and the selectivity of the assay. The QqQ-MS can also be operated in full scan mode, where all of the ions in Q1 (or Q3) within a selected *m/z* range are detected, with or without fragmentation. QqQ-MS operated in full scan and MRM mode was used for method development and determination of insulin and other glucose regulatory peptides in **Paper II** and **Paper III**, respectively.

In a hybrid configuration, a quadrupole and an Orbitrap mass analyzer (Q-Orbitrap) are combined to utilize the mass filtration strength of the Q with the ultra-high mass resolution of the Orbitrap [90]. The Q-Orbitrap can be used in targeted peptidomics with parallel reaction monitoring (PRM) and in untargeted peptidomics with data dependent acquisition (DDA). Compared to MRM, PRM measures all of the product ions simultaneously following the user-defined precursor selection in the Q and fragmentation by higher energy collisional dissociation (HCD), **Figure 7B**.

Conversely, DDA (**Figure 7C)** does not depend on a user-defined *m/z* selection of the precursor ions or the product ions. Precursor ions are selected based on pre-defined criteria during analysis by e.g. a select number of the most abundant ions with exclusion of certain charge states. To increase the number of precursor ions measured in DDA, dynamic exclusion of the previously measured ions can be applied for a set amount of time.

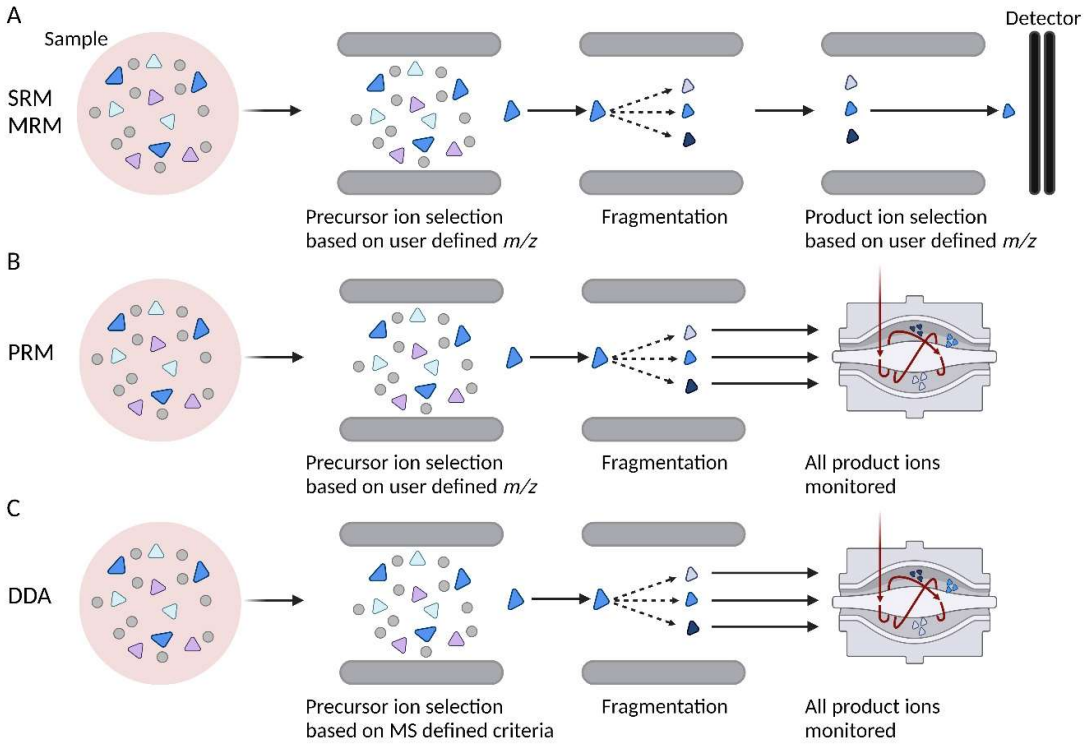

Figure 7: Schematic overview of acquisition modes in MS/MS explored in this dissertation. (**A**) Targeted SRM/MRM-based user-defined m/z selection of precursor and product ion par. (**B**) Targeted PRM based on user-defined m/z selection of precursor followed by monitoring of product ions. (**C**) Untargeted DDA, where the precursor ion is selected during analysis based on predefined criteria, e.g. top N abundant ions with exclusion of selected charge states), followed by monitoring of all product ions. Adapted from [91], and prepared in BioRender.com [15]. MS/MS analysis using DDA with Q-Orbitrap was explored in **Paper I**, while MRM using a QqQ-MS was applied in **Paper II** and **Paper III**.

1.2.2 Peptide identification in untargeted analysis

Identification of native peptides measured by DDA can be done using search engines, e.g. Mascot or Sequest-HT, to match with spectral libraries, e.g. UniProtKB/Swiss-Prot database, in a time-consuming non-enzyme specific search [84, 92]. However, careful considerations should be taken when applying these data engines for peptidomics, as the search engines were originally developed for bottom-up proteomics (i.e. proteins digested into peptides by specific enzymes) [84, 93].

The well-known behavior of e.g. the expected cleavage pattern of tryptic peptides, provides a much more suitable candidate for the preparation of *in silico* digested protein databases, compared to the unpredictable nature of endogenous peptides in peptidomics [93]. The non-enzyme specific search will generate an *in silico* digested protein database consisting of all possible cleavage sites of a protein, including cleavage sites that are not likely to be present in the sample [85]. The influx in the number of hypothetically generated amino acid sequences per protein increases the probability for false positive identifications [85, 93].

An alternative to the non-enzyme specific search is to prepare a database consisting of only the known bioactive peptide sequences expected in the samples [92, 93]. However, bioactive peptides are produced following enzymatic cleavage of larger precursor proteins (e.g. insulin formed from proinsulin). By applying a database with only the known bioactive peptide sequences, the search will be unable to match unintended products following incomplete biodegradation of precursor proteins [85, 92, 93].

Determination of insulin applying Q-Orbitrap operated in DDA mode, including unsupervised peptide identification using the Sequest-HT search engine, was explored in **Paper I.**

A common challenge for both targeted and untargeted MS/MS of peptides is intact disulfide bonds between cysteine residues. Disulfide bonds are specific PTMs with reduced fragmentation in collision-induced dissociation (CID) occurring in q2 of the QqQ-MS and the HCD process in the Q-Orbitrap [94]. When disulfide bonds remain intact, the fragmentation of the peptide backbone (**Figure 8**) between intact disulfide bonds may be less successful, which can limit identification with library search engines and lead to unstable product ion formation.

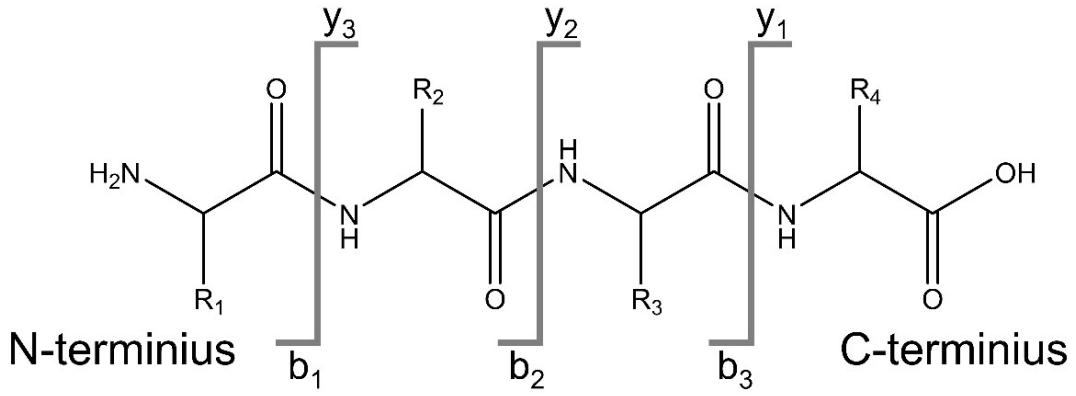

Figure 8: Fragmentation of the peptide backbone occurring due to CID in q2 of the QqQ-MS and the HCD process in the Q-Orbitrap.

The sensitivity and selectivity obtained combining MS peptidomics with OoC devices can be enhanced by including a separation step upstream to MS detection. Several separation techniques exist, e.g. capillary electrophoresis and chromatography, however, liquid chromatography (LC) combined with ESI-MS are most well-established and suitable for determination of non-volatile peptides [77, 84].

1.3 Liquid chromatography for peptidomics

Separation in chromatography is based on the principle that compounds in a mixture are distributed differently between a stationary phase (SP) and a mobile phase (MP), where the separation is obtained by applying a driving force on the MP (**Figure 9**) [95]. The inclusion of a separation step in an analysis method will increase the selectivity, as the compounds can be individually introduced to the hyphenated detector at different time points (i.e. retention time, t_R). In LC, a pump is applied to push the liquid MP through a separation column containing the SP. The characteristic of the MP and the SP should be selected based on the target analytes and sample matrix. For the separation of peptides, reversed phase (RP)-LC is most commonly applied due to high efficiency (per time unit), good repeatability, and compatibility with ESI-MS [84, 85]. RPLC applies a polar MP (e.g. aqueous buffer mixed with

usually methanol or acetonitrile) and a non-polar SP (e.g. C18-alkyl chains chemically bonded to the surface of silica particles) to separate compounds, where the retention increases with increasing hydrophobicity of the solutes, hydrophobicity of the SP, and polarity of MP [96]. Challenges for applying RPLC-ESI-MS in peptidomics have been related to insufficient sensitivity for low abundant peptides present in complex matrices and carry-over [88, 92].

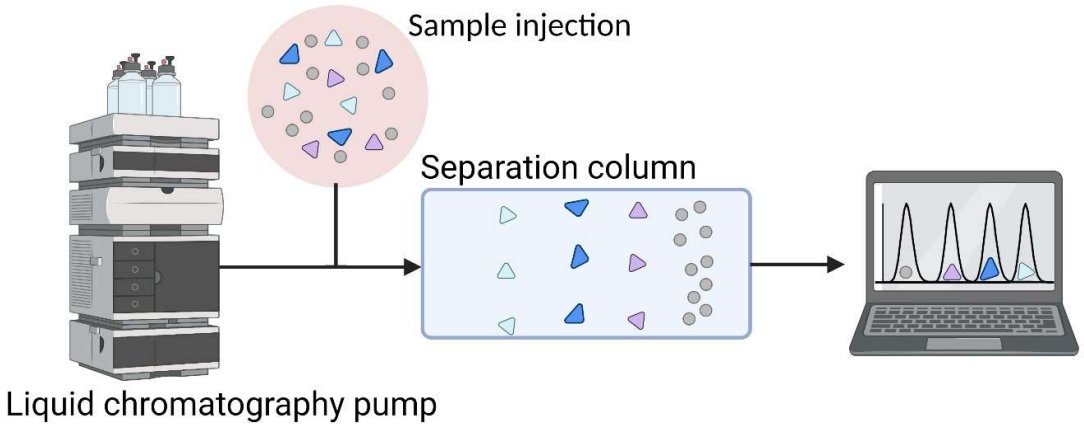

Figure 9: Simplified schematic overview of the separation of sample components by LC. Created with Biorender.com [15].

1.3.1 Peptidomics and non-defined adsorption

Native peptides, consisting of two to 100 amino acid residues, will have a wide range of characteristics affecting the determination in a RPLC-ESI-MS method; including the possibility of multiple charge states, secondary interactions due to side chains, and a wide range of hydrophobicity and sizes.

Surface adsorption can affect the peak shape, carry-over, detection limits, repeatability, reproducibility, and recovery in LC-based peptide determination [97, 98]. Non-defined adsorption (also called non-specific or aspecific) can occur at any time point from sample collection until detection, and there does not exist a universal strategy to avoid the adsorption of peptides [99]. Peptides consist of a wide range of acidic, basic, non-polar, and polar amino acids,

which can contribute to adsorption through both ionic and hydrophobic interactions [99], and also due to interaction with metal ions [100].

Technical advances for reducing the unpredictable adsorption have been made with coated vials (e.g. LoBind Eppendorf tubes and QuanRecovery autosampler vials) [101, 102], alternative hardware materials (e.g. polyetheretherketone (PEEK) and titanium) [103], surface modification (e.g. end-capping and hybrid organic-inorganic surface) [104], and with entire bio-inert or bio-compatible LC systems [97].

Fine-tuning of the applied LC method, including column format, MP composition, additional MP additives, and gradient vs isocratic elution still needs to be addressed in peptidomics. The LC method must also be compatible with the sample matrix (e.g. avoid precipitation during analysis) and compatible with ESI-MS obtaining sufficient ionization of the peptides [102, 103]. A multitude of column formats can be applied for determination of peptides, including particle packed columns and monolithic columns.

1.3.2 **Particles and column formats**

Particle packed columns in cylindrical steel-housings with 4.6 – 2.1 mm inner diameter (id) are the most commonly applied column format in LC [105]. The columns have typically been packed with fully porous silica particles (**Figure 10**). However, an emerging alternative is superficially porous silica particles (SPPs, **Figure 10)**, which consist of a solid nonporous core with a porous layer on the outside (also termed solid-core particles). The SPPs offer higher efficiency with reduced backpressure while maintaining sufficient loading capacity compared to fully porous particles [97, 106].

The increased efficiency of SPPs can be understood from the band broadening occurring in the column due to various physical processes summarized in the Van Deemter equation (**Equation 1**) [95, 107, 108]:

$$H = A + \frac{B}{u} + Cu = 2\lambda d_p + \frac{2\gamma D_m}{u} + \frac{c_{mp} d_p^2 u}{D_m} + \frac{c_s d_p^2 u}{D_s} \qquad \textbf{Equation 1}$$

where H is the plate height depending on the band broadening contribution of eddy dispersion (term A), longitudinal diffusion in the MP (term B), and resistance to mass transfer in the MP and the SP (term C). In the extended equation, d_p is the particle diameter, λ is the packing characterization factor, γ is the external obstruction factor, u is the linear flow rate, D_m is the diffusion coefficient in the MP, D_s is the diffusion coefficient in the SP, and c_{mp} and c_s are constants.

The improved efficiency of the SSPs is not fully understood and is still debated, but a reduction of the diffusion paths in the porous shell leads to faster mass transfer and the decrease in pore volume will reduce the contribution of longitudinal diffusion. Additionally, the SPPs can be produced with a more narrow size distribution improving the packing in the column, as a more uniform packing will reduce the eddy dispersion [109]. The reduction in the resistance to mass transfer is especially important for large molecules, such as peptides and proteins, with slow mass-transfer kinetics [110, 111]. Another advantage with the SPPs is that the backpressure is much smaller compared to equally sized fully porous particles, reducing the need for more complex and expensive instrumentation [109]. The size of the pores in the porous shell is also of importance as a too narrow pore will exclude the peptides from the internal pore volume, reducing the available surface and, subsequently the retention and loading capacity of peptides on the column [112, 113].

Band broadening also occurs outside of the column in the flow paths from the injection site to the point of the detection (i.e. extra-column volume) [95]. The column housing and the frits (filters to contain the particles in the column) applied at the end(s) of the particle packed columns may also contribute to carry-over and band broadening due to unpredictable adsorption [97, 114].

Monolithic columns produced from organic monomers or inorganic materials (e.g. silica) are alternative column formats independent of frits, as the rigid porous structure fills the entire column body and is covalently attached to the column wall (**Figure 10**) [115]. The different characteristics of the organic monolithic columns can be obtained by careful selection of the organic monomers, and silica monoliths can be functionalized with the desired stationary phase post-production [116].

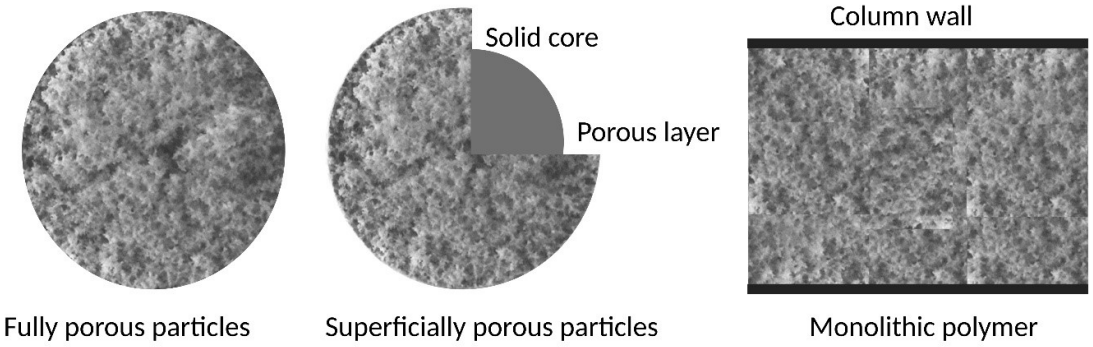

Figure 10: Alternative column materials: Fully porous particles, superficially porous particles (a solid nonporous core with a porous layer on the outside), and monolithic polymers (rigid porous structure filling the entire column). Created with Biorender.com [15].

Organic polymer monoliths, e.g. poly(styrene-co-divinylbenzene), have been successfully applied for the separation of large biomolecules [117], while e.g. methacrylate-based monoliths have been applied as solid supports for bio-reactors for on-line sample preparation [118-120]. Silica monoliths offer even less resistance to mass transfer and backpressure compared to particle packed columns due to the porous structure consisting of micro-meter throughpores (macropores) and nano-meter mesopores [116]. The large throughpores of the

silica monoliths make the columns rugged towards crude samples ("dirty samples") [116]. Silica monoliths offer low recovery of proteins, but are suitable for small molecules and peptide separations [117].

Theoretically increased sensitivity by downscaling

A well-known strategy for potentially obtaining higher sensitivity in LC-ESI-MS analysis is by miniaturization of the LC system [121]. ESI-MS is (generally) a concentration-sensitive detection technique, where the response is directly proportional to the concentration of the analyte at the point of detection [122]. The dilution of the analyte concentration in the column can be understood by **Equation 2** [123]:

$$D = \frac{C_0}{C_{max}} = \varepsilon\pi r^2(1+k)\frac{\sqrt{2\pi LH}}{V_{inj}} \qquad \textbf{Equation 2}$$

where D is the dilution, C_0 is the concentration of the analyte in the sample, C_{max} is the concentration of the analyte at the point of detection, ε is the porosity of the column particles, r is the inner radius of the column, k is the retention factor, L is the column length, H is the column plate height, and V_{inj} is the injection volume.

The theoretical gain in signal intensity following reduced radial dilution when comparing identical columns with different id (applying identical operational parameters and sample size) can be explained by the downscaling factor in **Equation 3** (**Figure 11**):

$$f_{theor} = \frac{C_{max,c1}}{C_{max,c2}} = \frac{d_{c1}^2}{d_{c2}^2} \qquad \textbf{Equation 3}$$

Downscaling from a 4.6 mm id column to an equivalent 2.1 mm id column should in theory increase the signal intensity with a factor of about 5. However, a significantly larger gain can be obtained by downscaling from a conventional

4.6 mm id column towards nano LC columns with ≤ 100 µm id [106], as the factor would be about 2100.

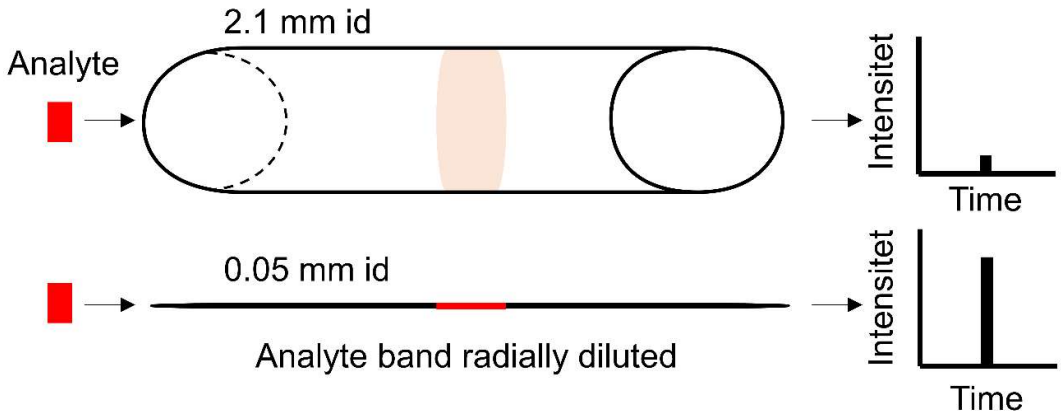

Figure 11: The reduced radial dilution of the analyte band in a 0.05 mm id column results in theory to a stronger analyte response in a concentration-sensitive detector, compared to the more radially diluted analyte band on an identical 2.1 mm id column operated with the same conditions. Adapted from [124].

In addition to the increased sensitivity, nanoLC is a "greener" alternative with reduced MP consumption, better suited for limited samples than conventional systems, and when coupled to ESI-MS enhances ionization and improved analyte transfer from liquid to gas phase is obtained (**Section 1.3.4**) [106, 121, 125]. The downscaling from conventional LC to nano LC does however offer challenges with reduced ruggedness (especially for crude samples) and limited loading capacity [125]. These challenges are often combated by using multiple columns and pumps in switching valve systems to include automated sample purification and allow for large-volume injections [126]. Extra-column volume and dead volume in ill-fitted connections in nano LC can detrimentally affect the peak shape due to the band broadening [121]. Other alternatives using columns with reduced id are micro LC (1 mm id columns) and capillary LC (0.2 – 0.5 mm id columns) [106].

A nanoLC-ESI-MS platform using both particle packed columns and monolithic columns was explored in **Paper I**, while a conventional LC-ESI-MS platform using particle packed columns was examined in **Paper II** and

Paper III. In addition, an organic methacrylate-based monolith was examined as solid support for insulin antibodies for on-line immunoaffinity enrichment of insulin on the nanoLC-ESI-MS platform of **Paper I** (**Section 3.2.3**).

1.3.3 Mobile phase composition

Carry-over, reduced recovery, and insufficient repeatability in peptide determination are consequences of the unpredictable adsorption behavior of peptides. Peptides may strongly adsorb to available adsorption sites found on the surfaces e.g. in the sample vials, in the injection system, and in the LC flow path from injector to detection [127, 128]. Composition and additives of the MP and the samples are countermeasures that seek to reduce surface adsorption (**Figure 12**). There is no universal strategy, but common additives are acids/bases, organic solvents, adsorption competitors, and surfactants [103, 128].

The use of acids (e.g. formic acid (FA) and acetic acid) as a pH-control additive for sufficient solubilization is unavoidable for RPLC-ESI determination of peptides due to the presence of multiple basic and acidic amino acid residues in each peptide [99]. However, multiple charge states may still occur following pH-adjustment (**Figure 12**), which can be a challenge in optimizing the LC separation and reduce the sensitivity of the ESI-MS detection [89]. Peptides are usually measured at acidic conditions, where the N-terminal amino group and the basic amino acid residues lysine, arginine, and histidine carry a positive charge.

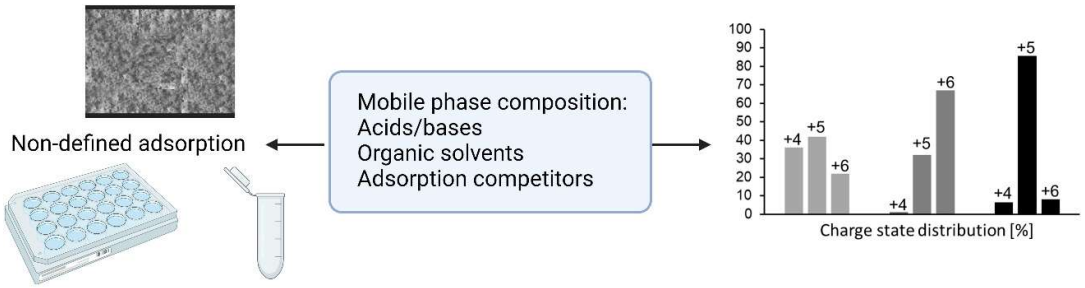

Figure 12: MP composition concerning the use of acids, bases, organic solvent, and adsorption competitors may affect both non-defined adsorption and the charge state distribution of peptides. Created with Biorender.com [15].

Ion pairing reagents, e.g. trifluoroacetic acid (TFA) and difluroacetic acid (DFA), can stabilize and neutralize the positively charged peptides by formation of an ion-pair complex [129]. The increased hydrophobicity of the neutralized peptides can increase the retention in RPLC, but also improve the peak shape due to a reduction in secondary interactions with e.g. rest-silanol groups on the SP, column housing (especially fused silica applied in nano LC) or other hydrophilic surfaces [127, 129]. Reduction in unwanted secondary interaction by an ion-pairing agent may lead to decreased carry-over and improved repeatability [99].

However, ion-pairing reagents may also negatively affect the ionization in ESI (**Section 1.3.4**) as the formed neutral complex is not sufficiently degraded in the ionization process leading to the peptide not being detected and thus increasing the detection limits [127]. The necessity of perfluoroalkyl reagents TFA and DFA should, however, be considered in a holistic view as these compounds show environmental persistence with known toxic effects, but also unknown ramifications on humans and wildlife [130, 131]. Various acids, including FA and DFA, were examined in the development of the method presented in **Paper I**. DFA was applied as in the final method in **Paper I**, while FA was used in **Paper II** and **Paper III**.

Another strategy to reduce the loss of analyte is to add an adsorption competitor with stronger interactions towards the surface than the analyte itself [98]. The competitor can be used to coat the vials before use or be added during sample preparation. Bovine serum albumin (BSA), hydrolyzed BSA, plasma, and LC-MS compatible surfactants have all been applied in this manner with success [132-135]. Saturation of possible adsorption sites in the LC system can be done by multiple injections of e.g. BSA or plasma [99]. However, the long-term stability of the saturation process can be insufficient, leading to leaking of the compounds from the adsorption sites and unpredictable adsorption can still occur of the target analyte giving an unreliable determination. BSA was one of the main compounds present in the sample matrices used to study SC-islets in **Paper II** and **Paper III**.

Standard MP for elution of target analytes in RPLC contain methanol (MeOH, suitable for more hydrophilic peptides) or acetonitrile (ACN, for the hydrophobic peptides). However, for the strongly hydrophobic peptides, isopropanol (IPA) is an organic solvent with stronger elution strength that can be used as MP or as an additive [99]. Dimethyl sulfoxide (DMSO) is another MP additive, which can improve both the elution of peptides and enhances peptide ionization [136, 137]. Additionally, DMSO can affect the charge state distribution of peptides to give a higher abundance of specific charge states (i.e. charge state coalescence), which will increase the signal intensity in targeted MS/MS methods focusing on specific precursor *m/z* (**Section 1.2.1**) [136, 138]. IPA was applied in the method presented in **Paper I**, while DMSO was used in **Paper II** and **Paper III**.

1.3.4 Electrospray ionization

As mentioned in **Section 1.2.1**, ESI is a soft ionization technique, which can generate intact protonated (most common in peptidomics) or deprotonated peptides in gas phase ($[M+nH]^{n+}$ or $[M+nH]^{n-}$. The transfer of peptides from the liquid phase into the gas phase occurs in three phases: 1) Production of charged droplets ejected from the emitter tip, 2) reduction in droplet size due to solvent evaporation and droplet fission, and 3) formation of gas phase peptide ions (**Figure 13**) [139].

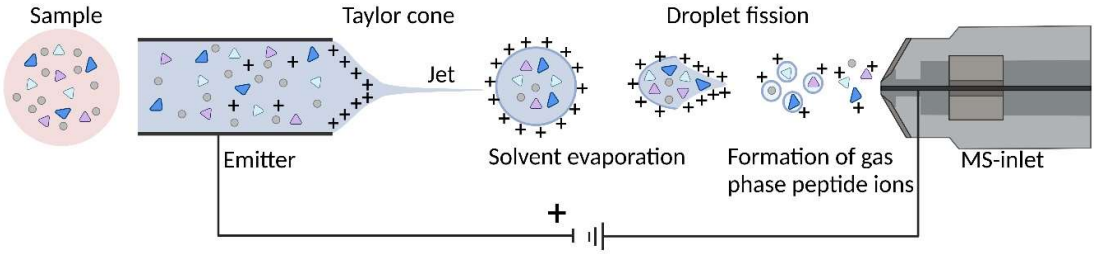

Figure 13: Schematic overview of the ESI process going from injected sample to free ions in gas phase. Adapted from [139] with permission under the Creative Commons Attribute licensing. Created with Biorender.com [15].

When LC is coupled to ESI operated in positive ionization mode, a positive voltage (3-5 kV) is normally applied on the emitter at the end of the LC flow path, while the MS inlet (the heated ion transfer capillary) acts as the counter electrode at ground potential [140, 141]. Oxidation of the solvent (typically water, MeOH, or ACN) pumped through the emitter feeds positive ions (protons) into the solution, which are then repelled by the positive voltage applied to the emitter [142]. The electrostatic repulsion of the positive charges leads to an accumulation at the emitter tip, where the meniscus eventually will be destabilized and deform into a Taylor cone [143]. In the strong electric field between the emitter and the ion transfer capillary at ground potential, the Taylor cone will eject the liquid in a jet forming a fine mist of positively charged droplets moving towards the ion transfer capillary [143].

The charged droplets contain the analytes in the center, while the protons and other positively charged ions are at the spherical surface. The electrostatic repulsion will try to break the spherical shape causing droplet jet fission and formation of smaller charged droplets. Droplet jet fission will eventually succeed as solvent evaporation occurs as the droplets move towards the heated ion transfer capillary, and the Rayleigh limit is reached (i.e. the surface tension cannot contain the Coulomb force of repulsion) [139]. The process is repeated until highly charged nanodroplets are obtained.

The transfer from highly charged nanodroplets to free peptide ions in gas phase is suggested obtained by three hypothetical ion release mechanisms: ion evaporation model, charged residue model, and/or chain ejection model [144, 145].

Biological samples (or solvents made to replicate biological systems e.g. cell culture medium and Krebs buffer) contain salt and other compounds, which may cause ion suppression or enhancement during the ESI process [146]. These compounds can be reduced through sample purification and by including an LC separation step upstream to the ESI interface.

When conventional LC with flow rates above 1 µL/min is coupled to ESI (**Figure 14A**), gases are applied to aid the ESI process. Sheath gas (typically nitrogen) assists in the nebulization of the solvent into a fine mist, while an auxiliary gas is applied to improve solvent evaporation (**Figure 14B**) [147]. Heated-ESI (HESI) improves solvent evaporation further by applying a vaporizer to heat the auxiliary gas [148]. The reduced flow rate (< 0.5 µL/min) and use of more narrow emitters in nanoLC, offers more efficient droplet formation and solvent evaporation without the need for sheath- or auxiliary gas (**Figure 14C**) [149]. Sheathless nanospray was applied in the nanoLC-ESI-MS

method presented in **Paper I**, while HESI was optimized and applied in **Paper II** and **Paper III**.

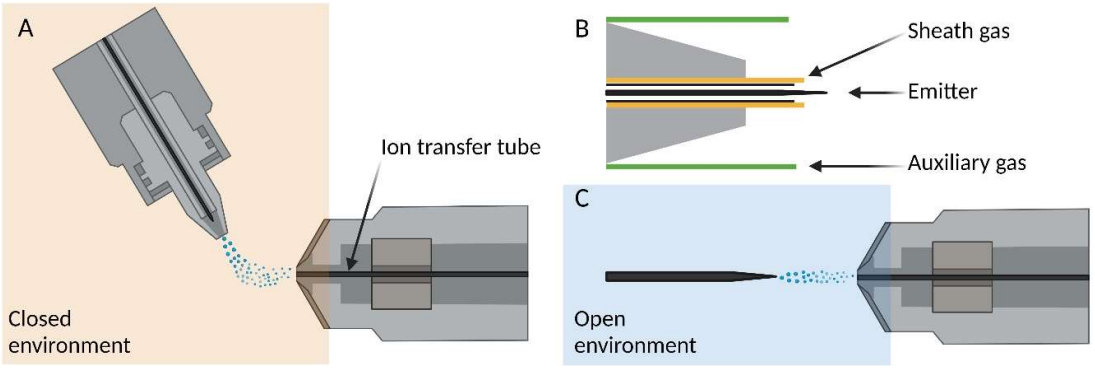

Figure 14: Schematic view of the technical set-up of; (**A**) a closed HESI system, where (**B**) the HESI needle is applied coaxial sheath- and auxiliary gas. (**C**) Sheathless nanospray in an open environment. Created with Biorender.com [15].

1.4 Towards liquid chromatography–electrospray ionization tandem mass spectrometry determination of bioactive peptides from stem cell-derived islet organoids and islet organoids-on-chip

LC-MS determination of insulin within anti-doping has recently been done in urine, plasma, and whole blood using traditional sampling methods and dried blood spot sampling [150-153]. LC-MS methods have also recently been developed for determination of glucagon in plasma [154-156], and somatostatin-14 in plasma from mice [157]. The mentioned methods require the inclusion of sample preparation steps for purification and enrichment to obtain sufficient ruggedness and low detection limits. The typically included sample preparation steps are protein precipitation combined with solid-phase extraction, [151, 153, 154, 156], solid-phase extraction [155-157] or immunoaffinity purification and enrichment [150, 152].

The most commonly applied strategy for protein analysis: bottom-up proteomics is typically not used as bioactive peptides must be determined

independently from their pro-form and similar by-products following degradation of the pro-form e.g. glucagon and glucagon-like peptide-1 [156]. This is due to the fact that the inclusion of reduction and alkylation of disulfide bonds followed by enzymatic cleavage of the peptide structure, would result in loss of all structural information leaving the origin of the enzymatic peptide fragments undetermined in an LC-MS method. The inclusion of a disulfide bond reduction can be applied, however, to separate endogenous insulin from synthetic variants, as is a usual requirement in anti-doping and diagnostic applications, the entire structure must remain intact during analysis [151].

OoC devices offer the possibility for on-line analysis of organoids, as the device can potentially be coupled upstream to a suitable analysis method including necessary sample preparation steps [76]. There is continuous progress reported toward coupling OoC with MS (and some cases with LC included) [77]. The benefit of an on-line OoC-LC-MS analysis is the reduction of sample handling steps and increased automation, and consequently, the sample is exposed to a reduced number of surfaces, which is of utmost importance for peptide determination, see **Section 1.3.1** and **Section 1.3.3**. The drawback of on-line LC-MS analysis, however, is the increased complexity, decreased flexibility, challenges with sample matrix compatibility, which may lead to reduced ruggedness [81, 126].

There are few reports concerning off- or on-chip LC-MS analysis of SC-islets, however, off-line LC-MS analysis has been applied to study secretion of small molecules from human and mice islets-on-chip [158, 159]. Quantification of glucagon and insulin was done using AlphaLISA, a down-scaled immunoassay [159]. A simultaneous LC-MS determination of insulin, somatostatin, glucagon, and C-peptide from 250 human islets equivalents with hydrolyzed BSA to reduce carry-over has been reported by Donohue et al. [132]. The method could successfully be used to determine secretion of insulin and C-

peptide. In another targeted LC-MS method, relative peptide abundances of insulin, islet amyloid polypeptide, glucagon, and somatostatin-14 were compared in secretions from islets from mice exposed to various storage conditions [160]. Untargeted peptidomics (of reduced and alkylated peptides) using nanoLC-MS has successfully been applied to probe the peptidome in secretions from human and mice islets, but also following islet lysis [161].

In this dissertation, sample preparation steps were limited to cleavage of disulfide bonds of insulin upstream a nano LC-MS method (**Paper I)**. Additionally, an immunoaffinity column for enrichment of insulin was explored (unpublished work included in **Section 3.2.3**). The final LC-MS method developed in **Paper II** and **Paper III,** applied a simple dilution with acidified internal standard following sample collection to obtain simultaneous determination of insulin, somatostatin-14, and glucagon in Krebs buffer and cell medium.

2 Aim of study

Understanding islet cell biology is important for multiple metabolic diseases, including diabetes and obesity. SC-islets developed from hESCs are cell models suitable for closing existing knowledge gaps concerning glucose regulatory hormones, such as insulin, somatostatin-14, glucagon, and urocortin-3.

The ultimate aim of this study was to obtain a highly selective, sensitive, versatile, and reliable determination of hormone secretion from SC-islets off- and on-chip device.

The overall hypothesis of the dissertation was that a method with the mentioned characteristics could be obtained by applying RPLC combined with ESI and MS detection. Model peptides used to examine the potential of RPLC-ESI-MS for the determination of hormone secretion from SC-islets were insulin, somatostatin-14, glucagon, and urocortin-3.

The dissertation seeks to comment on the following research question: *How far can we push LC separation and MS detection of native peptides secreted from SC-islets, and what are the limiting factors?*

3 Main results and discussion

The results and discussion will be focused on the challenges of applying liquid chromatography and mass spectrometry in the determination of low abundant bioactive peptides in complex matrices secreted from SC-islets. Alongside work presented in ***Papers I-III****, some unpublished work will be discussed. The main observations concerning the SC-islets and the developed RPLC-ESI-MS/MS methods are presented in the following brief overview of* ***Paper I-III*** *and a graphical overview is presented in* ***Figure 15****.*

The study aimed to examine the potential of LC-MS for the determination of bioactive peptides secreted from SC-islets. The final method should be compatible with samples collected directly from SC-islets-on-chip, and not be limited concerning the choice of sample matrix (**Section 3.1**). Determination of insulin applying miniaturized nano LC with high resolution (HR)MS was explored in **Paper I**, where unsupervised insulin identification was based on mass fragmentation spectra obtained following IPA-assisted radical inter-chain cleavage upstream of the nano LC-MS platform (**Section 3.2**). However, the detection limit was surprisingly high for a miniaturized system and insufficient for studying SC-islets, leading to the exploration of conventional liquid chromatography with triple quadruple mass spectrometry in **Paper II** (**Section 3.3**). Here, a sufficient limit of quantification for insulin was obtained, and insulin secretion in SC-islets challenged with glucose was determined in Krebs buffer. In **Paper III**, the RPLC-MS/MS method developed in **Paper II** was further expanded to include somatostatin-14 and glucagon, while being compatible with cell medium in addition to Krebs buffer. The final RPLC-MS/MS method showed that the SC-islets produced and released insulin, somatostatin-14, and glucagon. As a proof-of-concept in **Paper III**, background secretion was examined in supernatant collected from a limited number of SC-islets incubated on-chip. The final RPLC-MS/MS method was

successful in determination of insulin secretion from SC-islets-on-chip, however, the quantification limits were too high for determination of somatostatin-14 and glucagon (**Section 3.3.3**). In a last application, the ruggedness of the RPLC-MS/MS method for determination of insulin in complex samples was further examined by studying the co-culture of SC-islets and SC-liver on-chip (**Section 3.3.4**).

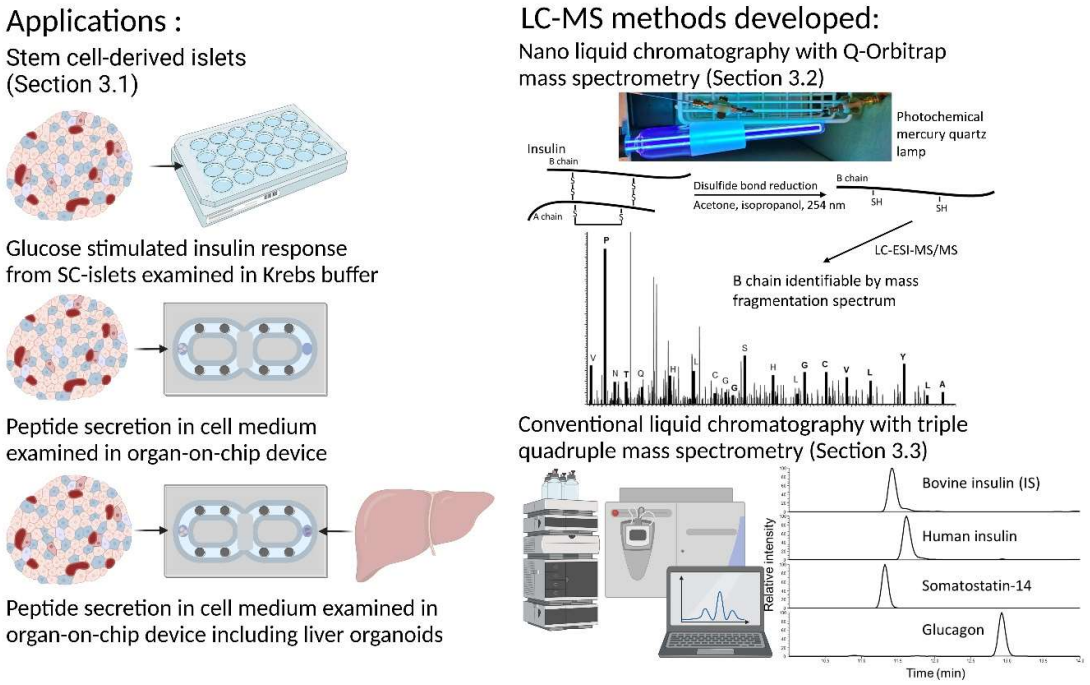

Figure 15: Graphical overview of the dissertation.

3.1 Stem cell-derived islet organoids

The SC-islets studied in the dissertation were generated from human pluripotent stem cell line H1 (i.e. a type of hESCs) according to the protocol given in **Supplementary data 1** of **Paper II**. The batches of SC-islets were characterized by bright field imaging, flow cytometry, and immunofluorescence staining (**Supplementary data 2** of **Paper II** and **Supplementary material** in **Paper III**).

The SC-islets showed a uniform shape with a diameter of around 100 μm (**Paper II**). In the batch of SC-islets examined in **Paper II**, flow cytometry determined that > 83% of the cells were insulin-producing cells (**Supplementary data 2** of **Paper II)**, while > 66% of cells were insulin-producing cells (Q2 in **Figure 16A** and **Figure 16B**) in the batch of SC-islets examined in **Paper III**. Additionally, for the SC-islets studied in **Paper III**, it was determined that > 22% of cells were glucagon-producing cells (Q10 in **Figure 16C** and **Figure 16D**) and > 17% were somatostatin-producing cells (Q6 in **Figure 16E** and **Figure 16F**). For both batches of SC-islets studied, flow cytometry quantification showed that > 95% of the cells were endocrine cells (represented by chromogranin A (CHGA) Q2 and Q3 in **Figure 16A**). The batch-to-batch variation in the distribution of specific hormone-producing cells, but also of unwanted products or not-differentiated cells (not characterized here), is one of the limiting bottlenecks for the establishment of SC-islets for application in e.g. cell replacement therapy for T1D patients [58].

The development of the protocol, production, and characterization of the SC-islet using bright field imaging, flow cytometry, and immunofluorescence staining was done by Ph.D. student Chencheng Wang at the hybrid technology hub-center of Excellence at the University of Oslo and the department of transplant medicine and institute for surgical research at Oslo university hospital.

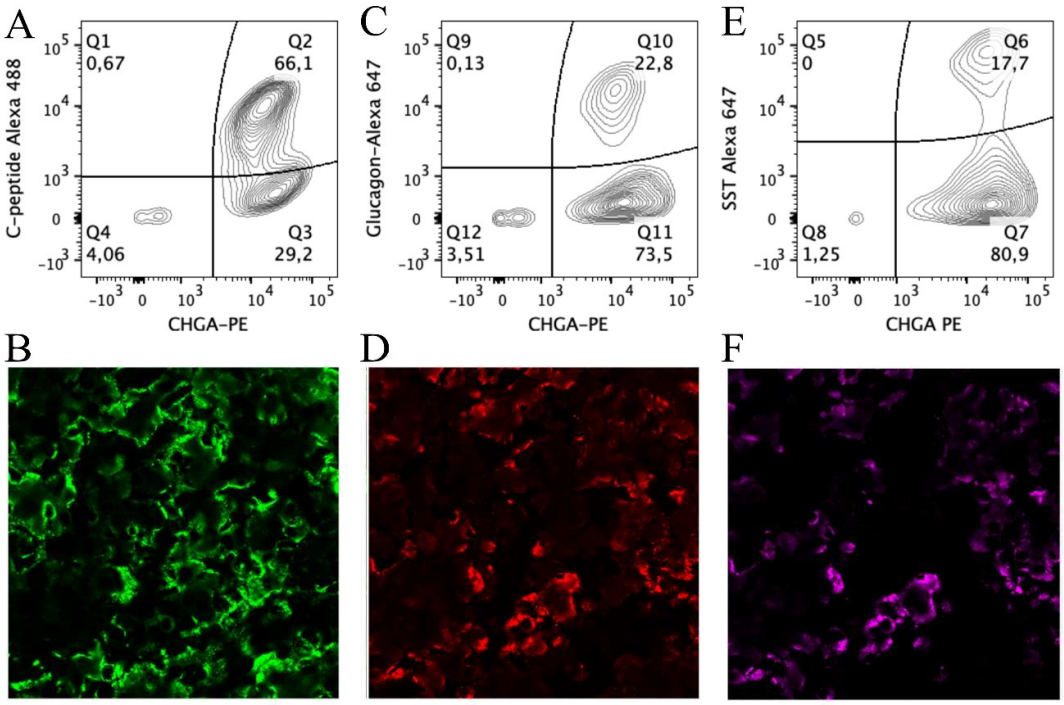

Figure 16: Representative flow cytometry quantification (%) of dispersed SC-islets stained for (**A**) C-peptide and chromogranin A (CHGA), (**C**) glucagon and CHGA, and (**E**) somatostatin-14 and CHGA. Representative immunostaining images of SC-islets stained for (**B**) C-peptide (green), (**D**) glucagon (red), and (**F**) somatostatin-14 (magenta). Adapted from manuscript of **Paper III**.

A common characterization of importance for SC-islets is the determination of glucose stimulated insulin secretion (GSIS) using Krebs buffer (a balanced salt solution used to mimic physiological conditions) [162, 163]. Another possibility is to use high levels of potassium in Krebs buffer to cause membrane depolarization to examine the ability of the SC-islets to produce and store hormones [4, 22, 164]. Cell medium, which is used for short- and long-term cultivation of SC-islets, is another important matrix in which to monitor hormone secretion [47, 64, 65]. An LC-MS method for determination of peptides should therefore be established for Krebs buffer and cell medium. The recipes for Krebs buffer and cell medium applied in **Paper III** is given in **Table 1** and **Table 2**.

BSA is an important addition in both Krebs buffer (**Table 1**) and cell medium (**Table 1** and **Table 2**). BSA (and human albumin in the body) has beneficial

capabilities improving cell growth and viability e.g. transportation of growth factors, hormones, and vitamins, maintaining proper osmotic pressure, and antioxidant properties [165].

Table 1: Contents of Krebs buffer and cell medium applied in **Paper II** and **Paper III.**

Krebs buffer	Cell medium
0.1% BSA (w/v)	2% BSA (w/v)
2.7 mM $CaCl_2$	1% GlutaMAX™ stock solution (v/v), **Table 2**.
10 mM HEPES	10 µg/mL heparin
5 mM KCl	1% of minimum essential medium non-essential amino acids stock solution (MEM NEAA) (v/v), **Table 2**.
1.2 mM KH_2PO_4	1% penicillin/streptavidin (v/v)
1.2 mM $MgSO_4$	0.1% of trace elements A and B stock solutions (v/v), **Table 2**.
128 mM NaCl	10 µM $ZnSO_4$
5 mM $NaHCO_3$	Added to MCDB131 basal cell medium containing e.g. essensial amino acids and vitamins [166].
1 mM Na_2HPO_4	

Table 2: Description of the stock solutions used to prepare cell medium.

Trace elements A stock solution	Trace elements B stock solution	GlutaMAX™ stock solution	MEM NEAA stock solution
1.60 mg/L $CuSO_4 * 5H_2O$	0.17 mg/L $MnSO_4 * H_2O$	0.85 % NaCl (w/v)	10 mM glycine
836.00 mg/L $ZnSO_4 * 7H_2O$	140 mg/L $Na_2SiO_3 * 9H_2O$	200 mM L-alanyl-L-glutamine	10 mM L-alanine
17.30 mg/L Selenite * 2Na	1.24 mg/L Molydbic acid, ammonium salt		10 mM L-asparagine
1155.10 mg/L Ferric citrate	0.65 mg/L NH_4VO_3		10 mM L-aspartic acid
	0.13 mg/L $NiSO_4 * 6H_2O$		10 mM L-glutamic acid
	0.12 mg/L $SnCl_2$ (anhydrous)		10 mM L-serine

*To summarize, the SC-islets studied in **Paper II-III** were shown to contain cells enabling secretion and production of insulin, somatostatin, and glucagon with flow cytometry and immunostaining. Compatibility with Krebs buffer and cell medium is predicted to be a crucial consideration regarding the*

*development of an LC-MS method suitable for determination of secreted hormones from SC-islets in **Paper I-III**.*

3.2 Unsupervised determination of insulin with high resolution mass spectrometry

To aid in the understanding of islet cell biology and the development of SC-islets, the goal in **Paper I** was to obtain an untargeted LC-MS method (**Section 1.2.1**) to examine the secretion output from SC-islets. The production of bioactive peptides in SC-islets may be affected by incomplete biodegradation of the prohormones resulting in by-products with slightly different amino acid sequences. The benefit of an untargeted LC-MS method is the possibility to look for a combination of bioactive hormones, residues of pro-forms, and by-products following complete/incomplete degradation of the pro-forms [161]. Insulin (of human origin unless stated otherwise), which should be produced in the β-cells of SC-islets following degradation of proinsulin, was used as a model analyte to examine the potential of a nano RPLC-nanospray-Q-Orbitrap-MS platform for unsupervised identification of peptides in **Paper I**. The determination of insulin faced various challenges with non-defined adsorption (**Section 3.2.1**), and limited fragmentation on the Q-Orbitrap introducing the need for an on-line reactor for cleavage of disulfide bonds present in insulin (**Section 3.2.2**).

3.2.1 Carry-over of insulin depending on column format and non-defined adsorption

A bottleneck for determination of intact insulin (i.e. insulin with three disulfide bonds) on the nanoRPLC-ESI-Q-Orbitrap platform in **Paper I** was carry-over. Intact insulin displayed extreme levels of carry-over (> 90%) and tailing (asymmetry factor of 5) on the investigated commercial particle packed trap column (75 µm id x 2 cm, Acclaim PepMap™ C18, 3 µm, 100Å) and the in-

house prepared separation column using fused silica capillary (50 µm id x 5 cm, Accucore C18, 2.6 µm, 80 Å) in **Paper I** (**Figure 17A**). The carry-over effect was neither improved by exploring the alternative acids FA, TFA, or acetic acid in place for DFA, nor by replacing ACN in the MP with MeOH (results not shown). The carry-over effect was first eliminated by applying in-house prepared silica-based monolithic columns (50 µm id, C18, 1-1.6 µm pores), **Figure 17B**. Based on these observations, it was assumed that insulin interacted with the frits and/or the column walls in the particle packed nano columns, as these features were eliminated with the use of monolithic columns.

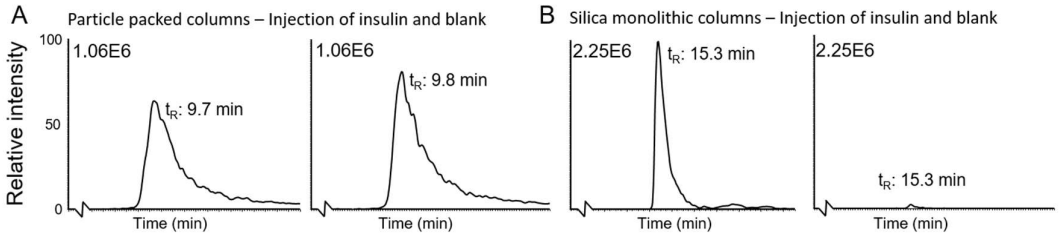

Figure 17: Extracted ion chromatogram of m/z 1162.3 from injections of intact insulin and following blanks on the LC-MS set-up in **Paper I** with the following columns: (**A**) 75 µm x 2 cm Acclaim PepMap™ 100 (C18, 3 µm, 100 Å) trap column and 50 µm x 5 cm Accucore (C18, 2.6 µm, 80 Å) analytical column, (**B**) 50 µm ID silica-based C18 monolithic trap column and analytical column. Adapted from **Paper I** with permission under the Creative Commons Attribute licensing.

Carry-over and loss of signal due to non-defined adsorption of intact insulin on various types of tubings (e.g. untreated fused silica capillary and PEEK tubing, **Figure 18A**) was also a key challenge in the establishment of a conventional LC-system in **Paper II**. The conventional RPLC-HESI-MS method was not successful in determination of insulin in water-based solutions at concentrations below 1 ng/µL, until intact insulin was only in contact with shielded fused silica nanoViper™ connectors, see **Figure 18B**, using a glass syringe coupled to a shielded fused silica connector for manual injection (**Figure 18C**).

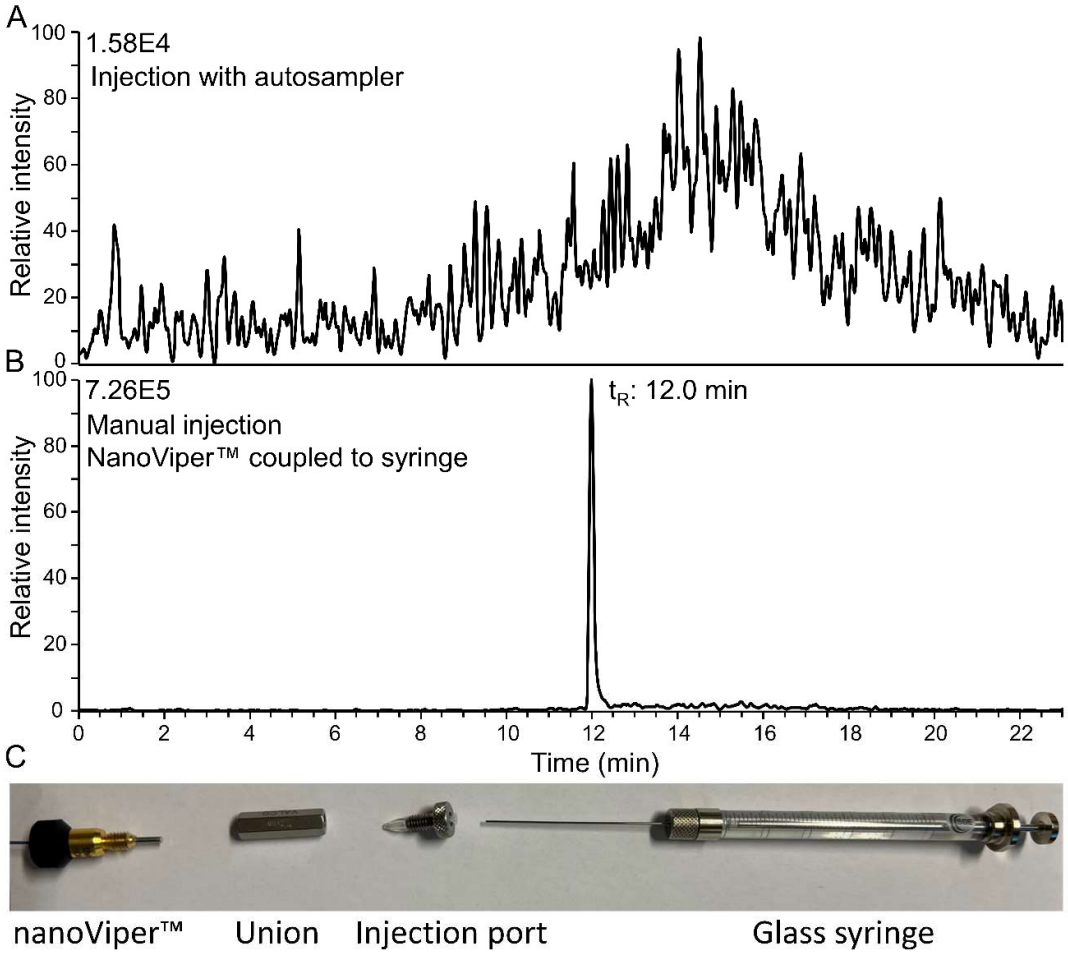

Figure 18: Extracted ion chromatogram of intact insulin (m/z 1162.0-1163.0) following injection of 125 pg/µL insulin in 0.1% FA in water on the RPLC-ESI-QqQ-MS system in **Paper II**. (**A**) 1 µL of the solution was injected with the autosampler including various types of tubings. (**B**) Manual injection of 1.08 µL of the insulin solution which was only allowed contact with shielded fused silica connectors. (**C**) Manual injection was done using a glass syringe which was coupled to the shielded fused silica nanoViper™ connector by a 250 µm id union and an injection port. The other end of the connector was attached following filling to a 6-port-2-position valve fitted with a 50 µm id x 550 mm shielded fused silica loop (1.08 µL). Adapted from **Paper II** with permission under the Creative Commons Attribute licensing.

The shielded fused silica connectors had been surface-treated by the producers (the information about the type of surface-treatment is inaccessible to the general public). The type of shielded fused silica connector is the standard tubing applied on the nanoLC pump used in **Paper I**, however, untreated fused silica capillary was used as column housing in the in-house prepared particle packed separation columns.

In **Paper III**, a commercial guard cartridge (10 x 2.1 mm id) with the same particles (Accucore C18, 2.6 µm, 80 Å) as the separation column in **Paper I**, showed dramatic tailing (asymmetry factor 5.6) and contributed to carry-over. In comparison, an Accucore phenyl/hexyl guard cartridge (10 x 2.1 mm id, 2.6 µm, 80 Å) offered an asymmetry factor of 2.3 without any detectable contribution to carry-over. The Poroshell C18 separation column used with both guard cartridges for examination of the asymmetry factor had been extensively used for samples in both Krebs buffer and cell medium. Initially in **Paper II**, the Accucore phenyl/hexyl guard cartridge and Poroshell C18 separation column obtained an insulin peak with an asymmetry factor of 1.4.

These findings in **Paper I-III**, indicate that both the Accucore C18 particles and the untreated fused silica column housing used in preparation of particle packed nano columns were not suitable for separation of intact insulin because of non-defined adsorption causing band broadening and carry-over. In hindsight, other particle packed nano columns with e.g. phenyl/hexyl stationary phase and other column housings may have provided better chromatographic performance in the nano RPLC system in **Paper I**.

To summarize, determination of intact insulin faces the challenge of non-defined adsorption causing high levels of carry-over and tailing on various tubings and separation columns. The choice of particles and column housing significantly influences chromatographic performance, indicating that alternative particle packed nano columns with different stationary phases and column housings could have provided better results in the developed method in ***Paper I****.*

3.2.2 Detection limits affected by yield of inter-chain cleavage reactor and charge state distribution

With three disulfide bonds present in intact insulin, the mass fragmentation spectra (**Figure 19A**) obtained on the Q-Orbitrap in **Paper I** were insufficient for identification using either a non-enzyme specific search towards a Swissprot database or directly towards the amino acid sequence of insulin. The identification could be enhanced by incorporation of an IPA-assisted radical inter-chain cleavage reactor, based on Adhikari et al. [167, 168] placed upstream to the nano LC-MS platform. The inter-chain cleavage rector separated the A- and B chains of insulin, and insulin could be successfully identified by the mass fragmentation spectra obtained from B chain in simple water-based solutions (**Figure 19B**). For solutions prepared in Krebs buffer, the developed IPA-assisted radical inter-chain cleavage reactor coupled to the nanoLC-MS platform suffered from clogging and high detection limits above 10 ng/µL (results not shown). For cell medium, the method was successful down to 1 ng/µL of insulin, however, only following dilution of the cell medium with water (1+1, v+v).

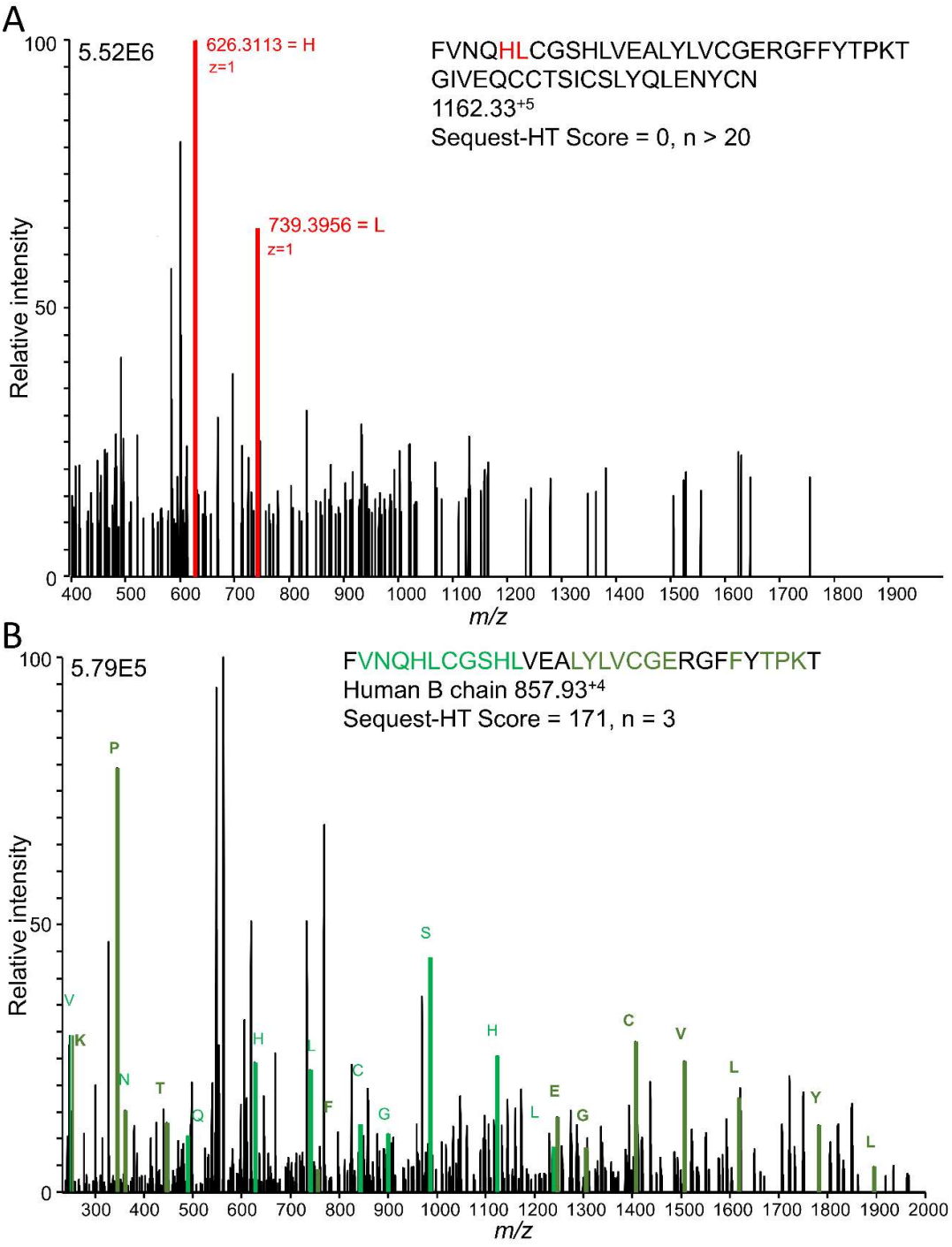

Figure 19: (**A**) Mass fragmentation spectrum of intact insulin in water-based solution obtained with nanospray-Q-Orbitrap-MS. (**B**) Mass fragmentation spectrum of insulin B chain following on-line IPA-assisted radical inter-chain cleavage of insulin in water-based solution upstream to nanospray-Q-Orbitrap-MS. Fragments of the amino acid sequence identified by Sequest-HT are colored in green, while manually recognized fragments of amino acids are colored in red (e.g. *m/z* 626.3^{+} = FVNQH is marked with an H). Applied precursor mass tolerance of 10 ppm and fragment mass tolerance of 0.02 Da. Adapted from **Paper I** with permission under the Creative Commons Attribute licensing.

In hindsight, the effect on the detection limits due to the degree of reduction of intact insulin, the distribution of B-chain with zero, one or two IPA modifications following radical cleavage, and the charge state distribution of the reduced B-chains (**Figure 20)** was not sufficiently examined in **Paper I**. The developers of the IPA-assisted radical cleavage reactor successfully applied a similar reactor in-front of the ESI source for mapping of disulfide bridges with close to 100% reduction of disulfide bonds in 5 s [167, 168]. However, the cleavage of intact insulin to reduced B chain in the examined platform was not 100%, as the peak area ratio of the reduced B chain (represented as *m/z* 858) and the remaining intact insulin (measured as *m/z* 1162.3) was 0.9 (RSD = 27%, N = 6) in cell medium (**Paper I**). The reason for the reduced cleavage efficiency in **Paper I** is difficult to pin-point, but it may be related to the placement of the reactor as the reactor was placed upstream to the LC system in **Paper I**, while it was placed directly in-front of the ESI source in the original article [167]. Also, in **Paper I**, the amount of IPA was reduced from 50% to 20% to allow for trapping and separation on the LC system. This reduction may have caused the initially formed acetone radicals to interact with other compounds in the solutions rather than IPA, giving a reduced formation of hydroxyalkyl radicals which cleaves the disulfide bonds [167].

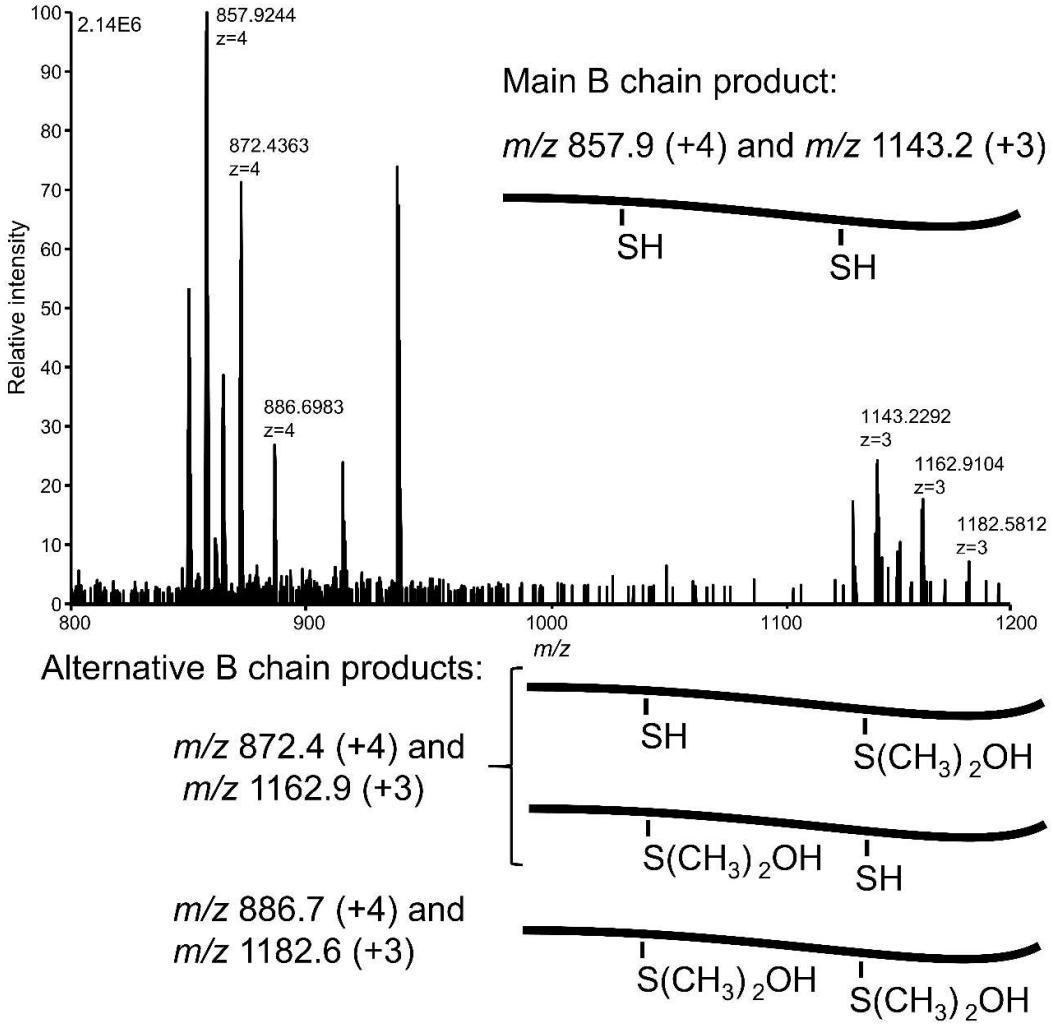

Figure 20: The IPA-assisted radical inter-chain cleavage reactor can cleave insulin into B chain with zero, one, or two IPA modification $(CH_3)_2OH$, where the main B chain product was without IPA modification. The mass spectrum shows the distribution of the various B chain products with zero to two IPA modifications and their charge state distribution.

A possibility to improve the detection limit is to summarize the signal obtained for all of the various B chain products at both charge states. The summation of multiple MRM transitions has been shown successful for ubiquitin giving increased detection limits and dynamic range [169]. In addition, summation would improve insulin determination as the effect of variation in the produced B chain products and the charge state distribution is accounted for.

Another option is to affect the charge state distribution of B chain products (and intact insulin), which depends on the MP additives (added in water-based

MP A and ACN-based MP B) and sample matrix. The pH of all sample matrices applied in **Paper I-III** were manually controlled to have a pH 3 using addition of acid and pH-paper. For the examined B chain product in **Paper I**, the distribution of *m/z* 857.9 and *m/z* 1143.2 was dependent on the sample matrix as shown in **Table 3**. The charge state distribution shifted towards a significantly higher percentage of *m/z* 857.9 when the injected solutions contained cell medium in addition to water.

Table 3: Charge state distribution of B chain product with zero IPA modifications (including relative standard deviation, RSD) in different solutions obtained with the IPA-assisted radical inter-chain cleavage reactor coupled upstream to the nanoRPLC-ESI-MS platform in **Paper I**. The distribution was calculated based on peak area. Technical replicates (N) ≥ 3.

MP A additive	MP B additive	Solution matrix	*m/z* 857.9 (+4)	*m/z* 1143.2 (+3)
0.05 % DFA	10% IPA 10% water 0.05% DFA	80/20 water/IPA (v/v) 0.05% DFA	56% RSD = 2%	44% RSD = 2%
0.05 % DFA	10% IPA 10% water 0.05% DFA	40/40/20 water/cell medium/IPA (v/v) 0.05% DFA	74% RSD = 4%	26% RSD = 12%

For intact insulin, the distribution of *m/z* 968.6, *m/z* 1162.5, and *m/z* 1452.5 was largely dependent on the MP additives, but also to a degree the sample matrix, as shown in **Table 4**. Independent of sample matrix or MP additives, the only ion which had a stable and repeatable percentage in the charge state distribution of intact insulin with RSD ≤ 6 % for N ≥ 3 was *m/z* 1162.5. In **Paper I**, using FA and DFA as MP additives, between 32% and 44% of intact insulin was present as *m/z* 1162.5. However, in **Paper II**, using DMSO and FA as MP additives, < 85% of intact insulin was present as *m/z* 1162.5. Having a shifted charge state distribution towards a single charge state offers lower detection limits favorable for determination of low abundant peptides independent of untargeted (**Paper I**) or targeted (**Paper II-III**) MS acquisition.

Table 4: Charge state distribution of intact insulin with different MP additives and different solutions obtained with: (top three rows) the IPA-assisted radical inter-chain cleavage reactor coupled upstream to the nanoRPLC-ESI-Q-Orbitrap platform in **Paper I**, and (bottom two rows) using the conventional RPLC-ESI-QqQ-MS system in **Paper II**. The distribution was calculated based on peak area. Technical replicates (N) ≥ 3.

MP A additive	MP B additive	Solution matrix	*m/z* 968.6 (+6)	*m/z* 1162.5 (+5)	*m/z* 1452.5 (+4)
0.1% FA	10% IPA 10% water 0.1% FA	Water 0.1% FA	36% RSD = 11%	42% RSD = 5%	22% RSD = 27%
0.05% DFA	10% IPA 10% water 0.05% DFA	Water 0.05% DFA	< 1% RSD = 21%	32% RSD = 2%	67% RSD = 1%
0.05% DFA	10% IPA 10% water 0.05% DFA	50/50 water/cell medium (v/v) 0.05% DFA	< 1% RSD = 29%	44% RSD = 6%	55% RSD = 4%
1% DMSO 0.1% FA	1% DMSO 0.1% FA	Water 0.1% FA	6.5% RSD = 15%	85.5% RSD = 1%	8% RSD = 8%
1% DMSO 0.1% FA	1% DMSO 0.1% FA	Cell medium 1.0% FA	< 0.1%	90% RSD = 6%	10% RSD = 43%

Another downside of the method in **Paper I,** was quite extensive run time due to the need to ensure repeatable exposure time in-front of the UV lamp, **Figure 21**. The samples were loaded with a controlled flow rate of 300 nL/min, with a total loading volume being: injection volume + extra column volume + 1 µL. Subsequently, a 2 µL injection volume was loaded with a total of 4.5 µL over the course of 15 min giving a UV light exposure time of approx. 2 min. In addition, the gradient run time was 30 min, giving a minimum run time of 45 min per injection.

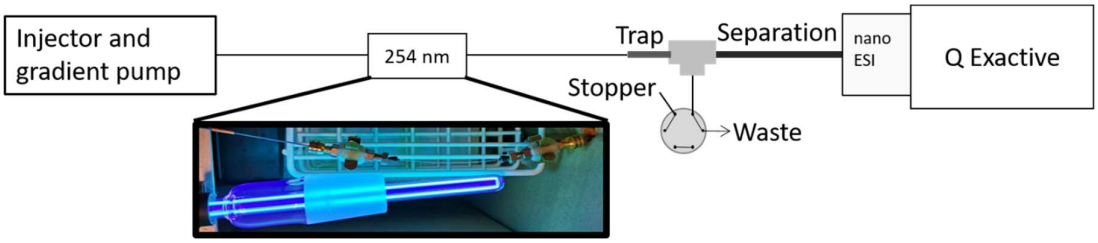

Figure 21: Schematic overview of instrumental set-up for incorporation of IPA-assisted radical inter-chain cleavage reactor using a high intensity 254 nm mercury quartz lamp and UV transparent tubing. Adapted from **Paper I** with permission under the Creative Commons Attribute licensing.

A benefit concerning method development was that the Q-Orbitrap operated in DDA mode allowed for continuous monitoring of charge state distribution in **Paper I**. In **Paper II-III**, the QqQ-MS was operated in MRM mode, which does not offer information about the precursor ions in the same manner. To monitor charge state distribution with the QqQ-MS, an additional injection using full scan mode would have been necessary.

*To summarize, the limiting factors of the developed method in **Paper I** were poor fragmentation in the Q-Orbitrap of intact insulin, which was combated with the incorporation of an inter-chain cleavage reactor enabling identification based on mass fragmentation spectrum. However, there were still compatibility issues with Krebs buffer and cell medium, high detection limits, and extensive sample loading and run times. Concerning peptides, special care should also be taken when selecting MP additives and changing sample matrices as shifts in charge state distribution may occur.*

3.2.3 **Immunoaffinity column: A possible tool for enrichment (unpublished work)**

Immunoaffinity techniques for purification and enrichment are common in insulin determination using magnetic beads with immobilized antibodies or ELISA plates [150, 170, 171]. An immunoaffinity column for enrichment of insulin was briefly examined in the nano RPLC-MS set-up of **Paper I**, **Figure 22A**. The column was prepared by immobilizing insulin antibodies onto a poly(vinyl azlactone-co-ethylene dimethacrylate) monolith, **Figure 22B**, by flushing a 0.1 mg/mL antibody solution in 50 mM phosphate buffer (pH 8) for 4 h (approx. 0.5 mL). The procedure for preparing the monoliths is described by Olsen et al. [120], which was based on Geiser et al. [172]. In addition, the monoliths have previously been used for selective fishing of a proteotypic peptide [119], and in drug-target studies [120].

The prepared insulin immunoaffinity columns were applied a total of 25 ng of reduced and alkylated insulin in a water-based solution (using dithiothreitol and iodoacetamide). The flow through the column was collected (termed Flow through) and added 2 µL 100% FA before injection. Additionally, the column was washed with 50 mM ammonium acetate (pH 8.2) following the application of insulin, this fraction was also collected (term Wash) and added 2 µL 100% FA before injection. The elution from the immunoaffinity column was done by injecting 5 µL of 0.8 M of acetic acid in 20/80 IPA/water (v/v) (termed Elution). In addition, an injection of 10 ng of reduced and alkylated insulin in 0.1% FA in H2O was done bypassing the immunoaffinity column (termed Control). The peak of B chain of insulin obtained in the Elution was much greater than the peak obtained in the fraction Control, Flow through, or Wash, indicating that the immunoaffinity columns could trap and release reduced and alkylated insulin (N = 3 on the same immunoaffinity column), **Figure 22C**.

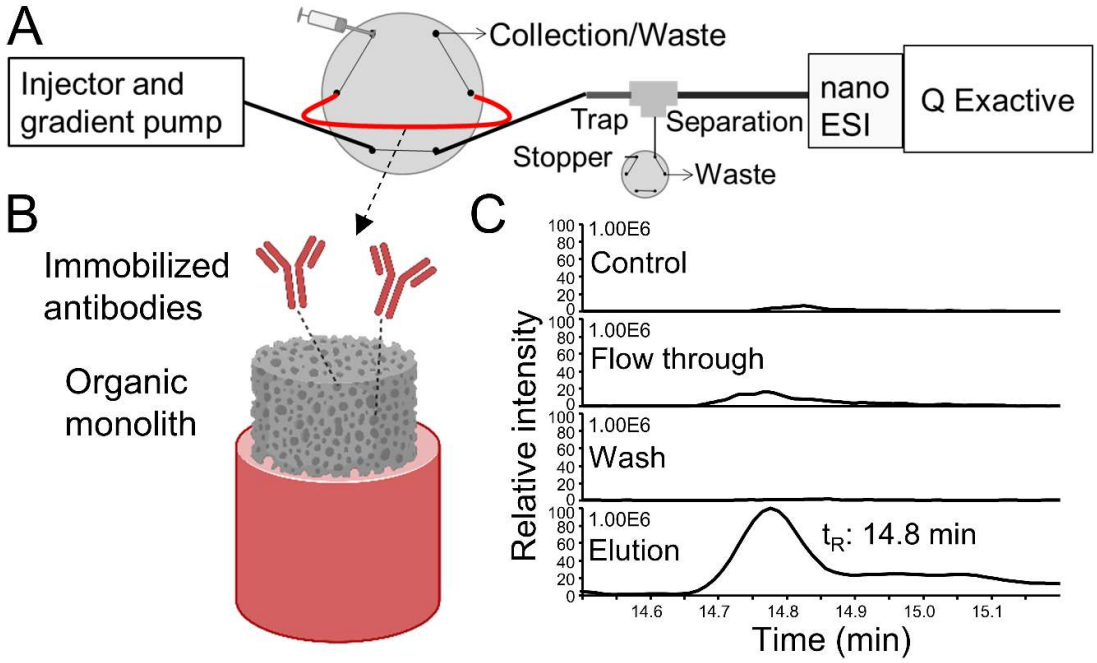

Figure 22: (**A**) Immunoaffinity column incorporated in the nano RPLC-ESI-MS platform in **Paper I**. (**B**) Visualization of insulin antibody attached to poly(EDMA-co-VDM) organic monolith. Created with BioRender.com [15]. (**C**) Crude peak comparison of the B chain of insulin obtained from 10 ng injection of insulin (Control), 4 µL injection of the solution collected during application of insulin solution on immunoaffinity column (Flow through), 4 µL injection of the solution collected during application of washing solution (Wash), and injection of 5 µL of 0.8 M of acetic acid in 20/80 IPA/water (v/v) (Elution).

To summarize, the immunoaffinity columns need to be characterized much more extensively and in more complex sample matrices, but the technique shows promise as a possible tool for on-line enrichment.

3.2.4 Nano liquid chromatography and Q-Orbitrap: Not suited for insulin determination in Krebs buffer and cell medium

The Q-Orbitrap was unable to fragment intact insulin in a manner suitable for untargeted or targeted MS analysis, leading to the necessity of incorporation of an inter-chain cleavage reactor in **Paper I**. The high detection limits of insulin following on-line inter-chain cleavage could have possibly been reduced following an extensive optimization of the inter-chain reactor yield of B chain product and charge state distribution (**Section 3.2.2**), or by obtaining enrichment with an immunoaffinity column (**Section 3.2.3**). However, there

appears to be an incompatibility between nano RPLC-MS, determination of insulin, and the intended sample matrices; Krebs buffer and cell medium. Actual samples collected as supernatant from SC-islets could contain cell debris and other particles, which would also contribute to clogging the vulnerable narrow id columns and tubings in a nano LC system. Inclusion of sample preparation steps for reduction and alkylation, purification, and enrichment could provide a better outlook for obtaining an untargeted LC-MS method to examine the secretion output from SC-islets. Examination of the peptidome of islets from mice and human donors has been successfully done with nano-LC-MS determination following reduction and alkylation [161].

The IPA-assisted radical inter-chain cleavage reactor coupled with RPLC-MS may hold a potential for on-line determination of higher abundant peptides and proteins with disulfide bonds in simple matrices (e.g. water-based solutions). However, in the particular case of **Paper I**, the obtained performance in measuring insulin in diluted cell medium (≥ 1 ng/µL), incompatibility with Krebs buffer, and the long run time per sample (> 45 min) does not justify the effort to maintain or optimize a nano LC-MS system. Conventional systems using low resolution QqQ-MS can determine insulin including other peptides with better detection limits in salt-based matrices (with or without extensive sample preparation) with run times ≤ 15 min [132, 173].

*To summarize, the developed nano RPLC-MS method in **Paper I** applying narrow id silica-based monolithic columns and IPA-assisted radical inter-chain cleavage reactor showed surprisingly high detection limits for insulin in cell medium and incompatibility with Krebs buffer. Larger id column formats offering better ruggedness were deemed a more appropriate future route for obtaining a method for determination of secreted hormones from SC-islets.*

3.3 Conventional liquid chromatography with targeted low resolution mass spectrometry: A better match for determination of secretion in stem cell-derived islet organoids

A multitude of LC-MS methods for determination of insulin or synthetic analogues apply particle packed column with id > 1 mm, where 2.1 mm id is the most common format [132, 151, 170, 171, 173-175]. Having difficulties obtaining sufficient detection limits for insulin, the expected main secretion product of the β-cells in the SC-islets, in a nanoRPLC-ESI-HRMS/MS approach in **Paper I**, separation using larger column formats and QqQ-MS was considered possible alternatives. A conventional RPLC-HESI-QqQ-MS system focused on insulin determination was explored in **Paper II**, and later examined for the inclusion of other peptides; somatostatin-14, glucagon, and urocortin-3 in **Paper III**.

The QqQ-MS applied in **Paper II**, obtained a highly repeatable fragmentation of intact insulin (*m/z* 1162.5 (+5) → *m/z* 226.1, 345.0, and 1159.2, **Figure 23**), which is in contrast to the limited and unstable fragmentation of intact insulin obtained with Q-Orbitrap in **Paper I**. The conventional RPLC-HESI-QqQMS system was examined in **Paper II** for the possibility of obtaining a "dilute and shoot" method for the determination of intact insulin secretion from SC-islets incubated in Krebs buffer and cell medium (**Section 3.1**). Key challenges concerning non-defined adsorption in the LC-system and charge state distribution of intact insulin at three charge states were solved by applying shielded fused silica connectors (see **Section 3.2.1**) and using DMSO and FA as MP additives (see **Section 3.2.2**), respectively. Matrix components in Krebs buffer and cell medium proved to be a challenge to obtain sufficiently low detection limits from determination of peptides in a conventional RPLC-ESI-MS system (**Paper II** and **Paper III**).

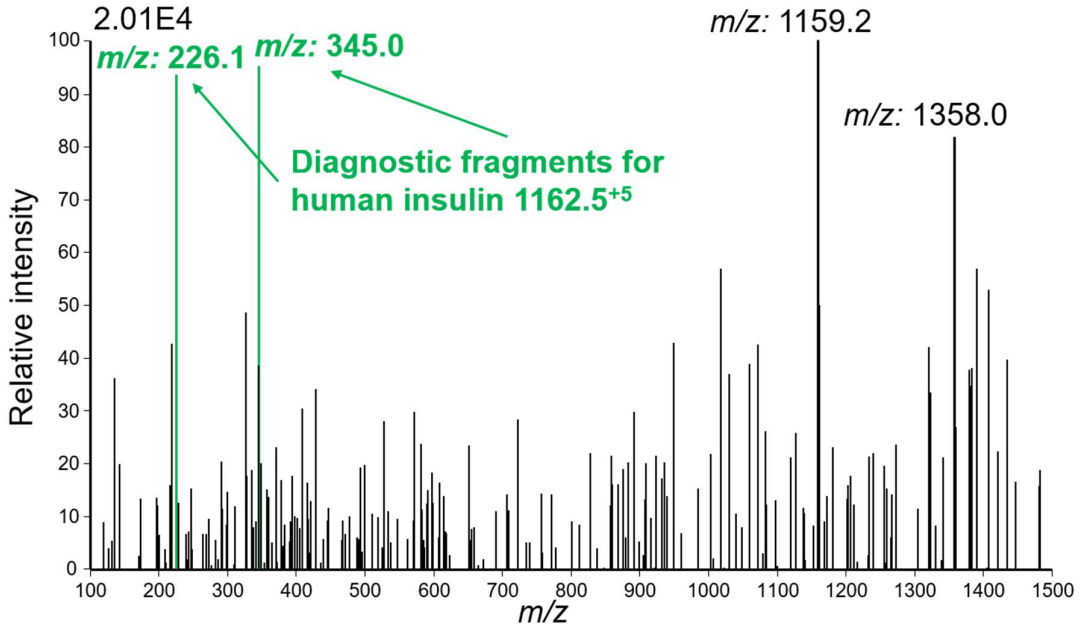

Figure 23: Product ions obtained following fragmentation of intact insulin using the QqQ-MS in **Paper II**, the green fragments are the diagnostic fragments used in determination of endogenous human insulin separate from synthetic variants [151]. Adapted from **Paper II** with permission under the Creative Commons Attribute licensing.

3.3.1 Successful determination of insulin secretion from stem cell-derived islet organoids in Krebs buffer

To reach a suitable detection limit for intact insulin secreted from SC-islets (approx. 1 pg/µL) in **Paper II**, Box-Behnken (BB) experimental design was used to optimize HESI- and MS-inlet settings for optimal precursor (*m/z* 1162.5) peak area in full scan MS mode. The settings optimized in the BB were spray voltage, temperature of the vaporizer and the ion transfer tube, and the flow rate of sheath gas, auxiliary gas, and sweep gas. A 3.2-fold increase in peak area was obtained by changing the recommended default settings of sheath gas levels from 27 arbitrary units (Arb) to 20 Arb and reducing the ion transfer tube temperature from 325 °C to 210 °C.

Recently, Krmar et al. [147], conducted a thorough examination into the prediction of various LC- and ESI settings' effect on analyte response in LC-ESI-MS. The study found that spray voltage and ion transfer tube temperature

were the main factors affecting obtained analyte response, but also flow rate of sheath- and auxiliary gas. The findings in **Paper II** are in agreement with the findings of Krmar et al. [147], and show that using a simple and split BB-design (2 x 15 injection) was a powerful, highly effective, and unbiased way to optimize six different HESI- and MS-inlet settings at three levels.

Following BB-optimization, intact insulin was successfully detected in cell medium containing approx. 8 pg/µL insulin using an injection volume of 1.08 µL (fixed loop attached to a 6-port-2-position valve for manual injection) in MRM mode. To pursue a detection limit of around 1 pg/µL, the injection volume was increased to 20 µL, but resulted in co-elution of insulin and BSA present in the cell medium, **Figure 24A**. However, in Krebs buffer, which contains 20 times less BSA than cell medium, insulin was still successfully detected with 20 µL injection volume without being co-eluted with BSA, **Figure 24B**. The correct amount of BSA present in Krebs buffer and cell medium was 1 µg/µL and 20 µg/µL, respectively, not 1 ng/µL and 20 ng/µL as stated in **Paper II**.

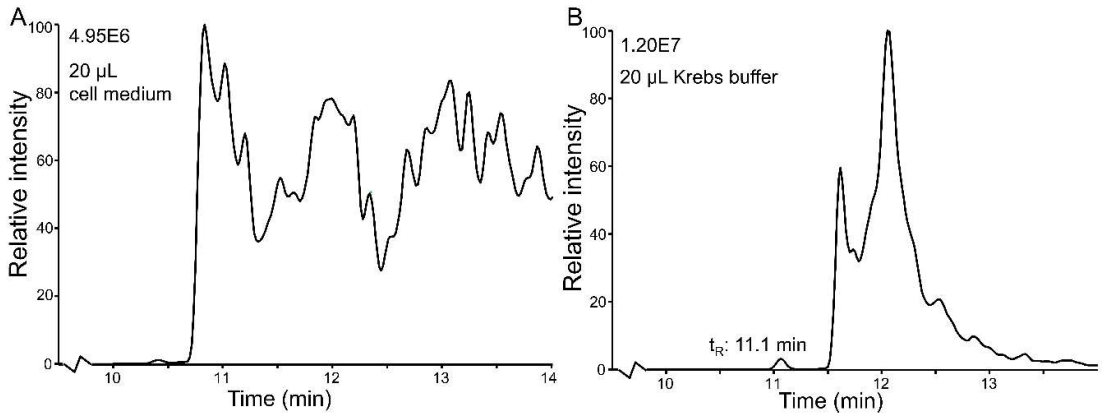

Figure 24: Extracted ion chromatogram (m/z 1162-1163) showing: (**A**) Insulin not detected in 20 µL injection of 6.25 pg/µL insulin in 1% FA in cell medium, while (**B**) insulin was detected at 11.1 min after 20 µL injection of 5 pg/µL insulin in 0.5% FA in Krebs buffer. Adapted from **Paper II** with permission under the Creative Commons Attribute licensing.

The developed conventional RPLC-HESI-QqQ-MS method in **Paper II** was successfully applied for determination of insulin secretion from SC-islets

incubated in Krebs buffer with different concentrations of glucose and KCl. The insulin concentrations found with the LC-MS method were not significantly different from the concentrations found with an established ELISA kit.

*To summarize, the conventional RPLC-HESI-QqQ-MS of **Paper II** was able to determine insulin secretion from SC-islets in Krebs buffer. The detection limit allowing for determination of insulin secretion from SC-islets in Krebs buffer was obtained following optimization of HESI-MS using experimental design and increasing the injection volume. However, determination of insulin in cell medium was not possible due to co-elution with BSA under the same conditions.*

3.3.2 Bovine serum albumin: A bottleneck for inclusion of other peptides and determination in cell medium

The developed LC-MS method in **Paper II** obtained determination of insulin secretion from SC-islets with the following method characteristics: an estimated limit of detection of 0.2 pg/µL, ± 10% relative error, < 10% RSD, and negligible carry-over. Fulfilling three out of four method characteristics mentioned in the ultimate aim of the study; being highly selective, sensitive, and reliable. However, the method did not show versatility concerning simultaneous determination of multiple analytes or sample matrices, where BSA was the limiting factor for successful determination of insulin in cell medium. Therefore, efforts to obtain determination of insulin in cell medium and to enable measurement of additional bioactive peptides were made in **Paper III**.

Somatostatin-14, glucagon, and urocortin-3 (all of human origin) were included in a peptide mix along with insulin. By optimizing the gradient applied on the LC, the interfering BSA peak could be removed from insulin in

both Krebs buffer (**Figure 25A**) and cell medium (**Figure 25B**). However, urocortin-3 was not successfully separated from BSA in Krebs buffer (**Figure 25A**), subsequently, urocortin-3 was not examined in cell medium which contains even more BSA than Krebs buffer.

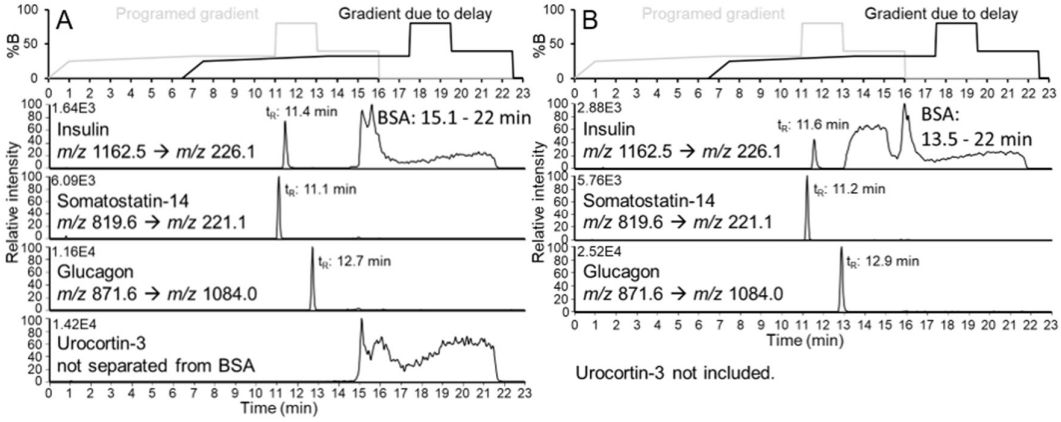

Figure 25: Separation of insulin, somatostatin-14, glucagon, and urocortin-3 with the optimized gradient from **Paper III**: (**A**) 20 µL injection of 5 pg/µL of each peptide in 0.5% FA in Krebs buffer and (**B**) 20 µL injection of 5 pg/µL of each peptide in 1.0% FA in cell medium. Adapted from manuscript of **Paper III**.

The precursors of insulin (*m/z* 1162.5) and urocortin-3 (*m/z* 1035.5) are within *m/z* 1000-1500, where BSA produces a multitude of peaks (**Supplementary materials** in **Paper II**). Additionally, a product ion scan confirmed that BSA produces the same precursor and product ion pair of insulin: *m/z* 1162.5 → *m/z* 226.1 and *m/z* 345.1 (**Figure 26A**), and *m/z* 1162.5 → *m/z* 1159.0 (**Figure 26B**). BSA was also proved to produce the same precursor and product ion pair as urocortin-3 in another product ion scan (results not shown). Somatostatin-14 and glucagon were not affected as the applied precursor (< *m/z* 900) was outside the range of interfering peaks originating from BSA, also confirmed by product ion scans (results not shown).

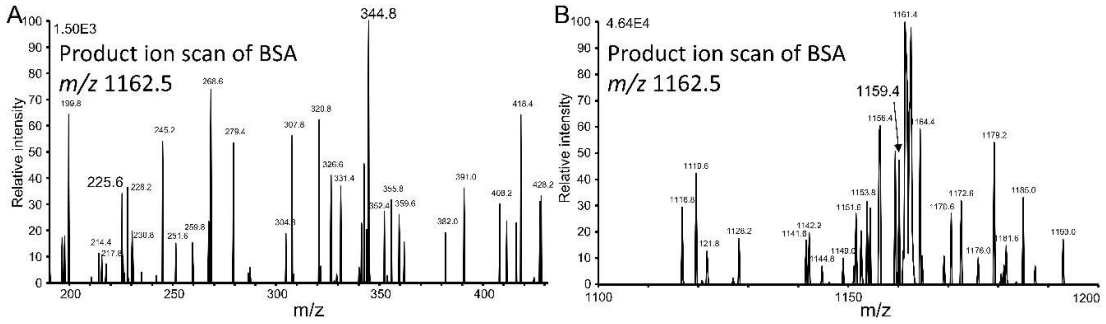

Figure 26: Mass fragmentation spectrum obtained from direct injection of 10 ng/µL BSA in 50/50 ACN/H2O with 0.1% FA with QqQ-MS operated product ion scan mode with the same settings applied in the MRM mode used for determination of insulin. The mass fragmentation spectra show that BSA produces (**A**) fragments at 226 and 345, and (**B**) a fragment at 1159.

The final conventional RPLC-HESI-QqQ-MS method developed in **Paper III**, was applied to measure peptide secretion of SC-islets incubated in Krebs buffer with different concentrations of glucose and KCl. Insulin was successfully determined in all of the samples with the RPLC-HESI-QqQ-MS method. The obtained detection limits for somatostatin-14 and glucagon allowed for determination of the peptides following membrane depolarization of the SC-islets, however, not by glucose stimulation alone.

To summarize, determination of insulin in cell medium could be obtained following optimization of the applied gradient elution profile in ***Paper III****. In addition, somatostatin-14 and glucagon could be included, even though the detection limits were insufficient for glucose stimulated somatostatin-14 and glucagon secretion from SC-islets incubated in Krebs buffer.*

3.3.3 Determination of secretion from stem cell-derived islet organoids-on-chip device in cell medium

In **Paper III,** the final conventional RPLC-HESI-QqQ-MS method was applied for determination of peptides in supernatant collected from 3-6 SC-islets incubated in cell medium for 24h (with 5.5 mM glucose) on an organ-on-chip device based on Busek et al. [176] (**Figure 27A**). Dr. Mathias Busek and Dr. Aleksandra Aizenshtadt at the hybrid technology hub-center of Excellence at the University of Oslo were responsible for the preparation of the chips and sample collection.

The secretion of insulin from SC-islets-on-chip in cell medium was successfully determined. The amount of insulin in supernatant was 5 pg/µL per SC-islet (RSD = 52%, n = 4, N = 1) after five days of culture, while on day 7 the insulin amount in the supernatant was 3 pg/µL per SC-islet (RSD = 30%, n = 4, N = 1). These findings show that the SC-islets have a rather large variation in secretion of insulin, and that the method can be used to study insulin secretion in a single SC-islet (estimated limit of detection was 0.2 pg/µL for insulin). Somatostatin-14 and glucagon were not successfully determined as the secretions were below lower limit of quantification (0.1 pg/µL in cell medium), **Figure 27B**. Glucagon was determined in a 24-well plate with 14-19 SC-islets incubated in cell medium for 24 h. This indicates that a larger batch of SC-islets combined with the use of potassium for membrane depolarization (used in Krebs buffer in **Section 3.3.2**) will be needed to study somatostatin-14 and glucagon production in SC-islets with the current method.

Thus, the final conventional RPLC-HESI-QqQ-MS method offered reliable determination of insulin, somatostatin-14, and glucagon in cell medium. The method offered a negligible variation in retention time (≤ 0.5% RSD), repeatable quantifier/qualifier transition ratios in standards and samples for

insulin and glucagon (**Figure 27C**), and negligible levels of carry-over (< 2% for glucagon, < 0.5% for human insulin, and < 0.1% for somatostatin-14). The characteristics of the developed method was similar to a reported LC-MS based method applied for peptide determination from human islets [132].

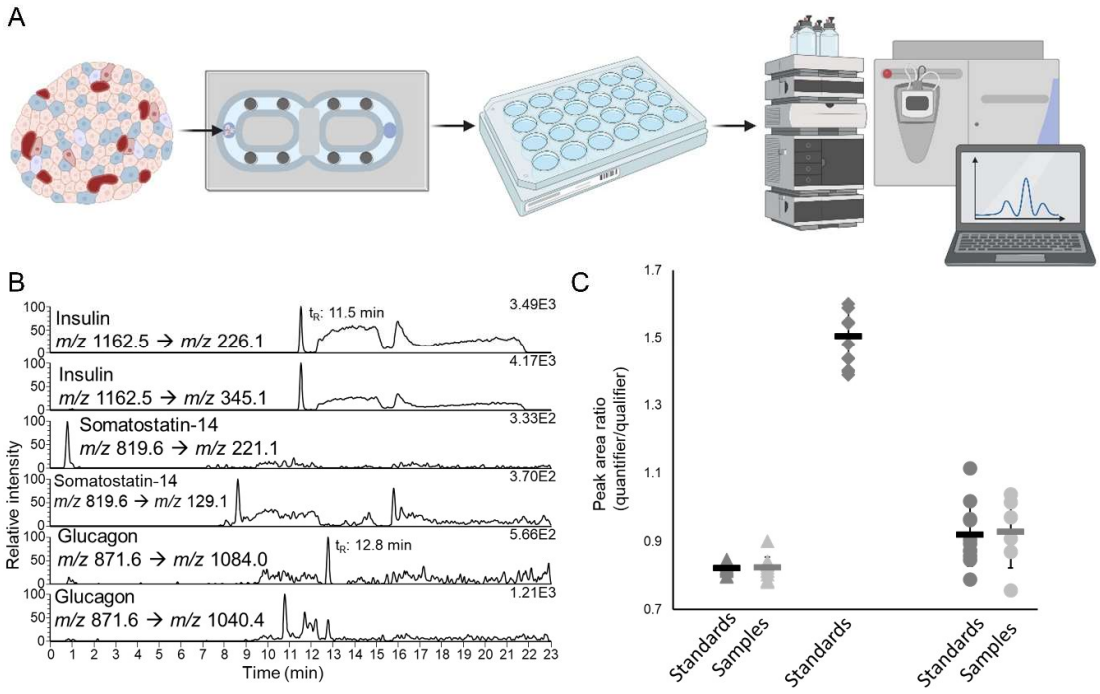

Figure 27: (**A**) Schematic overview of proof-of-concept for combining determination of peptide secretion from SC-islets-on-chip with LC-MS. (**B**) Successful determination of insulin separated from BSA in cell medium-based supernatant collected from SC-islets-on-chip. Somatostatin-14 and glucagon were below lower limit of quantification. (**C**) The ratio of quantifier/qualifier transitions for insulin (triangles), somatostatin-14 (diamonds), and glucagon (circle) were obtained for calibration standards and quality controls (QCs) (dark grey), and samples (light grey). None of the transitions of somatostatin-14 were detected in any of the examined samples. Adapted from manuscript of **Paper III**.

*To summarize, insulin secretion from limited number of SC-islets-on-chip cultivated in cell medium was successfully determined with the final conventional RPLC-HESI-QqQ-MS method in **Paper III**. In addition, glucose stimulated secretion of glucagon could be determined from a larger number of SC-islets cultivated in well-plates.*

3.3.4 Increased sample complexity: Supernatant collected from stem cell-derived islet organoids co-cultured with stem cell-derived liver organoids-on-chip (unpublished work)

The ruggedness of the final conventional RPLC-HESI-QqQ-MS method was further examined for determination of peptides in cell medium-based supernatant from co-culture of SC-islets and SC-liver-on-chip, **Figure 28A** [data from an ongoing unpublished study]. The SC-liver was generated from H1 cell line as described in Busek et al. [176], by Dr. Aleksandra Aizenshtadt. Samples from a total of 16 OoCs with co-culture of 2-9 SC-islets and 3-11 SC-liver were examined, where obesity had been induced in the SC-liver (by treatment of oleic acid, palmitic acid, and fructose) in eight of the co-cultures.

In most of the collected samples, insulin could be determined within a range of 5-36 pg/µL) with repeatable insulin quantifier/qualifier transition ratios as found in standards. Somatostatin-14 and glucagon were again below lower limit of quantification. In one of the co-cultures of SC-islets and SC-liver (not induced with obesity), insulin could not be determined as the insulin peak co-eluted with interferences shown in **Figure 28B**. In healthy co-culture, the amount of insulin in supernatant was determined to be 2.5 pg/µL per SC-islet (RSD = 40%, n = 7, N = 1), while in induced obesity state, the amount of insulin in the supernatant was 4 pg/µL per SC-islet (RSD = 59%, n = 8, N =1). There was no significant difference in the determined insulin concentration in the cell medium from co-culture with induced obesity compared to supernatant from healthy co-culture. This may be due to the rather large variances in insulin secretion between organoids (**Section 3.3.3**).

Gel electrophoresis followed by Coomassie blue staining (procedure explained in **Paper III**) was used to compare the presence of proteins in the different samples collected from co-culture of SC-islets and SC-liver with standard cell medium (not incubated with any organoids or spiked with analytes) and a

mixture of BSA and insulin in water. While the water solution showed protein band from insulin and BSA, including most likely dimers and trimers of BSA (Lane 1, **Figure 28C**), the standard cell medium also had some proteins bands visible in the range between the band BSA and insulin (Lane 2, **Figure 28C**) equal to the size range 15 to 40 kDa based on the pre-stained protein ladder (Lane 10, **Figure 28C**). The samples collected from the co-culture with induced obesity showed an increased amount of proteins in the same range compared to standard cell medium (Lane 5, 6, 8, and 9 in **Figure 28C**). However, the healthy co-culture showed even more proteins present in the same range (Lane 3, 4, and 7 in **Figure 28C**). The sample in Lane 7 was from the co-culture of SC-islets and SC-liver, where insulin co-eluted with interferences (**Figure 28B**). In addition, the bands belonging to BSA appeared to be even more saturated in Lane 3-9, which is likely due to the SC-liver producing and secreting human albumin into the cell medium [176]. Both the proteins are in the range between 15 to 40 kDa and the increase in albumin (human + bovine) may be the cause for the co-elution with insulin.

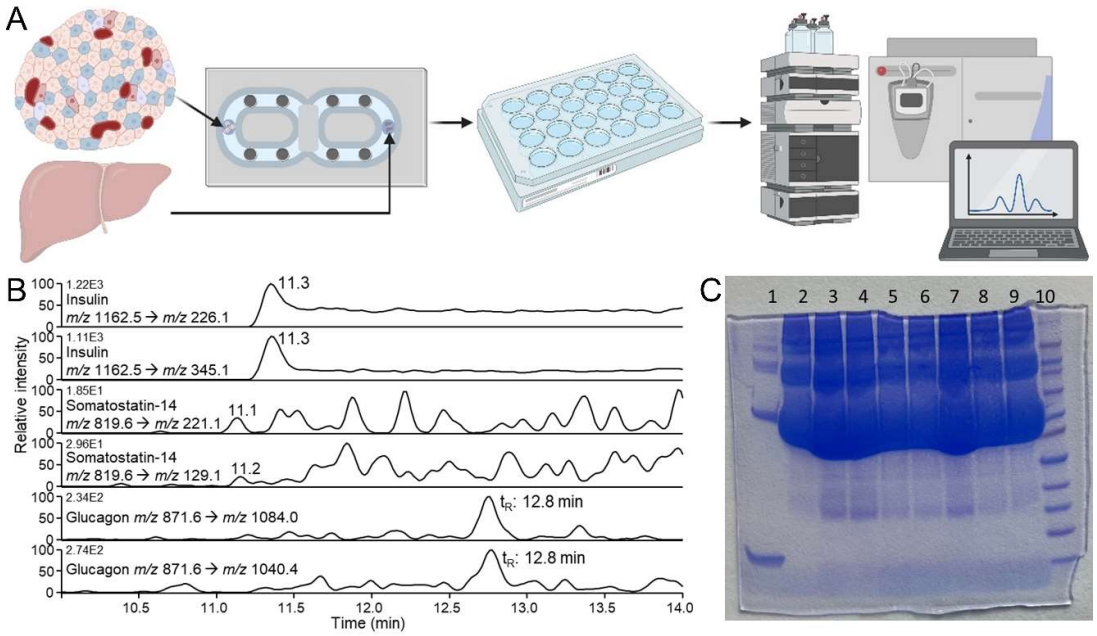

Figure 28: (**A**) Schematic overview showing SC-islets and liver organoids co-cultured on OoC device before LC-MS determination of peptide secretion. (**B**) Co-elution of insulin

with interfering compound(s) in cell medium-based supernatant collected from SC-islets and liver organoids-on-chip. Somatostatin-14 and glucagon were below lower limit of quantification. (**C**) Stained protein band after gel electrophoresis of the following samples: (**1**) 100 ng/µL of insulin and 100 ng/µL of bovine serum albumin in water. (**2**) 1.0% formic acid in cell medium. (**3**, **4**, **7**) Supernatant collected from SC-islets and SC-liver incubated in cell medium on OoC device at day 11 of co-culture. (**5**, **6**, **8**, **9**) Supernatant collected from SC-islets and SC-liver (treated with 200 µM oleic acid, 200 µM palmitic acid, and fructose to induce obesity) incubated in cell medium on OoC device at day 11 of co-culture. (**10**) 10 µL of Novex® sharp pre-stained protein standard.

*To summarize, the RPLC-HESI-QqQ-MS method from **Paper III** provided reliable, highly selective, sensitive, and rugged determination of insulin secretion in highly complex samples collected from co-culture of SC-islets and SC-liver-on-chip.*

3.3.5 Final comments about the conventional liquid chromatography triple quadrupole mass spectrometry-based method

The ruggedness of the conventional RPLC-HESI-QqQ-MS in **Paper III** was far superior to the nano RPLC-ESI-Q-Orbitrap-MS method developed in **Paper I**. The conventional method allowed for > 1000 injections without loss of sensitivity or any substantial wash of the separation columns, even though the peak shape of insulin did gain more tailing (**Section 3.2.1**). The QqQ-MS required at minimum a thorough wash of the MS-inlet once a week when running > 30 injections in cell medium per day. As a precaution, the MS was washed daily when running samples collected from OoC experiments to avoid sensitivity drop.

Another challenge with cell medium was the increase in the variation of the peak area obtained from bovine insulin, which was applied as internal standard in **Paper II** and **Paper III**. While the bovine insulin peak area showed a consistent RSD of < 5% for the calibration standards prepared in Krebs buffer, the RSD of the bovine insulin peak area increased to over > 7% for calibration standards prepared in cell medium. The increase in variation of bovine insulin peak area negatively affected the method's accuracy in determination of

known insulin concentration in quality control (QC) solutions examined alongside the samples in **Paper III** (**Section 3.3.3** and **Section 3.3.4**). In Krebs buffer applying bovine insulin as internal standard, QCs with known concentrations of insulin were determined within ± 15% relative error. However, in cell medium, the known insulin concentrations were determined within ± 20% relative error using bovine insulin as internal standard, and within ± 10% relative error without use of internal standard. This indicates that bovine insulin was not an appropriate internal standard for insulin in cell medium.

Determination of somatostatin-14 and glucagon was done without use of internal standard (as bovine insulin was not a suitable match due to different structure and retention time, and other suitable options were not available at the time of analysis). QCs with known concentrations of somatostatin-14 and glucagon were also examined in Krebs buffer and cell medium. In Krebs buffer, the known concentration of somatostatin-14 and glucagon were determined within ± 15% relative error (except for single QC for glucagon) in **Paper II** and **Paper III**. In cell medium, known concentrations of somatostatin-14 and glucagon were determined within ± 15% relative error for QCs analysed in the same sequence as the samples collected from SC-islets-on-chip (**Section 3.3.3**). However, for the QCs included during peptide determination of samples collected from co-culture of SC-islets and SC-liver-on-chip (**Section 3.3.4**), the relative error increased dramatically during the sequence. For somatostatin-14, known concentration was determined within ± 15% at the start of the sequence. However, the detectable response of somatostatin-14 in QCs dropped following several injections of samples of co-culture, and the relative error increased to between -30 % to -60%. The signal from glucagon dropped in the same manner, leading to determination of known concentrations with over -50% relative error. These observations indicate that

the presence of secreted components in the samples collected from co-culture of SC-islets and SC-liver caused a drop in the measurable response of somatostatin-14 and glucagon. These components also limited the method's ability to accurately determine samples with unknown concentrations of somatostatin-14 and glucagon.

To improve the method, the matrix effects in cell medium following incubation of SC-liver need to be examined concerning e.g. ion suppression and protein binding. Also, inclusion of deuterated internal standards could improve the reliability of the determination. As discussed in **Paper II**, particle packed columns using particles with pore sizes over 220 Å (three times the hydrodynamic dimension of BSA) should reduce band broadening of proteins and may provide better separation of target peptides from co-eluting proteins [112, 177]. These changes may also allow for separation of urocortin-3 from BSA. Another option would be to include sample preparation for purification and enrichment, e.g. immunoaffinity purification (**Section 3.2.3**) or electromembrane extraction [178]. Electromembrane extraction has been successfully incorporated on-line in a capillary LC-ESI-QqQ-MS system for determination of methadone metabolism from SC-liver organoids in cell medium [179].

In hindsight, the effect of dimerization and hexamerization of insulin in the presence of Zn^{2+} (a component found in the applied cell medium) should have been examined during method development in **Paper II** and **Paper III**. Insulin was determined in a concentration range from 35 pM to 25 nM at pH 3 based on the monomeric structure of insulin. It has been reported that insulin does not show oligomeric species below μM range and that oligomerization is more favorable at higher pH [180]. However, a recent report by Bohr et al. [175], found that insulin was in fact present as oligomeric species in the nM range at physiological pH. These findings by Bohr et al. may indicate that the

therapeutic doses of insulin used for treatment of diabetes patients have been to low (as there is less monomeric insulin present), and show the importance of research and its output for improved patient safety and treatment.

To summarize, the final conventional RPLC-HESI-QqQ-MS in ***Paper III*** *showed superior ruggedness towards determination of insulin in highly complex samples. BSA and possibly other proteins or compounds secreted by SC-liver organoids caused significant signal drop for somatostatin-14 and glucagon revealed with the use of QCs. Further improvements may be obtained by using particle packed columns with larger pore sizes in the particles, or with the addition of sample preparation steps for purification and enrichment.*

4 Concluding remarks

The determination of bioactive peptides secreted from SC-islets incubated off- and on-chip has been dominated by immunoassays. This dissertation has examined the potential for determination of bioactive peptides secreted by SC-islets using LC in nano and conventional formats, with MS/MS in both an untargeted and a targeted approach. The combination of a conventional LC and targeted MS/MS was far superior concerning detection limits, versatility, reliability, and ruggedness compared to the nano LC coupled with untargeted MS/MS.

The developed nano RPLC-ESI-Q-Orbitrap-MS method showed limited performance due to poor fragmentation of intact insulin in the Q-Orbitrap requiring incorporation of disulfide bond cleavage. An IPA-assisted radical inter-chain cleavage reactor was coupled upstream of the nano LC-MS platform to obtain successful unsupervised peptide identification. However, the platform showed limited capabilities concerning detection limits, compatibility with Krebs buffer and cell medium, and required extensive sample loading and run time per injection.

Therefore, the tailored conventional RPLC-HESI-QqQ-MS method was optimized concerning the use of tubing material, MP composition, gradient elution profile, settings of the HESI and MS-inlet, CID performance, and monitored with the use of QCs with known analyte concentrations. The thorough optimization offered a method with superior ruggedness, negligible variation in retention time, negligible levels of carry-over, repeatable quantifier/qualifier transition ratios in standards and samples, and sufficient precision and accuracy. The method could successfully determine insulin secretion in Krebs buffer and cell medium from SC-islets off- and on-chip, and in co-culture with SC-liver. Somatostatin-14 and glucagon could be

determined in both Krebs buffer, cell medium, and fractions collected from SC-islets following membrane depolarization.

The exploration of LC and MS for determination of bioactive peptides showed that LC-MS was a potential competitor to immunoassays, offering simultaneous and highly selective determination of multiple analytes in the same sample/injection. The limiting factors concerning LC separation of bioactive peptides were; 1) non-defined adsorption depending on column format, tubing material, and sample matrices, 2) charge state distribution of multiply charged peptides combated with MP composition, and 3) compatibility towards biologically relevant sample matrices: Krebs buffer and cell medium, requiring rugged columns and instrumental set-up.

Concerning MS, the poor fragmentation in the Q-Orbitrap due to the presence of disulfide bonds in insulin was detrimental to the attempted "dilute-and-shoot" method, requiring either on-line inter-chain cleavage or traditional reduction and alkylation of disulfide bonds prior to injection. The use of QqQ-MS solved the issues with fragmentation, but limited the MS/MS approach to pre-selected target peptides.

The dissertation found that successful determination could be obtained by tailoring the LC-MS platform toward the desired analyte and sample matrices. The method fulfilled the desired characteristics of being highly selective, sensitive, versatile, and reliable for hormone secretion, even though the detection limits could be better concerning somatostatin-14 and glucagon. The work presented her confirms the overall hypothesis of this dissertation which was that LC-MS could provide a method with the above-mentioned characteristics for determination of hormone secretion from SC-islets off- and on-chip.

5 Future aspects

This dissertation contributes to the field of peptidomics with greater insight into determination of bioactive peptides using LC-MS, but also towards the development and characterization of organoids off- and on-chip.

The final conventional LC-MS method can for instance be applied for monitoring of insulin secretion in a single SC-islet during cultivation, as the method's quantification limits for insulin are suitable for the expected insulin secretion of one SC-islets following 24 h incubation in cell medium on-chip. Being able to study SC-islet variation could aid in improving the current variation in insulin secretion per SC-islet which was over 30% in the present study. The method is readily applicable to study insulin secretion in SC-islets following e.g. injections of synthetic analogs (which may be determined by the developed method), drug screening, and exposure to perfluoroalkyl substances. Concerning, somatostatin-14 and glucagon, the detection limits require a much larger batch of SC-islets.

Being able to reduce the amount of BSA in the samples appears to be the key to enable determination of other peptides e.g. urocortin-3 in the same method. The method may be improved by including sample preparation for purification and enrichment using immunoaffinity tools (e.g. immunoaffinity column or magnetic beads with immobilized antibodies) or possibly electromembrane extraction. The effect of BSA might also be reduced by using a separation column with particles with larger pores compared to the 120 Å pores studied here. Alternative separation columns might also improve the chromatographic performance obtained on the nanoLC system combined with reduction and alkylation prior to injection. A column format between nano and conventional may prove to be the best trade-off concerning ruggedness and sensitivity.

The final method developed in the dissertation can be applied to study SC-islets and human donor islets to obtain a further understanding of islet cell biology, which may eventually benefit patients with diabetes.

References

[1] H. Sun, P. Saeedi, S. Karuranga, M. Pinkepank, K. Ogurtsova, B.B. Duncan, C. Stein, A. Basit, J.C.N. Chan, J.C. Mbanya, M.E. Pavkov, A. Ramachandaran, S.H. Wild, S. James, W.H. Herman, P. Zhang, C. Bommer, S. Kuo, E.J. Boyko, D.J. Magliano, *IDF Diabetes Atlas: Global, regional and country-level diabetes prevalence estimates for 2021 and projections for 2045*, Diabetes Research and Clinical Practice, 183 (2022) 109119. https://www.sciencedirect.com/science/article/pii/S0168822721004782.

[2] G.A. Gregory, T.I.G. Robinson, S.E. Linklater, F. Wang, S. Colagiuri, C. de Beaufort, K.C. Donaghue, J.L. Harding, P.L. Wander, X. Zhang, X. Li, S. Karuranga, H. Chen, H. Sun, Y. Xie, R. Oram, D.J. Magliano, Z. Zhou, A.J. Jenkins, R.C.W. Ma, D.J. Magliano, J. Maniam, T.J. Orchard, P. Rai, G.D. Ogle, *Global incidence, prevalence, and mortality of type 1 diabetes in 2021 with projection to 2040: a modelling study*, The Lancet Diabetes & Endocrinology, 10 (2022) 741-760. https://www.sciencedirect.com/science/article/pii/S2213858722002182.

[3] O. Cabrera, D.M. Berman, N.S. Kenyon, C. Ricordi, P.-O. Berggren, A. Caicedo, *The unique cytoarchitecture of human pancreatic islets has implications for islet cell function*, Proceedings of the National Academy of Sciences of the United States of America, 103 (2006) 2334-2339. https://www.pnas.org/doi/abs/10.1073/pnas.0510790103.

[4] P. Rorsman, M.O. Huising, *The somatostatin-secreting pancreatic δ-cell in health and disease*, Nature Reviews Endocrinology, 14 (2018) 404-414. https://doi.org/10.1038/s41574-018-0020-6.

[5] C.J. Hedeskov, *Mechanism of glucose-induced insulin secretion*, Physiological reviews, 60 (1980) 442-509. https://journals.physiology.org/doi/abs/10.1152/physrev.1980.60.2.442.

[6] A.R. Saltiel, C.R. Kahn, *Insulin signalling and the regulation of glucose and lipid metabolism*, Nature, 414 (2001) 799-806. https://doi.org/10.1038/414799a.

[7] R.H. Unger, *Glucagon physiology and pathophysiology in the light of new advances*, Diabetologia, 28 (1985) 574-578. https://doi.org/10.1007/BF00281991.

[8] G. Jiang, B.B. Zhang, *Glucagon and regulation of glucose metabolism*, American Journal of Physiology-Endocrinology and Metabolism, 284 (2003) E671-E678. https://journals.physiology.org/doi/abs/10.1152/ajpendo.00492.2002.

[9] J.-C. Henquin, *Paracrine and autocrine control of insulin secretion in human islets: evidence and pending questions*, American Journal of Physiology-Endocrinology and Metabolism, 320 (2021) E78-E86. https://journals.physiology.org/doi/abs/10.1152/ajpendo.00485.2020.

[10] M.F. Flisher, D. Shin, M.O. Huising, *Urocortin3: Local inducer of somatostatin release and bellwether of beta cell maturity*, Peptides, 151 (2022) 170748. https://www.sciencedirect.com/science/article/pii/S0196978122000146.

[11] K.V. Grunddal, S.A.J. Trammell, C. Bæch-Laursen, D.B. Andersen, S.F.S. Xu, H. Andersen, M.P. Gillum, S.M. Ghiasi, I. Novak, B. Tyrberg, C. Li, M.M. Rosenkilde, B. Hartmann, J.J. Holst, R.E. Kuhre, *Opposing roles of the entero-pancreatic hormone urocortin-3 in glucose metabolism in rats*, Diabetologia, 65 (2022) 1018-1031. https://doi.org/10.1007/s00125-022-05675-9.

[12] J. Hutton, *The insulin secretory granule*, Diabetologia, 32 (1989) 271-281. https://link.springer.com/article/10.1007/BF00265542.

[13] Y. Rouillé, G. Westermark, S.K. Martin, D.F. Steiner, *Proglucagon is processed to glucagon by prohormone convertase PC2 in alpha TC1-6 cells*, Proceedings of the National Academy of Sciences of the United States of America, 91 (1994) 3242-3246. https://www.ncbi.nlm.nih.gov/pmc/articles/PMC43552/.

[14] B.H. Francis, D.G. Baskin, D.R. Saunders, J.W. Ensinck, *Distribution of somatostatin-14 and somatostatin-28 gastrointestinal-pancreatic cells of rats and humans*, Gastroenterology, 99 (1990) 1283-1291. https://www.sciencedirect.com/science/article/pii/001650859091151U.
[15] BioRender.com, (2023). https://app.biorender.com/biorender-templates.
[16] B.O. Roep, S. Thomaidou, R. van Tienhoven, A. Zaldumbide, *Type 1 diabetes mellitus as a disease of the β-cell (do not blame the immune system?)*, Nature Reviews Endocrinology, 17 (2021) 150-161. https://doi.org/10.1038/s41574-020-00443-4.
[17] D.L. Eizirik, F. Szymczak, R. Mallone, *Why does the immune system destroy pancreatic β-cells but not α-cells in type 1 diabetes?*, Nature Reviews Endocrinology, (2023). https://doi.org/10.1038/s41574-023-00826-3.
[18] C.J. Nolan, P. Damm, M. Prentki, *Type 2 diabetes across generations: from pathophysiology to prevention and management*, The Lancet, 378 (2011) 169-181. https://www.sciencedirect.com/science/article/pii/S0140673611606144.
[19] A.S. Al-Goblan, M.A. Al-Alfi, M.Z. Khan, *Mechanism linking diabetes mellitus and obesity*, Diabetes Metab Syndr Obes, 7 (2014) 587-591. https://www.ncbi.nlm.nih.gov/pmc/articles/PMC4259868/.
[20] P. Shah, A. Vella, A. Basu, R. Basu, W.F. Schwenk, R.A. Rizza, *Lack of suppression of glucagon contributes to postprandial hyperglycemia in subjects with type 2 diabetes mellitus*, The Journal of Clinical Endocrinology & Metabolism, 85 (2000) 4053-4059. https://doi.org/10.1210/jcem.85.11.6993.
[21] C.J. Greenbaum, R.L. Prigeon, D.A. D'Alessio, *Impaired β-cell function, incretin effect, and glucagon suppression in patients with type 1 diabetes who have normal fasting glucose*, Diabetes, 51 (2002) 951-957. https://doi.org/10.2337/diabetes.51.4.951.
[22] J.E. Campbell, C.B. Newgard, *Mechanisms controlling pancreatic islet cell function in insulin secretion*, Nature Reviews Molecular Cell Biology, 22 (2021) 142-158. https://doi.org/10.1038/s41580-020-00317-7.
[23] V.H. Maier, G.W. Gould, *Long-term insulin treatment of 3T3-L1 adipocytes results in mis-targeting of GLUT4: implications for insulin-stimulated glucose transport*, Diabetologia, 43 (2000) 1273-1281. https://doi.org/10.1007/s001250051523.
[24] F.G. Banting, C.H. Best, J.B. Collip, W.R. Campbell, A.A. Fletcher, *Pancreatic extracts in the treatment of diabetes mellitus*, Canadian Medical Association Journal, 12 (1922) 141-146. https://www.ncbi.nlm.nih.gov/pmc/articles/PMC1524425/.
[25] M. Fralick, B. Zinman, *The discovery of insulin in Toronto: beginning a 100 year journey of research and clinical achievement*, Diabetologia, 64 (2021) 947-953. https://doi.org/10.1007/s00125-020-05371-6.
[26] R. Retnakaran, B. Zinman, *The ongoing evolution of basal insulin therapy over 100 years and its promise for the future*, Diabetes, Obesity and Metabolism, 24 (2022) 17-26. https://dom-pubs.onlinelibrary.wiley.com/doi/abs/10.1111/dom.14552.
[27] C.K. Kramer, R. Retnakaran, B. Zinman, *Insulin and insulin analogs as antidiabetic therapy: A perspective from clinical trials*, Cell Metabolism, 33 (2021) 740-747. https://www.sciencedirect.com/science/article/pii/S1550413121001212.
[28] Y.H. Lee, M.-Y. Wang, X.-X. Yu, R.H. Unger, *Glucagon is the key factor in the development of diabetes*, Diabetologia, 59 (2016) 1372-1375. https://doi.org/10.1007/s00125-016-3965-9.
[29] S. Knight, T. Vogel, P. Friend, *Pancreas transplantation*, Surgery (Oxford), 38 (2020) 418-424. https://www.sciencedirect.com/science/article/pii/S0263931920300922.
[30] G. Lanzoni, C. Ricordi, *Transplantation of stem cell-derived pancreatic islet cells*, Nature Reviews Endocrinology, 17 (2021) 7-8. https://doi.org/10.1038/s41574-020-00430-9.

[31] L.H. Story, L.M. Wilson, *New developments in glucagon treatment for hypoglycemia*, Drugs, 82 (2022) 1179-1191. https://doi.org/10.1007/s40265-022-01754-8.
[32] D.A. Domingo-Lopez, G. Lattanzi, L. H. J. Schreiber, E.J. Wallace, R. Wylie, J. O'Sullivan, E.B. Dolan, G.P. Duffy, *Medical devices, smart drug delivery, wearables and technology for the treatment of diabetes mellitus*, Advanced Drug Delivery Reviews, 185 (2022) 114280. https://www.sciencedirect.com/science/article/pii/S0169409X22001703.
[33] A.M.J. Shapiro, J.R.T. Lakey, E.A. Ryan, G.S. Korbutt, E. Toth, G.L. Warnock, N.M. Kneteman, R.V. Rajotte, *Islet transplantation in seven patients with type 1 diabetes mellitus using a glucocorticoid-free immunosuppressive regimen*, New England Journal of Medicine, 343 (2000) 230-238. https://www.nejm.org/doi/full/10.1056/NEJM200007273430401.
[34] E.A. Ryan, J.R.T. Lakey, R.V. Rajotte, G.S. Korbutt, T. Kin, S. Imes, A. Rabinovitch, J.F. Elliott, D. Bigam, N.M. Kneteman, G.L. Warnock, I. Larsen, A.M.J. Shapiro, *Clinical outcomes and insulin secretion after islet transplantation with the Edmonton protocol*, Diabetes, 50 (2001) 710-719. https://doi.org/10.2337/diabetes.50.4.710.
[35] A.M.J. Shapiro, C. Ricordi, B.J. Hering, H. Auchincloss, R. Lindblad, R.P. Robertson, A. Secchi, M.D. Brendel, T. Berney, D.C. Brennan, E. Cagliero, R. Alejandro, E.A. Ryan, B. DiMercurio, P. Morel, K.S. Polonsky, J.-A. Reems, R.G. Bretzel, F. Bertuzzi, T. Froud, R. Kandaswamy, D.E.R. Sutherland, G. Eisenbarth, M. Segal, J. Preiksaitis, G.S. Korbutt, F.B. Barton, L. Viviano, V. Seyfert-Margolis, J. Bluestone, J.R.T. Lakey, *International trial of the Edmonton protocol for islet transplantation*, New England Journal of Medicine, 355 (2006) 1318-1330. https://www.nejm.org/doi/full/10.1056/NEJMoa061267.
[36] M.-C. Vantyghem, E.J.P. de Koning, F. Pattou, M.R. Rickels, *Advances in β-cell replacement therapy for the treatment of type 1 diabetes*, The Lancet, 394 (2019) 1274-1285. https://www.sciencedirect.com/science/article/pii/S0140673619313340.
[37] P. Siwakoti, C. Rennie, Y. Huang, J.J. Li, B.E. Tuch, L. McClements, X. Xu, *Challenges with cell-based therapies for type 1 diabetes mellitus*, Stem Cell Reviews and Reports, 19 (2023) 601-624. https://doi.org/10.1007/s12015-022-10482-1.
[38] S. Abadpour, C. Wang, E.M. Niemi, H. Scholz, *Tissue engineering strategies for improving beta cell transplantation outcome*, Current Transplantation Reports, 8 (2021) 205-219. https://doi.org/10.1007/s40472-021-00333-2.
[39] J.A. Thomson, J. Itskovitz-Eldor, S.S. Shapiro, M.A. Waknitz, J.J. Swiergiel, V.S. Marshall, J.M. Jones, *Embryonic stem cell lines derived from human blastocysts*, Science, 282 (1998) 1145-1147. https://www.science.org/doi/abs/10.1126/science.282.5391.1145.
[40] K. Takahashi, S. Yamanaka, *Induction of pluripotent stem cells from mouse embryonic and adult fibroblast cultures by defined factors*, Cell, 126 (2006) 663-676. https://www.sciencedirect.com/science/article/pii/S0092867406009767.
[41] K. Takahashi, K. Tanabe, M. Ohnuki, M. Narita, T. Ichisaka, K. Tomoda, S. Yamanaka, *Induction of pluripotent stem cells from adult human fibroblasts by defined factors*, Cell, 131 (2007) 861-872. https://www.sciencedirect.com/science/article/pii/S0092867407014717.
[42] H. Clevers, *Modeling development and disease with organoids*, Cell, 165 (2016) 1586-1597. https://www.sciencedirect.com/science/article/pii/S0092867416307292.
[43] X.-Y. Tang, S. Wu, D. Wang, C. Chu, Y. Hong, M. Tao, H. Hu, M. Xu, X. Guo, Y. Liu, *Human organoids in basic research and clinical applications*, Signal Transduction and Targeted Therapy, 7 (2022) 168. https://doi.org/10.1038/s41392-022-01024-9.
[44] A. Marsee, F.J.M. Roos, M.M.A. Verstegen, A. Marsee, F. Roos, M. Verstegen, H. Clevers, L. Vallier, T. Takebe, M. Huch, W.C. Peng, S. Forbes, F. Lemaigre, E. de

Koning, H. Gehart, L. van der Laan, B. Spee, S. Boj, P. Baptista, K. Schneeberger, C. Soroka, M. Heim, S. Nuciforo, K. Zaret, Y. Saito, M. Lutolf, V. Cardinale, B. Simons, S. van Ijzendoorn, A. Kamiya, H. Chikada, S. Wang, S.J. Mun, M.J. Son, T.T. Onder, J. Boyer, T. Sato, N. Georgakopoulos, A. Meneses, L. Broutier, L. Boulter, D. Grün, J. Ijzermans, B. Artegiani, R. van Boxtel, E. Kuijk, G. Carpino, G. Peltz, J. Banales, N. Man, L. Aloia, N. LaRusso, G. George, C. Rimland, G. Yeoh, A. Grappin-Botton, D. Stange, N. Prior, J.E.E. Tirnitz-Parker, E. Andersson, C. Braconi, N. Hannan, W.-Y. Lu, S. Strom, P. Sancho-Bru, S. Ogawa, V. Corbo, M. Lancaster, H. Hu, S. Fuchs, D. Hendriks, H. Gehart, E. de Koning, F. Lemaigre, S.J. Forbes, W.C. Peng, M. Huch, T. Takebe, L. Vallier, H. Clevers, L.J.W. van der Laan, B. Spee, *Building consensus on definition and nomenclature of hepatic, pancreatic, and biliary organoids*, Cell Stem Cell, 28 (2021) 816-832. https://www.sciencedirect.com/science/article/pii/S1934590921001624.

[45] C.L. Basford, K.J. Prentice, A.B. Hardy, F. Sarangi, S.J. Micallef, X. Li, Q. Guo, A.G. Elefanty, E.G. Stanley, G. Keller, E.M. Allister, M.C. Nostro, M.B. Wheeler, *The functional and molecular characterisation of human embryonic stem cell-derived insulin-positive cells compared with adult pancreatic beta cells*, Diabetologia, 55 (2012) 358-371. https://doi.org/10.1007/s00125-011-2335-x.

[46] Felicia W. Pagliuca, Jeffrey R. Millman, M. Gürtler, M. Segel, A. Van Dervort, Jennifer H. Ryu, Quinn P. Peterson, D. Greiner, Douglas A. Melton, *Generation of functional human pancreatic β cells in vitro*, Cell, 159 (2014) 428-439. https://www.sciencedirect.com/science/article/pii/S0092867414012288.

[47] P.U. Mahaddalkar, K. Scheibner, S. Pfluger, Ansarullah, M. Sterr, J. Beckenbauer, M. Irmler, J. Beckers, S. Knöbel, H. Lickert, *Generation of pancreatic β cells from CD177+ anterior definitive endoderm*, Nature Biotechnology, 38 (2020) 1061-1072. https://doi.org/10.1038/s41587-020-0492-5.

[48] S.G. Yabe, S. Fukuda, J. Nishida, F. Takeda, K. Nashiro, H. Okochi, *Induction of functional islet-like cells from human iPS cells by suspension culture*, Regenerative Therapy, 10 (2019) 69-76. https://www.sciencedirect.com/science/article/pii/S2352320418300488.

[49] H. Bi, S.S. Karanth, K. Ye, R. Stein, S. Jin, *Decellularized tissue matrix enhances self-assembly of islet organoids from pluripotent stem cell differentiation*, ACS Biomaterials Science & Engineering, 6 (2020) 4155-4165. https://doi.org/10.1021/acsbiomaterials.0c00088.

[50] G.G. Nair, J.S. Liu, H.A. Russ, S. Tran, M.S. Saxton, R. Chen, C. Juang, M.-l. Li, V.Q. Nguyen, S. Giacometti, S. Puri, Y. Xing, Y. Wang, G.L. Szot, J. Oberholzer, A. Bhushan, M. Hebrok, *Recapitulating endocrine cell clustering in culture promotes maturation of human stem-cell-derived β cells*, Nature Cell Biology, 21 (2019) 263-274. https://doi.org/10.1038/s41556-018-0271-4.

[51] E.S. Heaton, S. Jin, *Importance of multiple endocrine cell types in islet organoids for type 1 diabetes treatment*, Translational Research, 250 (2022) 68-83. https://www.sciencedirect.com/science/article/pii/S1931524422001487.

[52] D. Balboa, J. Saarimäki-Vire, D. Borshagovski, M. Survila, P. Lindholm, E. Galli, S. Eurola, J. Ustinov, H. Grym, H. Huopio, J. Partanen, K. Wartiovaara, T. Otonkoski, *Insulin mutations impair beta-cell development in a patient-derived iPSC model of neonatal diabetes*, eLife, 7 (2018) e38519. https://doi.org/10.7554/eLife.38519.

[53] Y. Hosokawa, T. Toyoda, K. Fukui, M.Y. Baden, M. Funato, Y. Kondo, T. Sudo, H. Iwahashi, M. Kishida, C. Okada, A. Watanabe, I. Asaka, K. Osafune, A. Imagawa, I. Shimomura, *Insulin-producing cells derived from 'induced pluripotent stem cells' of patients with fulminant type 1 diabetes: Vulnerability to cytokine insults and increased*

expression of apoptosis-related genes, Journal of Diabetes Investigation, 9 (2018) 481-493. https://onlinelibrary.wiley.com/doi/abs/10.1111/jdi.12727.
[54] A.M.J. Shapiro, K. Verhoeff, *A spectacular year for islet and stem cell transplantation*, Nature Reviews Endocrinology, 19 (2023) 68-69. https://doi.org/10.1038/s41574-022-00790-4.
[55] H. Nichols, *Vertex announces positive day 90 data for the first patient in the phase 1/2 clinical trial dosed with VX-880, a novel investigational stem cell-derived therapy for the treatment of type 1 diabetes*, Businesswire, 18.10.2021. https://www.businesswire.com/news/home/20211018005226/en/.
[56] A. Ramzy, D.M. Thompson, K.A. Ward-Hartstonge, S. Ivison, L. Cook, R.V. Garcia, J. Loyal, P.T.W. Kim, G.L. Warnock, M.K. Levings, T.J. Kieffer, *Implanted pluripotent stem-cell-derived pancreatic endoderm cells secrete glucose-responsive C-peptide in patients with type 1 diabetes*, Cell Stem Cell, 28 (2021) 2047-2061.e2045. https://www.sciencedirect.com/science/article/pii/S193459092100415X.
[57] A.M.J. Shapiro, D. Thompson, T.W. Donner, M.D. Bellin, W. Hsueh, J. Pettus, J. Wilensky, M. Daniels, R.M. Wang, E.P. Brandon, M.S. Jaiman, E.J. Kroon, K.A. D'Amour, H.L. Foyt, *Insulin expression and C-peptide in type 1 diabetes subjects implanted with stem cell-derived pancreatic endoderm cells in an encapsulation device*, Cell Reports Medicine, 2 (2021) 100466. https://www.sciencedirect.com/science/article/pii/S2666379121003384.
[58] X. Zhang, Z. Ma, E. Song, T. Xu, *Islet organoid as a promising model for diabetes*, Protein & Cell, 13 (2022) 239-257. https://doi.org/10.1007/s13238-021-00831-0.
[59] J. Rogal, A. Zbinden, K. Schenke-Layland, P. Loskill, *Stem-cell based organ-on-a-chip models for diabetes research*, Advanced Drug Delivery Reviews, 140 (2019) 101-128. https://www.sciencedirect.com/science/article/pii/S0169409X18302606.
[60] M.L. Coluccio, G. Perozziello, N. Malara, E. Parrotta, P. Zhang, F. Gentile, T. Limongi, P.M. Raj, G. Cuda, P. Candeloro, E. Di Fabrizio, *Microfluidic platforms for cell cultures and investigations*, Microelectronic Engineering, 208 (2019) 14-28. https://www.sciencedirect.com/science/article/pii/S016793171930019X.
[61] D.E. Ingber, *Human organs-on-chips for disease modelling, drug development and personalized medicine*, Nature Reviews Genetics, 23 (2022) 467-491. https://doi.org/10.1038/s41576-022-00466-9.
[62] R. Edmondson, J.J. Broglie, A.F. Adcock, L. Yang, *Three-dimensional cell culture systems and their applications in drug discovery and cell-based biosensors*, ASSAY and Drug Development Technologies, 12 (2014) 207-218. https://www.liebertpub.com/doi/abs/10.1089/adt.2014.573.
[63] H. Kutluk, E.E. Bastounis, I. Constantinou, *Integration of extracellular matrices into organ-on-chip systems*, Advanced Healthcare Materials, (2023) 2203256. https://onlinelibrary.wiley.com/doi/abs/10.1002/adhm.202203256.
[64] T. Tao, Y. Wang, W. Chen, Z. Li, W. Su, Y. Guo, P. Deng, J. Qin, *Engineering human islet organoids from iPSCs using an organ-on-chip platform*, Lab on a Chip, 19 (2019) 948-958. http://dx.doi.org/10.1039/C8LC01298A.
[65] T. Tao, P. Deng, Y. Wang, X. Zhang, Y. Guo, W. Chen, J. Qin, *Microengineered multi-organoid system from hiPSCs to recapitulate human liver-islet axis in normal and type 2 diabetes*, Advanced Science, 9 (2022) 2103495. https://onlinelibrary.wiley.com/doi/abs/10.1002/advs.202103495.
[66] S. Abadpour, A. Aizenshtadt, P.A. Olsen, K. Shoji, S.R. Wilson, S. Krauss, H. Scholz, *Pancreas-on-a-chip technology for transplantation applications*, Current Diabetes Reports, 20 (2020) 72. https://doi.org/10.1007/s11892-020-01357-1.

[67] A.-D. Luong, I. Roy, B.D. Malhotra, J.H.T. Luong, *Analytical and biosensing platforms for insulin: A review*, Sensors and Actuators Reports, 3 (2021) 100028. https://www.sciencedirect.com/science/article/pii/S2666053921000047.
[68] J. Yin, H. Meng, J. Lin, W. Ji, T. Xu, H. Liu, *Pancreatic islet organoids-on-a-chip: how far have we gone?*, Journal of Nanobiotechnology, 20 (2022) 308. https://doi.org/10.1186/s12951-022-01518-2.
[69] H. Ahsan, *Monoplex and multiplex immunoassays: approval, advancements, and alternatives*, Comparative Clinical Pathology, 31 (2022) 333-345. https://doi.org/10.1007/s00580-021-03302-4.
[70] S. Hædersdal, A. Andersen, F.K. Knop, T. Vilsbøll, *Revisiting the role of glucagon in health, diabetes mellitus and other metabolic diseases*, Nature Reviews Endocrinology, (2023). https://doi.org/10.1038/s41574-023-00817-4.
[71] J.J. Holst, N.J. Wewer Albrechtsen, *Methods and guidelines for measurement of glucagon in plasma*, International Journal of Molecular Sciences, 20 (2019) 5416. https://www.mdpi.com/1422-0067/20/21/5416.
[72] L. Kothegala, C. Miranda, M. Singh, J.-P. Krieger, N.R. Gandasi, *Somatostatin containing δ-cell number is reduced in type-2 diabetes*, International Journal of Molecular Sciences, 24 (2023) 3449. https://www.mdpi.com/1422-0067/24/4/3449.
[73] N. Rosli, H.-J. Kwon, J. Lim, Y.A. Yoon, J.-S. Jeong, *Measurement comparability of insulin assays using conventional immunoassay kits*, Journal of Clinical Laboratory Analysis, 36 (2022) e24521. https://onlinelibrary.wiley.com/doi/abs/10.1002/jcla.24521.
[74] T. Wu, C.K. Rayner, K.L. Jones, M. Horowitz, C. Feinle-Bisset, S.D. Standfield, C. Xie, C.F. Deacon, J.J. Holst, N.J. Wewer Albrechtsen, *Measurement of plasma glucagon in humans: A shift in the performance of a current commercially available radioimmunoassay kit*, Diabetes, Obesity and Metabolism, 24 (2022) 1182-1184. https://dom-pubs.onlinelibrary.wiley.com/doi/abs/10.1111/dom.14673.
[75] A. Ramzy, P.J. Belmonte, M.J.S. Braam, S. Ida, E.M. Wilts, M.K. Levings, A. Rezania, T.J. Kieffer, *A Century-long Journey From the Discovery of Insulin to the Implantation of Stem Cell–derived Islets*, Endocrine Reviews, 44 (2022) 222-253. https://doi.org/10.1210/endrev/bnac021.
[76] A. Shinde, K. Illath, U. Kasiviswanathan, S. Nagabooshanam, P. Gupta, K. Dey, P. Chakrabarty, M. Nagai, S. Rao, S. Kar, T.S. Santra, *Recent advances of biosensor-integrated organ-on-a-chip technologies for diagnostics and therapeutics*, Analytical chemistry, 95 (2023) 3121-3146. https://doi.org/10.1021/acs.analchem.2c05036.
[77] S. Kogler, K.S. Kømurcu, C. Olsen, J.-y. Shoji, F.S. Skottvoll, S. Krauss, S.R. Wilson, H. Røberg-Larsen, *Organoids, organ-on-a-chip, separation science and mass spectrometry: An update*, TrAC, Trends in Analytical Chemistry, (2023) 116996. https://doi.org/10.1016/j.trac.2023.116996.
[78] K. Lian, H. Feng, S. Liu, K. Wang, Q. Liu, L. Deng, G. Wang, Y. Chen, G. Liu, *Insulin quantification towards early diagnosis of prediabetes/diabetes*, Biosensors and Bioelectronics, 203 (2022) 114029. https://www.sciencedirect.com/science/article/pii/S0956566322000690.
[79] L. Beck, T. Geiger, *MS-based technologies for untargeted single-cell proteomics*, Current Opinion in Biotechnology, 76 (2022) 102736. https://www.sciencedirect.com/science/article/pii/S0958166922000702.
[80] P. Zhong, X. Wei, X. Li, X. Wei, S. Wu, W. Huang, A. Koidis, Z. Xu, H. Lei, *Untargeted metabolomics by liquid chromatography-mass spectrometry for food authentication: A review*, Comprehensive Reviews in Food Science and Food Safety, 21 (2022) 2455-2488. https://ift.onlinelibrary.wiley.com/doi/abs/10.1111/1541-4337.12938.

[81] A. Lin, F. Sved Skottvoll, S. Rayner, S. Pedersen-Bjergaard, G. Sullivan, S. Krauss, S. Ray Wilson, S. Harrison, *3D cell culture models and organ-on-a-chip: Meet separation science and mass spectrometry*, Electrophoresis, 41 (2020) 56-64. https://onlinelibrary.wiley.com/doi/abs/10.1002/elps.201900170.
[82] X. Shao, Y. Huang, G. Wang, *Microfluidic devices for protein analysis using intact and top-down mass spectrometry*, VIEW, 4 (2023) 20220032. https://onlinelibrary.wiley.com/doi/abs/10.1002/VIW.20220032.
[83] H.A. Favre, W.H. Powell, *Nomenclature of organic chemistry: IUPAC recommendations and preferred names 2013*, Royal Society of Chemistry, 2013.
[84] R.E. Foreman, A.L. George, F. Reimann, F.M. Gribble, R.G. Kay, *Peptidomics: A review of clinical applications and methodologies*, Journal of Proteome Research, 20 (2021) 3782-3797. https://doi.org/10.1021/acs.jproteome.1c00295.
[85] K.-T. Fan, C.-W. Hsu, Y.-R. Chen, *Mass spectrometry in the discovery of peptides involved in intercellular communication: From targeted to untargeted peptidomics approaches*, Mass Spectrometry Reviews, n/a (2022) e21789. https://analyticalsciencejournals.onlinelibrary.wiley.com/doi/abs/10.1002/mas.21789.
[86] G.P. Moss, P.A.S. Smith, D. Tavernier, *Glossary of class names of organic compounds and reactivity intermediates based on structure (IUPAC Recommendations 1995)*, Pure and Applied Chemistry, 67 (1995) 1307-1375. https://doi.org/10.1351/pac199567081307.
[87] Y.-C. Chen, A.J. Taylor, C.B. Verchere, *Islet prohormone processing in health and disease*, Diabetes, Obesity and Metabolism, 20 (2018) 64-76. https://dom-pubs.onlinelibrary.wiley.com/doi/abs/10.1111/dom.13401.
[88] A. Descamps, K. Van der borght, A. De Spiegeleer, E. Wynendaele, B. De Spiegeleer, *Peptidomics: LC–MS operational parameters do matter*, Journal of Pharmaceutical and Biomedical Analysis, 229 (2023) 115348. https://www.sciencedirect.com/science/article/pii/S0731708523001176.
[89] S. Caira, G. Picariello, G. Renzone, S. Arena, A.D. Troise, S. De Pascale, V. Ciaravolo, G. Pinto, F. Addeo, A. Scaloni, *Recent developments in peptidomics for the quali-quantitative analysis of food-derived peptides in human body fluids and tissues*, Trends in Food Science & Technology, 126 (2022) 41-60. https://www.sciencedirect.com/science/article/pii/S0924224422002072.
[90] C. Li, S. Chu, S. Tan, X. Yin, Y. Jiang, X. Dai, X. Gong, X. Fang, D. Tian, *Towards higher sensitivity of mass spectrometry: A perspective from the mass analyzers*, Frontiers in Chemistry, 9 (2021). https://www.frontiersin.org/articles/10.3389/fchem.2021.813359.
[91] A. Hu, W.S. Noble, A. Wolf-Yadlin, *Technical advances in proteomics: new developments in data-independent acquisition*, F1000Res, 5 (2016). https://www.ncbi.nlm.nih.gov/pmc/articles/PMC4821292/.
[92] J. Peng, H. Zhang, H. Niu, R.a. Wu, *Peptidomic analyses: The progress in enrichment and identification of endogenous peptides*, TrAC, Trends in Analytical Chemistry, 125 (2020) 115835. https://www.sciencedirect.com/science/article/pii/S0165993619302596.
[93] E. Maes, E. Oeyen, K. Boonen, K. Schildermans, I. Mertens, P. Pauwels, D. Valkenborg, G. Baggerman, *The challenges of peptidomics in complementing proteomics in a clinical context*, Mass Spectrometry Reviews, 38 (2019) 253-264. https://analyticalsciencejournals.onlinelibrary.wiley.com/doi/abs/10.1002/mas.21581.
[94] M.J.P. Rush, N.M. Riley, M.S. Westphall, J.J. Coon, *Top-down characterization of proteins with intact disulfide bonds using activated-ion electron transfer dissociation*, Analytical chemistry, 90 (2018) 8946-8953. https://doi.org/10.1021/acs.analchem.8b01113.

[95] E. Lundanes, L. Reubsaet, T. Greibrokk, *Chromatography: basic principles, sample preparations and related methods*, John Wiley & Sons, 2013.
[96] P. Žuvela, M. Skoczylas, J. Jay Liu, T. Bączek, R. Kaliszan, M.W. Wong, B. Buszewski, *Column characterization and selection systems in reversed-phase high-performance liquid chromatography*, Chemical Reviews, 119 (2019) 3674-3729. https://doi.org/10.1021/acs.chemrev.8b00246.
[97] V. D'Atri, A. Murisier, S. Fekete, J.-L. Veuthey, D. Guillarme, *Current and future trends in reversed-phase liquid chromatography-mass spectrometry of therapeutic proteins*, TrAC, Trends in Analytical Chemistry, 130 (2020) 115962. https://www.sciencedirect.com/science/article/pii/S0165993620301916.
[98] F. Verbeke, N. Bracke, N. Debunne, E. Wynendaele, B. De Spiegeleer, *LC–MS compatible antiadsorption diluent for peptide analysis*, Analytical chemistry, 92 (2020) 1712-1719. https://doi.org/10.1021/acs.analchem.9b01840.
[99] K. Maes, I. Smolders, Y. Michotte, A. Van Eeckhaut, *Strategies to reduce aspecific adsorption of peptides and proteins in liquid chromatography–mass spectrometry based bioanalyses: An overview*, Journal of Chromatography A, 1358 (2014) 1-13. https://www.sciencedirect.com/science/article/pii/S0021967314010152.
[100] J. Yang, I. Wilson, P. Rainville, *Evaluation of hybrid surface technology for the analysis of the B-group vitamins by LC-ESI-MS/MS*, Journal of Chromatography B, 1204 (2022) 123336. https://www.sciencedirect.com/science/article/pii/S1570023222002409.
[101] M.C. Jung, *Strategies to improve recoveries of proteins and peptides from sample containers before LC–MS analyses*, Column, 15 (2019) 11–16-11–16. https://www.chromatographyonline.com/view/strategies-improve-recoveries-proteins-and-peptides-sample-containers-lc-ms-analyses.
[102] J. Bongaerts, D. De Bundel, I. Smolders, D. Mangelings, Y. Vander Heyden, A. Van Eeckhaut, *Improving the LC-MS/MS analysis of neuromedin U-8 and neuromedin S by minimizing their adsorption behavior and optimizing UHPLC and MS parameters*, Journal of Pharmaceutical and Biomedical Analysis, 228 (2023) 115306. https://www.sciencedirect.com/science/article/pii/S0731708523000754.
[103] G.J. Guimaraes, M.G. Bartlett, *Managing nonspecific adsorption to liquid chromatography hardware: A review*, Analytica Chimica Acta, 1250 (2023) 340994. https://www.sciencedirect.com/science/article/pii/S0003267023002155.
[104] M. DeLano, T.H. Walter, M.A. Lauber, M. Gilar, M.C. Jung, J.M. Nguyen, C. Boissel, A.V. Patel, A. Bates-Harrison, K.D. Wyndham, *Using hybrid organic–inorganic surface technology to mitigate analyte interactions with metal surfaces in UHPLC*, Analytical chemistry, 93 (2021) 5773-5781. https://doi.org/10.1021/acs.analchem.0c05203.
[105] S. Perchepied, H. Ritchie, G. Desmet, S. Eeltink, *Insights in column packing processes of narrow bore and capillary-scale columns: Methodologies, driving forces, and separation performance – A tutorial review*, Analytica Chimica Acta, 1235 (2022) 340563. https://www.sciencedirect.com/science/article/pii/S0003267022011345.
[106] S.R. Wilson, C. Olsen, E. Lundanes, *Nano liquid chromatography columns*, Analyst, 144 (2019) 7090-7104. https://doi.org/10.1039/C9AN01473J.
[107] J.J. van Deemter, F.J. Zuiderweg, A. Klinkenberg, *Longitudinal diffusion and resistance to mass transfer as causes of nonideality in chromatography*, Chemical Engineering Science, 50 (1995) 3869-3882. https://www.sciencedirect.com/science/article/pii/0009250996818136.
[108] F. Gritti, G. Guiochon, *The van Deemter equation: Assumptions, limits, and adjustment to modern high performance liquid chromatography*, Journal of

Chromatography A, 1302 (2013) 1-13. https://www.sciencedirect.com/science/article/pii/S0021967313009278.
[109] M. Gumustas, P. Zalewski, S.A. Ozkan, B. Uslu, *The history of the core–shell particles and applications in active pharmaceutical ingredients via liquid chromatography*, Chromatographia, 82 (2019) 17-48. https://doi.org/10.1007/s10337-018-3670-6.
[110] K. Kaczmarski, G. Guiochon, *Modeling of the mass-transfer kinetics in chromatographic columns packed with shell and pellicular particles*, Analytical chemistry, 79 (2007) 4648-4656. https://doi.org/10.1021/ac070209w.
[111] B. Bobály, J.-L. Veuthey, D. Guillarme, S. Fekete, *New developments and possibilities of wide-pore superficially porous particle technology applied for the liquid chromatographic analysis of therapeutic proteins*, Journal of Pharmaceutical and Biomedical Analysis, 158 (2018) 225-235. https://www.sciencedirect.com/science/article/pii/S0731708518310811.
[112] F. Gritti, K. Horvath, G. Guiochon, *How changing the particle structure can speed up protein mass transfer kinetics in liquid chromatography*, Journal of Chromatography A, 1263 (2012) 84-98. https://www.sciencedirect.com/science/article/pii/S002196731201415X.
[113] S. Jaag, C. Wen, B. Peters, M. Lämmerhofer, *Kinetic performance comparison of superficially porous, fully porous and monolithic reversed-phase columns by gradient kinetic plots for the separation of protein biopharmaceuticals*, Journal of Chromatography A, 1676 (2022) 463251. https://www.sciencedirect.com/science/article/pii/S0021967322004447.
[114] D. Stoll, J. Hsiao, G. Staples, *Troubleshooting LC separations of biomolecules, part I: background, and the meaning of inertness*, LCGC North America, 38 (2020). https://www.chromatographyonline.com/view/troubleshooting-lc-separations-biomolecules-part-i-background-and-meaning-inertness.
[115] S. Ma, Y. Li, C. Ma, Y. Wang, J. Ou, M. Ye, *Challenges and advances in the fabrication of monolithic bioseparation materials and their applications in proteomics research*, Advanced Materials, 31 (2019) 1902023. https://onlinelibrary.wiley.com/doi/abs/10.1002/adma.201902023.
[116] K.B. Lynch, J. Ren, M.A. Beckner, C. He, S. Liu, *Monolith columns for liquid chromatographic separations of intact proteins: A review of recent advances and applications*, Analytica Chimica Acta, 1046 (2019) 48-68. http://www.sciencedirect.com/science/article/pii/S0003267018310900.
[117] O. Vyviurska, Y. Lv, B.F. Mann, F. Svec, *Comparison of commercial organic polymer-based and silica-based monolithic columns using mixtures of analytes differing in size and chemistry*, Journal of separation science, 41 (2018) 1558-1566. https://analyticalsciencejournals.onlinelibrary.wiley.com/doi/abs/10.1002/jssc.201701374.
[118] M. Nechvátalová, J. Urban, *Current trends in the development of polymer-based monolithic stationary phases*, Analytical Science Advances, 3 (2022) 154-164. https://chemistry-europe.onlinelibrary.wiley.com/doi/abs/10.1002/ansa.202100065.
[119] M.C.S. Levernæs, O.K. Brandtzaeg, S.F. Amundsen, L. Reubsaet, E. Lundanes, T.G. Halvorsen, S.R. Wilson, *Selective fishing for peptides with antibody-immobilized acrylate monoliths, coupled online with nanoLC-MS*, Analytical chemistry, 90 (2018) 13860-13866. https://doi.org/10.1021/acs.analchem.8b00935.
[120] C. Olsen, F.S. Skottvoll, O.K. Brandtzaeg, C. Schnaars, P. Rongved, E. Lundanes, S.R. Wilson, *Investigating monoliths (vinyl azlactone-co-ethylene dimethacrylate) as a support for enzymes and drugs, for proteomics and drug-target studies*, Frontiers in Chemistry, 7 (2019). https://www.frontiersin.org/article/10.3389/fchem.2019.00835.

[121] E. Vasconcelos Soares Maciel, A.L. de Toffoli, E. Sobieski, C.E. Domingues Nazário, F.M. Lanças, *Miniaturized liquid chromatography focusing on analytical columns and mass spectrometry: A review*, Analytica Chimica Acta, 1103 (2020) 11-31. https://www.sciencedirect.com/science/article/pii/S000326701931534X.
[122] G. Hopfgartner, K. Bean, J. Henion, R. Henry, *Ion spray mass spectrometric detection for liquid chromatography: A concentration- or a mass-flow-sensitive device?*, Journal of Chromatography A, 647 (1993) 51-61. https://www.sciencedirect.com/science/article/pii/002196739383323K.
[123] J.P.C. Vissers, H.A. Claessens, C.A. Cramers, *Microcolumn liquid chromatography: instrumentation, detection and applications*, Journal of Chromatography A, 779 (1997) 1-28. https://www.sciencedirect.com/science/article/pii/S0021967397004226.
[124] S.R. Wilson, T. Vehus, H.S. Berg, E. Lundanes, *Nano-LC in proteomics: recent advances and approaches*, Bioanalysis, 7 (2015) 1799-1815. https://www.future-science.com/doi/full/10.4155/bio.15.92.
[125] L. Shan, B.R. Jones, *Nano-LC: An updated review*, Biomedical Chromatography, 36 (2022) e5317. https://analyticalsciencejournals.onlinelibrary.wiley.com/doi/abs/10.1002/bmc.5317.
[126] M. Rogeberg, H. Malerod, H. Roberg-Larsen, C. Aass, S.R. Wilson, *On-line solid phase extraction–liquid chromatography, with emphasis on modern bioanalysis and miniaturized systems*, Journal of Pharmaceutical and Biomedical Analysis, 87 (2014) 120-129. https://www.sciencedirect.com/science/article/pii/S0731708513001994.
[127] V. Houbart, E. Rozet, A. Matagne, J. Crommen, A.C. Servais, M. Fillet, *Influence of sample and mobile phase composition on peptide retention behaviour and sensitivity in reversed-phase liquid chromatography/mass spectrometry*, Journal of Chromatography A, 1314 (2013) 199-207. https://www.sciencedirect.com/science/article/pii/S0021967313014672.
[128] E.L. Murphy, A.P. Joy, R.J. Ouellette, D.A. Barnett, *Improved intact peptide and protein quantitation by LC-MS: Battling the deleterious effects of analyte adsorption*, Analytical Science Advances, 2 (2021) 299-307. https://chemistry-europe.onlinelibrary.wiley.com/doi/abs/10.1002/ansa.202000102.
[129] D. Åsberg, A. Langborg Weinmann, T. Leek, R.J. Lewis, M. Klarqvist, M. Leśko, K. Kaczmarski, J. Samuelsson, T. Fornstedt, *The importance of ion-pairing in peptide purification by reversed-phase liquid chromatography*, Journal of Chromatography A, 1496 (2017) 80-91. https://www.sciencedirect.com/science/article/pii/S002196731730420X.
[130] L. Liang, Y. Pan, L. Bin, Y. Liu, W. Huang, R. Li, K.P. Lai, *Immunotoxicity mechanisms of perfluorinated compounds PFOA and PFOS*, Chemosphere, 291 (2022) 132892. https://www.sciencedirect.com/science/article/pii/S0045653521033646.
[131] B. Cara, T. Lies, G. Thimo, L. Robin, B. Lieven, *Bioaccumulation and trophic transfer of perfluorinated alkyl substances (PFAS) in marine biota from the Belgian North Sea: Distribution and human health risk implications*, Environmental Pollution, 311 (2022) 119907. https://www.sciencedirect.com/science/article/pii/S0269749122011216.
[132] M.J. Donohue, R.T. Filla, D.J. Steyer, W.J. Eaton, M.G. Roper, *Rapid liquid chromatography-mass spectrometry quantitation of glucose-regulating hormones from human islets of Langerhans*, Journal of Chromatography A, 1637 (2021) 461805. https://www.sciencedirect.com/science/article/pii/S0021967320310797.
[133] E.E. Chambers, C. Legido-Quigley, N. Smith, K.J. Fountain, *Development of a fast method for direct analysis of intact synthetic insulins in human plasma: the large peptide challenge*, Bioanalysis, 5 (2013) 65-81. https://www.future-science.com/doi/abs/10.4155/bio.12.290.

[134] M. Goebel-Stengel, A. Stengel, Y. Taché, J.R. Reeve, *The importance of using the optimal plasticware and glassware in studies involving peptides*, Analytical Biochemistry, 414 (2011) 38-46. https://www.sciencedirect.com/science/article/pii/S0003269711000960.
[135] S. Nie, R. O'Brien Johnson, Y. Livson, T. Greer, X. Zheng, N. Li, *Maximizing hydrophobic peptide recovery in proteomics and antibody development using a mass spectrometry compatible surfactant*, Analytical Biochemistry, 658 (2022) 114924. https://www.sciencedirect.com/science/article/pii/S0003269722003840.
[136] P. Judák, J. Grainger, C. Goebel, P. Van Eenoo, K. Deventer, *DMSO assisted electrospray ionization for the detection of small peptide hormones in urine by dilute-and-shoot-liquid-chromatography-high resolution mass spectrometry*, Journal of the American Society for Mass Spectrometry, 28 (2017) 1657-1665. https://doi.org/10.1007/s13361-017-1670-7.
[137] P.M. van Midwoud, L. Rieux, R. Bischoff, E. Verpoorte, H.A.G. Niederländer, *Improvement of recovery and repeatability in liquid chromatography−mass spectrometry analysis of peptides*, Journal of Proteome Research, 6 (2007) 781-791. https://doi.org/10.1021/pr0604099.
[138] J.G. Meyer, E. A. Komives, *Charge state coalescence during electrospray ionization improves peptide identification by tandem mass spectrometry*, Journal of the American Society for Mass Spectrometry, 23 (2012) 1390-1399. https://doi.org/10.1007/s13361-012-0404-0.
[139] S. Banerjee, S. Mazumdar, *Electrospray ionization mass spectrometry: A technique to access the information beyond the molecular weight of the analyte*, International Journal of Analytical Chemistry, 2012 (2012) 282574. https://doi.org/10.1155/2012/282574.
[140] L.C. Chen, *A plug-and-play high-pressure ESI source with an emitter at ground potential and its application to high-temperature capillary LC-MS*, Journal of the American Society for Mass Spectrometry, 31 (2020) 1015-1018. https://doi.org/10.1021/jasms.0c00052.
[141] L.C. Chen, *High-pressure ESI-MS made easy using a plug-and-play ion source and its application to highly conductive aqueous solutions*, Journal of Mass Spectrometry, 56 (2021) e4583. https://analyticalsciencejournals.onlinelibrary.wiley.com/doi/abs/10.1002/jms.4583.
[142] G. Diehl, U. Karst, *On-line electrochemistry–MS and related techniques*, Analytical and Bioanalytical Chemistry, 373 (2002) 390-398. https://link.springer.com/article/10.1007/s00216-002-1281-3.
[143] M.S. Wilm, M. Mann, *Electrospray and Taylor-cone theory, Dole's beam of macromolecules at last?*, International Journal of Mass Spectrometry and Ion Processes, 136 (1994) 167-180. https://www.sciencedirect.com/science/article/pii/0168117694040249.
[144] L. Konermann, E. Ahadi, A.D. Rodriguez, S. Vahidi, *Unraveling the mechanism of electrospray ionization*, Analytical chemistry, 85 (2013) 2-9. https://doi.org/10.1021/ac302789c.
[145] L. Konermann, H. Metwally, Q. Duez, I. Peters, *Charging and supercharging of proteins for mass spectrometry: recent insights into the mechanisms of electrospray ionization*, Analyst, 144 (2019) 6157-6171. http://dx.doi.org/10.1039/C9AN01201J.
[146] A. Nasiri, R. Jahani, S. Mokhtari, H. Yazdanpanah, B. Daraei, M. Faizi, F. Kobarfard, *Overview, consequences, and strategies for overcoming matrix effects in LC-MS analysis: a critical review*, Analyst, 146 (2021) 6049-6063. http://dx.doi.org/10.1039/D1AN01047F.

[147] J. Krmar, L.T. Stojadinović, T. Đurkić, A. Protić, B. Otašević, *Predicting liquid chromatography−electrospray ionization/mass spectrometry signal from the structure of model compounds and experimental factors; case study of aripiprazole and its impurities*, Journal of Pharmaceutical and Biomedical Analysis, 233 (2023) 115422. https://www.sciencedirect.com/science/article/pii/S0731708523001917.
[148] W. Lu, B.D. Bennett, J.D. Rabinowitz, *Analytical strategies for LC–MS-based targeted metabolomics*, Journal of Chromatography B, 871 (2008) 236-242. https://www.sciencedirect.com/science/article/pii/S1570023208002845.
[149] I. Kourtchev, P. Szeto, I. O'Connor, O.A.M. Popoola, W. Maenhaut, J. Wenger, M. Kalberer, *Comparison of heated electrospray ionization and nanoelectrospray ionization sources coupled to ultra-high-resolution mass spectrometry for analysis of highly complex atmospheric aerosol samples*, Analytical chemistry, 92 (2020) 8396-8403. https://doi.org/10.1021/acs.analchem.0c00971.
[150] A. Thomas, M. Thevis, *Analysis of insulin and insulin analogs from dried blood spots by means of liquid chromatography–high resolution mass spectrometry*, Drug Testing and Analysis, 10 (2018) 1761-1768. https://analyticalsciencejournals.onlinelibrary.wiley.com/doi/abs/10.1002/dta.2518.
[151] A. Thomas, R. Yang, S. Petring, L. Bally, M. Thevis, *Simplified quantification of insulin, its synthetic analogs and C-peptide in human plasma by means of LC-HRMS*, Drug Testing and Analysis, 12 (2020) 382-390. https://analyticalsciencejournals.onlinelibrary.wiley.com/doi/abs/10.1002/dta.2765.
[152] P. Judák, G. Coppieters, B. Lapauw, P. Van Eenoo, K. Deventer, *Urinary detection of rapid-acting insulin analogs in healthy humans*, Drug Testing and Analysis, 12 (2020) 1629-1635. https://analyticalsciencejournals.onlinelibrary.wiley.com/doi/abs/10.1002/dta.2817.
[153] A. Thomas, S. Thilmany, A. Hofmann, M. Thevis, *Probing for peptidic drugs (2–10 kDa) in doping control blood samples*, Analytical Science Advances, 3 (2022) 235-243. https://chemistry-europe.onlinelibrary.wiley.com/doi/abs/10.1002/ansa.202200027.
[154] A. Miyachi, M. Kobayashi, E. Mieno, M. Goto, K. Furusawa, T. Inagaki, T. Kitamura, *Accurate analytical method for human plasma glucagon levels using liquid chromatography-high resolution mass spectrometry: comparison with commercially available immunoassays*, Analytical and Bioanalytical Chemistry, 409 (2017) 5911-5918. https://doi.org/10.1007/s00216-017-0534-0.
[155] J. Farré-Segura, N. Fabregat-Cabello, C. Calaprice, L. Nyssen, S. Peeters, C. Le Goff, E. Cavalier, *Development and validation of a fast and reliable method for the quantification of glucagon by liquid chromatography and tandem mass spectrometry*, Clinica Chimica Acta, 512 (2021) 156-165. https://www.sciencedirect.com/science/article/pii/S000989812030526X.
[156] J.W. Howard, R.G. Kay, B. Jones, J. Cegla, T. Tan, S. Bloom, C.S. Creaser, *Development of a UHPLC–MS/MS (SRM) method for the quantitation of endogenous glucagon and dosed GLP-1 from human plasma*, Bioanalysis, 9 (2017) 733-751. https://www.future-science.com/doi/abs/10.4155/bio-2017-0021.
[157] G. Maasz, J. Schmidt, P. Avar, L. Mark, *Automated SPE and nanoLC–MS analysis of somatostatin*, Journal of Liquid Chromatography & Related Technologies, 40 (2017) 400-406. https://doi.org/10.1080/10826076.2017.1315722.
[158] E.O. Ogunkunle, M.J. Donohue, D.J. Steyer, D.I. Adeoye, W.J. Eaton, M.G. Roper, *Small molecules released from islets of Langerhans determined by liquid chromatography - mass spectrometry*, Anal Methods, 14 (2022) 2100-2107. https://pubs.rsc.org/en/content/articlehtml/2022/ay/d2ay00402j.

[159] A.E. Lenhart, R.T. Kennedy, *Monitoring hormone and small molecule secretion dynamics from islets-on-chip*, Analytical and Bioanalytical Chemistry, 415 (2023) 533-544. https://doi.org/10.1007/s00216-022-04460-2.
[160] N. Dolezalova, A. Gruszczyk, K. Barkan, J.A. Gamble, S. Galvin, T. Moreth, K. O'Holleran, K.T. Mahbubani, J.A. Higgins, F.M. Gribble, F. Reimann, J. Surmacki, S. Andrews, J.J. Casey, F. Pampaloni, M.P. Murphy, G. Ladds, N.K.H. Slater, K. Saeb-Parsy, *Accelerating cryoprotectant diffusion kinetics improves cryopreservation of pancreatic islets*, Scientific reports, 11 (2021) 10418. https://doi.org/10.1038/s41598-021-89853-6.
[161] S.G. Galvin, R.G. Kay, R. Foreman, P. Larraufie, C.L. Meek, E. Biggs, P. Ravn, L. Jermutus, F. Reimann, F.M. Gribble, *The human and mouse islet peptidome: Effects of obesity and type 2 diabetes, and assessment of intraislet production of glucagon-like peptide-1*, Journal of Proteome Research, 20 (2021) 4507-4517. https://doi.org/10.1021/acs.jproteome.1c00463.
[162] J.C. Davis, T.C. Alves, A. Helman, J.C. Chen, J.H. Kenty, R.L. Cardone, D.R. Liu, R.G. Kibbey, D.A. Melton, *Glucose response by stem cell-derived β cells in vitro is inhibited by a bottleneck in glycolysis*, Cell Reports, 31 (2020) 107623. https://www.sciencedirect.com/science/article/pii/S2211124720305763.
[163] T. Barsby, T. Otonkoski, *Maturation of beta cells: lessons from in vivo and in vitro models*, Diabetologia, 65 (2022) 917-930. https://doi.org/10.1007/s00125-022-05672-y.
[164] M. Omar-Hmeadi, P.-E. Lund, N.R. Gandasi, A. Tengholm, S. Barg, *Paracrine control of α-cell glucagon exocytosis is compromised in human type-2 diabetes*, Nature communications, 11 (2020) 1896. https://doi.org/10.1038/s41467-020-15717-8.
[165] G.L. Francis, *Albumin and mammalian cell culture: implications for biotechnology applications*, Cytotechnology, 62 (2010) 1-16. https://doi.org/10.1007/s10616-010-9263-3.
[166] MCDB131-fomulation, (2023). https://www.thermofisher.com/no/en/home/technical-resources/media-formulation.85.html.
[167] S. Adhikari, X. Yang, Y. Xia, *Acetone/isopropanol photoinitiating system enables tunable disulfide reduction and disulfide mapping via tandem mass spectrometry*, Analytical chemistry, 90 (2018) 13036-13043. https://doi.org/10.1021/acs.analchem.8b04019.
[168] S. Adhikari, Y. Xia, S.A. McLuckey, *Top-down analysis of disulfide-linked proteins using photoinduced radical reactions and ET-DDC*, International journal of mass spectrometry, 444 (2019) 116173. https://doi.org/10.1016/j.ijms.2019.06.009.
[169] L. Tang, R.R. Swezey, C.E. Green, J.C. Mirsalis, *Enhancement of sensitivity and quantification quality in the LC–MS/MS measurement of large biomolecules with sum of MRM (SMRM)*, Analytical and Bioanalytical Chemistry, 414 (2022) 1933-1947. https://doi.org/10.1007/s00216-021-03829-z.
[170] P. Judák, P. Van Eenoo, K. Deventer, *Utilizing ELISA-plate based immunopurification and liquid chromatography-tandem mass spectrometry for the urinary detection of short- and long acting human insulin analogues*, Journal of Pharmaceutical and Biomedical Analysis, 153 (2018) 76-81. http://www.sciencedirect.com/science/article/pii/S0731708517331990.
[171] M. Mazzarino, M. Senofonte, F. Martinelli, X. de la Torre, F. Botrè, *Detection of recombinant insulins in human urine by liquid chromatography–electrospray ionization tandem mass spectrometry after immunoaffinity purification based on monolithic microcolumns*, Analytical and Bioanalytical Chemistry, 411 (2019) 8153-8162. https://doi.org/10.1007/s00216-019-02203-4.

[172] L. Geiser, S. Eeltink, F. Svec, J.M. Fréchet, *In-line system containing porous polymer monoliths for protein digestion with immobilized pepsin, peptide preconcentration and nano-liquid chromatography separation coupled to electrospray ionization mass spectroscopy*, Journal of Chromatography A, 1188 (2008) 88-96. https://doi.org/10.1016/j.chroma.2008.02.075.
[173] A. Thomas, L. Benzenberg, L. Bally, M. Thevis, *Facilitated qualitative determination of insulin, its synthetic analogs, and C-peptide in human urine by means of LC–HRMS*, Metabolites, 11 (2021) 309. https://www.mdpi.com/2218-1989/11/5/309.
[174] C. Bottinelli, F. Bévalot, N. Cartiser, L. Fanton, J. Guitton, *Detection of insulins in postmortem tissues: an optimized workflow based on immunopurification and LC–MS/HRMS detection*, International Journal of Legal Medicine, 135 (2021) 1813-1822. https://doi.org/10.1007/s00414-021-02598-9.
[175] F. Bohr, S.S.R. Bohr, N.K. Mishra, N.S. González-Foutel, H.D. Pinholt, S. Wu, E.M. Nielsen, M. Zhang, M. Kjaergaard, K.J. Jensen, N.S. Hatzakis, *Enhanced hexamerization of insulin via assembly pathway rerouting revealed by single particle studies*, Communications Biology, 6 (2023) 178. https://doi.org/10.1038/s42003-022-04386-6.
[176] M. Busek, A. Aizenshtadt, T. Koch, A. Frank, L. Delon, M.A. Martinez, A. Golovin, C. Dumas, J. Stokowiec, S. Gruenzner, E. Melum, S. Krauss, *Pump-less, recirculating organ-on-a-chip (rOoC) platform*, Lab on a Chip, (2023). http://dx.doi.org/10.1039/D2LC00919F.
[177] F. Gritti, G. Guiochon, *Comparison between the loading capacities of columns packed with partially and totally porous fine particles: What is the effective surface area available for adsorption?*, Journal of Chromatography A, 1176 (2007) 107-122. https://www.sciencedirect.com/science/article/pii/S0021967307018547.
[178] J.-K. Huang, Y.-W. Hsiao, W.-C. Chen, S.Y. Chang, *Nylon membrane-based electromembrane extraction coupled with matrix-assisted laser desorption/ionization mass spectrometry for the determination of insulin*, Separations, 9 (2022) 286. https://www.mdpi.com/2297-8739/9/10/286.
[179] F.S. Skottvoll, A. Aizenshtadt, F.A. Hansen, M.A. Martinez, J.M. Andersen, I.L. Bogen, J.P. Kutter, S. Pedersen-Bjergaard, E. Lundanes, S. Krauss, S.R. Wilson, *Direct electromembrane extraction-based mass spectrometry: A tool for studying drug metabolism properties of liver organoids*, Analysis & Sensing, (2022) e202100051. https://chemistry-europe.onlinelibrary.wiley.com/doi/abs/10.1002/anse.202100051.
[180] M. Østergaard, N.K. Mishra, K.J. Jensen, *The ABC of insulin: The organic chemistry of a small protein*, Chemistry – A European Journal, 26 (2020) 8341-8357. https://chemistry-europe.onlinelibrary.wiley.com/doi/abs/10.1002/chem.202000337.

I

Received: 15 February 2022 | Revised: 15 March 2022 | Accepted: 19 March 2022

DOI: 10.1002/sscp.202200022

RESEARCH ARTICLE

On-line reduction of insulin disulfide bonds with photoinduced radical reactions, upstream to nano liquid chromatography-mass spectrometry

Christine Olsen[1] | **Elisa Wiborg**[1] | **Elsa Lundanes**[1] | **Shadab Abadpour**[2,3] | **Hanne Scholz**[2,3] | **Steven Ray Wilson**[1,2]

[1]Department of Chemistry, University of Oslo, Blindern, Oslo, Norway

[2]Hybrid Technology Hub-Centre of Excellence, Faculty of Medicine, Institute of Basic Medical Sciences, University of Oslo, Oslo, Norway

[3]Department of Transplant Medicine and Institute for Surgical Research, Oslo University Hospital, Oslo, Norway

Correspondence
Steven Ray Wilson, Department of Chemistry, University of Oslo, P.O. Box 1033, Blindern, NO-0315 Oslo, Norway.
Email: s.r.h.wilson@kjemi.uio.no

A current focus of our research is dedicated to investigating tools that can be used to couple pancreas-on-a-chip systems on-line with mass spectrometry. To enable on-line-cleavage of insulin's disulfide bonds, we coupled an inter-chain cleavage reactor with a nano liquid chromatography-mass spectrometry system. The reactor featured a high intensity 254 nm photochemical mercury quartz lamp radiating upon an ultraviolet transparent tubing where acetone and isopropanol form hydroxyalkyl radicals which cleave insulin disulfide bridges. The cleavage allowed for robust fragmentation mass spectra of insulin using nanospray/Q-Exactive mass spectrometry. A nano liquid chromatography separation column was placed downstream to the reactor. We found that for the nano liquid chromatography format, a silica monolith provided substantially less carry-over and improved chromatographic performance to the investigated particle-packed columns. The photochemical reactor/silica monolithic nano liquid chromatography/nanospray/Q-Exactive mass spectrometry was compatible with cell culture medium, and will be further investigated for on-line coupling with pancreas-on-a-chip systems.

KEYWORDS
Insulin, mass spectrometry, monolithic columns, nano liquid chromatography, sample preparation

1 | INTRODUCTION

A current bioanalytical focus of our joint research is to study and monitor the traits of organoids and organ-on-a-chip platforms [1]. These biomaterials/microphysiological systems, which may be grown from, for example, induced pluripotent stem (iPS) cells or patient cells, are emerging as powerful tools for, for example, drug discovery and development biology, serving as alternatives to animal models

Abbreviations: AGC, automatic gain control; DDMS^2, data dependent tandem mass spectrometry; DFA, difluoroacetic acid; EME, electromembrane extraction; IPA, isopropanol; iPS, induced pluripotent stem; MeOH, methanol; NCE, normalized collision energy; THF, tetrahydrofuran; TMOS, tetramethyl orthosilicate

and conventional cell cultures [2]. Recently, we have studied drug metabolism traits of liver organoids, using 96-well electromembrane extraction (EME) [3] and on-chip EME [4]. In the latter study, we coupled the on-chip format directly with mass spectrometry, allowing a high degree of automation and specificity, leading us to conclude that organoids/chip systems and mass spectrometry is a well-suited pairing. In this project, we shift focus towards pancreatic islets, the site of insulin production. iPS cell-based models and pancreas on a chip models are currently under development [5, 6], and we wished to explore potential tools for on-line MS coupling. Insulin is an endocrine hormone produced in the pancreatic islets, which is responsible for regulation of the blood glucose level in collaboration with glucagon [7]. Monitoring the production and secretion of insulin and other molecules is of great relevance for evaluating the stages of organoid/chip development for, for example, diabetes research [5].

Insulin consists of two peptide chains, A chain and B chain, with 21 and 30 amino acids, respectively. The chains are bound together by two disulfide bridges, and the A chain has in addition one internal disulfide bond. The inter-chain disulfide bonds can present a challenge for achieving an on-line Pancreas-on-a-chip-LC-MS method with secure identification, as information about the amino acid sequence between disulfide bridges are not obtained, "on a level suitable for protein identification by library search with a Sequest-HT engine", due to limited fragmentation in traditional collision cells used in MS methods for protein analysis [8]. For miniaturized LC-format (nano LC, often suited for limited samples), we have here found that reduction of the two inter-chain disulfide bonds enables secure identification of insulins based on de novo sequencing from tandem MS spectra. Therefore, we wished to couple on-line reduction of intact insulin to identifiable β-chains, and here investigate the potential of a photochemical system similar to Adhikari et al. [9, 10], placed for the first time upstream to a nano LC-MS system. An alternative on-line method for reduction of disulfide bridges is the use of electrochemical cells which has been shown successful for immunoglobins [11, 12]. The inter-chain cleavage reactor, a high intensity 254 nm photochemical mercury quartz lamp radiating upon a UV transparent tubing where acetone and isopropanol (IPA) form hydroxyalkyl radicals which cleave disulfide bridges, was placed upstream to a silica-based monolithic separation system with mass spectrometry for detection of insulin.

In this paper, we describe the development of an on-line reduction/nano LC-MS platform for monitoring insulin (including choice of nanoLC column, which was a crucial parameter for reducing carry-over), present findings of detecting insulin in various biological islet matrices, and discuss further steps towards coupling with islets-on-a-chip.

2 | MATERIALS AND METHODS

2.1 | Chemicals

ACN (LC-MS grade), acetone (99%), chloro(dimethyl)octadecylsilane (95%), difluoroacetic acid (DFA, 98%), insulin human (recombinant, ≥ 98%), insulin from bovine pancreas (≥25 USP units/mg), IPA (hypergrade LC-MS), urea (98%), polyethyleneglycol (M_n = 10000 g/mol), sodium hydroxide (NaOH, 99%), tetramethyl orthosilicate (TMOS, ≥ 99%) were all purchased from Sigma-Aldrich. Water (LC-MS grade), methanol (MeOH, LC-MS grade) and tetrahydrofuran (THF) were obtained from VWR Chemicals (Radnor, PA, USA). Para-xylene (>99.0%) was acquired from Fluka (Buchs, Switzerland). Fused silica capillary with 50 μm i.d. × 360 μm o.d. with polymide coating and Polymicro UV Flexible Fused Silica Capillary Tubing with 100 μm i.d. × 360 μm o.d. were obtained from Polymicro Technologies (Phoenix, AZ, USA). For column preparation, type 1 water was acquired from a Milli-Q Integral water purification system equipped with a Q-POD dispenser (0.22-μm filter) from Merck Millipore (Billercia, MA, USA). Nitrogen gas (99.99%) was obtained from Nippon gases (Oslo, Norway). Islet cell medium Corning CMRL 1066 without phenol red, L-glutamine (99-663-CV) was acquired from Corning (Corning, NY, USA), and added 200 mM L-glutamine, 10 mol/L HEPES, 1% Penecilin/Streptovidin and 5% human AB serum. In-house prepared KREBS buffer, a solvent consisting of 20 mmol/L HEPES, 11.5 mmol/L NaCl, 0.5 mmol/L KCl, 2 mmol/L $CaCl_2$, 1 mmol/L $MgCl_2$, 2.4 mmol/L NaHCO, and 0.2% human serum albumin in water. In addition, 1.7 mmol/L glucose was added to the KREBS buffer.

2.2 | Preparation of standards

Aqueous water standards of human and bovine insulin (internal standard) were prepared individually by dissolving 1 mg of insulin powder in 1 mL of 0.05% DFA in water. The standards were further diluted to working solutions consisting of 100 ng/μL human or bovine insulin, divided into 100 μL aliquots, and kept at −20°C until use or for a maximum of three months. From freshly thawed aliquots, aqueous standards diluted to 1–5 ng/μL in 20/80 IPA/water (v/v) was added 1% of acetone prior to injection. Solutions

with islet cell medium were spiked with the same working solutions of insulins, diluted to 1–5 ng/μL in 20/40/40 IPA/Cell medium/0.05% DFA in water (v/v/v), and added 1% of acetone prior to injection.

2.3 | Instrumentation

The UV lamp was incorporated between an Easy nLC 1000 pump and a Q-Exactive Orbitrap MS, both instruments were from Thermo Scientific (Waltham, MA, USA), by coupling the pump output to a 100 μm i.d. × 80 mm UV transparent tubing, which was placed at a distance of 0.5 cm to the 254 nm photochemical mercury quartz lamp from Pen-Ray a part of PLZ Corp (Downers Grove, IL, USA). To prevent direct exposure to high intensity 254 nm UV-light, the reaction set-up was enclosed in a cardboard box. Silica-based monoliths functionalized with C18-groups were used as a 50 μm i.d. × 50 mm trap-column and 50 μm i.d. × 100 mm analytical column. The columns were coupled to a 150 μm id stainless steel T-port using Cheminert C360IZR1 fitting adapters from Valco Instruments (Houston, TX, USA). The analytical column was connected to a 30 μm i.d. stainless steel LC/MS emitter from Thermo Scientific with a polyetheretherketone MicroTight Union Assembly from IDEX Health & Science (Oak Harbor, WA, USA).

2.4 | Preparation of C18 functionalized silica-based monolithic columns

The silica monolithic columns were prepared with an adapted procedure based on Hara et al. [13]. A fused silica capillary was filled with 1 M NaOH and kept at room temperature for 24 h. Subsequently, the capillary was washed with water, 1 M HCl, water, MeOH, and dried with nitrogen gas. The skeleton formation solution was prepared by adding 0.9 g of urea and 1.2 g of PEG to an Erlenmeyer flask before adding 10.0 g of 0.01 M acetic acid filtered with a 0.20 μm nylon filter. The solution was stirred at 1°C until all components were dissolved. Subsequently, 5.7 g of TMOS was added and the solution was stirred for another 40 min at 1°C and 10 min at room temperature. The solution was filtered with a 0.20 μm nylon filter before being filled in a 1 m NaOH-treated capillary using the in-house pressure bombs previously described by Berg et al. [14]. The capillary was sealed with septa before being placed in a water bath at 25°C for 18 h. Afterwards, the capillary was placed in an oven at 30°C running the following heating program: The temperature was increased with 0.1°C/min from 30 to 80°C, kept at 80°C for 15 h and cooled at a rate of 0.2°C/min down to 30°C. After heat treatment, the capillary was washed with MeOH at a flow rate of 0.2 μL/min using a nanoAcquity UPLC pump from Waters (Milford, MA, USA). Subsequently, the capillary, without being sealed, was placed back into an oven running a second heat treatment: The temperature was raised from 30 to 330°C at a rate of 5°C/min, kept at 330°C for 22 h, and cooled at a rate of 5°C/min down to 30°C.

Functionalization of the silica monoliths were done by filling a homogenized solution of 0.600 g chloro(dimethyl)octadecylsilane in 0.257 g of para-xylene in the capillaries. The filled capillary was subsequently placed in an oven at 30°C, and the temperature was increased with 5°C/min up to 110°C, kept at 110°C for 18 h and cooled at a rate of 5°C/min down to 30°C. Finally, the capillary was washed with THF, MeOH, a 1+1 solution of MeOH and water, and finally MeOH for 6 min at 150 bar using the in-house pressure bomb. The finalized silica monolithic columns were stored in MeOH at room temperature until use.

2.5 | Mobile phases and gradient settings for LC

The mobile phase (MP) reservoirs contained 0.05% DFA in water (MP A) and 0.05% DFA in 80/10/10 ACN/IPA/water (v/v/v) (MP B). The sample was loaded with a controlled flow rate at 300 nL/min and with a volume equal to (injection volume + extra column volume + 1 μL), for instance an injection volume of 2 μL, gave a total injection volume of 4.5 μL. A 300 nL/min gradient was started at: 3% B for 0–3 min, linearly increased to 34% B between 3 to 13 min, further increased to 95% B at 13–19 min, kept at 95% B for 4 min, quickly decreased to 3% B in 1 min and kept at 3% B for 6 min.

2.6 | Acquisition settings for MS

Comprehensive acquisition was performed in data dependent tandem MS mode (Full MS/DDMS^2). Full MS was run with resolution of 70 000, automatic gain control (AGC) target at 5e5, maximum injection time of 100 ms and a scan range of *m/z* 500–1500. DDMS^2 was run with a resolution of 17 500, AGC target at 5e4, maximum injection time of 60 ms, normalized collision energy (NCE) of 28 and an isolation window of 1.4 *m/z*. Data dependent settings was configured with a minimum AGC target of 8e3 and intensity threshold of 1.3e5. Dynamic exclusion was not active, but species with charges 1, 2, 7, 8, and >8 were excluded. Capillary temperature was set to 250°C.

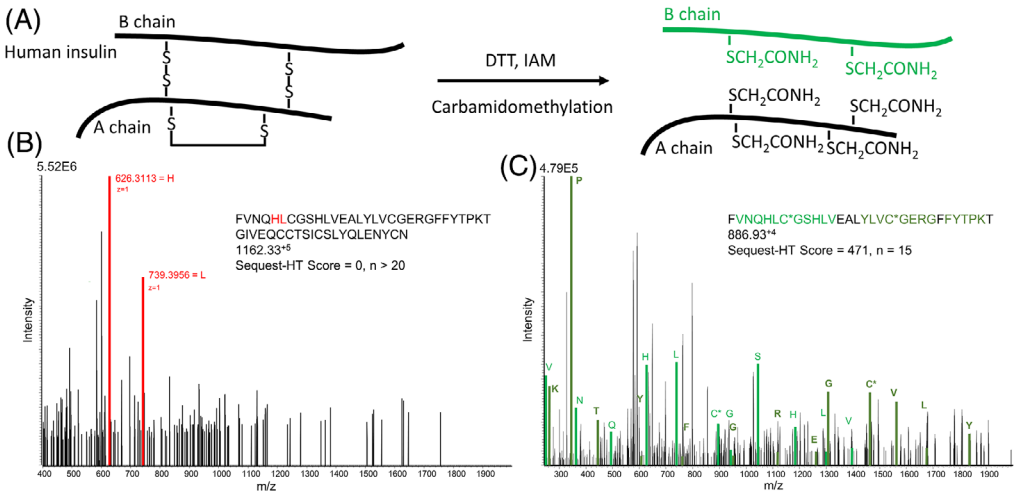

FIGURE 1 Mass fragmentation spectra of (A) intact insulin and (B) in-solution inter-chain cleaved insulin. Fragments of the amino acid sequence identified by Sequest-HT are colored in green, while manually recognized fragments of amino acids are colored in red. Carbamidomethyl modifications on cysteine residues due to inter-chain cleavage are indicated with "*"

3 | RESULTS AND DISCUSSION

3.1 | Improved MS fragmentation of insulin after disulfide bridge reduction

In, for example, anti-doping analysis, intact insulin can be measured with selected reaction monitoring using triple quadrupole (qqq) mass spectrometers [15, 16]. We have here used a nanospray-equipped Q-Exactive mass spectrometer, suited for higher resolution and can be expanded for subsequent untargeted peptidomics analysis. Initially, we examined if intact insulin (i.e. no inter-chain cleavage steps, Figure 1A) could be identified with Sequest-HT database searches by way of robust fragmentation spectra using our nanospray interface/Q-Exactive mass spectrometer. Mass fragmentation spectra acquired by LC-MS of intact insulin did not lead to unsupervised identifications (Sequest-HT score = 0, $n > 20$ at 20–44 NCE) due to a narrow coverage of the amino acid sequence (Figure 1B). Only fragments of two consecutive amino acids (m/z 626.3$^+$ = FVNQH and m/z 739.4$^+$ = FVNQHL) were frequently present with unstable intensities, insufficient for unsupervised and unambiguous identification. Neither of these fragments are utilized in earlier methods [16–18]. From LC-MS determination of in-solution inter-chain cleaved insulin, the B chain of insulin was without exception successfully identified (Sequest-HT score = 471, $n = 15$) in the obtained mass fragmentation spectra (Figure 1C).

Hence, to obtain robust fragmentation mass spectra of insulin using nanospray/Q-Exactive MS towards islet analysis, inter-chain cleavage was further explored.

3.2 | Silica-based monolithic columns reduce carry-over compared to traditional particle packed columns

In addition to challenges with MS fragmentation, using our nanospray/Q-Exactive MS setup, intact insulin displayed non-defined adsorption ("stickiness") on particle packed nano LC columns at room temperature, which caused tailing (asymmetry factor of 5, $n = 3$), variable peak area and extreme levels of carry-over (>90%, Figure 2A). Having previously experienced that intact myoglobin caused carry-over on C18 particle packed nano LC columns, while not on an organic monolith [19], we tested both organic poly(vinyl azlactone-co-ethylene dimethacrylate) monoliths and silica-based monoliths as alternative columns. An optimized system utilizing the C18 silica-based monolithic columns as both trap and analytical columns offered a significantly improved peak shape (asymmetry factor of 2, n = 3) and significantly reduced carry-over (<3%) of insulin compared to particle-packed columns (Figure 2B). The procedure utilized in preparation of silica-based monoliths produced monoliths with varying through-pores in a range from 1 to 1.7 μm. Silica monoliths with larger through-pores (estimated size of 1.6 μm) were utilized as trap columns, while monoliths with smaller through-pores (estimated size of 1 μm) were utilized as analytical columns (Figure 2C). Concerning variation on the optimized system, the retention times (t_R) were stable with less than 0.5% relative standard deviation (RSD, $n = 3$) and the peak area (without internal standard correction) had an RSD of 24% ($n = 3$); further investigations related to

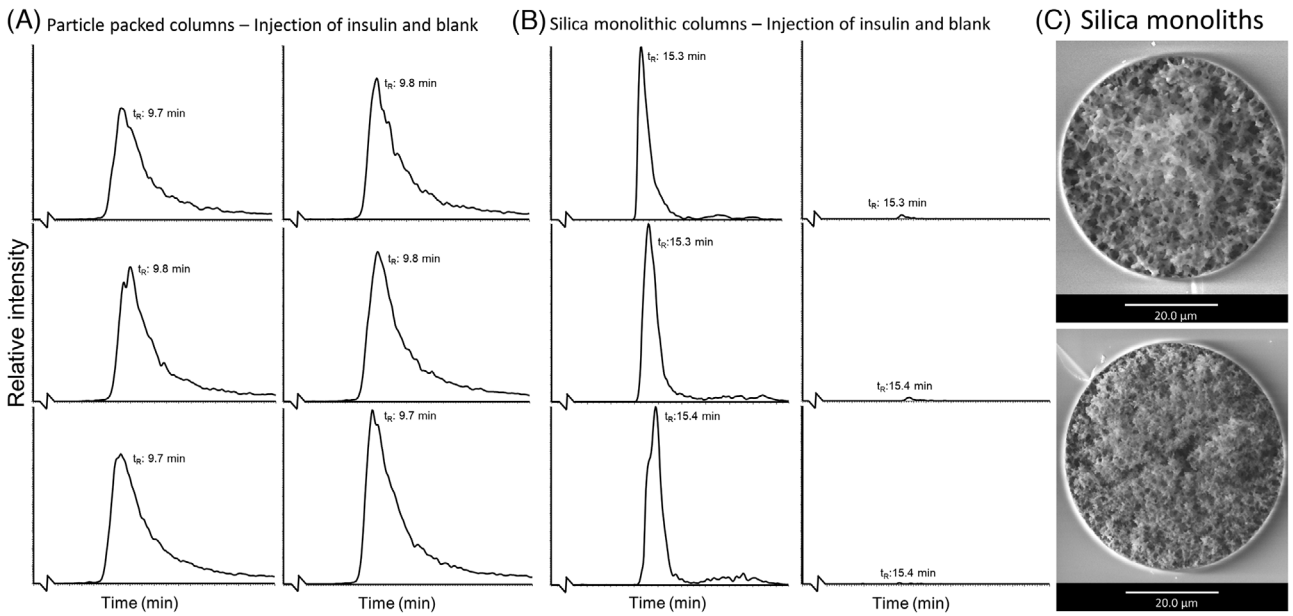

FIGURE 2 Extracted ion chromatogram of *m/z* 1162.3 from three injections of intact insulin and following blanks on the LC-MS set-up with the following columns: (A) 75 µm × 2 cm Acclaim PepMap 100 (C18, 3 µm, 100 Å) trap column and 50 µm × 5 cm Accucore (C18, 2.6 µm, 80 Å) analytical column, (B) 50 µm i.d. silica-based C18 monolithic trap column and analytical column. (C) Micrographs of the cross-sections of the silica monoliths captured with a Quanta 200 FEG-E scanning electron microscope from FEI Company (Hillsboro, OR, USA) by applying a large field detector (LFD) at 12.5 kV, 12 mm working distance and a spot size of 4.0 in low vacuum

RSD improvement using internal standards are described below.

Hence, to secure improved chromatographic performance, a silica-based monolithic separation system was employed instead of particle-packed columns.

3.3 | On-line cleavage of inter-chains between A and B chain in insulin by photoinduced radical reactions

To achieve a robust method for monitoring of insulin, we found that inter-chain cleavage led to unsupervised identification based on mass fragmentation spectra. However, in-solution carbamidomethylation (as performed above) is not readily compatible with on-line analysis (e.g., islets-on-a-chip coupled to nanoLC-MS, a future step of our work). Hence, implementation of inter-chain cleavage on-line the nanoLC-MS platform was adapted from Adhikari et al. [9], which utilized a 50/50 IPA/water (v/v) + 1% acetone solvent system to achieve inter-chain cleavage of insulin (Figure 3A).

The most common separation principle utilized for peptide separations is RP-LC [20], where organic solvents are strong eluates. To achieve compatibility between RP-LC and inter-chain cleavage with IPA/acetone solvent system, the amount of organic solvents needed to be reduced prior to the chromatographic system to avoid plug elution. Kuo et al. resolved the compatibility issue by adding acetone and IPA in the MPs, when they coupled an on-line UV reactor in front of a conventional LC-MS set-up [21].

Initially, to enable analysis of insulin standards in 50/50 IPA/water (v/v) + 1% acetone, we coupled a make-up pump, running 3 µL/min of MP A, in a T-port coupled to the outlet of the UV reactor, which consisted of a UV transparent tubing and a mercury UV lamp from a standard LC-detector. This initial system suffered from variations in retention time (back-to-back injection had over 1 min shift in t_R), variation in trapping of insulin (unstable peak area and breakthrough), and unstable signal of fragments of consecutive amino acids in the obtained mass fragmentation spectra of the B chain (Sequest-HT score of 16, $n = 6$). The UV lamp also presented different technical challenges due to long warm-up period (>24 h) and elevated temperatures (> 40°C). Subsequently, to achieve a more robust method concerning trapping and on-line inter-chain cleavage of insulin, the amount of IPA in the standard solutions needed to be reduced prior to injection and a higher intensity 254 nm mercury quartz lamp (stable at 25°C) was used.

The effect of IPA amount was examined in a simplified technical set-up, included the optimized silica-based monolithic separation system, with 5 ng/µL insulin standards (Figure 3B). Standards with > 25% IPA was not successfully trapped, while standards containing 10% IPA resulted in small, unstable peaks of intact insulin (peak area in order 10^6, RSD of 39%, $n = 3$), and no successfully

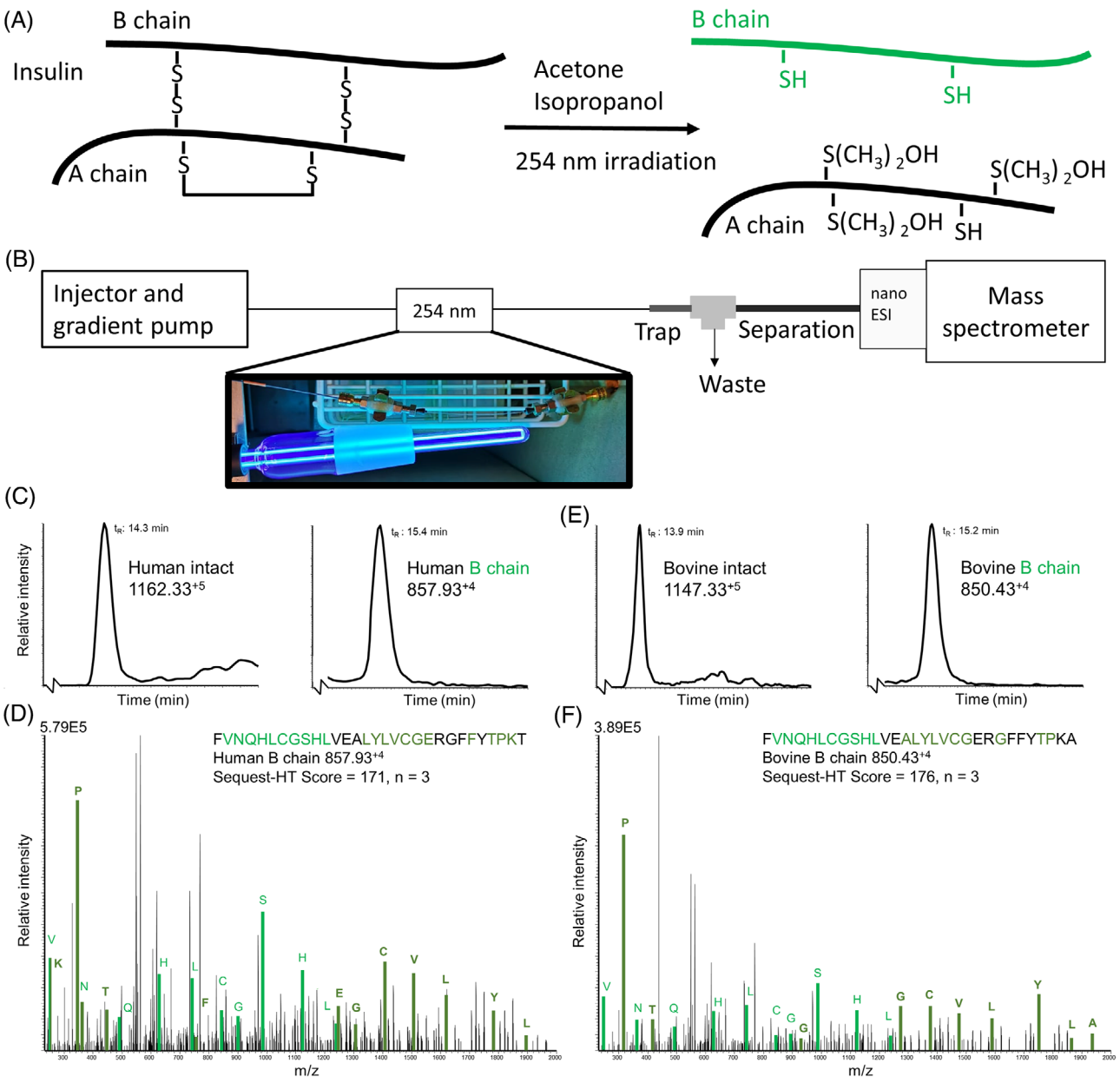

FIGURE 3 (A) Reduction of inter-chains in insulins by photoinduced radical reactions using acetone and isopropanol irradiated at 254 nm, can result in B chain with zero, one or two isopropanol (IPA) modification = $(CH_3)_2OH$. (B) Online set up with inter-chain cleavage upstream a nanoLC-MS. (C) Extracted ion chromatogram of human insulin with intact inter-chains *m/z* 1162.3 and reduced inter-chains *m/z* 857.9. (D) Mass fragmentation spectra of B chain from human insulin. (E) Extracted ion chromatogram of bovine insulin with intact inter-chains *m/z* 1147.3 and reduced inter-chains *m/z* 850.4 (F) Mass fragmentation spectra of B chain from bovine insulin

cleavage of the inter-chains to obtain a detectable signal of the B chain. Standards analyzed with 15 and 20% IPA was successfully trapped on the trap-column and the peak area (order of 10^8) of reduced B chain *m/z* 857.93 (without internal standard correction) had an RSD of 21% ($n = 3$) with 15% IPA, and RSD of 5.5% ($n = 3$) with 20% IPA (Figure 3C). The UV reactor successfully cleaved the inter-chains of insulin, and we obtained robust mass fragmentation spectra with Sequest-HT score of 171 for human insulin ($n = 3$, Figure 3D).

Hence, IPA-assisted radical inter-chain cleavage and online trapping RP-nano LC was compatible.

3.4 | Internal standard considerations

Insulin from bovine has two different amino acids in A chain and a different C-term amino acid in B chain (A instead of T) compared to human insulin, and was hence considered an appropriate internal standard. For 5 ng/μL

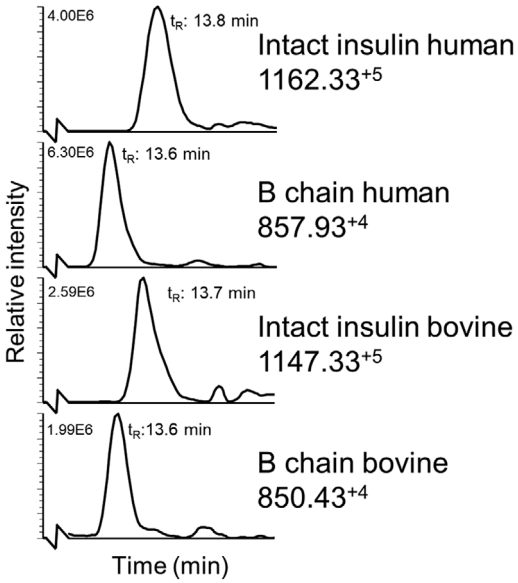

FIGURE 4 Extracted ion chromatogram of: human insulin with intact inter-chains *m/z* 1162.3, and human insulin with reduced inter-chains *m/z* 857.9, bovine insulin with intact inter-chains *m/z* 1147.3, and bovine insulin with reduced inter-chains *m/z* 850.4

standards of bovine insulin with 20% IPA added 1% acetone, the B chain *m/z* 850.43 was successfully detected with a peak area in order of 10^8 with an RSD of 5% ($n = 3$, Figure 3E). The inter-chain cleavage reactor lead to robust mass fragmentation spectra with Sequest-HT score of 176 for bovine insulin ($n = 3$, Figure 3F).

3.5 | Online inter-chain cleavage – nanoLC-MS is compatible with relevant biological islet matrices

The online inter-chain cleavage reactor needs to be compatible with relevant matrices such as KREBS buffer (a high salt content buffer often used in glucose-stimulated insulin secretion models) and islet cell medium. In KREBS buffer, the set-up suffered from clogging and consecutive injections proved to be a challenge, B chain of human and bovine insulin was detected in injection with ≥10 ng/μL (results not shown).

In cell medium, the B chain of human and bovine insulin was successfully detected for injections of ≥ 1 ng/μL bovine and human insulin. The obtained fragmentation spectra showed fragments of 5–6 consecutive amino acids, which gave a Sequest-HT score between 10 and 50. Concerning the chromatography (Figure 4), analyzing 2 μL of a standard solution containing 2.5 ng/μL of human and 2.5 ng/μL of bovine insulin gave peak areas in the order of 10ˆ8 of both human B chain *m/z* 857.93 with RSD of 20% ($n = 6$) and bovine B chain *m/z* 850.43 with RSD of 12% ($n = 6$). The ratio of human B chain and bovine B chain was between 3.1 and 4.1 with an average of 3.5 (RSD = 11%, $n = 6$).

Hence, IPA-assisted radical inter-chain cleavage and RP-nano LC remained compatible for insulins in cell medium, and bovine insulin appears to be a suitable choice as an internal standard.

4 | CONCLUDING REMARKS

We have shown that on-line inter-chain cleavage is compatible with nano LC-MS, here demonstrated with insulin. This coupling can be highly useful for on-line sample preparation, which is encouraging for, for example, further developments of a pancreas-on-a-chip systems. We observe that carry-over effects in nano LC format can be highly dependent on the analyte and column chemistry, seeing that monolithic columns can have advantages in this particular case. In next steps, we explore various column dimensions, including capillary/microbore format, for insulin analysis towards on-line action.

ACKNOWLEDGMENTS

Financial support was obtained from the Research Council of Norway through its Centres of Excellence funding scheme, project number 262613. S.R.W. is a member of the National Network of Advanced Proteomics Infrastructure (NAPI), which is funded by the Research Council of Norway INFRASTRUKTUR-program (project number: 295910).

CONFLICT OF INTEREST

The authors have declared no conflict of interest.

DATA AVAILABILITY STATEMENT

Data available (e.g., MS raw files and Excel calculations) on request from the authors.

REFERENCES

1. Lin A, Sved Skottvoll F, Rayner S, Pedersen-Bjergaard S, Sullivan G, Krauss S, Ray Wilson S, Harrison S. 3D cell culture models and organ-on-a-chip: meet separation science and mass spectrometry. Electrophoresis 2020;41:56–64.
2. Sakalem ME, De Sibio MT, Costa FAdS, de Oliveira M. Historical evolution of spheroids and organoids, and possibilities of use in life sciences and medicine. Biotechnol J. 2021;16:2000463.
3. Skottvoll FS, Hansen FA, Harrison S, Boger IS, Mrsa A, Restan MS, Stein M, Lundanes E, Pedersen-Bjergaard S, Aizenshtadt A, Krauss S, Sullivan G, Bogen IL, Wilson SR. Electromembrane extraction and mass spectrometry for liver organoid drug metabolism studies. Anal Chem. 2021;93:3576–85.
4. Skottvoll FS, Aizenshtadt A, Hansen FA, Martinez MA, Andersen JM, Bogen IL, Kutter JP, Pedersen-Bjergaard S,

Lundanes E, Krauss S, Wilson SR. Direct electromembrane extraction-based Mass spectrometry: A tool for studying drug metabolism properties of liver organoids. Anal Sens. 2022;e202100051.
5. Abadpour S, Aizenshtadt A, Olsen PA, Shoji K, Wilson SR, Krauss S, Scholz H. Pancreas-on-a-chip technology for transplantation applications. Curr Diabetes Rep. 2020;20:72.
6. Glieberman AL, Pope BD, Zimmerman JF, Liu Q, Ferrier JP, Kenty JHR, Schrell AM, Mukhitov N, Shores KL, Tepole AB, Melton DA, Roper MG, Parker KK. Synchronized stimulation and continuous insulin sensing in a microfluidic human Islet on a Chip designed for scalable manufacturing. Lab Chip. 2019;19:2993–3010.
7. Xavier GDaS. The cells of the islets of Langerhans. J Clin Med. 2018;7:54.
8. Rush MJP, Riley NM, Westphall MS, Coon JJ. Top-down characterization of proteins with intact disulfide bonds using activated-ion electron transfer dissociation. Anal Chem. 2018;90:8946–53.
9. Adhikari S, Yang X, Xia Y. Acetone/isopropanol photoinitiating system enables tunable disulfide reduction and disulfide mapping via tandem mass spectrometry. Anal Chem. 2018;90:13036–43.
10. Adhikari S, Xia Y, McLuckey SA. Top-down analysis of disulfide-linked proteins using photoinduced radical reactions and ET-DDC. Int J Mass Spectrom. 2019;444:116173.
11. Morgan TE, Jakes C, Brouwer H-J, Millán-Martín S, Chervet J-P, Cook K, Carillo S, Bones J. Inline electrochemical reduction of NISTmAb for middle-up subunit liquid chromatography-mass spectrometry analysis. Analyst 2021;146:6547–55.
12. Vanduijn MM, Brouwer H-J, Sanz de la Torre P, Chervet J-P, Luider TM. Online electrochemical reduction of both inter- and intramolecular disulfide bridges in immunoglobulins. Anal Chem. 2022;94:3120–5.
13. Hara T, Desmet G, Baron GV, Minakuchi H, Eeltink S. Effect of polyethylene glycol on pore structure and separation efficiency of silica-based monolithic capillary columns. J Chromatogr A. 2016;1442:42–52.
14. Berg HS, Seterdal KE, Smetop T, Rozenvalds R, Brandtzaeg OK, Vehus T, Lundanes E, Wilson SR. Self-packed core shell nano liquid chromatography columns and silica-based monolithic trap columns for targeted proteomics. J Chromatogr A. 2017;1498:111–9.
15. Judák P, Van Eenoo P, Deventer K. Utilizing ELISA-plate based immunopurification and liquid chromatography-tandem mass spectrometry for the urinary detection of short- and long acting human insulin analogues. J Pharm Biomed Anal. 2018;153:76–81.
16. Chambers EE, Fountain KJ, Smith N, Ashraf L, Karalliedde J, Cowan D, Legido-Quigley C. Multidimensional LC-MS/MS enables simultaneous quantification of intact human insulin and five recombinant analogs in human plasma. Anal Chem. 2014;86:694–702.
17. Rosting C, Sæ CØ, Gjelstad A, Halvorsen TG. Evaluation of water-soluble DBS for small proteins: A conceptual study using insulin as a model analyte. Bioanalysis 2016;8:1051–65.
18. Judák P, Coppieters G, Lapauw B, Van Eenoo P, Deventer K. Urinary detection of rapid-acting insulin analogs in healthy humans. Drug Test Anal. 2020;12:1629-1635.
19. Olsen C, Skottvoll FS, Brandtzaeg OK, Schnaars C, Rongved P, Lundanes E, Wilson SR. Investigating monoliths (vinyl azlactone-co-ethylene dimethacrylate) as a support for enzymes and drugs, for proteomics and drug-target studies. Front Chem. 2019;7:835.
20. Foreman RE, George AL, Reimann F, Gribble FM, Kay RG. Peptidomics: a review of clinical applications and methodologies. J Proteome Res. 2021;20:3782–97.
21. Kuo C-M, Wei S-Y, Du S-H, Lin J-L, Chu C-H, Chen C-H, Tai J-H, Chen S-H. Comprehensive workflow for mapping disulfide linkages including free thiols and error checking by on-line UV-induced precolumn reduction and spiked control. Anal Chem. 2021;93:1544–52.

How to cite this article: Olsen C, Wiborg E, Lundanes E, Abadpour S, Scholz H, Wilson SR. On-line reduction of insulin disulfide bonds with photoinduced radical reactions, upstream to nano liquid chromatography-mass spectrometry. Sep Sci plus. 2022;5:220–227.
https://doi.org/10.1002/sscp.202200022

II

Journal of Chromatography B 1215 (2023) 123577

Contents lists available at ScienceDirect

Journal of Chromatography B

journal homepage: www.elsevier.com/locate/jchromb

Determination of insulin secretion from stem cell-derived islet organoids with liquid chromatography-tandem mass spectrometry

Christine Olsen [a,b], Chencheng Wang [b,c], Shadab Abadpour [b,c], Elsa Lundanes [a], Audun Skau Hansen [a], Frøydis Sved Skottvoll [d], Hanne Scholz [b,c], Steven Ray Wilson [a,b,*]

[a] Department of Chemistry, University of Oslo, Blindern, Oslo, Norway
[b] Hybrid Technology Hub-Centre of Excellence, Institute of Basic Medical Sciences, Faculty of Medicine, University of Oslo, Oslo, Norway
[c] Department of Transplant Medicine and Institute for Surgical Research, Oslo University Hospital, Oslo, Norway
[d] Department of Smart Sensors and Microsystems, SINTEF Digital, Oslo, Norway

ARTICLE INFO

Keywords:
Stem cell-derived islets
Islet organoids
Insulin secretion
Box-Behnken design
Liquid chromatography-mass spectrometry

ABSTRACT

Organoids are laboratory-grown 3D organ models, mimicking human organs for e.g. drug development and personalized therapy. Islet organoids (typically 100–200 μm), which can be grown from the patients own cells, are emerging as prototypes for transplantation-based therapy of diabetes. Selective methods for quantifying insulin production from islet organoids are needed, but sensitivity and carry-over have been major bottlenecks in previous efforts. We have developed a reverse phase liquid chromatography-tandem mass spectrometry (RPLC-MS/MS) method for studying the insulin secretion of islet organoids. In contrast to our previous attempts using nano-scale LC columns, conventional 2.1 mm inner diameter LC column (combined with triple quadrupole mass spectrometry) was well suited for sensitive and selective measurements of insulin secreted from islet organoids with low microliter-scale samples. Insulin is highly prone to carry-over, so standard tubings and injector parts were replaced with shielded fused silica connectors. As samples were expected to be very limited, an extended Box-Behnken experimental design for the MS settings was conducted to maximize performance. The finale method has excellent sensitivity, accuracy and precision (limit of detection: ≤0.2 pg/μL, relative error: ≤±10%, relative standard deviation: <10%), and was well suited for measuring 20 μL amounts of Krebs buffer containing insulin secreted from islet organoids.

1. Introduction

Hormonal imbalance, i.e. endocrine disorders (ED), is typically treated with lifelong daily hormone replacement therapy (HRT). However, HRT is limited in achieving physiological mimicry, e.g. in type 1 diabetes (T1D) patients, where injections of exogenous insulin do not match the precise control over the blood glucose as that achieved by the insulin-producing beta cells (found in pancreatic islets) in healthy individuals, leading to incidents of hyper- and hypoglycemia [1,2]. An alternative is beta cell replacement either of donor-derived solid pancreas or isolated islets transplantation, but the approach is adversely affected by the scarcity of donors and the use of immunosuppressive medications due to risk of rejection [1,3]. Ex vivo generated islet organoids is largely thought to be one possible solution to an unlimited source and achieve treatment of T1D patients [3–7]. However, protocols for generating organoids (i.e. laboratory-grown 3D organ models) are still under development, and there is a need for analytical tools for studying the traits and dynamics of organoids, including stem cell-derived islet (SC-islet) organoids [8].

Renewable in-vitro-produced SC-islets provide virtually unlimited cell resources for diabetes transplantation-based therapy. A critical feature to characterize SC-islet is their ability to secrete insulin in response to glucose [7,9]. Insulin secretion is typically measured with enzyme-linked immunosorbent assay (ELISA), but ELISA methods have selectivity weaknesses, i.e. inability to distinguish insulin from structural analogs [10].

Our research group focuses on applying liquid chromatography-mass spectrometry (LC-MS) to study the traits of various organoids [11–14], and we here describe the first MS-based method for highly selective monitoring of insulin excreted from islet organoids. Main ingredients of the method were: The use of conventional-sized columns rather than columns in the nano-format, which we previously found were prone to

* Corresponding author at: Department of Chemistry, University of Oslo, Blindern, Oslo, Norway.
E-mail address: s.r.h.wilson@kjemi.uio.no (S.R. Wilson).

https://doi.org/10.1016/j.jchromb.2022.123577
Received 24 October 2022; Received in revised form 5 December 2022; Accepted 13 December 2022
Available online 16 December 2022

carry-over and surprisingly unsatisfactory sensitivity for islet organoids [15]; Exploring tubing and injection hardware for reduced carry-over of insulin, which is highly prone to non-defined adsorption [15,16]; Applying experimental design to maximize mass spectrometric sensitivity for very limited samples. As a proof-of-concept, we present findings concerning the determination of insulin secretion in SC-islets incubated in Krebs buffer with various levels of glucose and KCl, which stimulate insulin secretion [17].

2. Materials and methods

2.1. Chemicals

Acetonitrile (ACN, LC-MS grade), bovine serum albumin (BSA, ≥98%), dimethyl sulfoxide (DMSO, ≥99.7%), formic acid (FA, 98%), insulin from bovine pancreas (HPLC grade), and recombinant insulin human (≥98%) were all purchased from Sigma-Aldrich. Water (LC-MS grade), and methanol (MeOH, LC-MS grade) were obtained from VWR Chemicals (Radnor, PA, USA). Gibco™ basal cell medium MCDB131, GlutaMAX™ supplement (cat. no. 35050061) and minimum essential medium non-essential amino acids (MEM NEAA) stock solution by Gibco™ was acquired from Thermo Fisher Scientific (Waltham, MA, USA). Krebs buffer was prepared in-house and consists of the following chemicals of analytical grade: 10 mM HEPES, 128 mM NaCl, 5 mM KCl, 2.7 mM $CaCl_2$, 1.2 mM $MgSO_4$, 1 mM Na_2HPO_4, 1.2 mM KH_2PO_4, 5 mM $NaHCO_3$, and 0.1% BSA.

2.2. Preparation of islet maturation cell medium

Islet maturation cell medium was prepared in-house by adding 1% Penicillin/Streptavidin (Pen/Strep), 2.5 mM of glucose (final concentration in cell medium being 8 mM of glucose), 2% BSA, 10 μg/mL of heparin, 1 μM of $ZnSO_4$, 1% of GlutaMAX™ stock solution and 1% of MEM NEAA stock solution to basal cell medium MCDB131 stock solution.

2.3. Preparation of human and bovine insulin solutions

Aqueous water solutions of human and bovine insulin (internal standard) were prepared individually by dissolving 1 mg of insulin powder in 1 mL of 0.1% FA in water. All solutions containing proteins were prepared in protein low binding tubes from Sarstedt (Nümbrecht, Germany). The 1 mg/mL stock solutions were further diluted to working solutions consisting of 10 ng/μL human or bovine insulin, divided into 100 μL aliquots, and kept at −20 °C until use or for a maximum of three months. Separate standard solutions of 10 ng/μL of human and bovine insulin in a 1 + 1 mixture of ACN and water were prepared for direct injections on the MS. For assessment of the LC method (method evaluation solutions), the working solution of human insulin was further diluted to 125 pg/μL with water and spiked with 2 ng/μL of bovine insulin solution to give a concentration of 125 pg/μL of bovine insulin.

Working and method evaluation solutions with human and bovine insulin in islet maturation cell medium and Krebs buffer were prepared in the same manner as described for water-based solutions, with the exception being the amount of FA; 1% FA in cell medium and 0.5% FA in Krebs buffer.

2.4. Preparation of calibration standard solutions and quality controls

Calibration standard solutions and quality controls (QC) were prepared by mixing freshly thawed working solutions of human and bovine insulin and diluted to appropriate concentrations. Calibration standard solutions in 1.0% FA cell medium consisted of [7.8, 15.6, 31.25, 62.5, 125.0, and 250.0] pg/μL human insulin with 125.0 pg/μL bovine insulin. Calibration standard solutions in 0.5% FA Krebs buffer consisted of [0.2, 0.5, 1.0, 3.0, 5.0, and 10.0] pg/μL human insulin with 5.0 pg/μL bovine insulin.

2.5. Cell culture and differentiation

SC-islets were generated from human pluripotent cell line H1 (WA01, WiCell, Madison, WI, USA). Undifferentiated H1 cells were cultured in Essential 8™ Medium (Gibco) on tissue culture plates coated with Geltrex™ in a humidified incubator containing 5% CO_2 at 37 °C. Undifferentiated cells were passaged with 0.5 mM EDTA. To initiate differentiation, undifferentiated cells were seeded at 2×10^5 cells/cm^2 in Geltrex-coated cell culture plates. The subsequent stepwise differentiation schedules and media recipes are provided in **SI-Table 1**. On day 7 of stage 6, the differentiated cells were dissociated with TrypLE and seeded at 1×10^6 cells/mL in ultra-low attachment cell culture plates from Corning (Corning, NY, USA). The cells were then maintained and aggregated as spheroids on an orbit-shaker (Thermo Fisher) at 100 RPM for over 7 days until analysis.

2.6. Glucose stimulated insulin secretion in stem cell-derived islets

A total of 30 SC-islets were hand-picked into transwells (CLS3414, Merck, Billercia, MA, USA) and placed in 24-well cell culture plates. The SC-islets were washed three times with 1 mL Krebs buffer and equilibrated in 1 mL Krebs buffer containing 2 mM glucose for 60 min at 37 °C. The SC-islets were then sequentially incubated in 1 mL Krebs buffer containing 2 mM and 20 mM glucose for 60 min each, and up to 900 μL of supernatant was collected. Last, the cells were incubated in 1 mL Krebs buffer containing 20 mM glucose and 30 mM KCl for 30 min, and up to 900 μL of supernatant was collected. Cells were placed in a 37 °C humidified incubator with 5% CO_2 for all incubations. Insulin in the supernatant was quantified with human insulin ELISA kit (Mercodia, Uppsala, Sweden). Prior to insulin determination with the LC-MS/MS method, the collected supernatants were spiked with a total of 5.0 pg/μL of bovine insulin and added 100% FA to a total of 0.5%.

2.7. Liquid chromatography instrumentation

The conventional LC-HESI-MS system was a modified Agilent 1100 series (Santa Clara, CA, USA) employing only shielded fused silica connectors (shielded fused silica nanoViper™ sheathed in polyetheretherketone (PEEK) tubing from Thermo Fisher) in the entire system. Injection was achieved by coupling a 6-port-2-position valve, with a 50 μm inner diameter (id) × 550 mm shielded fused silica loop or a 20 μL shielded fused silica loop, between the output from the pump and in front of the column set-up. A 25 μL or 250 μL glass syringe was used for introduction of solutions and samples onto the loop. Introduction of method evaluation solutions onto the loop was done using a 150 μm id × 750 mm shielded fused silica connector coupled to a 250 μL glass syringe using a 250 μm id union and an injection port, where the solutions were filled into the syringe through the shielded fused silica connector. The column set-up consisted of an Accucore™ phenyl/hexyl guard column (2.1 mm id × 10 mm, 2.6 μm, 80 Å) attached with a Uniquard drop-in holder to the InfinityLab Poroshell EC-C18 separation column (2.1 mm id × 50 mm, 2.7 μm, 120 Å). For experiments with elevated column temperature, a 10 cm Butterfly portfolio heater coupled to a column heater controller, both from Phoenix S&T (Chester, PA, USA) was used.

2.8. Mobile phases and gradient settings for LC

The mobile phase (MP) reservoirs contained 0.1% FA in water added 1% DMSO (MP A) and 0.1% FA in ACN added 1% DMSO (MP B). A 150 μL/min solvent gradient was started at 1% B and linearly increased to 60% B in 8 min, further increased to 80% B at 8–10 min, kept at 80% B for 2 min, quickly decreased to 40% B, and kept at 40% B for 4 min, before being further decreased to 1% B and kept at 1% B for 7 min. The

gradient had a total runtime of 23 min, including column re-equilibration for 7 min at 1% B.

2.9. Mass spectrometry instrumentation

A TSQ Quantiva triple quadrupole (QQQ) MS equipped with an H-ESI-II probe ionization source, both from Thermo Fisher, was used for all of the experiments. A syringe pump (model pump 11 elite) from Harvard Apparatus (Holliston, MA, USA) was used for direct injection on the MS by using a 250 μL glass syringe (Trajan Scientific and Medical, Ringwood, Australia) coupled to a 150 μm id × 750 mm shielded fused silica tubing. Initial experiments, prior to optimization with Box-Behnken, were attained with the MS operated in fullscanQ1 mode with the following recommended default settings at 150 μL/min LC flow rate: The vaporizer temperature was set to 210 °C, and a spray voltage of 3.5 kV. Sheath gas was set at 27 arbitrary units (Arb), while auxiliary gas was set at 9 Arb, and sweep gas was not applied. The ion transfer tube temperature was kept at 325 °C.

2.10. Optimization of peak areas in untargeted acquisition on the MS in fullscanQ1 mode with Box-Behnken experimental design

The H-ESI settings were optimized using a three-factor design with the MS operated in fullscanQ1 mode. A scan range from *m/z* 500–1500 was applied with 0.7 Q1 resolution. Box-Behnken was repeated twice to include six selected parameters related to the ionization source: Sheath gas, vaporizer temperature, and spray voltage were included in the first design, while the second design included sweep gas, auxiliary gas, and ion transfer tube temperature. Settings used for sweep gas, auxiliary gas and ion transfer tube temperature in the first set-up of Box-Behnken were the default settings used in the initial experiments, mentioned in **Section 1.8**. The three-factor designs were considered for the peak area of the most abundant precursor ion related to human insulin. The three-factor designs are described with the minimum and maximum value of each parameter in Table 1. The script written for Box-Behnken is available as an open source code using the code named "btjenesten" version 0.26 and "scikit-learn" version 1.0.2 and version 1.1.1 found at https://pypi.org/project/btjenesten/0.26/. The first BB-design applied "scikit-learn" version 1.0.2, while the second BB-design applied "scikit-learn" version 1.1.1.

2.11. Targeted analysis with MS operated in selected reaction monitoring mode

The transitions, used in selected reaction monitoring (SRM), including collision energies, are listed in Table 2. The collision energies and radio frequency (RF) lens voltage were optimized using the compound optimization provided in Xcalibur. The collision gas (argon) pressure in q2 was 2.5 mTorr, the RF Lens was set at 210 V and the cycle time was set to 1 sec (equal to 167 ms dwell time per transition in this method). The vaporizer temperature was set to 210 °C, and a spray voltage of 3.5 kV was applied to the H-ESI-II probe. Sheath gas was set at 20 Arb (approx. 2.71 L/min), while auxiliary gas was set at 9 Arb (approx. 7.49 L/min), and sweep gas was not applied. The ion transfer tube temperature was kept at 275 °C.

Table 1
Description of parameters, including minimum and maximum value, used in two three-factor Box-Behnken designs for optimization of peak area of human insulin precursor.

Parameter	Minimum value	Maximum value
Sheath gas (Arb)	20	36
Vaporizer temperature (°C)	170	250
Spray voltage (kV)	1.8	3.5
Sweep gas (Arb)	0	10
Auxiliary gas	5	13
Ion transfer tube temperature (°C)	275	375

Table 2
SRM transitions used for human and bovine insulin (internal standard) including quantifier/qualifier status, precursor ion, product ion, and collision energy.

Compound	Identity	Precursor ion (*m/z*)	Product ion (*m/z*)	Collision energy (V)
Human insulin	Quantifier	1162.5	226.1	41
	Qualifiers	1162.5	345.1; 1159.0	42; 22
Bovine insulin	Quantifier	1147.8	226.2	41
(Internal standard)	Qualifiers	1147.8	315.2; 1144.5	42; 20

3. Results and discussion

3.1. Repeatable and stable fragmentation of intact insulin was attained on a QQQ mass spectrometer

Based on ELISA measurements, it was expected that insulin secretion from SC-islets would be in the lower pg/μL range, and that the developed LC-MS/MS method would need a ≤1 pg/μL detection limit. In addition, we aimed for developing a method which was independent of sample preparation, apart from adding internal standard to the samples. Therefore, effort was placed on optimizing the signal of the most abundant precursor of human insulin in the MS to achieve the lowest possible detection limit in biologically relevant matrices for characterization of SC-islet organoids (i.e. cell medium and Krebs buffer). The addition of DMSO as an organic modifier is beneficial for peptides and proteins when applying electrospray ionization [18], suitable for reduction of carry-over in the LC-system [19], and DMSO has successfully been applied in several LC-MS methods for insulin analysis [20–22]. Initial MS/MS settings were established: *m/z* 1162.5 (+5) → *m/z* 226.1, 345.0, 1159.2, 1358.0, see Fig. 1**A**. These repeatable and stable MS/MS transitions, also commonly applied in insulin analysis [20,22], allow for highly selective measurements, distinguishable from structural analogs e.g. insulin from animals, synthetic insulins, and proinsulin. See **SI-1** for more details.

3.2. Non-defined adsorption of intact human insulin in autosampler and on glass syringe eliminated by shielded fused silica tubing

For initial attempts of direct injection of intact insulin in the previous **Section 2.1**, we examined a multitude of tubings (e.g. untreated fused silica capillary, PEEK tubing, fused silica/PEEK capillary from Agilent, and shielded fused silica tubing) to achieve a continuously stable signal of human insulin in the MS. A stable signal of human insulin was only obtained with the shielded fused silica connector, while insulin appeared to be retained on the other types of tubings due to non-defined adsorption (results not shown). The shielded fused silica connecters have been surface-treated by the producers, however the proprietary information about the treatment is inaccessible for the general public. Based on the reduced non-defined adsorption, we replaced all available tubings in the LC-system with the shielded fused silica connectors. However, some tubings (i.e. seat capillary, load capillary and a fused silica/PEEK capillary from Agilent) could not easily be replaced due to different formats not suitable for the fittings on the shielded fused silica connectors. The effect of the remaining unchangeable tubing was obvious when comparing autosampler injection with manual injection using a 6-port-2-position valve with an 1.08 μL shielded fused silica loop: for 125 pg/μL human insulin in an aqueous standard, poor signal was associated with the autosampler (Fig. 2**A**), while a high intensity peak belonging to human insulin at *m/z* 1162.5 was attained with manual injection (Fig. 2**B**). For injection of higher concentrations of

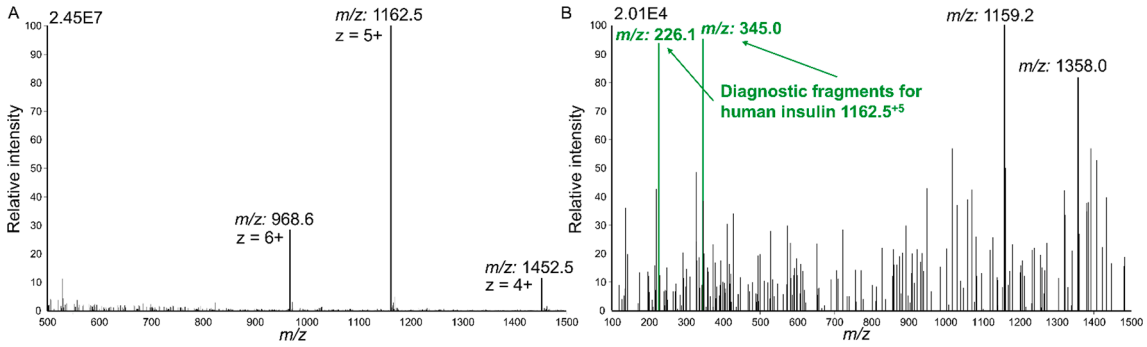

Fig. 1. (**A**) Charge distribution of intact human insulin found in FullscanQ1 mode by continuously flow of a 1 + 1 mixture of acetonitrile and water with 10 ng/μL human insulin, (**B**) product ions fragmented from *m/z* 1162.5, the most abundant precursor of human insulin.

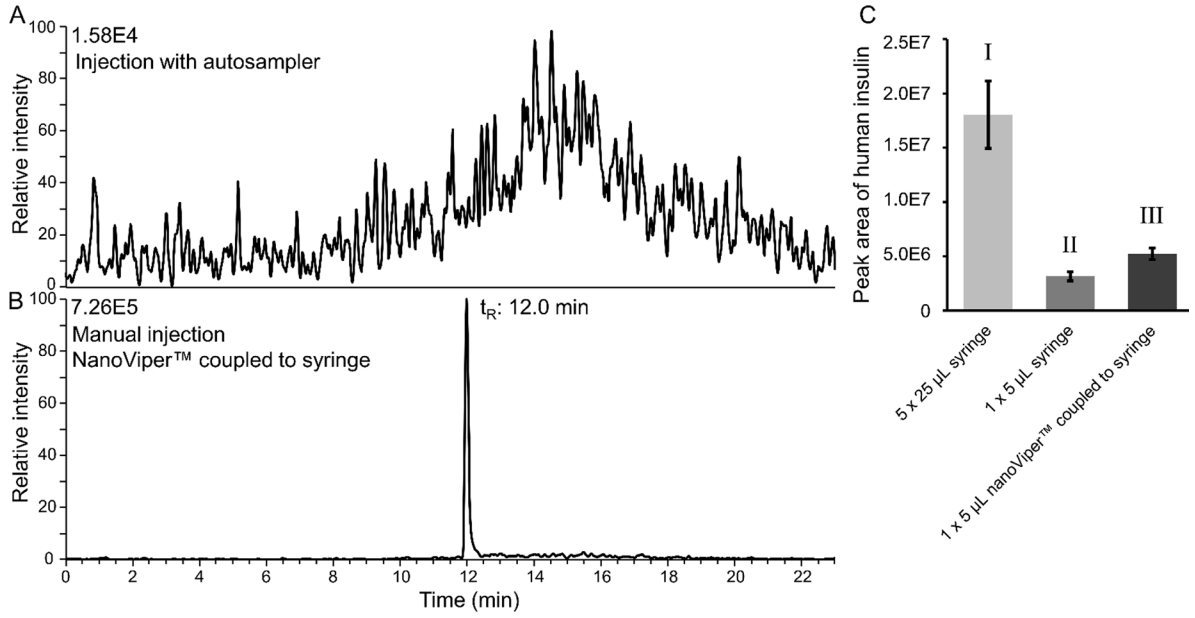

Fig. 2. Extracted ion chromatogram of intact human insulin (*m/z* 1162.0–1163.0). (**A**) 1 μL injection of 125 pg/μL human insulin in 0.1% FA in water using autosampler, and (**B**) 1.08 μL injection of 125 pg/μL human insulin in 0.1% FA in water using a 6-port-2-position valve with 50 μm id × 550 mm shielded fused silica loop, and the solution was filled in the loop with a 25 μL glass syringe coupled to a 150 μm id × 750 mm shielded fused silica connector. Solutions were examined with the MS operated in fullscanQ1 mode. (**C**) Comparison of peak areas of human insulin obtained with manual injection of 125 pg/μL insulin solution. (**I**) Shows that insulin accumulated on the syringe when 125 μL (5 × 25 μL) of solutions was used for wash and filling of the syringe and the loop prior to injection (n = 3), compared to (**II**) when the syringe was filled once with 25 μL and 5 μL applied over the 1.08 μL loop (1 × 5 μL, n = 3). (**III**) A compromise was coupling a 13.2 μL shielded fused silica connector to the syringe, and filling 40 μL (2 × 20 μL) solution through the shielded fused silica tubing connected to the syringe and applying 5 μL over the 1.08 μL loop (1 × 5 μL, n = 3).

insulin on the autosampler, the peak shape was drastically worse with an asymmetry factor of 2.4 (results not shown), while the peak obtained by manual injection had an asymmetry factor of 1.4 (Fig. 2**B**). Similar chromatograms were obtained for bovine insulin (results not shown). In addition, we found that glass parts for e.g. syringes would also contribute to carry-over and should be avoided, visualized in Fig. 2**C** (see **SI-2** for details). Although manual injections were performed here, contemporary autosamplers can be modified accordingly.

3.3. Optimization of precursor peak areas with Box-Behnken led to lower detection limits

The peak area of precursor *m/z* 1162.5 of human insulin was optimized using Box-Behnken (BB) experimental design with a quadratic model on the six selected variables in the H-ESI and MS-inlet settings. The design was split into two BB for three variables at three levels requiring 15 experiments per design, seeing as a six variables BB with three levels (which could be useful for assessing the interactions between all of the selected variables) would require 54 measurements [23]. The manual injection and the runtime of 23 min per samples meant that a design with 54 measurements would have to be run over a minimum of two days and could be exposed to a potential drift in the sensitivity. In the first set-up of a three factor BB-design: Sheath gas (SG, Arb) [20, 28, 36], vaporizer temperature (VT, °C) [170, 210, 250], and spray voltage (SV, kV) [1.8, 2.65, 3.5] was evaluated for the highest peak area of *m/z* 1162.5 in water-based insulin solutions, with a coefficient of determination of 0.83. In the second set-up of a three factor BB design: Sweep gas (SWG, Arb) [0, 5, 10], auxiliary gas (AUX, Arb) [5,9,13], and ion transfer tube temperature (ITT, °C) [275, 325, 375] were examined in insulin solutions prepared in cell medium, with a coefficient of determination of 0.61. Column temperature was kept at ambient, as temperature did not affect peak shape or peak area, see **SI-3** for more details.

The suggested optimal settings found with BB for sheath gas (SG, Arb), vaporizer temperature (VT, °C), and spray voltage (SV, kV) were 36 Arb, 210 °C and 3.5 kV, see Fig. 3**A**. However, as described in **SI-4**,

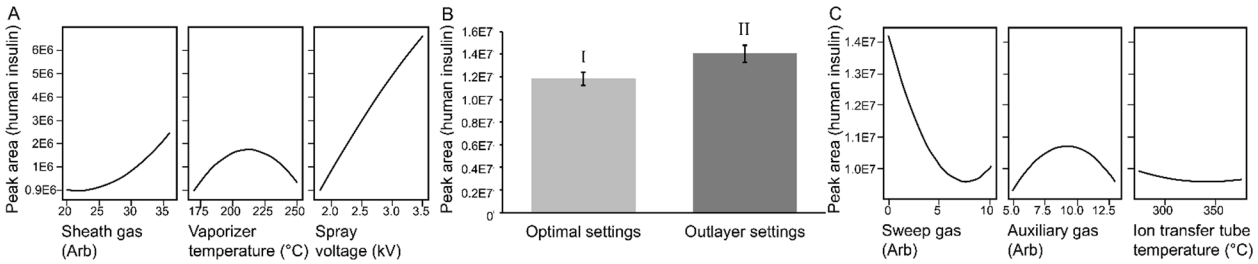

Fig. 3. Optimization of peak area of human insulin *m/z* 1162.5 with Box-Behnken. (**A**) Main effects plot showing effect of sheath gas levels, vaporizer temperature and spray voltage, (**B**) comparison of peak areas obtained with (**I**) optimal settings [SG = 36, VT = 210, SV = 3.5] and (**II**) outlayer settings [SG = 20, VT = 210, SV = 3.5], and (**C**) main effects plot showing effect of sweep gas levels, auxiliary gas levels and ion transfer tube temperature.

another experiment included in the BB-design run at 20 Arb SG, 210 °C VT and 3.5 kV SV, had a peak area of insulin 39% larger than the suggested optimal setting. Therefore, by comparing the peak areas obtained when applying sheath gas levels of 36 Arb (Fig. 3**B-I**) to peak areas obtained with sheath gas level of 20 Arb (Fig. 3**B-II**), an even higher peak area of human insulin was obtained and sheath gas level of 20 Arb was applied moving forward. BB-optimized settings for sweep gas, auxiliary gas, and ion transfer tube temperature were found to be 0 Arb, 9 Arb and 275 °C (See Fig. 3**C**).

Comparing the recommended default settings to the final optimized settings of the method, sheath gas level was reduced from 27 Arb to 20 Arb and ion transfer tube temperature was decreased from 325 °C to 210 °C, the BB-optimization led to a 3.2-fold sensitivity increase. See **SI-4** for a detailed description of the experiment design and evaluation.

3.4. Diagnostic fragment m/z 226 from human and bovine insulin established a calibration curve in cell medium for determining concentrations in quality controls with sufficient accuracy

The linearity, carry-over and the accuracy of the fully optimized SRM method with the following settings; SG = 20, VT = 210, SV = 3.5, SWG = 0, AUX = 9, ITT = 275, and collision gas pressure = 2.5 mTorr, were examined. Three transitions belonging to human insulin: *m/z* 1162.5 → *m/z* 226.1, *m/z* 345.0, or *m/z* 1159.2, and three transitions from bovine insulin: *m/z* 1147.8 → *m/z* 226.2, *m/z* 315.2, or *m/z* 1144.5, were monitored. A calibration curve was established in the range from 7.8 pg/μL to 250 pg/μL human insulin with 125 pg/μL bovine insulin as internal standard in cell medium for each possible combination of SRM transition from human and bovine insulin. Quality control (QC) samples with [10, 20, 50, 80, 100, 150, 200] pg/μL human insulin and 125 pg/μL bovine insulin were analyzed and the concentrations were determined using the established calibration curves. The calibration curves, which achieved the most accurate determination of the insulin concentrations in the QC's, are shown with their respective SRM transitions for human and bovine insulin in Fig. 4**A-C**. Only the QC standard with the lowest amount of human insulin (10 pg/μL) could not be determined with an accuracy<10% relative error. The combination of the transition *m/z* 1162.5 → *m/z* 226.1 for human insulin, and *m/z* 1147.8 → *m/z* 226.2 for bovine insulin (Fig. 4**A**) provided on average an absolute relative error of 3% for the other six QC standards, and were therefore selected as the quantifiers. The four other remaining transitions *m/z* 1162.5 → *m/z* 345.0 or *m/z* 1159.2, and *m/z* 1147.8 → *m/z* 315.2, or *m/z* 1144.5, were used as qualifiers. Although an internal standard was employed in subsequent studies, it can be noted that also without the use of an IS, the precision and accuracy was excellent (see **SI-7**).

The carry-over was examined after the injection of the calibration standard with the highest concentration of human insulin (250 pg/μL). For all of the six transitions applied as quantifier or qualifier, carry-over in the following blank was ≤ 3%.

3.5. Detection limit below 1 pg/μL was reached in Krebs buffer by increasing the injection volume

To reach the target detection limit below 1 pg/μL, an increase in the injection volume was examined. The increase in injection volume was easily achieved by exchanging the 1.08 μL loop with a 20 μL loop and using only a syringe for injection (see **SI-5** for discussion concerning use of only a syringe for injection). The increase in injection volume caused a collapse of the chromatography for standards in cell medium. With 1.08 μL injection of a solution consisting of 125 pg/μL human and 125 pg/μL bovine insulin, insulins were eluted at 11.2 min and were separated from the other compounds in the cell medium, which were eluted after 11.6 min, see Fig. 5**A**. When the injection volume was increased to 20 μL of a solution consisting of 6.25 pg/μL human and 6.25 pg/μL bovine insulin, no peaks corresponding to human or bovine insulin was distinguishable from the other compounds present in cell medium, as

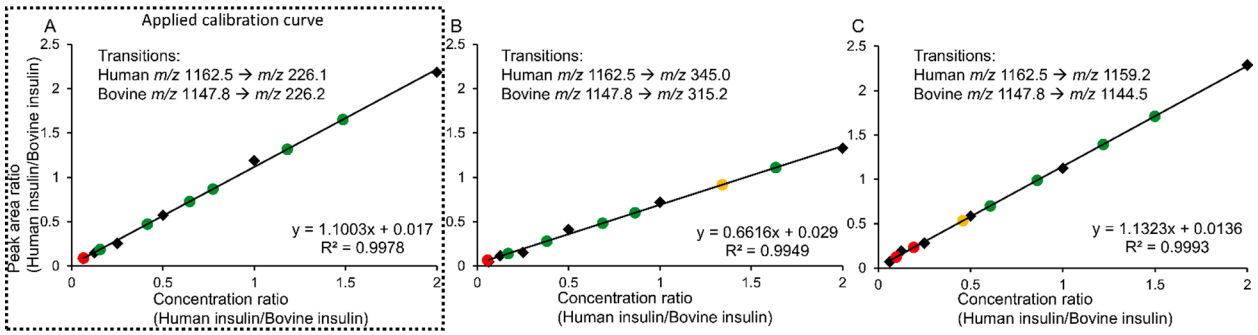

Fig. 4. Calibration curve in 1.0% FA cell medium, obtained by SRM, from 7.8 pg/μL to 250 pg/μL human insulin with 125 pg/μL bovine insulin (IS) (points marked in black were used for calibration). Seven quality control standards at [10, 20, 50, 80, 100, 150, 200] pg/μL human insulin and 125 pg/μL bovine insulin are color-coded based on relative error (e_r). green = $e_r \leq 10\%$), yellow = $10\% < e_r < 15\%$, and red = $e_r \geq 15\%$. SRM calibration curves were established using the following transitions. (**A**) *m/z* 1162.5 → *m/z* 226.1 for human insulin, and *m/z* 1147.8 → *m/z* 226.2 for bovine insulin, (**B**) *m/z* 1162.5 → *m/z* 345.0 and *m/z* 1147.8 → *m/z* 315.2, and (**C**) *m/z* 1162.5 → *m/z* 1159.2 and *m/z* 1147.8 → *m/z* 1144.5.

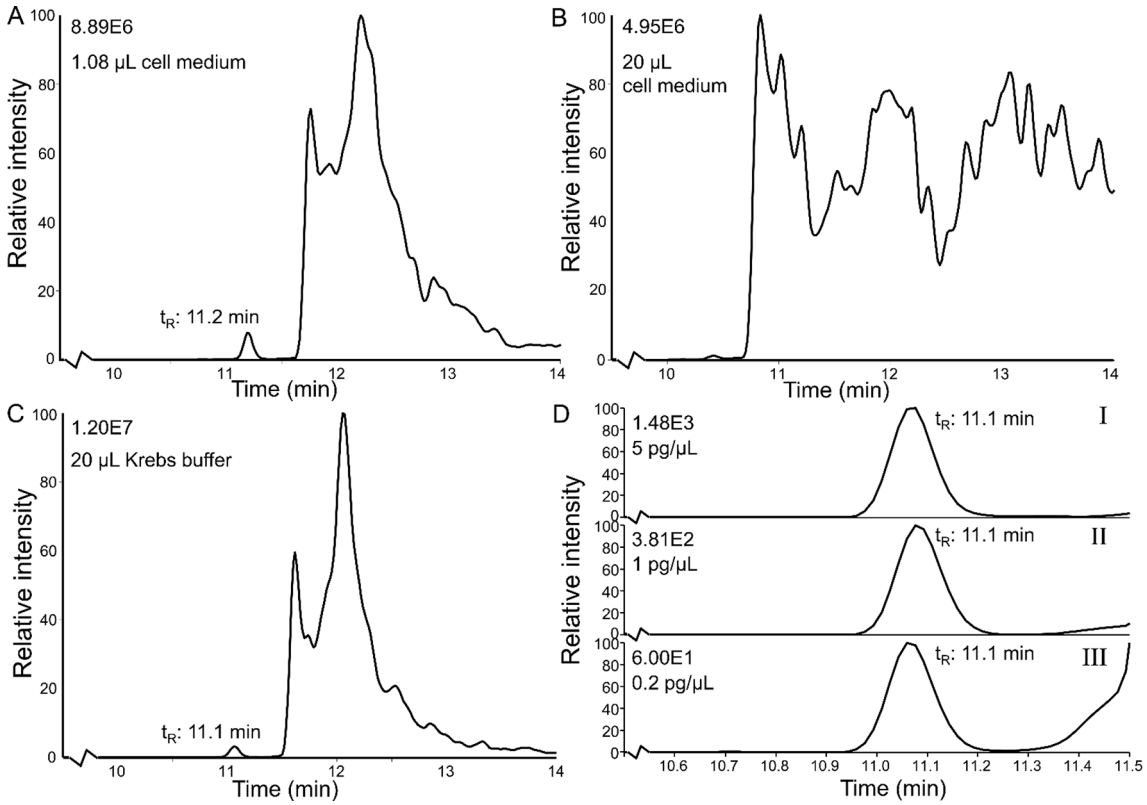

Fig. 5. Effect of injection volume and sample matrix on the separation was examined in FullscanQ1 mode. Extracted ion chromatogram (*m/z* 1162–1163) showing. (**A**) Human insulin detected at 11.2 min after 1.08 µL injection of 125 pg/µL human insulin in 1% FA in cell medium, (**B**) human insulin not detected in 20 µL injection of 6.25 pg/µL human insulin in 1% FA in cell medium, and (**C**) human insulin detected at 11.1 min after 20 µL injection of 5 pg/µL human insulin in 0.5% FA in Krebs buffer. (**D**) Peaks obtained in SRM mode of human insulin in a dilution series in 0.5% Krebs buffer with the quantifier transition *m/z* 1162.5 → *m/z* 226.1. (**I**) 5 pg/µL human insulin, (**II**) 1 pg/µL human insulin, and (**III**) 0.2 pg/µL human insulin.

shown in Fig. 5**B**.

Besides cell medium, Krebs buffer is another biologically relevant matrix for assessing SC-islets. When 20 µL of Krebs buffer with 5 pg/µL human and 5 pg/µL bovine insulin was injected, human and bovine insulin were eluted at 11.1 min and were separated from other compounds in the buffer and residue of cell medium on the column, shown in Fig. 5**C**. The detection limit was successfully lowered, shown here by detection of human insulin in a dilution series in Krebs buffer at the following concentrations: 5 pg/µL (Fig. 5**D-I**), 1 pg/µL (Fig. 5**D-II**), and 0.2 pg/µL (Fig. 5**D-III**), with the MS operated in SRM mode. Results shown in Fig. 5**D** used the quantifier SRM transition (*m/z* 1162.5 → *m/z* 226.1), but detection was also successful with the other selected qualifier transitions (*m/z* 1162.5 → *m/z* 345.0, or *m/z* 1159.2).

The large peak present in the chromatograms in Fig. 5A-C were assumed to contain BSA based on the mass spectrum of the peak, as the pattern of the peak was visually confirmed to match a mass spectrum of BSA obtained by direct injection on the MS (see **SI-6** for details). The particles of the columns applied in this study have a pore size of 80 Å in the guard cartridge and 120 Å in the separation column. To have sufficient column loading ability and avoid exclusion of the peptides from the pores in the particles, the average pore size should be approximately three times the size of the peptide [24]. The hydrodynamic dimension of insulin is 32 Å, while BSA is much larger at 72 Å, meaning a much larger area of the particles are available for insulin compared to BSA and the selected particles are appropriate for peptides with similar hydrodynamic dimensions as insulin. The cell medium used in this study contains 2% BSA (20 ng/µL), while the Krebs buffer contains 0.1% BSA (1 ng/µL). The effect of reduced loading capabilities of BSA on the columns is obvious in the lack of separation in the injection of 20 µL of cell medium (400 ng of BSA injected, Fig. 5B), as the peak from BSA is distorted showing effects of a large degree of band broadening [25]. While the peak from BSA in the injection of 20 µL of Krebs buffer (20 ng of BSA, Fig. 5C) does not show such effects of band broadening due to 20 times lower amount of BSA loaded on the column.

The 80 Å and 120 Å pore sizes of the particles in the guard column and separation column are too small to be accessible to BSA without a size exclusion effect, giving a slow pore diffusion which consequently results in a very broad peak shape for BSA [24,25]. It is also worth noting that following injections in cell medium and Krebs buffer, the residue of BSA was impossible to fully remove even after extensive washing of the columns. The continuous carry-over of BSA and loss of separation of insulins from BSA indicates that the system is not suitable for large injection of highly concentrated BSA solutions. An increasing of the pore sizes to over 220 Å, which is a more suitable pore size for BSA [24], may give a narrower peak shape of BSA and improve the separation of insulin, BSA and other potential compounds co-eluting with BSA. The combination of a short analysis column (50 mm) and a relatively steep gradient may not be suitable when looking to separate bovine and human insulin, which only has three different amino acids when comparing their respective amino acid sequences [20]. However, as we apply bovine insulin in this method as the internal standard, it can be viewed as beneficial that the two insulins co-elute.

Thus by increasing the injection volume to 20 µL, a detection limit of $\leq$ 0.2 pg/µL (34.4 pM) was achieved in standards prepared in Krebs buffer with 0.5% FA. For standards prepared in cell medium with 1.0% FA, the increased injection volume compromised the separation. Cell medium and Krebs buffer are common matrices used in characterization of human islets and islets organoids, and we found that with our LC-MS method the highest sensitivity for insulin analysis were achieved in Krebs buffer.

3.6. Optimized LC-MS/MS method determined insulin secretion in stem cell-derived islets.

To determine insulin secretion from SC-islets (Fig. 6**A-B**, and see more details in **SI-7**) exposed to three different glucose environments, a calibration curve was established from 0.2 pg/μL to 10 pg/μL human insulin with 5.0 pg/μL bovine insulin as internal standard, see Fig. 6**C**. The accuracy of the calibration and potential drift in the system during a long sample sequence was monitored by running a quality control standard with 2.0 pg/μL human insulin (with 5.0 pg/μL bovine insulin as internal standard) as the first injection following the calibration standards, in the middle of the sample sequence and as the last injection. The quality controls were individually determined with a relative error of −2%, −9% and 2%, and the average concentration was found to be 1.9 pg/μL with an RSD of 6%. The quality controls indicated that the LC-MS/MS method provide sufficient accuracy in determining insulin concentrations by a single injection of a sample and that there was no drift in the system in the course of a relatively long sequence (37 injections).

Analyses by the LC-MS/MS method showed that SC-islets exposed to 2 mM glucose (low glucose) secreted 1.9 pg/μL of human insulin (n = 4, RSD = 36%). Contradictory, in 20 mM glucose (high glucose), 1.9 pg/μL of human insulin (n = 4, RSD = 18%) was also secreted by the SC-islets. However, when the SC-islets were exposed to 20 mM glucose combined with 30 mM KCl, a total of 12 pg/μL of human insulin (n = 4, RSD = 18%) was secreted (it should be noted that the concentration of insulin in the KCl samples were outside of the calibration range). The values obtained by the LC-MS/MS method was compared to that of an established ELISA method, which determined human insulin secretion to be 2.0 pg/μL (n = 4, RSD = 15%) in low glucose, 2.3 pg/μL (n = 4, RSD = 17%) in high glucose, and 13 pg/μL (n = 4, RSD = 20%) in KCl environment. An independent two sample *t*-test, at 95% confidence, showed that the average insulin concentration found for the three different exposures determined with ELISA and LC-MS/MS were not significantly different, and this is visualized in Fig. 6**D**. For quality SC-islets, it was expected that the insulin secretion in response to high glucose should be more than 1.5 times higher than the insulin secretion in response to low glucose. The SC-islets used in these experiments did not show this difference in insulin secretion based on glucose environment. However, it should be noted that the SC-islets used in these experiments were examined in the first days after completion of the differential protocol, and we would expect SC-islets that have matured further to display a difference in insulin secretion profile depending on glucose concentration [26,27]. The experiments with KCl show however, that the SC-islets are producing larger amount of insulin, and are able to control how much is secreted pending on exposure. The LC-MS/MS method shows sufficiently low detection limit as we are able to detection insulin secretion from not functionally mature SC-islets.

4. Brief comparison to previously published LC-MS methods for determination of human insulin.

In a balanced salt solution, equivalent to the Krebs buffer applied in this study, Donohue *et al.* [16] developed a conventional RPLC-MS/MS method for human insulin secreted by human donor islets with a precision of RSD = 13–16% and a detection limit of 0.5 nM (2.9 pg/μL). Another multi-element conventional RPLC-MS/MS method achieved simultaneous detection of human insulin, synthetic analogous, and C-peptide from blood/plasma samples by combining protein precipitation and a mixed-mode cation-exchange solid-phase extraction sample preparation. The method was fully validated with a LOD of 0.2 pg/μL, LOQ of 0.6 pg/μL, 78–128% accuracy, and < 21% precision [22].

The method presented in this study, tailored for islet organoid samples, has negligible carry-over, an LOD of ≤ 0.2 pg/μL, ≤ ±10% accuracy, and < 10% precision for human insulin, which is in the same range as achieved in the previously mentioned methods.

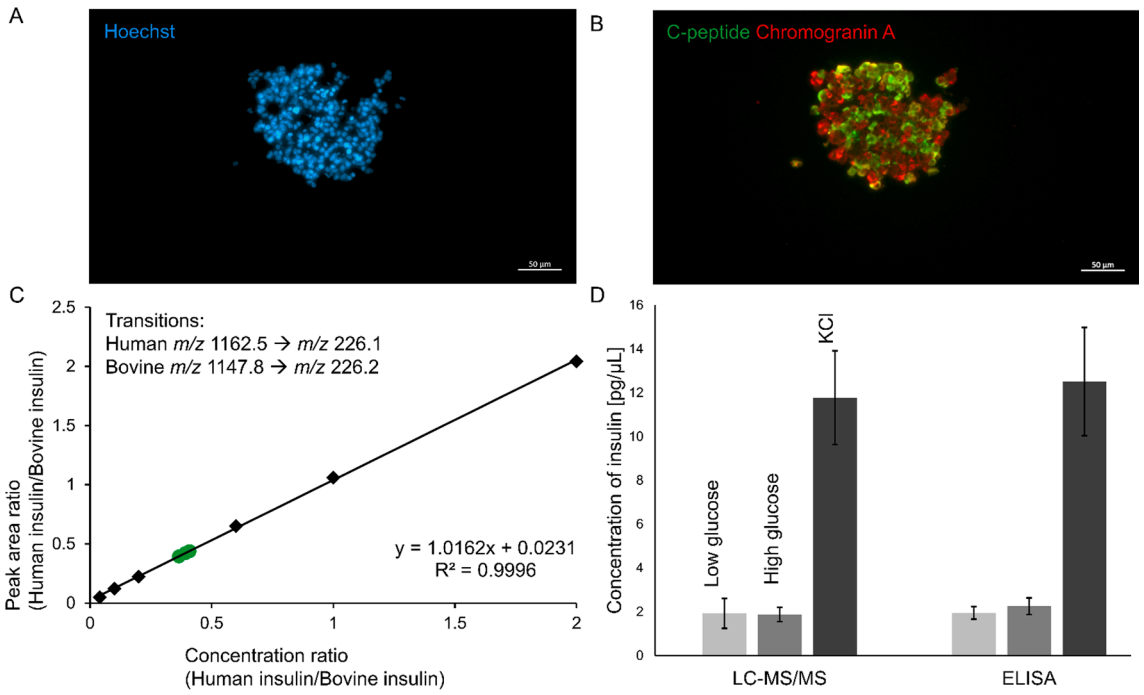

Fig. 6. Representative immunostaining images of SC-islets. (**A**) Nuclei DNA stained with Hoechst (blue), and (**B**) endocrine secretory vesicles stained with chromogranin A (red) and production of insulin is represented by C-peptide (green). (**C**) Calibration curve in 0.5% FA Krebs buffer, obtained by SRM, from 0.2 pg/μL to 10 pg/μL human insulin with 5 pg/μL bovine insulin (IS) (points marked in black), and three quality control standards (marked green as relative error was<10%) at 2 pg/μL human insulin with 5 pg/μL bovine insulin (IS). (**D**) Insulin secretion determined by LC-MS/MS and ELISA from SC-islets exposed to low glucose (2 mM), high glucose (20 mM) and KCl (20 mM glucose with 30 mM KCl).

5. Conclusions

We have developed an RPLC-MS/MS method tailored for measuring insulin secreted from organoid islets. The method is highly sensitive and selective, with excellent quantitative properties. Conventional LC columns were compatible with low μL-scale samples, and next steps will be direct coupling of the system with pancreas-on-a-chip systems [8]. A limitation is that the method is sensitive to the type of medium applied; additional fine-tuning can eventually be performed, e.g. focusing on LC column selectivity to avoid medium specific matrix effects. Possible expansions include adding additional analytes to the method, for example cytokines and other islets-related peptides (e.g. somatostatin, glucagon, and C-peptide).

Declaration of Competing Interest

The authors declare that they have no known competing financial interests or personal relationships that could have appeared to influence the work reported in this paper.

Data availability

Data will be made available on request.

Acknowledgements

Financial support was obtained from the Research Council of Norway through its Centres of Excellence funding scheme, project number 262613 and partly from UiO:Life Science, University of Oslo. S.R.W. is a member of the National Network of Advanced Proteomics Infrastructure (NAPI), which is funded by the Research Council of Norway INFRASTRUKTUR-program (project number: 295910). This work was partially supported by the Research Council of Norway through its Centres of Excellence scheme, project number 262695.

Appendix A. Supplementary data

Supplementary data to this article can be found online at https://doi.org/10.1016/j.jchromb.2022.123577.

References

[1] Y. Aghazadeh, M.C. Nostro, Cell therapy for type 1 diabetes: Current and future strategies, Curr. Diabetes Rep. 17 (2017) 37, https://doi.org/10.1007/s11892-017-0863-6.

[2] B.J. Hering, W.R. Clarke, N.D. Bridges, T.L. Eggerman, R. Alejandro, M.D. Bellin, K. Chaloner, C.W. Czarniecki, J.S. Goldstein, L.G. Hunsicker, D.B. Kaufman, O. Korsgren, C.P. Larsen, X. Luo, J.F. Markmann, A. Naji, J. Oberholzer, A. M. Posselt, M.R. Rickels, C. Ricordi, M.A. Robien, P.A. Senior, A.M.J. Shapiro, P. G. Stock, N.A. Turgeon, Phase 3 trial of transplantation of human islets in type 1 diabetes complicated by severe hypoglycemia, Diabetes Care 39 (7) (2016) 1230–1240.

[3] S. Pathak, T.T. Pham, J.-H. Jeong, Y. Byun, Immunoisolation of pancreatic islets via thin-layer surface modification, J Control Release 305 (2019) 176–193. https://www.sciencedirect.com/science/article/pii/S0168365919302342.

[4] A.M.J. Shapiro, J.R.T. Lakey, E.A. Ryan, G.S. Korbutt, E. Toth, G.L. Warnock, N. M. Kneteman, R.V. Rajotte, Islet transplantation in seven patients with type 1 diabetes mellitus using a glucocorticoid-free immunosuppressive regimen, N. Engl. J. Med. 343 (2000) 230–238. https://www.nejm.org/doi/full/10.1056/NEJM200007273430401.

[5] C.-H. Wassmer, F. Lebreton, K. Bellofatto, L. Perez, D. Cottet-Dumoulin, A. Andres, D. Bosco, T. Berney, V. Othenin-Girard, B. Martinez De Tejada, M. Cohen, C. Olgasi, A. Follenzi, E. Berishvili, t.V.C. , C. Borsotti, S. Merlin, L. Piemonti, A. Citro, S. Pellegrini, J. Seissler, L. Wolf-van Buerck, M. Honarpisheh, O. Thaunat, E. Massey, A. Cronin, E. Bunnik, D. de Jongh, L. Segantini, G. Rossi, P. Kugelmeier, P. Wolint, M. Cavallaro, J. Götz, J. Müller, Bio-engineering of pre-vascularized islet organoids for the treatment of type 1 diabetes, Transpl. Int., 35 (2022). https://www.frontierspartnerships.org/articles/10.3389/ti.2021.10214.

[6] M. Khosravi-Maharlooei, E. Hajizadeh-Saffar, Y. Tahamtani, M. Basiri, L. Montazeri, K. Khalooghi, M. Kazemi Ashtiani, A. Farrokhi, N. Aghdami, A. Sadr Hashemi Nejad, M.-B. Larijani, N. De Leu, H. Heimberg, X. Luo, H. Baharvand, Theraphy of endocrine disease: Islet transplantation for type 1 diabetes: so close and yet so far away, Eur. J. Endocrinol., 173 (2015) R165-R183. https://eje.bioscientifica.com/view/journals/eje/173/5/R165.xml.

[7] X. Zhang, Z. Ma, E. Song, T. Xu, Islet organoid as a promising model for diabetes, Protein, Cell 13 (2022) 239–257, https://doi.org/10.1007/s13238-021-00831-0.

[8] S. Abadpour, A. Aizenshtadt, P.A. Olsen, K. Shoji, S.R. Wilson, S. Krauss, H. Scholz, Pancreas-on-a-chip technology for transplantation applications, Curr. Diabetes Rep. 20 (2020) 72, https://doi.org/10.1007/s11892-020-01357-1.

[9] Y. Du, Z. Liang, S. Wang, D. Sun, X. Wang, S.Y. Liew, S. Lu, S. Wu, Y. Jiang, Y. Wang, B. Zhang, W. Yu, Z. Lu, Y. Pu, Y. Zhang, H. Long, S. Xiao, R. Liang, Z. Zhang, J. Guan, J. Wang, H. Ren, Y. Wei, J. Zhao, S. Sun, T. Liu, G. Meng, L. Wang, J. Gu, T. Wang, Y. Liu, C. Li, C. Tang, Z. Shen, X. Peng, H. Deng, Human pluripotent stem-cell-derived islets ameliorate diabetes in non-human primates, Nat. Med. 28 (2022) 272–282, https://doi.org/10.1038/s41591-021-01645-7.

[10] A.-D. Luong, I. Roy, B.D. Malhotra, J.H.T. Luong, Analytical and biosensing platforms for insulin: A review, Sensors and Actuators Reports 3 (2021), 100028. https://www.sciencedirect.com/science/article/pii/S2666053921000047.

[11] A. Lin, F. Sved Skottvoll, S. Rayner, S. Pedersen-Bjergaard, G. Sullivan, S. Krauss, S. Ray Wilson, S. Harrison, 3D cell culture models and organ-on-a-chip: Meet separation science and mass spectrometry, Electrophoresis 41 (2020) 56–64. https://onlinelibrary.wiley.com/doi/abs/10.1002/elps.201900170.

[12] F.S. Skottvoll, A. Aizenshtadt, F.A. Hansen, M.A. Martinez, J.M. Andersen, I. L. Bogen, J.P. Kutter, S. Pedersen-Bjergaard, E. Lundanes, S. Krauss, S.R. Wilson, Direct electromembrane extraction-based mass spectrometry: A tool for studying drug metabolism properties of liver organoids, Anal. Sens. (2022) e202100051. https://chemistry-europe.onlinelibrary.wiley.com/doi/abs/10.1002/anse.202100051.

[13] F.S. Skottvoll, F.A. Hansen, S. Harrison, I.S. Boger, A. Mrsa, M.S. Restan, M. Stein, E. Lundanes, S. Pedersen-Bjergaard, A. Aizenshtadt, S. Krauss, G. Sullivan, I. L. Bogen, S.R. Wilson, Electromembrane extraction and mass spectrometry for liver organoid drug metabolism studies, Anal. Chem. 93 (2021) 3576–3585, https://doi.org/10.1021/acs.analchem.0c05082.

[14] S. Kogler, S. Harrison, A. Aizenshtadt, F.S. Skottvoll, S. Abadpour, S. Krauss, H. Scholz, G. Sullivan, E. Lundanes, S.R. Wilson, “Organoid-in-a-column” coupled on-line with liquid chromatography-mass spectrometry, bioRxiv, (2020) 2020.2009.2008.282756. https://www.biorxiv.org/content/biorxiv/early/2020/09/19/2020.09.08.282756.full.pdf.

[15] C. Olsen, E. Wiborg, E. Lundanes, S. Abadpour, H. Scholz, S.R. Wilson, On-line reduction of insulin disulfide bonds with photoinduced radical reactions, upstream to nano liquid chromatography-mass spectrometry, Sep. Sci. plus 5 (2022) 220–227. https://analyticalsciencejournals.onlinelibrary.wiley.com/doi/abs/10.1002/sscp.202200022.

[16] M.J. Donohue, R.T. Filla, D.J. Steyer, W.J. Eaton, M.G. Roper, Rapid liquid chromatography-mass spectrometry quantitation of glucose-regulating hormones from human islets of Langerhans, J. Chromatogr. A 1637 (2021), 461805. https://www.sciencedirect.com/science/article/pii/S0021967320310797.

[17] D. Brüning, K. Reckers, P. Drain, I. Rustenbeck, Glucose but not KCl diminishes submembrane granule turnover in mouse beta-cells, J Mol Endocrinol 59 (2017) 311–324. https://jme.bioscientifica.com/view/journals/jme/59/3/JME-17-0063.xml.

[18] P. Judák, J. Grainger, C. Goebel, P. Van Eenoo, K. Deventer, DMSO assisted electrospray ionization for the detection of small peptide hormones in urine by dilute-and-shoot-liquid-chromatography-high resolution mass spectrometry, J. Am. Soc. Mass Spectrom. 28 (2017) 1657–1665, https://doi.org/10.1007/s13361-017-1670-7.

[19] K. Maes, I. Smolders, Y. Michotte, A. Van Eeckhaut, Strategies to reduce aspecific adsorption of peptides and proteins in liquid chromatography–mass spectrometry based bioanalyses: An overview, J. Chromatogr. A 1358 (2014) 1–13. https://www.sciencedirect.com/science/article/pii/S0021967314010152.

[20] C. Rosting, C.Ø. Sæ, A. Gjelstad, T.G. Halvorsen, Evaluation of water-soluble DBS for small proteins: A conceptual study using insulin as a model analyte, Bioanalysis 8 (2016) 1051–1065. https://www.future-science.com/doi/abs/10.4155/bio-2016-0002.

[21] P. Judák, G. Coppieters, B. Lapauw, P. Van Eenoo, K. Deventer, Urinary detection of rapid-acting insulin analogs in healthy humans, Drug Test. Anal. 12 (2020) 1629–1635. https://analyticalsciencejournals.onlinelibrary.wiley.com/doi/abs/10.1002/dta.2817.

[22] A. Thomas, R. Yang, S. Petring, L. Bally, M. Thevis, Simplified quantification of insulin, its synthetic analogs and C-peptide in human plasma by means of LC-HRMS, Drug Test. Anal. 12 (2020) 382–390. https://analyticalsciencejournals.onlinelibrary.wiley.com/doi/abs/10.1002/dta.2765.

[23] G.E.P. Box, D.W. Behnken, Some New Three Level Designs for the Study of Quantitative Variables, Technometrics 2 (1960) 455–475. https://www.tandfonline.com/doi/abs/10.1080/00401706.1960.10489912.

[24] F. Gritti, K. Horvath, G. Guiochon, How changing the particle structure can speed up protein mass transfer kinetics in liquid chromatography, J. Chromatogr. A 1263 (2012) 84–98. https://www.sciencedirect.com/science/article/pii/S002196731201415X.

[25] F. Gritti, G. Guiochon, Comparison between the loading capacities of columns packed with partially and totally porous fine particles: What is the effective surface

area available for adsorption? J. Chromatogr. A 1176 (2007) 107–122. https://www.sciencedirect.com/science/article/pii/S0021967307018547.
[26] J.C. Davis, T.C. Alves, A. Helman, J.C. Chen, J.H. Kenty, R.L. Cardone, D.R. Liu, R. G. Kibbey, D.A. Melton, Glucose response by stem cell-derived β cells in vitro is inhibited by a bottleneck in glycolysis, Cell Rep. 31 (2020), 107623. https://www.sciencedirect.com/science/article/pii/S2211124720305763.
[27] T. Barsby, T. Otonkoski, Maturation of beta cells: lessons from in vivo and in vitro models, Diabetologia 65 (2022) 917–930, https://doi.org/10.1007/s00125-022-05672-y.

Supplementary Table: Differentiation medium formulation

Stage 1 medium: 4 days		
Basal medium	Pen/Strep	1 %
	$NaHCO_3$	1.174g/L
	Glutamax (100x)	1x
	Glucose	+4.5mM to10mM
	BSA	0.50 %
Suplementary	Activin A	100ng/ml
	Chir99021	3µM*
*only added in the first 24 hours		
Stage 2 medium: 2 days		
Basal medium	Same as stage 1 basal medium	
Suplementary	vitamin C	0.25mM
	FGF7	50ng/ml
	IWP-2	1.25µM
Stage 3 medium: 2 days		
Basal medium	Pen/Strep	1 %
	$NaHCO_3$	1.754g/L
	Glutamax (100x)	1x
	Glucose	+4.5mM to10mM
	BSA	2 %
	ITS-X	1:200
	vitamin C	0.25mM
Suplementary	Retinoid Acid	2µM
	SANT1	0.25µM
	FGF7	50ng/ml
	LDN193189	0.2µM
	TPPB	0.2µM
Stage 4 medium: 4 days		
Basal medium	Same as stage 3 basal medium	
Suplementary	Retinoid Acid	0.1µM
	SANT1	0.25µM
	FGF7	50ng/ml
	LDN 193189	0.2µM
	TPPB	0.2µM

Stage 5 medium: 7 days		
Basal medium	Pen/Strep	1 %
	$NaHCO_3$	1.754g/L
	Glutamax (100x)	1x
	Glucose	+14.5mM to 20mM
	BSA	2 %
	ITS-X	1:200
	Heparin	10ug/ml
	vitamin C	0.25mM
Suplementary	Retinoid Acid	0.1µM
	SANT1	0.25µM
	ALK5 inh II	10µM
	T3	1µM
	LDN 193189	0.1µM
	Xxi	1µM
	Latrunculin A**	1µM
**Latrunculin A only added at day 1 of stage 5.		
Stage 6 medium: >14 days		
	Pen/Strep	1 %
	Glutamax (100x)	1x
	MEM NEAA (100X)	1x
	BSA	2 %
	Trace Elements A (1000X)	1X
	Trace Elements B (1000X)	1X
	Heparin	10ug/ml
	$ZnSO_4$	10µM

Supplementary Material for: Determination of insulin secretion from stem cell-derived islets with liquid chromatography-tandem mass spectrometry

Christine Olsen[a,b], Chencheng Wang[b,c], Shadab Abadpour[b,c], Elsa Lundanes[a], Audun Skau Hansen[a], Frøydis Sved Skottvoll[d], Hanne Scholz[b,c], and Steven Ray Wilson[a,b*]

[a]University of Oslo, Department of Chemistry, Blindern, Oslo, Norway

[b]Hybrid Technology Hub-Centre of Excellence, Institute of Basic Medical Sciences, Faculty of Medicine, University of Oslo, Oslo, Norway

[c]Department of Transplant Medicine and Institute for Surgical Research, Oslo University Hospital, Oslo, Norway

[d]Department of Smart Sensors and Microsystems, SINTEF Digital, Oslo, Norway

*Corresponding author: Steven Ray Wilson E-mail: s.r.h.wilson@kjemi.uio.no.

1 Discussion concerning selection of collision gas pressure for stable fragmentation of intact insulin

Assessment of an aqueous standard containing 10 ng/µL human insulin by direct injection on a QQQ MS operated in fullscanQ1 mode showed that intact insulin (*i.e.* no changes to the structure of the peptide from its natural form) was present with expected charge states: *m/z* 968.6 (z = +6), *m/z* 1162.5 (z = +5) and *m/z* 1452.5 (z = +4), see **Figure S1A**. The fragmentation of the most abundant ion *m/z* 1162.5 was examined at various collision gas pressures from 1 mTorr to 4 mTorr. Commonly used diagnostic fragments in targeted insulin determination (*i.e. m/z* 226.1 and *m/z* 345.0) and larger fragments (*m/z* 1159.2 and *m/z* 1358.0, see **Figure S1B**) was found with increasing intensity when applying increasing collision gas pressures from 1.0 mTorr to 3.0 mTorr, see **Figure S1C** [1, 2]. At gas pressures of 2.5 mTorr and 3.0 m Torr, the signal intensity of the smaller fragments were in equal range, but with a larger intensity variance at 3.0 mTorr. The larger fragment *m/z* 1159.2 was present at sufficient intensities at both 2.5 mTorr and 3.0 mTorr gas pressures. At higher gas pressures over 3.5 mTorr, more of the precursor ion remained intact and the larger product ions were present at a higher intensity, however, the smaller fragment ions *m/z* 226.1 and *m/z* 345.0 were not present in all of the product scans. Therefore, 2.5 mTorr was selected as the collision gas pressure in the targeted experiments.

Bovine insulin has three amino acids which are different compared to that of human insulin and was selected as the internal standard in the method due to its availability and being an inexpensive alternative to a deuterated compound. A similar evaluation of bovine insulin by direct injection showed a highly abundant and stable precursor at *m/z* 1147.8 (z = +5) and high-intensity product fragments at *m/z* 226.2, *m/z* 315.2, and *m/z* 1144.5 at 2.5 mTorr collision gas pressure.

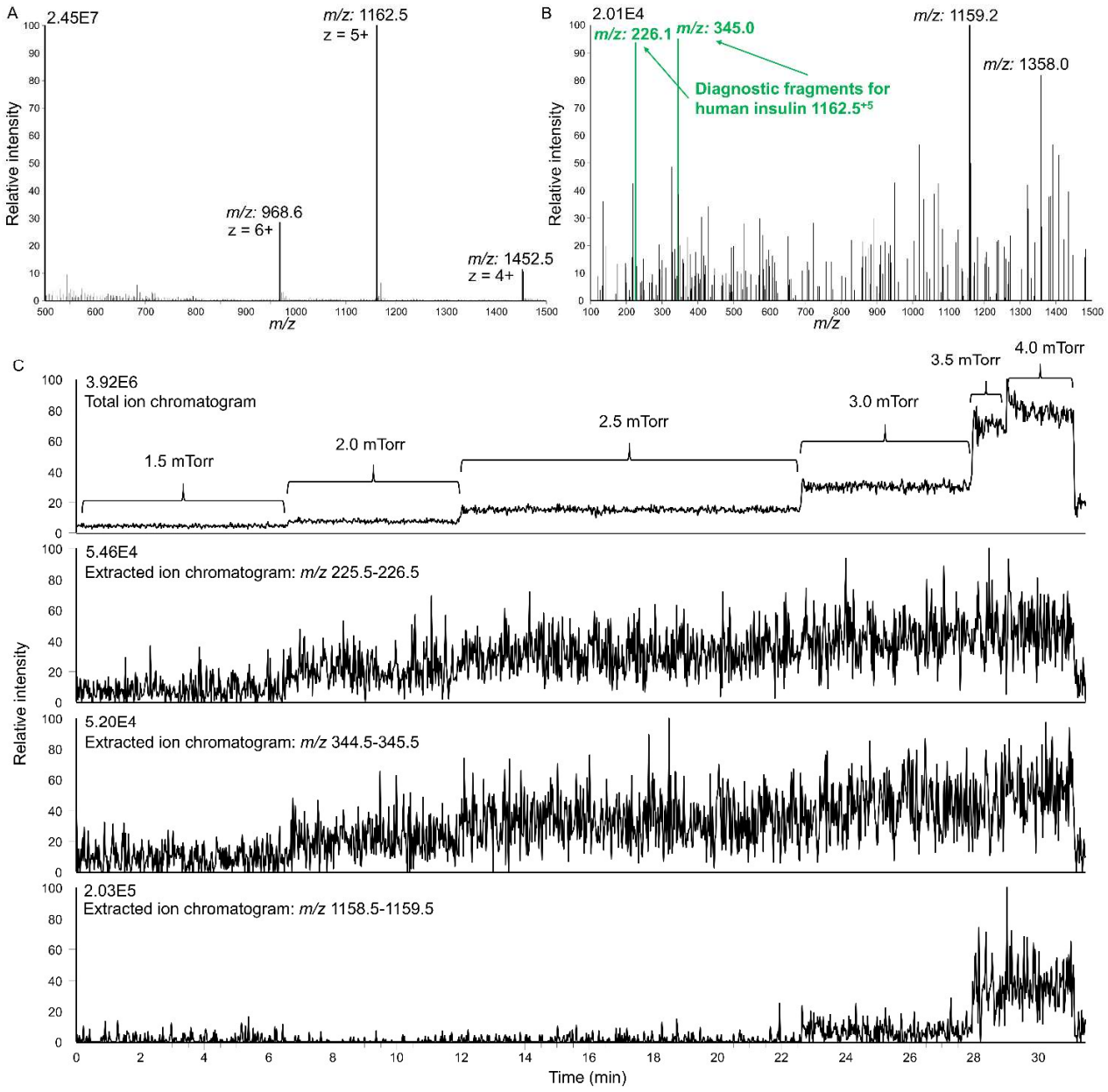

Figure S1: (**A**) Charge distribution of intact human insulin found in FullscanQ1 mode, (**B**) product ions fragmented from *m/z* 1162.5, the most abundant precursor of human insulin, and (**C**) evaluation of the stability and signal intensity of three selected product ions (i.e. *m/z* 226.1, *m/z* 345.0, and *m/z* 1159.2) from *m/z* 1162.5 at different collision gas pressures (1.5 mTorr – 4.0 mTorr).

2 Non-defined adsorption of intact human insulin on glass syringe eliminated by shielded fused silica tubing

The glass syringe used for manual injection was another critical point to assess for non-defined adsorption of insulins. Initially, insulin solutions were introduced directly onto the loop with a 25 µL glass syringe. When the glass syringe and the loop was washed with 25 µL of the insulin solution five times prior to loading and injection, the average peak area of human insulin was 1.8E7 with a relative standard deviation (RSD) of 17% (n = 3, see **Figure S2C-I**). The peak areas of human insulin also steadily increased for each subsequent injection: 1.5E7, 1.8E7 and 2.1E7. By reducing the amount of insulin solution filled on the syringe, syringe filled only once with 25 µL and directly fill 5 µL onto the loop for injection, the average peak area of human insulin was 3.2E6 with a RSD of 13% (n = 6, see **Figure S2C-II**). Seeing as the peak areas varied 83% between the two injection procedures, the glass syringe and the loop was examined for insulin accumulation by assessing the signal in a blank injection following a regular insulin injection. The carry-over signal of human insulin was ≥ 9% when only the loop had been cleaned with a 50/50 MeOH/H_2O solution and 0.1% FA in water, while the carry-over signal was ≤ 2% when only the glass syringe was cleaned with 50/50 MeOH/H_2O solution prior to filling with blank solution 0.1% FA in water. The carry-over indicated that insulin displayed non-defined adsorption towards the surface of the glass syringe, but not on the shielded fused silica loop.

To avoid insulin accumulation on the glass syringe during injection, the syringe was coupled to a 150 µm id x 750 mm shielded fused silica connector (volume of tubing = 13.2 µL), shown in **Figure S2D**). When the insulin solution was filled into the glass syringe through the shielded fused silica connector (two times 20 µL), and 5 µL of the volume in the tubing was filled onto the loop for injection, the average peak area of human insulin was 5.2E6 with a RSD of 10% (n = 6, **Figure S2C-III**). An independent two sample t-test, at 95% confidence, showed that the average peak area found for human insulin by injection with and without a shielded fused silica connector attached to the syringe were significantly different. In addition, the average peak area of human insulin obtained with injection using a syringe coupled to a shielded fused silica connector was between the average peak areas achieved with the previously examined injection procedures. Hence, it was even more probable that insulin had non-defined adsorption on the glass syringe, which accumulated during multiple fillings of the syringe giving a higher peak area, and when the syringe was filled only once led to a reduced peak area.

Injection technique and selection of tubing was of great importance in achieving LC-MS determination of intact insulin in low pg/µL range. A fully modified system, where insulin only came in contact with shielded fused silica shielded fused silica connector offered a repeatable chromatographic performance based on peak area examination. Utilizing a shielded fused silica connector coupled to the syringe eliminated the effect of non-defined adsorption on the syringe, and possible carry-over from the glass syringe was easily removed by washing with a 1+1 MeOH/water (v/v) solution.

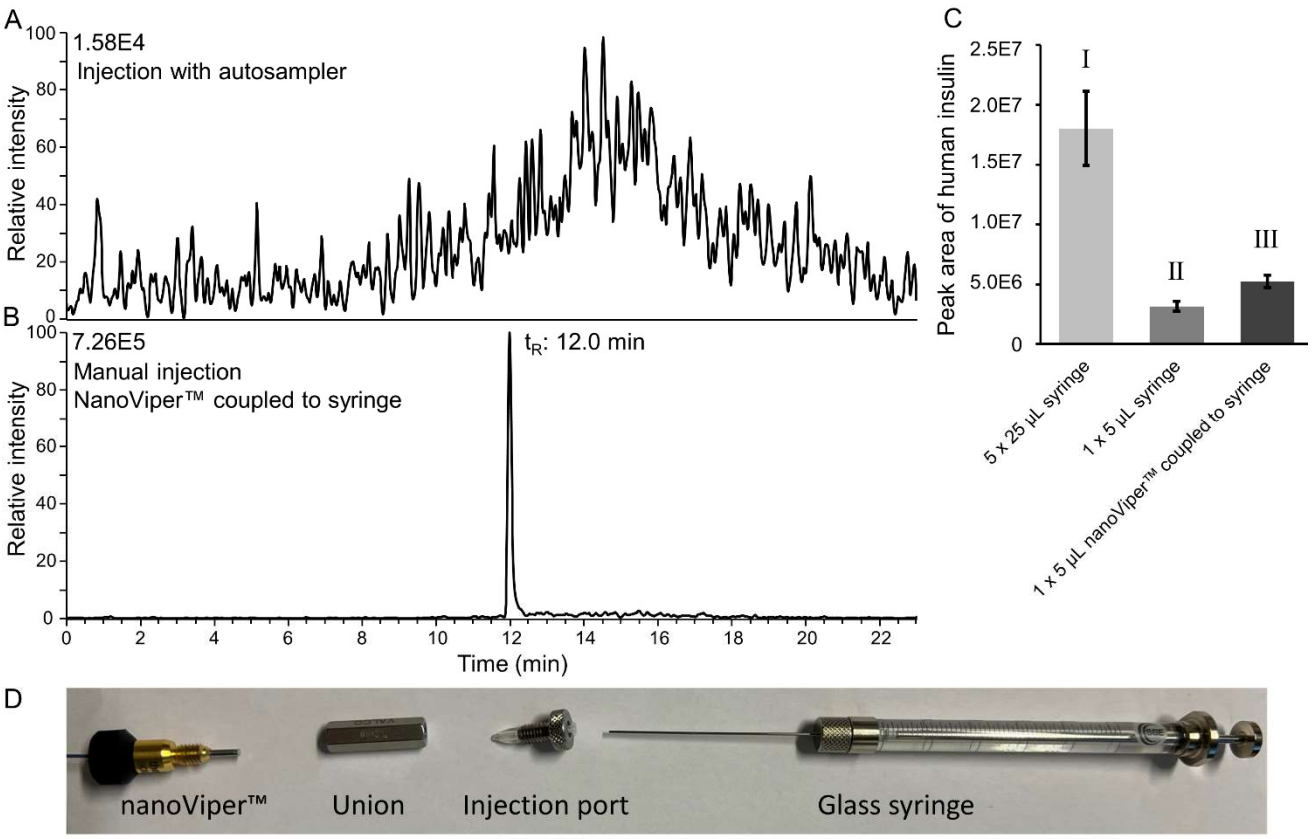

Figure S2: Extracted ion chromatogram of intact human insulin (*m/z* 1162.0-1163.0): (**A**) 1 µL injection of 125 pg/µL human insulin in 0.1% FA in water using autosampler, and (**B**) 1.08 µL injection of 125 pg/µL human insulin in 0.1% FA in water using a 6-port-2-position valve with 50 µm id x 550 mm shielded fused silica loop, and the solution was filled in the loop with a 25 µL glass syringe coupled to a 150 µm id x 750 mm shielded fused silica connector. Solutions were examined with the MS operated in fullscanQ1 mode. (**C**) Comparison of peak areas of human insulin obtained with manual injection of 125 pg/µL insulin solution: (**I**) Syringe and loop filled five times with 25 µL, (**II**) syringe filled once with 25 µL and 5 µL applied on loop, or (**III**) 40 µL solution filled through a 13.2 µL shielded fused silica connector coupled to the syringe, and 5 µL were applied on the loop. (**D**) Showing how the glass syringe was coupled to the shielded fused silica connector by a 250 µm id union and an injection port.

3 Discussion concerning effect of column temperature on peak area or peak shape

To examine if insulin peak shape/areas could be affected by the column temperature, the guard cartridge and separation column was placed in a column heater. Prior to injections, heating was applied for one hour to avoid a temperature gradient in the cross section of the columns. By injection of 1.08 µL of 125 pg/µL of human insulin and 125 pg/µL of bovine insulin dissolved in cell medium, no difference in peak area was found between 20 °C, 30 °C and 40 °C, as the average peak areas of human insulin was 4.4E6 (n = 3), 4.3E6 (n = 3) and 4.3E6 (n = 2), respectively. There was no difference found for bovine insulin either as the average peak areas of *m/z* 1147.8 was 4.2E6 (20 °C, n = 2), 4.1E6 (30 °C, n = 3) and 4.5E6 (40 °C, n = 2). Concerning the peak shape, no obvious difference was seen in the asymmetry factor as the factor was calculated to be 1.25 (n = 3) at 20 °C, 1.23 (n = 3) at 30 °C and 1.14 (n = 2) at 40 °C for human insulin.

4 Expanded discussion concerning optimization of precursor peak areas with Box-Behnken

The peak area of precursor *m/z* 1162.5 of human insulin was optimized using Box-Behnken (BB) experimental design on the six selected variables in the H-ESI and MS-inlet settings.

In the first set-up of a three factor BB-design: Sheath gas (SG, Arb) [20, 28, 36], vaporizer temperature (VT, °C) [170, 210, 250], and spray voltage (SV, kV) [1.8, 2.65, 3.5] was evaluated for the highest peak area of *m/z* 1162.5 in water standards. BB reported [SG = 36, VT = 210, SV = 3.5] to be the optimized settings, as shown in main effects plot in **Figure S3A**. However, the suggested optimized settings were included as one of the experiments in the BB-design and produced a peak with an area of 5.5E6. Another of the experiments included in the BB-design [SG = 20, VT = 210, SV = 3.5] (referred to as outlayer settings) achieved a peak area of 9E6, which was 39% larger than the peak area found by the settings deemed optimal by BB. Therefore, to be able to select between having sheath gas levels of 36 Arb or 20 Arb, the two settings were examined further.

Based on the three experiments run at the same settings in the BB-design, [SG = 28, VT = 210, SV = 2.65], it was clear that the experiments were subjected to uncertainty, as the obtained average peak area of 4E6 showed a large variation with RSD = 34%. There was also a significant signal found in the blank injection following the 15 injections of 125 pg/µL human and 125 pg/µL bovine insulin, where the signal was equal to 7% carry-over of human insulin and 8% carry-over of bovine insulin.

Therefore, three additional replicates of each experiments were compared after allowing the selected settings to run for one hour to reach a more stable condition to reduce random errors, and a blank injection was run between each injection of insulin solutions to remove effects of carry-over. When applying sheath gas at 36 Arb, the peak area of *m/z* 1162.5 = 1.18e7 (RSD = 5%, n = 3, **Figure S3B-I**), while sheath gas levels of 20 Arb showed a higher peak area of *m/z* 1162.5 = 1.40e7 (RSD = 5%, n =3, **Figure S3B-II**). The carry-over after a single injection was between 1-3% for both human and bovine insulin (n = 3), and no difference in carry-over was found depending on sheath gas levels applied.. An independent two sample t-test, at 95% confidence, showed that the average peak areas of the two settings (36 Arb and 20 Arb) were significantly different, and therefore sheath gas levels of 20 Arb were selected to be applied in the method going forward.

In the second set-up of a three factor BB design: Sweep gas (SWG, Arb) [0, 5, 10], auxiliary gas (AUX, Arb) [5, 9, 13], and ion transfer tube temperature (ITT, °C) [275, 325, 375] were examined in standards prepared in cell medium. The optimized H-ESI settings for *m/z* 1162.5 were found to be [SWG = 0, AUX = 9, ITT = 275], as shown in main effects plot in **Figure S3C**, and had a peak area of *m/z* 1162.5 = 1.7E7. The three experiments, which were examined at the same settings; [SWG = 5, AUX = 9, ITT = 325] gave an average peak area of 1.1E7 with an RSD = 22% in this case. Another important feature shown for the method with the second BB-design, was that the blank injection following 15 injections of 125 pg/µL human and 125 pg/µL bovine insulin in cell medium had a signal of human insulin equal to 1% carry-over and there was no distinguishable peak corresponding to bovine insulin, indicating that the carry-over was distinctly reduced in cell medium standard compared to water standards.

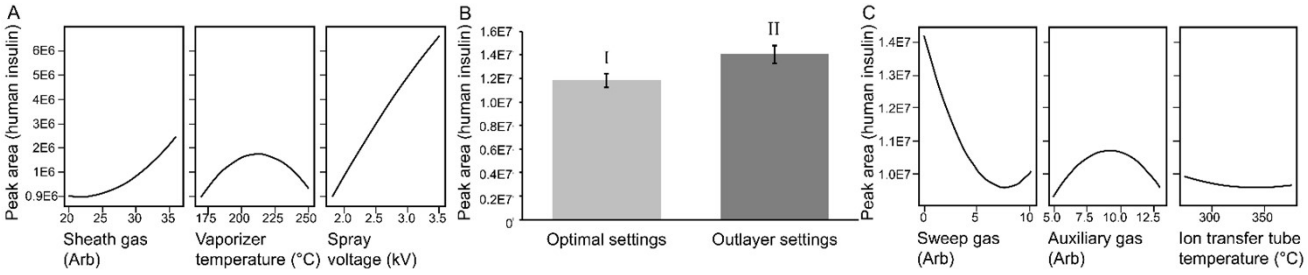

Figure S3: Optimization of peak area of human insulin *m/z* 1162.5 with Box-Behnken.: (**A**) Main effects plot showing effect of sheath gas levels, vaporizer temperature and spray voltage, (**B**) comparison of peak areas obtained with (**I**) optimal settings [SG = 36, VT = 210, SV = 3.5] and (**II**) outlayer settings [SG = 20, VT = 210, SV = 3.5], and (**C**) main effects plot showing effect of sweep gas levels, auxiliary gas levels and ion transfer tube temperature.

5 Discussion concerning manual injection technique based on peak areas obtained in SRM mode

The reduced carry-over of human and bovine insulin when working with standards prepared in cell medium compared to water standards, as described in previous **Section SI-2 and SI-4**, indicated that compounds present in the cell medium reduced the non-defined adsorption of insulins. Bovine serum albumin (BSA) was a possible candidate to examine, as BSA has been described as a sacrificial protein to block adsorption of proteins and peptides [3]. To examine if BSA could block non-defined adsorption, water standards with 125 pg/µL human and 125 pg/µL bovine insulin was prepared with and without 5 ng/µL BSA. The two solutions were then injected using only a glass syringe and a glass syringe coupled to a shielded fused silica connector, a repeat of the same experiments used to establish that the glass syringe showed non-defined adsorption of insulin in water standards in **Section SI-2**. The experiments was done using SRM, as it was assumed SRM had a higher sensitivity, than a FullscanQ1 method, to examine potential carry-over, and SRM was the intended method to be applied in determination of insulin in SC-islets. Water standards without BSA injected with a shielded fused silica connector coupled to a glass syringe resulted in an average peak area for human insulin of 1.4E4 (n = 3, RSD = 10%), and injection using only a glass syringe gave a similar average peak area and variance (1.4E4 and RSD = 13%). The carry-over in a blank injection after three injections was in both cases less than 0.5%. When BSA was added to the water standard and injected with a shielded fused silica connector coupled to a glass syringe the average peak area for human insulin was 1.5E4 (n = 3, RSD = 7%), while injection using only a glass syringe gave a similar average peak area and variance (1.4E4 and RSD = 2%). The carry-over in a blank injection after three injection of BSA water standard was also less than 0.5% independent of injection technique. By two-way analysis of variance (ANOVA), there was no significant difference in the obtained average peak areas with or without BSA or depending on the injection technique. From the information gained when comparing the injection techniques and the presence of BSA, it could not be confirmed whether or not BSA reduced non-defined adsorption of human insulin.

The injection technique with the shielded fused silica connector coupled to the glass syringe is much more laborious and more exposed to errors in the execution than injection with only a glass syringe. In addition, more sample is required when the shielded fused silica connector syringe technique is applied and frothing was an issue with the cell medium standards. Therefore, injection of cell medium standards were examined with both injection techniques as well to see if the peak areas where significantly different or not with the SRM method. Cell medium standards injected with shielded

fused silica connector coupled syringe technique had an average peak area of 1.56E4 (n = 3, RSD = 2%) for human insulin, while injection with only the syringe had an average peak area of 1.8E4 (n = 3, RSD = 8%). An independent two sample t-test, at 95% confidence, showed that the average peak area of human insulin found for the two different injection techniques were not significantly different for cell medium standards. The standard deviations of the two injection techniques were also not significantly different. Based on these findings, only a glass syringe was used for injection of samples and standards in cell medium.

6 Bovine serum albumin assumed responsible for unsuccessful separation of insulins in large injections of cell medium

When the injection volume was increased to 20 µL of a solution consisting of 6.25 pg/µL human and 6.25 pg/µL bovine insulin, no peaks corresponding to human or bovine insulin was distinguishable from the other compounds present in cell medium, as shown in **Figure S4A**. The mass spectrum obtained from the large peak in the chromatogram shows an *m/z* pattern with regular intervals, which can be expected for a large protein such as BSA with multiple charges, shown in **Figure S4B.** Being unable to completely remove the residue from the column, even after extensive washing, we have not been able to inject a BSA water standard for confirmation. However, a mass spectrum obtained from direct injection of 10 ng/µL of BSA confirms that BSA produces ions with signal in the same *m/z* interval, see **Figure S4C**.

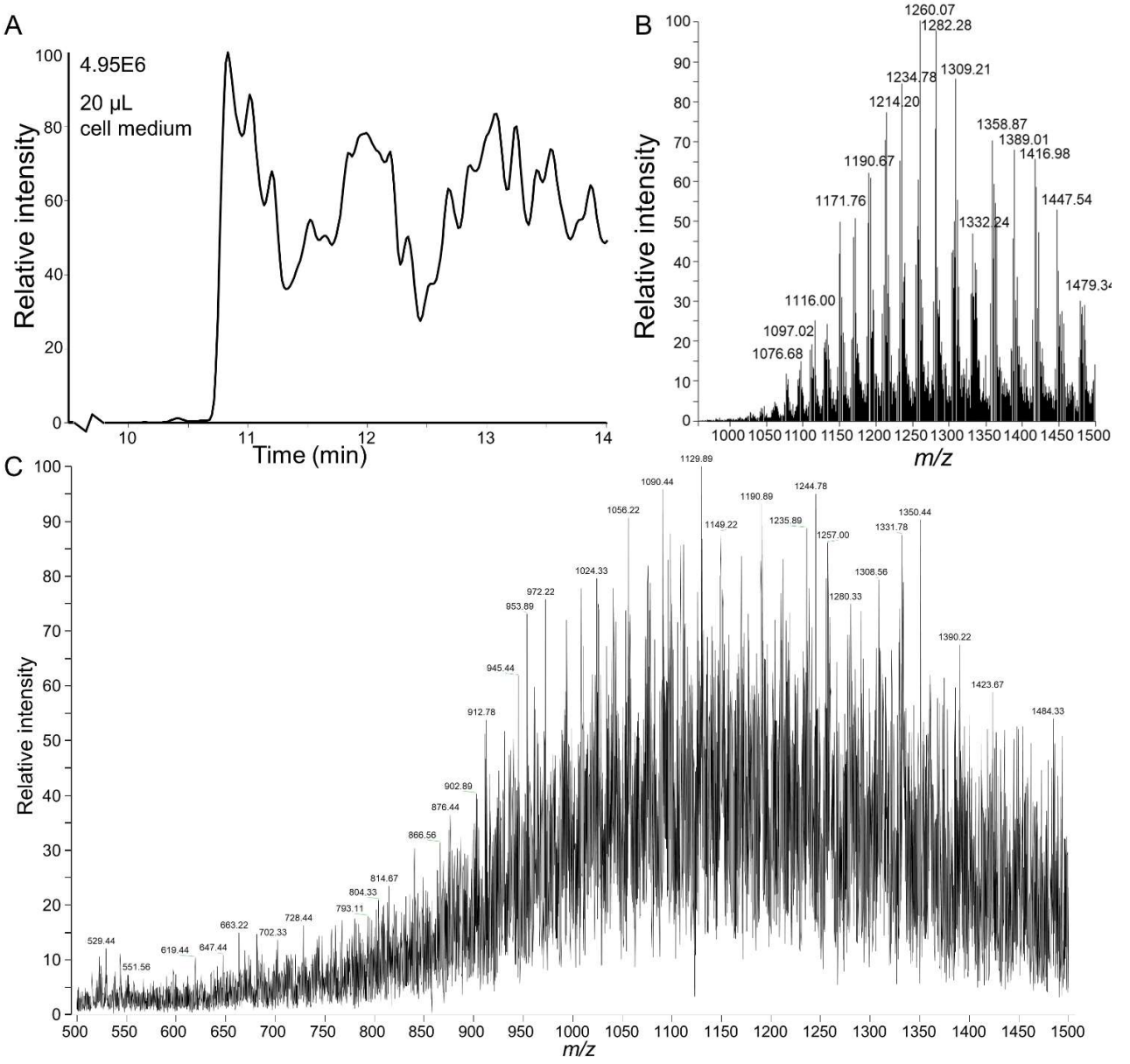

Figure S4: Effect of injection volume and sample matrix on the separation was examined in FullscanQ1 mode. **(A)** Extracted ion chromatogram (*m/z* 1162-1163) showing human insulin not detected in 20 µL injection of 6.25 pg/µL human insulin in 1% FA in cell medium. (**B**) The mass spectrum obtained from the large distorted peak visible in the chromatogram. (**C**) The mass spectrum obtained from direct injection of 10 ng/µL BSA in 50/50 ACN/H2O with 0.1% FA.

7 LC-MS/MS method sufficiently robust to maintain accuracy and precision without internal standard

The LC-MS/MS method robustness was evaluated by removing the internal standard and examining whether the method provided sufficient accuracy and precision without the internal standard. The three replicates of the 2.0 pg/µL human insulin quality control standard were individually determined

with a relative error of -7%, -11% and -11%, and the average concentration was found to be 1.9 pg/µL with an RSD of 11%, results visualized in **Figure S5**. The quality controls indicates that the accuracy and precision of the LC-MS/MS method was not compromised by removing the internal standard. Without internal standard, the LC-MS/MS determined human insulin secretion to be 1.8 pg/µL (n = 4, RSD = 37%) in low glucose, 1.8 pg/µL (n = 4, RSD = 21%) in high glucose, and 11.3 pg/µL (n = 4, RSD = 14%) in KCl environment. An independent two sample t-test, at 95% confidence, showed that the average insulin concentration found for the three different exposures determined by LC-MS/MS with and without internal standard were not significantly different.

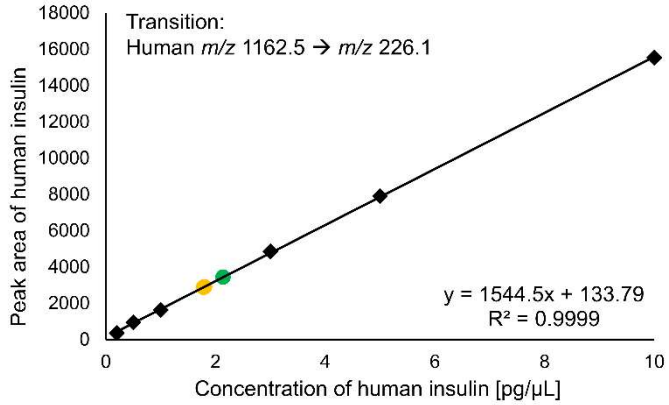

Figure S5: Calibration curve in 0.5% FA Krebs buffer, obtained by SRM, from 0.2 pg/µL to 10 pg/µL human insulin without internal standard(points marked in black), and three quality control standards at 2 pg/µL human insulin. Two quality controls are marked in yellow as the relative error was -10% and -11%, and the third QC is marked in green as the relative error was 7%.

8 Characterization of stem cell-derived islets

The SC-islets were generated from human pluripotent cell line H1 and maintained in suspension culture condition over 7 days until analysis. As shown in the bright field image, SC-islets were uniform in shape, with a diameter of around 100 µm at day 7 of aggregation (**Figure S6A**). Before being used for glucose-stimulated insulin secretion assay, SC-islets were further characterized with flow cytometry and immunofluorescence staining. Primary antibodies including human C-peptide (Developmental studies Hybridoma Bank, University of Iowa, IA, USA) and chromogranin A (CHGA, Novus Biologicals, Centennial, CO, USA) represent insulin-producing cells and pan-endocrine cells in the organoids respectively [4]. Representative flow cytometry quantification shows that > 96% of cells are endocrine cells (Q2 and Q3, **Figure S6B**), and > 83% of cells are insulin-producing cells (Q1 and Q2, **Figure S6B**). SC-islets were fixed with 4% PFA at room temperature for 30 min and embedded for cryosection. Section slides immunofluorescence staining corresponded

with flow cytometry results, showing that the majority of the cells are CHGA and human C-peptide-positive cells (**Figure S6C**).

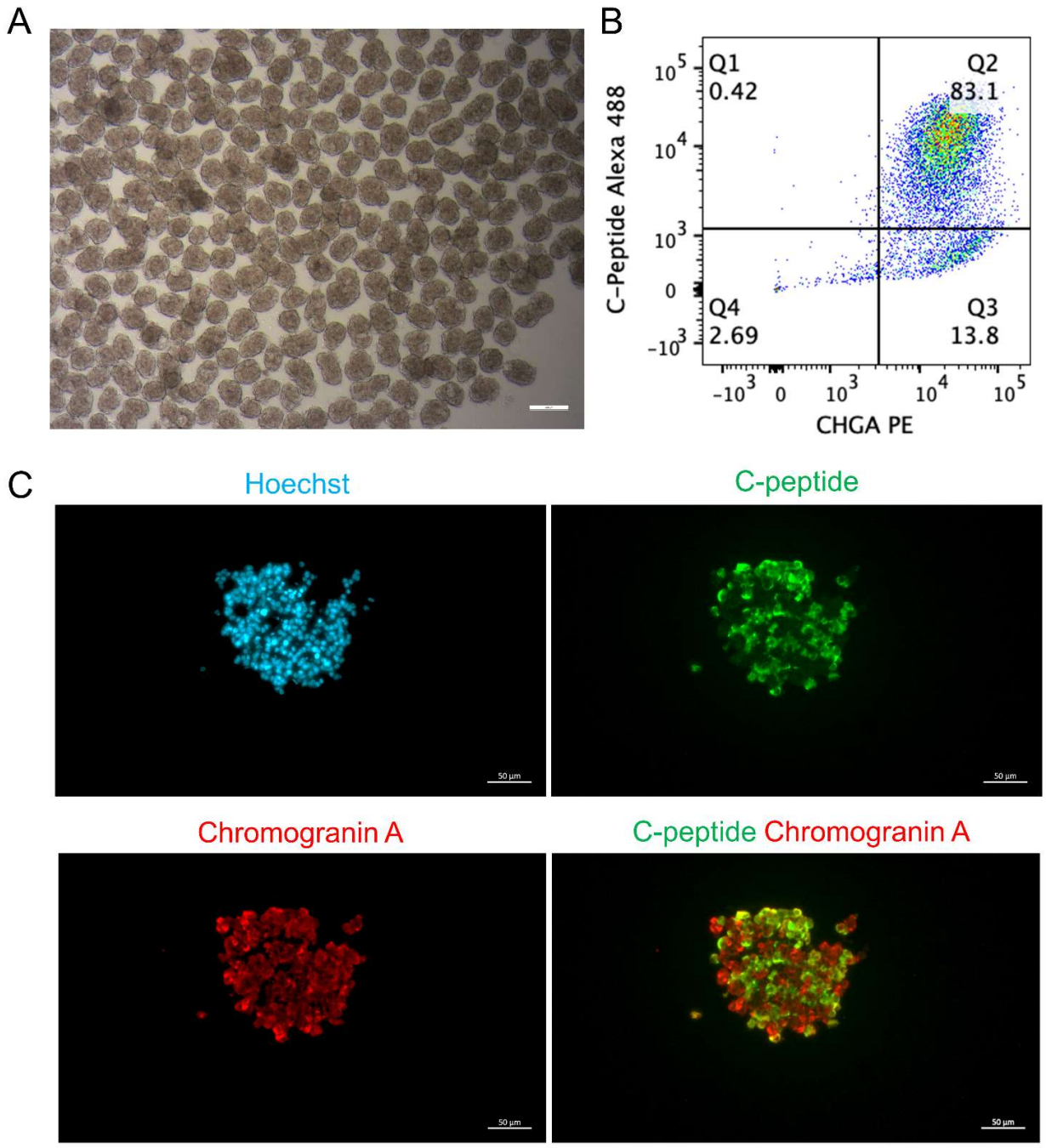

Figure S6: (**A**) Bright filed image of SC-islets. Scale bar = 200 µm. (**B**) Representative flow cytometry quantification (%) of dispersed SC-islets stained for C-peptide and Chromogranin A (CHGA). (**C**) Representative immunostaining images of SC-islets stained for Chromogranin A (red), C-peptide (green), and nuclei DNA with Hoechst (blue). Scale bar = 50 µm.

9 References in supplementary

[1] C. Rosting, C.Ø. Sæ, A. Gjelstad, T.G. Halvorsen, Evaluation of water-soluble DBS for small proteins: A conceptual study using insulin as a model analyte, Bioanalysis, 8 (2016) 1051-1065. https://www.future-science.com/doi/abs/10.4155/bio-2016-0002.

[2] A. Thomas, R. Yang, S. Petring, L. Bally, M. Thevis, Simplified quantification of insulin, its synthetic analogs and C-peptide in human plasma by means of LC-HRMS, Drug Test. Anal., 12 (2020) 382-390. https://analyticalsciencejournals.onlinelibrary.wiley.com/doi/abs/10.1002/dta.2765.

[3] K. Stejskal, D. Potěšil, Z. Zdráhal, Suppression of peptide sample losses in autosampler vials, J. Proteome Res., 12 (2013) 3057-3062. https://doi.org/10.1021/pr400183v.

[4] A. Lukinius, E. Wilander, B. Eriksson, K. Öberg, A chromogranin peptide is co-stored with insulin in the human pancreatic islet B-cell granules, Histochem. J., 24 (1992) 679-684. https://doi.org/10.1007/BF01047589.

III

Simultaneous LC-MS determination of glucose regulatory peptides secreted by stem cell-derived islet organoids

Christine Olsen[1,2], Chencheng Wang[2,3], Aleksandra Aizenshtadt[2], Shadab Abadpour[2,3], Elsa Lundanes[1], Frøydis Sved Skottvoll[4], Alexey Golovin[5], Mathias Busek[2], Stefan Krauss[2,5], Hanne Scholz[2,3], and Steven Ray Wilson[2,3]*

[1] Department of Chemistry, University of Oslo, Blindern, Oslo, Norway

[2] Hybrid Technology Hub-Centre of Excellence, Institute of Basic Medical Sciences, Faculty of Medicine, University of Oslo, Oslo, Norway

[3] Department of Transplant Medicine and Institute for Surgical Research, Oslo University Hospital, Oslo, Norway

[4] Department of Smart Sensors and Microsystems, SINTEF Digital, Oslo, Norway

[5] Department of Immunology and Transfusion Medicine, Oslo University Hospital, Oslo, Norway

*Correspondence should be addressed to the following author(s):

Prof. Steven Ray Wilson

Department of Chemistry

University of Oslo

Postboks 1033, Blindern 0315 Oslo

s.r.h.wilson@kjemi.uio.no.

Keywords: *Glucose regulatory hormones, liquid chromatography-tandem mass spectrometry, organ-on-chip, stem cell-derived islet organoids*

Abbreviations:

A_s	Asymmetry factor
FA	Formic acid
MEM NEAA	Minimum essential medium non-essential amino acids
N	Technical replicate
n	Biological replicate
RF	Radio frequency
rOoC	Recirculating organ-on-chip
SC-islets	Stem cell-derived islet organoids
SRM	Selected reaction monitoring
QC	Quality control

Abstract

For studying stem cell-derived islet organoids (SC-islets) in an organ-on-chip platform, we have developed a reversed phase liquid chromatography tandem mass spectrometry (RPLC-MS/MS) method allowing for simultaneous determination of insulin, somatostatin-14, and glucagon, with improved matrix robustness compared to earlier methodology. Combining phenyl/hexyl-C18 separations using 2.1 mm inner diameter LC columns and triple quadrupole mass spectrometry, identification and quantification were secured with negligible variance in retention time and quantifier/qualifier ratios, negligible levels of carry-over (< 2%), and sufficient precision (± 10% RSD) and accuracy (± 15% relative error) with and without use of internal standard. The here developed RPLC-MS/MS method showed that the SC-islets have an insulin response dependent on glucose concentration, and the SC-islets produce and release somatostatin-14 and glucagon. The RPLC-MS/MS method for these peptide hormones was compatible with an unfiltered off-line sample collection from SC-islets cultivated on a pump-less, recirculating organ-on-chip (rOoC) platform. The SC-islets background secretion of insulin was not significantly different on the rOoC device compared to a standard cell culture well-plate. Taken together, RPLC-MS/MS is well suited for multi-hormone measurements of SC-islets on an organ-on-chip platform.

1 Introduction

The development of organoids, i.e. laboratory-grown 3D organ models, is a rapidly growing field with broad implications on biomedical research [1, 2]. By combining organoids with microfluidics in an organ-on-chip (OoC) device, it has been possible to improve aspects of organ functionality *in vitro* compared to static 3D culture systems [3, 4]. Our research group focuses on applying separation science and mass spectrometry technology for studying metabolism of organoids under static conditions and on OoC devices [5, 6].

Pancreatic islets are composed of several endocrine cells, the majority of the cells being insulin-producing beta cells, somatostatin-14-producing delta cells, and glucagon-producing alpha cells [7]. The precise regulation of glucose homeostasis is controlled by the hormone secretion from these cells [8]. In type 1 and type 2 diabetes mellitus, both insulin secretion and glucagon secretion are impaired [9, 10]. Somatostatin-14 is a paracrine inhibitor of the secretion of insulin and glucagon, however, the role of somatostatin-14 in diabetes is not yet fully understood [11].

Stem cell-derived pancreatic islet organoids (SC-islets) are an emerging alternative for disease modeling of diabetes and cell replacement therapy [12, 13]. Similar to natural islets, SC-islets differentiated from embryonic stem cells consist of multiple types of endocrine cells [14, 15]. SC-islets should therefore be suitable for disease modeling and may serve as a source for islet transplantation in beta cell replacement therapy for type 1 diabetes patients [13, 15]. Another important hormone produced in the pancreatic islets is urocortin-3, which is a general maturation marker for both alpha and beta cells in humans [16, 17]. Urocortin-3 would also be beneficial to study in disease modelling, as it is a marker for dedifferentiated beta cells under diabetic conditions (i.e. altered phenotype with loss of insulin capabilities) [17].

The characterization of SC-islets, both under static conditions and on-chip, would benefit from a sensitive and robust methodology for simultaneous determination of multiple hormones. We have previously developed a sensitive reversed phase liquid chromatography – tandem mass spectrometry (RPLC-MS/MS) method for measuring insulin secreted from SC-islets [18]. However, we experienced limitations regarding sample matrix compatibility, i.e. the method was compatible with Krebs buffer (a balanced salt solution used to mimic physiological conditions), but not compatible with cell medium commonly applied in cultivation of organoids. We hypothesized that, by

improving the LC separation, the method could be improved to also include other hormones and be suitable for several biologically relevant sample matrices.

We here describe an expanded and more versatile RPLC-MS/MS method for simultaneous determination of insulin, somatostatin-14, and glucagon secreted by SC-islets, and show that the method is compatible with supernatant collected from SC-islets cultivated in a pump-less, recirculating organ-on-chip (rOoC) device [4]. We show that the SC-islets display an insulin response that is dependent on glucose concentrations. In addition, we were able to detect and quantify the release of somatostatin-14 and glucagon from the SC-islets, confirming that the SC-islets contain functional beta-, delta-, and alpha cells.

2 Materials and methods

2.1 Chemicals and solutions

Acetonitrile (ACN, LC-MS grade), bovine serum albumin (BSA, ≥ 98%), dimethyl sulfoxide (DMSO, ≥ 99.7%), formic acid (FA, 98%), insulin from bovine pancreas (HPLC grade), synthetic glucagon (≥ 95%, human HPLC grade), recombinant insulin human (≥ 98%), somatostatin-14 (≥ 97%, human HPLC grade), and urocortin-3 (≥ 97%, human HPLC grade) were all purchased from Sigma-Aldrich. Taxonomy will only be indicated for insulin, as all other peptides have human origin. Water (LC-MS grade), and methanol (MeOH, LC-MS grade) were obtained from VWR Chemicals (Radnor, PA, USA). Gibco™ basal cell medium MCDB131, GlutaMAX™ supplement (cat. no. 35050061) and minimum essential medium non-essential amino acids (MEM NEAA) stock solution by Gibco™ was acquired from Thermo Fisher Scientific (Waltham, MA, USA).

Krebs buffer was prepared in-house and consists of the following chemicals of analytical grade: 10mM HEPES, 128mM NaCl, 5mM KCl, 2.7mM $CaCl_2$, 1.2mM $MgSO_4$, 1mM Na_2HPO_4, 1.2mM KH_2PO_4, 5mM $NaHCO_3$, and 0.1% BSA.

Islet maturation cell medium was prepared in-house by adding 1% Penicillin/Streptavidin, 2% BSA, 10 µg/mL of heparin, 10 µM of ZnSO4, 0.1% of trace elements A and B stock solution, 1% of GlutaMAX™ stock solution and 1% of MEM NEAA stock solution to basal MCDB131 cell medium.

2.2 Preparation of individual hormone solutions and calibration solutions

Aqueous water solutions of human insulin, somatostatin-14, glucagon, urocortin-3, and bovine insulin (applied as internal standard for human insulin) were prepared individually by dissolving 1 mg of peptide powder in 1 mL of 0.1% FA in water. The 1 mg/mL stock solutions were further diluted to working solutions consisting of 10 ng/µL of each individual peptide, and divided into 100 µL aliquots. Aliquots of human and bovine insulin were kept at -20 °C until use or for a maximum of three months. Aliquots of somatostatin-14, glucagon, and urocortin-3 were kept at -80 °C until use. All

solutions containing proteins were prepared in protein low binding tubes from Sarstedt (Nümbrecht, Germany).

Separate standard solutions of 10 ng/µL of somatostatin-14, glucagon, and urocortin-3 in a 1+1 mixture of ACN and water were prepared for direct injections on the MS.

Solutions with human and bovine insulin in Krebs buffer and islet maturation cell medium were prepared in the same manner as described for water-based solutions, with the exception being the amount of FA: 0.5% FA in Krebs buffer and 1% FA in cell medium. Krebs buffer and cell medium solutions were spiked with separate water-based solutions of 10 ng/µL somatostatin-14, glucagon, and urocortin-3 and further diluted with the appropriate matrix to obtain the desired concentrations.

For assessment of the LC-MS method and the preparation of calibration solutions, freshly thawed working solutions of the peptides were further diluted to the desired pg/µL concentration with the experiment appropriate matrix, and spiked with bovine insulin to a concentration of 5 pg/µL unless stated otherwise. Quality controls (QC) were prepared in the same manner.

2.3 Cell culture, differentiation, and glucose stimulated insulin secretion for stem cell-derived islets

The SC-islets examined in this study, are prepared according to a previously described differentiation protocol [18]. In brief, SC-islets were generated from the human pluripotent cell line H1 (WA01, WiCell, Madison, WI, USA) with a stepwise differentiation protocol. Following the differentiation, the cells were aggregated as spheroids on an orbit-shaker for 7 days prior to analysis. For static conditions in Krebs buffer, batches of 30 SC-islets were placed in 24-well cell culture plates, hormone secretion was assessed by exposure to: 1 mL Krebs buffer with 2 mM glucose for 60 min at 37 °C, 1 mL Krebs buffer with 20 mM glucose for 60 min at 37 °C, and 1 mL Krebs buffer containing 20 mM glucose plus 30 mM KCl for 30 min at 37 °C. Up to 900 µL of supernatant was collected.

Insulin in the supernatant was quantified with human insulin enzyme-linked immunosorbent assay (ELISA) kit (Mercodia, Uppsala, Sweden) and with the LC-MS/MS method described in this study. Prior to injection on the LC-MS/MS system,

the collected supernatants were spiked with a total of 5 pg/µL of bovine insulin and 100% FA was added to a total of 0.5%.

2.4 Adsorption experiments on a poly(methylmethacrylate)-based organ-on-chip platform

Experiments were performed on the poly(methylmethacrylate) (PMMA)-based rOoC platform, which was fabricated in-house using laser-cutting and thermobonding as previously described in [4]. The rOoC platform consists of two nested circuits of perfusion channels separated with two organoids chambers. Channels are separated from the organoid chambers by a step reservoir with a height of 300 µm.

To evaluate surface adsorption in the rOoC platform, a solution consisting of 2 ng/µL of human insulin in Krebs buffer was incubated on-chip and in standard cell culture 24-wells plate from Corning (Corning, NY, USA) for 20 hours, and compared to an aliquot stored in the freezer.

2.5 Background secretion experiments from stem cell-derived islets cultivated on-chip and in static system

SC-islets were cultured in islet maturation cell medium in a rOoC platform with a modified design compared to [4], where the chamber for SC-islets was placed under the perfusion channel to facilitate media and oxygen exchange. In the organoids chamber, batches of 3-6 SC-islets were embedded in extracellular matrix (Geltrex, Gibco, cat. n A1569601) and cultured for 7 days under perfusion. The cell medium in the channels was collected after 24 h of incubation on day 5 and day 7. In the off-chip control culture, batches of 14-19 SC-islets were cultured in 24-well plates for 7 days, and cell medium was collected after 24 h of incubation on day 5 and day 7.

2.6 Gel electrophoresis

A water-based solution consisting of 10 ng/µL human insulin and 10 ng/µL BSA was used as a protein marker during gel electrophoresis. To 30 µL of the sample, 10 µL of Bolt™ LDS sample buffer (4x) was added prior to heating at 70 °C for 10 min on a Thermo-Shaker from Grant instruments (Shepreth, UK). The samples were loaded

with ultrafine pipettes, from VWR, onto a Bolt™ 4-12% 2-(bis(2-hydroxyethyl)amino)-2-(hydroxymethyl)propane-1,3-diol (bis-tris) plus gel inserted in a mini gel tank. The chamber was filled with Bolt™ 2-(N-morpholino)ethanesulfonic acid (MES) SDS running buffer (20x), diluted to 1x with water. All Bolt™ products and the mini gel tank were from Thermo Fischer Scientific. For 20 min, a voltage of 200 V was applied to the gel by a power supply from Delta Elektronika (Zierikzee, Netherlands).

Subsequently, the gel was washed four times with water for five minutes on a shaker. Following the wash, the gel was covered with Imperial™ protein stain (from Thermo Fischer Scientific) and left on shaking for 15 min. Before photographing the gel using a smartphone camera, the gel was washed with water four times for five minutes, followed by washing with gentle shaking in water overnight (18 hours).

2.7 Liquid chromatography - mass spectrometry instrumentation

The LC-MS system applied in this study has been used for insulin determination previously [18]. In brief, the conventional LC system was a modified Agilent 1100 series pump (Santa Clara, CA, USA) employing only shielded fused silica connectors (shielded fused silica nanoViper™ sheated in polyetheretherketone tubing from Thermo Fisher). Injection was achieved by coupling a 6-port-2-position valve, with a 50 µm inner diameter (id) x 550 mm (1.08 µL) shielded fused silica loop or a 20 µL shielded fused silica loop. A 250 µL glass syringe was used for injection, following injection the syringe and the loop was washed by flushing the syringe three times with 50/50 MeOH/water, before washing the loop twice with the MeOH/water solution. Prior to next injection, the syringe was washed once with 0.1% FA in water and the loop was washed twice with 0.1% FA in water. The column set-up consisted of an Accucore™ phenyl/hexyl guard column (2.1 mm id x 10 mm, 2.6 µm, 80 Å) attached within a Uniquard drop-in holder to the InfinityLab Poroshell EC-C18 separation column (2.1 mm id x 50 mm, 2.7 µm, 120 Å).

The applied MS was a TSQ Quantiva triple quadrupole MS equipped with a heated electrospray ionization source (H-ESI-II probe) both from Thermo Fisher. The vaporizer temperature was set to 210 °C, and a spray voltage of 3.5 kV was applied to the H-ESI-II probe. Sheath gas was set at 20 Arb (approx. 2.7 L/min), while auxiliary

gas was set at 9 Arb (approx. 7.5 L/min), and sweep gas was not applied. The ion transfer tube temperature was kept at 275 °C.

2.8 Optimized gradient settings for LC separation

The mobile phase reservoirs contained 0.1% FA in water added 1% DMSO and 0.1% FA in ACN added 1% DMSO, respectively. A 150 µL/min solvent gradient was started at 1% B, quickly increased to 25% B in 1 min, then linearly increased to 32.5% B in 6 min, and kept at 32.5% B for 4 min. In the following step, the %B was quickly increased to 80% B and kept at 80% for 2 min, before quickly decreased to 40% B, and kept at 40% B for 3 min, before being further decreased to 1% B and kept at 1% B for 7 min. The gradient had a total runtime of 23 min, including column re-equilibration for 7 min at 1% B.

2.9 Alternative guard and separation column

Other columns examined in this study included an Accucore™ C18 guard column (2.1 mm id x 10 mm, 2.6 µm, 80 Å) from Thermo Fisher, and a Cortecs Premier C18 separation column (2.1 mm id x 10 mm, 2.7 µm, 90 Å) from Waters (Milford, MA, USA).

2.10 Settings for selected reaction monitoring

The collision energies and radio frequency (RF) lens voltage were optimized using the compound optimization provided in Xcalibur. The transitions, used in selected reaction monitoring (SRM), including collision energies and RF lens voltage, are listed in **Table 1**. The collision gas (argon) pressure in q2 was 4.0 mTorr and the cycle time was set to 1 sec (equal to 77 ms or 91 ms dwell time per transition with and without urocortin-3, respectively).

Table 1: SRM transitions used for human insulin, bovine insulin (internal standard for human insulin), human somatostatin-14, human glucagon, and human urocortin-3 including quantifier/qualifier status, precursor ion, product ion, and collision energy. The settings applied for human urocortin-3 during method development are also included.

Compound	Identity	Precursor ion (*m/z*)	Product ion (*m/z*)	Collision energy (V)	RF lens (V)
Human insulin	Quantifier	1162.5	226.1	41	210
	Qualifiers	1162.5	345.1; 1159.0	42; 22	210
Bovine insulin	Quantifier	1147.8	226.2	41	210
	Qualifiers	1147.8	315.2; 1144.5	42; 20	210
Human somatostatin-14	Quantifier	819.6	221.1	40	182
	Qualifier	819.6	129.1	38	182
Human glucagon	Quantifier	871.6	1084.0	26	171
	Qualifiers	871.6	1040.4; 305.1	27; 43	171
Human Urocortin-3	Method development	1035.5	1121.7; 1193.1	29; 27	174

3 Results and discussion

3.1 Optimized gradient separation allowed for simultaneous determination of insulin, somatostatin-14 and glucagon in bovine serum albumin rich matrices

Initial MS/MS settings for somatostatin-14, glucagon, and urocortin-3 were established by direct injection: *m/z* 819.6 → *m/z* 221.1, 129.1 (somatostatin-14), *m/z* 871.6 → *m/z* 1084.0, 1040.4, 305.1 (glucagon), and *m/z* 1035.5 → *m/z* 1121.7, 1193.1 (urocortin-3). The MS/MS settings for human and bovine insulin were selected previously to be: *m/z* 1162.5 (+5) → *m/z* 226.1, 345.0, 1159.0 and *m/z* 1147.8 (+5) → *m/z* 226.2, 315.2, 1144.5, respectively [18]. The four analytes and the internal standard were successfully separated in a water-based solution with the originally applied gradient (8 min separation window from 1% B to 60% B [18]), shown in **Figure 1A**. However, when the analytes were dissolved in Krebs buffer, the separation of urocortin-3 from BSA was not possible, see **Figure 1B**. BSA is the main component in both Krebs buffer and in the cell medium that is used for culturing SC-islets, containing 0.1% BSA and 2% BSA, respectively. BSA produces a multitude of interfering peaks in the *m/z* range from 1000-1500 [18]. Effort was put towards optimization of the gradient, in order to achieve better separation of the peptide hormones from BSA.

By applying a shallow gradient from 25% B to 32.5% B, with an 1.25% B increase per minute, followed by an isocratic step at 32.5% B for 4 minutes, the BSA interference was removed from the insulins, somatostatin-14, and glucagon in both Krebs buffer (**Figure 1C**) and cell medium (**Figure 1D**). Urocortin-3 remained impossible to separate from the BSA in the Krebs buffer in the current set-up, as shown in **Figure 1C**, and was not examined further in this study (see Conclusions sections for further discussion). In addition, the collision gas pressure was increased from 2.5 mTorr used in the original method to 4.0 mTorr due to significantly increased peak area for human insulin and glucagon, see **SI-1** for more details.

In conclusion, by optimizing the applied gradient in the LC separation, the existing RPLC-MS/MS method could be improved to include three of the main hormones produced in islets: Insulin, somatostatin-14, and glucagon, while not being limited by the sample matrix. However, the current column set-up was not suitable for the

inclusion of a more retained hormone, urocortin-3, which was not separated from the matrix components.

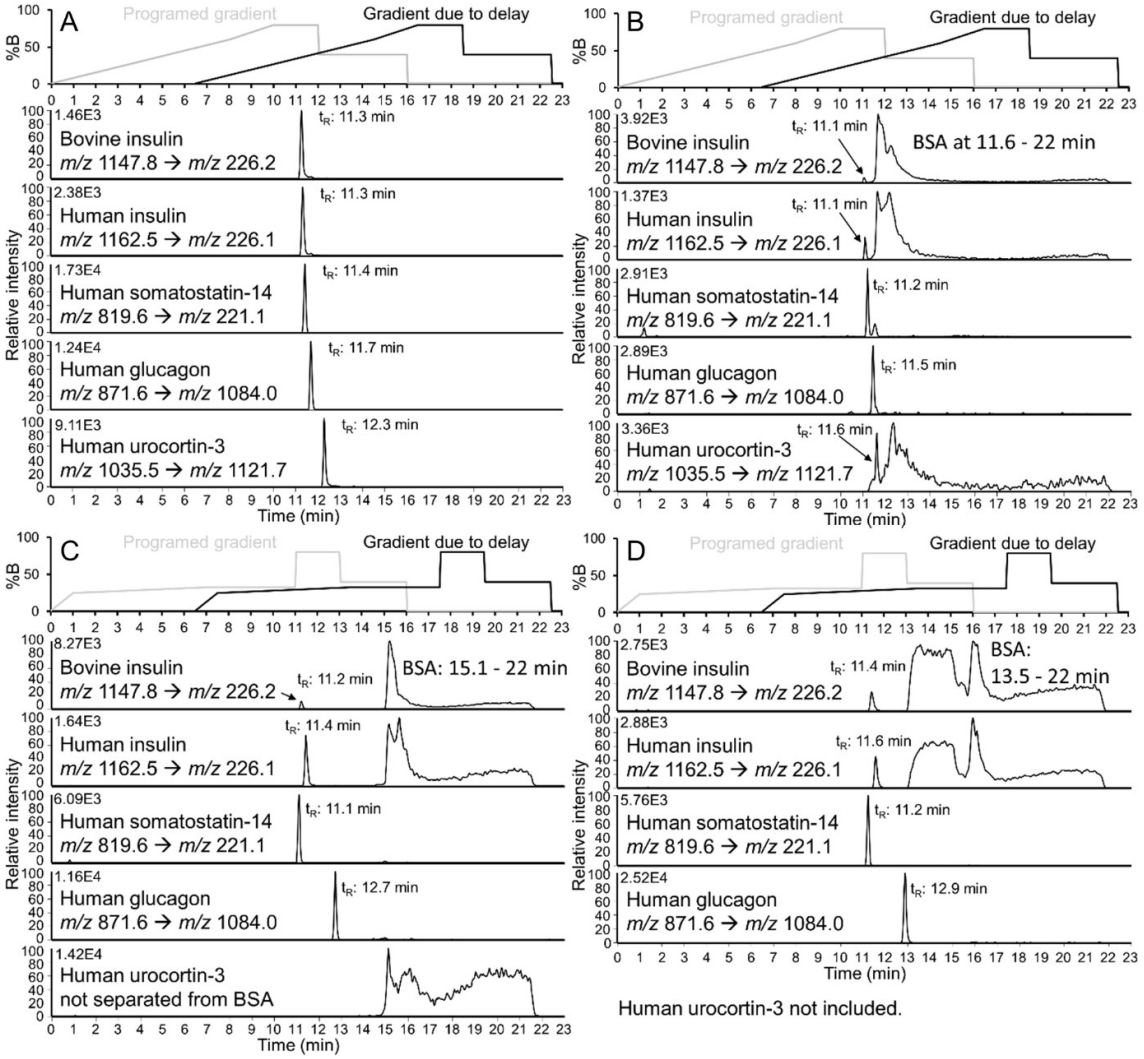

Figure 1: Separation of a peptide mix consisting of bovine insulin, human insulin, somatostatin-14, glucagon and urocortin-3 in different sample matrices. With the original steep gradient: (**A**) 1.08 µL injection of 250 pg/µL peptide mix in 0.1% FA in water, and (**B**) 20 µL injection of 2 pg/µL peptide mix in 0.5% FA in Krebs buffer. With an optimized shallow gradient: (**C**) 20 µL injection of 5 pg/µL peptide mix in 0.5% FA in Krebs buffer, and (**D**) 20 µL injection of 5 pg/µL peptide mix in 1.0% FA in cell medium. The first panel above each separation shows the programed gradient and the gradient due to system delay. The system delay of 6.5 min in the gradient delivery was estimated by running the analysis under non-retained conditions starting at 60% B, see **SI-2** for more details.

3.1.1 Guard cartridge: not one-size-fits-all for determination of intact peptides

In the previous section and in Olsen et al. [18], an Accucore phenyl/hexyl guard cartridge (80 Å, 2.6 µm particles, 2.1 mm inner diameter x 10 mm) combined with a Poroshell EC-C18 separation column (120 Å, 2.6 µm particles, 2.1 mm inner diameter x 50 mm) were applied in the LC-MS system. Traditionally, the guard column is packed with the same particles and stationary phase as the separation column. However, it is commonly accepted that combining different stationary phases on a two-column set-up, with a trapping column and a separation column, can improve the separation [19]. The combination of an Accucore phenyl/hexyl trapping column and Poroshell C18 separation column has previously been successfully applied for determination of insulin in urine matrix [20].

To examine in detail if the phenyl/hexyl guard cartridge significantly affected the separation, the separation was compared with and without the phenyl/hexyl guard. In addition, an equivalent Accucore C18 guard cartridge (80 Å, 2.6 µm particles, 2.1 mm inner diameter x 10 mm) was assessed as an alternative to the phenyl/hexyl guard. Asymmetry factors and peak areas obtained on different column set-ups for the peptides are summarized in **Table 2**.

The asymmetry factor obtained for human insulin increased from 2.3 (N = 3, technical replicates on LC-MS), **Figure 2A**) with the phenyl/hexyl guard to 5.6 (**Figure 2B**) on the C18 guard cartridge, and the peak area was reduced from 7.79 x 10^3 on the phenyl/hexyl to 6.71 x 10^3 on the C18. Without applying a guard cartridge, the asymmetry factor for human insulin was 1.8 (**Figure 2C**) and the peak area was 8.05 x 10^3. By one-factor analysis of variance (ANOVA), there was no significant difference in the obtained peak area of human insulin with or without guard cartridge or type of guard. However, the tailing effect for human insulin obtained on the C18 guard was significantly larger compared to that on the phenyl/hexyl guard or without applying a guard. Additionally, there was no signal detected of human insulin in a subsequent blank injection on the set-up without guard or with the phenyl/hexyl guard, but the C18 guard contributed to 5% carry-over of human insulin.

For bovine insulin, the asymmetry factor was not significantly different for the various column set-ups, however the peak area was significantly higher with the phenyl/hexyl

guard compared to the C18 guard. The peak area obtained with the phenyl/hexyl guard was not significantly different to the peak areas obtained without guard.

For somatostatin-14, the asymmetry was not significantly different for the different column set-up, however, the peak area was significantly increased without a guard cartridge being applied compared to the phenyl/hexyl guard, information summarized in **Table 2**. There was no significant difference between the C18 and the phenyl/hexyl guard or C18 and without guard applied concerning peak areas obtained for somatostatin-14.

For glucagon, the peak areas were significantly higher when applying the phenyl/hexyl guard cartridge compared to no guard cartridge applied or the C18 cartridge, while the asymmetry factor was not significantly different for the different column set-ups, summarized in **Table 2**.

The differences in the obtained chromatographic performances show that there isn't a "one-size-fits-all" approach when selecting guard cartridge for determination of various intact peptides, and large effects for asymmetry factor and peak areas can be seen based on changing the stationary phase. Based on our findings, it is hard to conclude why the C18 guard cartridge caused dramatic tailing for human and bovine insulin, and if there was an effect of having particles with smaller pore sizes in the guard cartridge compared to the separation column (80 Å vs 120 Å). When considering the use of guard cartridge, the LC-MS method was intended for experiments with supernatant collected directly from SC-islets possibly containing cell debris and particles, which would not be beneficial to inject directly onto the more expensive separation column without the protection from a guard cartridge.

In conclusion, we continued to employ a phenyl/hexyl guard cartridge based on the significantly higher peak areas obtained for glucagon and the guard cartridge's protection of the separation column when analyzing unfiltered samples collected directly from SC-islets.

Table 2: Chromatographic performance by injection of a peptide mix consisting of 5 pg/µL of bovine and human insulin, somatostatin-14, and glucagon. The obtained asymmetry factor (A_s) and peak area of the peptides are shown for the following guard cartridge options: Accucore phenyl/hexyl, Accucore C18, and no guard cartridge, combined with the Poroshell EC-C18 separation column (N = 3).

Columns	Accucore phenyl/hexyl-Poroshell C18	Accucore C18-Poroshell C18	No guard-Poroshell C18
Bovine insulin			
A_s	1.9 (14% RSD)	4.6 (13% RSD)	2.2 (13% RSD)
Peak area	8.64×10^3 (13% RSD)	4.92×10^3 (6% RSD)	5.63×10^3 (6% RSD)
Human insulin			
A_s	2.3 (14% RSD)	5.6 (7% RSD)	1.8 (13% RSD)
Peak area	7.79×10^3 (6% RSD)	6.71×10^3 (3% RSD)	8.05×10^3 (5% RSD)
Somatostatin-14			
A_s	1.5 (2% RSD)	1.7 (19% RSD)	1.4 (4% RSD)
Peak area	1.70×10^4 (10% RSD)	1.99×10^4 (2% RSD)	2.30×10^4 (4% RSD)
Glucagon			
A_s	1.5 (22% RSD)	2.1 (10% RSD)	1.8 (8% RSD)
Peak area	5.97×10^4 (4% RSD)	4.44×10^4 (3% RSD)	4.57×10^4 (1% RSD)

3.1.2 Success of intact hormone analysis is dependent on type of separation column

All three hormones and the internal standard have a minimum of one sulfur-containing amino acid residue (i.e. cysteine and methionine), which may cause adsorption on stainless steel column housing and contribute to band broadening [21, 22]. To see if this was the case in out set-up and if the chromatographic performance could be improved, a Premier column (C18, 2.6 µm, 90 Å) with modified metal surfaces in the column housing and filters to reduce non-defined adsorption was compared to the Poroshell column employed in previous sections [23]. For our particular application, the peaks of insulins and glucagon obtained on the Premier column were broader and not sufficiently separated from BSA or other matrix components in Krebs buffer, **Figure 2D**. The lack of separation indicated that the gradient optimized for the Poroshell column (C18, 2.7 µm, 120 Å) was not suitable for the Premier column. In the

attempt to optimize the separation, the peak area of glucagon was greatly reduced for each subsequent injection (from a peak area of approx. 2 x 10^5 to a peak area < 1 x 10^4, results not shown), and none of the insulins were successfully separated from BSA, **Figure 2E**. On the Accucore phenyl/hexyl-Poroshell C18 column set-up, an equivalent injection would give a stable peak area of glucagon around 250000. For somatostatin-14, the Premier column set-up was able to provide equivalent chromatographic performance as the phenyl/hexyl-Poroshell C18 column set-up.

Based on the lack of separation from BSA and the loss of signal for glucagon on the Premier column, the Premier column was not found appropriate for our application and was not examined further. One of the major differences between the Premier column and the Poroshell column is the pore size of the particles of 90 Å and 120 Å, respectively. In the previous **Section 3.1.1**, the guard cartridges with 80 Å particle pore size was sufficient for sample loading. However, from the comparison of the Premier and Poroshell column, it is clear that larger pores in the separation column was necessary to be able to separate the intact hormones from BSA and other matrix components [18, 24].

In conclusion: of the columns tested, the originally applied Poroshell C18 separation column was found to be the best option for the simultaneous determination of the three peptide hormones in complex matrices.

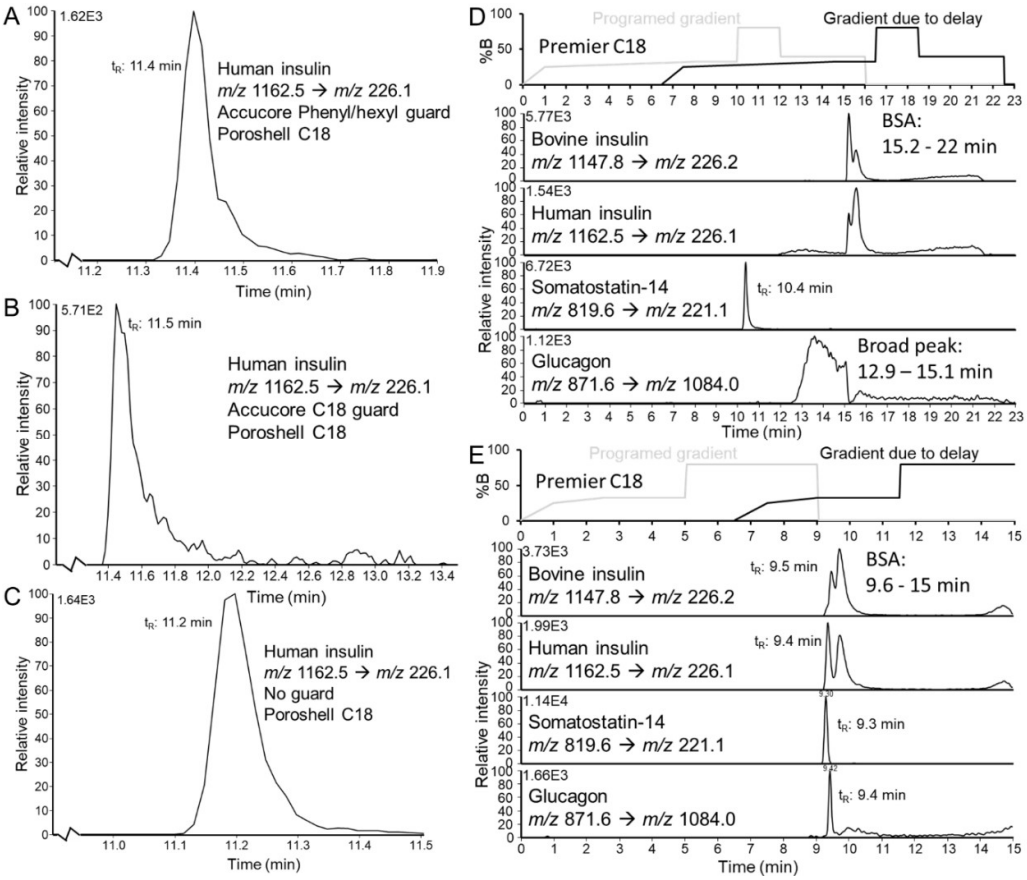

Figure 2: Comparison of peak shape obtained for human insulin on the following column set-ups (**A**) Accucore phenyl/hexyl guard – Poroshell C18, (**B**) Accucore C18 guard – Poroshell C18, and (**C**) only the Poroshell C18 column. Attempted separation of 5 pg/µL peptide mix in 0.5% Krebs buffer on the Premier column with different gradients: (**D**) Insufficient separation of insulins and glucagon from BSA with the same gradient as applied for the Poroshell Column. (**E**) Following attempted gradient optimization, still insufficient separation of insulins and BSA, and low signal intensity for glucagon.

3.2 Satisfactory accuracy and precision in determining concentration of insulin, somatostatin-14, and glucagon in quality controls in Krebs buffer

Glucose stimulated insulin secretion is a standard characterization experiment of insulin response in SC-islets using Krebs buffer [25, 26]. The experiments require highly accurate determinations of hormone concentrations in Krebs buffer. Therefore, the method's repeatability concerning linearity, precision, and accuracy in determination of the concentration of the three hormones was examined by establishing a linearity curve in the range from 5 pg/µL to 15 pg/µL in Krebs buffer over three days. The precision and accuracy for determination of hormone concentrations were evaluated based on concentration found in QCs containing 10 pg/µL of each analyte.

The established linearity curves for human insulin (with bovine insulin as internal standard, see **Figure 3A**), somatostatin-14 (**Figure 3C**), and glucagon (**Figure 3E**) did not show sign of heteroscedasticity (i.e. difference in variation of the response depending on the concentration level) as the residuals appear to fall randomly around the x-axis in the residual vs concentration plots in **Figure 3B**, **Figure 3D**, and **Figure 3F**, respectively [27]. The hypothesis of homoscedasticity was confirmed with an F-test comparing the variance in the response of the standard with the lowest and highest concentration levels for each of the analytes.

Bovine insulin was a suitable internal standard for human insulin due to similar structures, similar retention time and the variation of the peak area of bovine insulin was 4% RSD (N = 5) on day 1, 3% RSD (N = 5) on day 2, and 3% RSD (N = 5) on day 3. The variation in the peak area of bovine insulin was much smaller during these examinations compared to the examination done in **Section 3.1.1**, as changes to the system was not done between injections allowing for a better stability. Determination of somatostatin-14 and glucagon was done without use of bovine insulin as internal standard, due to large differences in the structures of the analytes compared to bovine insulin, and different retention time. These differences indicates that bovine insulin is not a suitable internal standard as it cannot compensate for differences in matrix effect (different retention time) nor the transfer from ions in solution into gas phase occurring during the ESI process (different structures). Bovine insulin could compensate for differences in injection volume, however, there is relatively small variation between

repeated injections that such compensation was not deemed necessary. The retention time variance over the three days was ≤ 0.5% RSD (N = 24) for all of the hormones, see **Figure 3G**.

In determination of QC analyte concentration using the same standard solutions to establish a calibration curve, the accuracy was within ± 10% relative error (N = 3, per day), ± 10% RSD (N = 3) intra-day precision and ± 10% RSD (N = 9) inter-day precision. Determination based on a single injection of the QC, only somatostatin-14 was not determined with an accuracy within ± 15% relative error, as shown in **Figure 3H** for injection number nine. The average concentration of each analyte found in the QCs on the three separate days was not significantly different determined with one-way ANOVA.

To summarize, the RPLC-MS/MS method, featuring a phenyl/hexyl guard and Poroshell C18 separation column combined with triple quadrupole mass spectrometry, was successful in simultaneous determination of the three analytes; human insulin (including bovine insulin as internal standard), somatostatin-14, and glucagon in Krebs buffer with sufficient accuracy, precision, and repeatability.

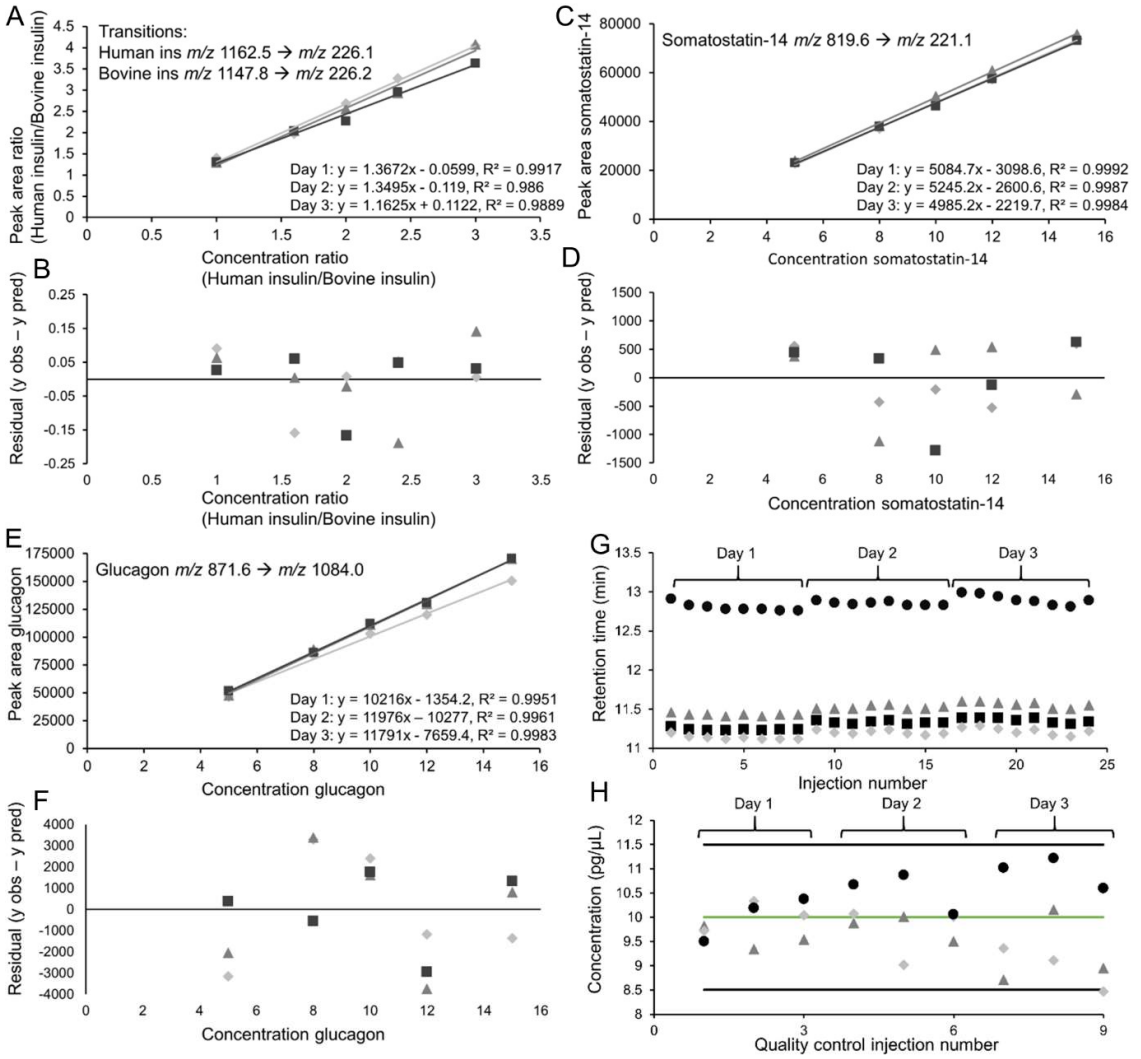

Figure 3: Established linearity curves in the range from 5 pg/µL to 15 pg/µL for (**A**) human insulin with bovine insulin as internal standard, (**C**) somatostatin-14, and (**E**) glucagon, where day 1 is represented with diamonds, triangles for day 2 and squars for day 3. Residual vs concentration plots for each curve belonging to (**B**) human insulin, (**D**) somatostatin-14, and (**F**) glucagon, where day 1 is represented with diamonds, triangles for day 2 and squars for day 3. (**G**) The retention time for bovine insulin (squares), human insulin (triangles), somatostatin-14 (diamonds), and glucagon (circles) over the 24 injections of calibration standards and QCs. (**H**) Determined concentration in QCs for human insulin (triangles), somatostatin-14 (diamonds), and glucagon (circles) in the nine injections.

3.3 Stem cell-derived islet organoids show glucose concentration dependent insulin response and potassium dependent release of somatostatin-14 and glucagon in Krebs buffer

As mentioned in the previous section, the secretion of peptide hormones in SC-islets can be examined by exposing the SC-islets to Krebs buffer containing various amounts of glucose. It has also been shown that the three major cell types found in islets, beta-, delta-, and alpha cells, release a large pool of stored hormones when exposed to high levels of potassium due to direct membrane depolarization [11, 28, 29]. Hence, to show compatibility between supernatant collected from SC-islets in Krebs buffer and RPLC-MS/MS, we attempted to measure the three hormones in Krebs buffer collected from SC-islets exposed to: (1) low amount of glucose (2 mM), (2) high amount of glucose (20 mM) and (3) a combination of 20 mM glucose and 30 mM KCl.

The concentration of insulin determined with RPLC-MS/MS in the supernatant collected from SC-islets challenged with low glucose (**Figure 4A**) was on average 2.2 pg/µL (RSD = 13%, n = 4 batches of SC-islets, N = 1), while there was 4.1 pg/µL insulin (RSD = 10%, n = 4, N = 1) secreted by SC-islets challenged with high glucose (**Figure 4B**). The stimulation index of insulin secretion during the glucose challenge was 1.86 (RSD = 5%, n = 4, N = 1). The amount of insulin determined in the samples collected with 20 mM glucose and 30 mM KCl (**Figure 4C**) was 18 pg/µL (RSD = 14%, n = 4, N = 1), which was eight times higher than the response in low glucose. Simultaneously, the reliability of the determination of insulin using the RPLC-MS/MS method was supervised by QCs, to see if the reported concentrations was within 15% relative error. QCs were included at 2 pg/µL (N = 2), 8 pg/µL (N = 3) and 18 pg/µL (N = 2), and the insulin concentration was determined within 15% relative error for each injection.

The insulin concentration in the supernatant collected from the SC-islets was also determined with an established ELISA method, which found the following insulin concentrations: 2.6 pg/µL (low glucose, RSD = 5%, n = 4, N = 1), 4.5 pg/µL (high glucose, RSD = 13%, n = 4, N = 1), and 20 pg/µL (KCl, RSD = 13%, n = 4, N = 1). An independent two sample t-test, at 95% confidence, showed that the concentrations determined by LC-MS/MS were not significantly different from the concentrations determined with ELISA.

The same samples were also simultaneously examined for somatostatin-14 and glucagon. Neither the quantifier nor the quantifier transition of somatostatin-14 and glucagon was detected in the supernatant from SC-islets exposed to low (**Figure 4A**) or high glucose (**Figure 4B**), however, in supernatant collected after exposure to KCl, detectable signals were obtained for both hormones and transitions (**Figure 4C**). For somatostatin-14, the average peak area was 1.3 x 10^3 (RSD = 7%, n = 4, N = 1) after KCl exposure, which was lower than the peak area of 1.9 x 10^3 obtained for the calibration standard with the least amount of somatostatin-14 of 0.25 pg/µL (**Figure 4D**). For glucagon, the concentration was determined to be 0.28 pg/µL (RSD = 18%, n = 4, N = 1) after KCl exposure. The QCs examined for somatostatin-14 and glucagon at 2 pg/µl and 8 pg/µL were determined within 11% relative error (RSD < 10 %), showing that the RPLC-MS/MS method for somatostatin-14 and glucagon has sufficient precision and accuracy without use of an internal standard.

For insulin, it was beneficial that the samples had been examined by a clinically approved ELISA kit prior to being analyzed by the LC-MS method [30], as a suitable calibration concentration range could easily be selected. For the other hormones, somatostatin-14 and glucagon, a gold standard for determination of the concentrations have not yet been established [31-33]. A calibration concentration range was selected without prior information about expected concentration of analytes in the sample, the concentration in the samples were found to be below or around the lowest concentration calibration standard (0.25 pg/µL). Therefore, the samples collected with 20 mM glucose and 30 mM KCl were reexamined with a calibration from 0.1 pg/µL to 3 pg/ µL for stomatostatin-14, and 0.05 pg/µL to 3 pg/µL for glucagon, including QCs at 0.4 pg/µL. The concentration for somatostatin-14 could now be determined and was found to be 0.27 pg/µL (RSD = 20%, n = 4, N = 1) in the samples collected with KCl. For glucagon, the concentration was determined with the new calibration curve to be 0.31 pg/µL (RSD = 18%, n = 4, N = 1), which was not significantly different form the concentration determined with the first calibration curve based on an independent two sample t-test (95 % confidence). The QCs examined at 0.4 pg/µL was all within 10% relative error for somatostatin-14 (N = 3), and 11% relative error for glucagon (N = 3).

The carry-over was less than 1% for all of the analytes and the internal standard, shown in a representative chromatogram from a blank injection of 0.5% FA in Krebs buffer following injections of the standards used to establish the curve in **Figure 4E**.

In addition, the carry-over was equal to less than 20% of the peak area obtained in the calibration standard with the smallest concentration of the analytes, giving a lower limit of quantification of 0.2 pg/µL for human insulin, 0.1 pg/µL for somatostatin-14, and 0.05 pg/µL for glucagon. The retention time variation was less than 0.2% RSD (N = 26) for all of the analytes and the internal standard.

A challenge when examining supernatant collected from SC-islets after exposure to different levels of glucose and KCl, is the change in the sample matrix. In this study, Krebs buffer without glucose or KCl was used as the solution for preparation of the calibration standards. Possible effects of glucose and KCl in the samples has not been examined. The ratio of the quantifier and qualifier transitions obtained for each hormone is shown in **Figure 4F**. For bovine and human insulin, the quantifier/qualifier ratio was not significantly different in samples with different amounts of glucose or KCl (determined with one-way ANOVA). In addition, for all analytes and bovine insulin, an independent two sample t-test, at 95% confidence, confirmed there was no significant difference in the quantifier/qualifier ratio obtained in the samples compared with the quantifier/qualifier ratio obtained in the calibration standards and QCs. The identification and quantification in the RPLC-MS/MS method is secured by negligible variance in retention time and quantifier/qualifier ratios, negligible levels of carry-over (< 1%), and sufficient precision and accuracy.

In conclusion, the RPLC-MS/MS method demonstrates sufficient detection limits for determination of insulin secretion in the supernatant of SC-islets (n = 30). In addition, we show that the SC-islets obtained through our differentiation protocol [18], have obtained a glucose dependent insulin secretion in response to 2 mM and 20 mM glucose. The method can also determine the production of somatostatin-14 and glucagon in 20 mM glucose and 30 mM KCl. However, better sensitivity is needed to determine secretion of somatostatin-14 and glucagon in SC-islets (n = 30) stimulated by glucose alone.

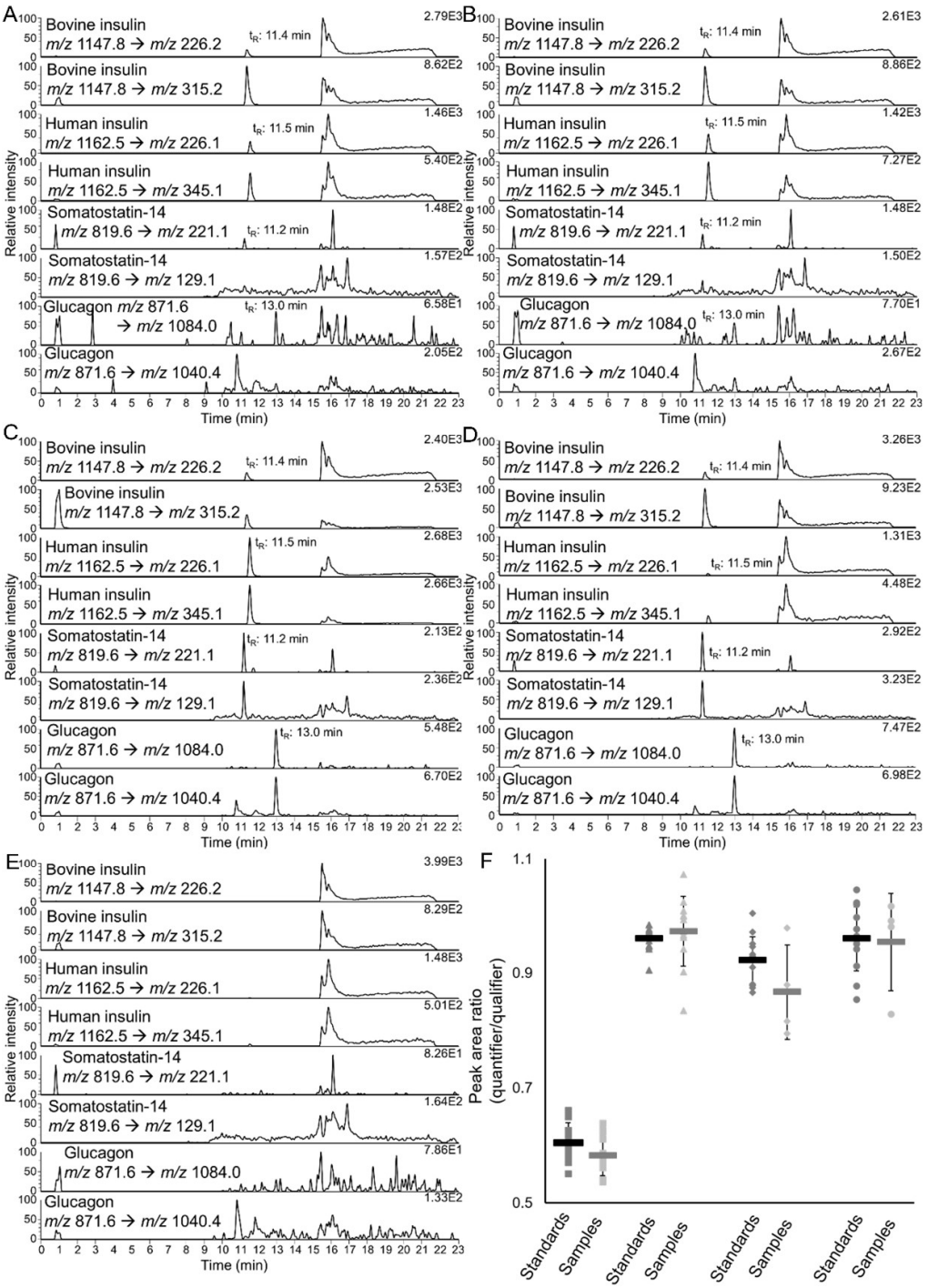

Figure 4: Representative chromatograms obtained in SRM mode of: Supernatant from SC-islets exposed to (**A**) 2 mM glucose, (**B**), 20 mM glucose, and (**C**) 20 mM glucose with 30 mM KCl. (**D**) Calibration standard with 0.25 pg/µL human insulin, somatostatin-14, and glucagon with 5 pg/µL bovine insulin in 0.5% FA in Krebs buffer and (**E**) blank injection of 0.5% FA in Krebs buffer. The first transition for each hormone is the quantifier, while the second transtion is the qualifier. (**F**) The ratio of quantifier/qualifier transitions for bovine insulin (squares),

human insulin (triangles), somatostatin-14 (diamonds), and glucagon (circle) obtained for calibration standards and QCs (dark grey), and samples (light grey).

3.4 Insulin could be determined in background secretion from a small number of stem cell-derived islet organoids cultivated in a pump-less, recirculating organ-on-a-chip device

Hormone secretion from isolated mouse or human islets-on-chip has been determined with the use of e.g. luminescent immunoassay (AlphaLISA) [34], or ELISA [35]. However, to the authors' knowledge, the combination of human SC-islets, organ-on-a-chip device, and hormone secretion determination with LC-MS has not been previously reported. As a proof-of-concept for combining RPLC-MS/MS determination of intact hormones from SC-islets cultured on an organ-on-chip device, we wanted to examine background secretion of the hormones. In addition, we wanted to show that the RPLC-MS/MS method was versatile concerning the applied sample matrix and therefore did not change the islet maturation cell medium (will be referred to as cell medium) with Krebs buffer for this experiment.

The background secretion over 24 h (in cell medium containing 5.5 mM glucose), from 3-6 SC-islets cultivated on-chip in a rOoC device was compared to 14-19 SC-islets cultivated in a standard cell culture well-plate.

To avoid introducing variation in the quantification, bovine insulin was not applied as an internal standard during the determination of human insulin in cell medium, due to a higher variation in the peak area (RSD > 7 %, N = 6) in cell medium compared to Krebs buffer (RSD < 5%, see **Section 3.2**). At day 5 on the rOoC, an average of 5 pg/µL of insulin was secreted per SC-islet (RSD = 52%, n = 4, N = 1), while on day 7 an average of 3 pg/µL of insulin was secreted per SC-islet (RSD = 30%, n = 4, N = 1). Similarly, on the well-plate at day 5, an average of 7 pg/µL of insulin was secreted per SC-islet (RSD = 24%, n = 4, N = 1), while on day 7 an average of 3.9 pg/µL of insulin was secreted per SC-islet (RSD = 7%, n = 4, N = 1). An independent two sample t-test, at 95% confidence, confirmed there was no significant difference in insulin secretion per SC-islet on the rOoC compared to the cell culture well-plate. The high variation in the determination of insulin secretion per SC-islet on the rOoC device (54% on day 5 and 30% on day 7) compared to the 24 well-plate (24% on day 5 and 7% on

day 7), can be explained by the number of SC-islets included on the different devices. There was 3-6 SC-islets on the rOoC, while there was 14-19 SC-islets included on the well-plate. Individual differences in the SC-islets may affect the reliability of the measurements when examining a small batch of SC-islets, and that the lower RSD values on the 24 well-plate indicates that a representative batch of SC-islets should be closer to 20 individual SC-islets.

Concerning background secretion of somatostatin-14 and glucagon in 3-6 SC-islets cultivated on rOoC device, the detection limits was not sufficient for quantification of secretion from limited number of SC-islets stimulated by only glucose, for details see **SI-3.** We were able to determine secretion of glucagon in the samples collected from 14-19 SC-islets on the cell culture well-plate.

The composition of the SC-islets was confirmed with flow cytometry quantification and immunostaining (**Figure 5A**), for details see **SI-4**. The SC-islets consisted of >66% insulin-positive cells, >17% somatostatin-positive cells, and >22% glucagon-positive cells, where >95% of the cells were endocrine cells (i.e. cells which can secrete hormones). The multicellular SC-islets have a composition, which is similar to the distribution of the cell types in human islets [13, 15].

To summarize, determination of secreted insulin from limited number SC-islets (n < 6) cultivated in cell medium on a rOoC device was possible with the applied RPLC-MS/MS method. It was found that the insulin secretion in the SC-islets was not significantly different on the rOoC device compared to the secretion occurring on a standard cell culture well-plate.

3.4.1 Discussion: concerning challenges with cell medium, the organ-on-chip device, and the applied liquid chromatography mass spectrometry method

In the present method an interfering peak (eluting after 13 min in standard solutions in cell medium) is eluting closer to the analytes and co-elute with glucagon in cell medium incubated with SC-islets on well-plate (**Figure 5B**) and on rOoC device (**Figure 5C**). In comparison, there is a baseline separation of the analytes and the interfering peak in the standard solution prepared with fresh cell medium spiked with the analytes and internal standard (**Figure 5D**). The separation in the samples may be affected by other

sample matrix components introduced following incubation of the SC-islets on the 24 well-plate or in the rOoC device. By gel electrophoresis, it was possible to confirm the presence of varius proteins in the size range between human insulin and BSA (See Lane 1, **Figure 5E**) in supernatant collected from SC-islets that were either cultivated in a 24 well-plate (Lane 8) or in the rOoC device (Lane 9 and 10). The observations suggest that the extra sample matrix components are released into the cell medium by the SC-islets or the extracellular matrix used for embedding the SC-islets on the two devices. Indeed, in cell medium neither incubated with SC-islets nor been in contact on either of the devices, significantly less protein bands were visible in the same size range. Gel electrophoresis was also used to compare cell medium with Krebs buffer concerning protein content, showing that there were more sample matrix components present in cell medium compared to Krebs buffer, see **SI-5** for more details.

It is worth nothing that during preliminary examination of the rOoC device with Krebs buffer, there was a significant loss of human insulin following incubation on the rOoC device compared to standard cell culture well-plates, see details in **SI-6**.

In the current experiment, the reliability of the determination of hormones with the RPLC-MS/MS method was not affected by the changes to the separation due to the presence of additional sample matrix components. The identification was secured by a stable ratio of the quantifier and qualifier transitions obtained for each hormone in calibration standards and sample is shown in **Figure 5F**, as there was no significant difference in the ratio obtained in calibration standards and samples. In addition, the retention time of each hormone varied ≤ 0.5% RSD (N = 30) and the carry-over was < 2% for glucagon, < 0.5% for human insulin, and < 0.1% carry-over for bovine insulin and somatostatin-14. Additionally, all QCs (examined before, within and after the sample-set) at 25 pg/µL of human insulin, and 0.8 pg/µL of somatostatin-14 and glucagon were determined within ± 15 relative error (N = 5). The only exception was for the determination of glucagon, where the relative error was 17% in the second replicate of the QC.

To summarize, the RPLC-MS/MS offers reliable determination of insulin, somatostatin-14 and glucagon in a complex matrix (cell culture supernatant in this study) without use of internal standard, with negligible variation in retention time, repeatable quantifier/qualifier transition ratios, and negligible levels of carry-over. With

the growing complexity of the cell medium samples following incubation with the SC-islets embedded with extracellular matrix on the 24 well-plate and in the rOoC device, we are approaching a limit where the RPLC-MS/MS method alone is not sufficient for reliable determination. In the case of even more complex samples, the inclusion of sample preparation steps might become necessary.

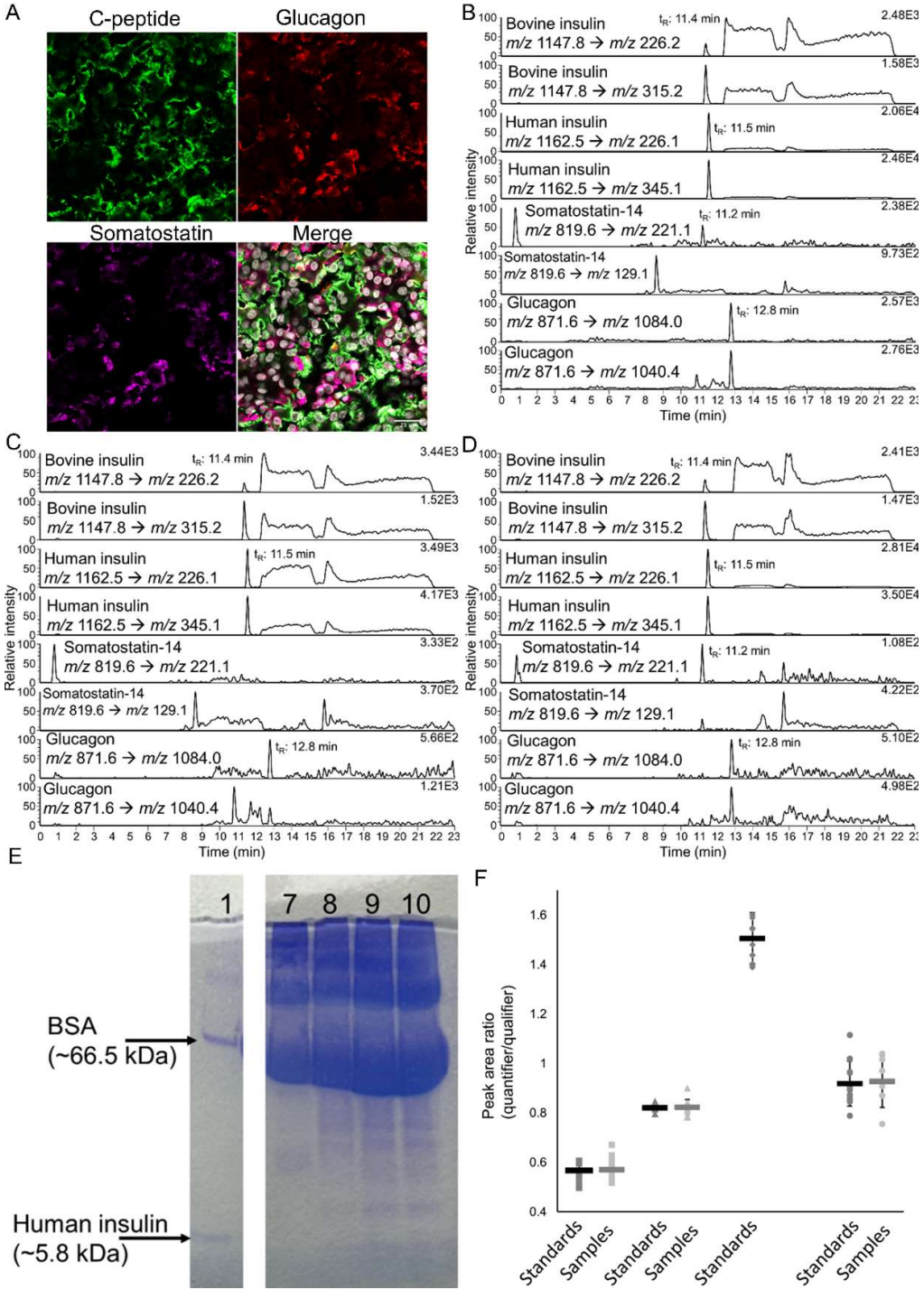

Figure 5: (**A**) Representative immunostaining images of SC-islets stained for C-peptide (green), glucagon (red), somatostatin-14 (magenta), and for cell nuclei with Hoechst 333242 (white). Scale bar = 25 µm. Representative chromatograms obtained in SRM mode of: Supernatant from SC-islets cultivated (**B**) in a 24 well-plate and (**C**) on the rOoC device, and (**D**) calibration standard with 100 pg/µL human insulin, 0.1 pg/µL somatostatin-14, and 0.1 pg/µL glucagon with 5 pg/µL bovine insulin in 1.0% FA in cell medium. The first transition for each hormone is the quantifier, while the second transtion is the qualifier. (**E**) Coomassie blue stained protein bands found by gel electrophoresis in the following samples: (**1**) 10 ng/µL og human insulin and 10 ng/µL of BSA in water, (**7**) 1.0% FA in cell medium, (**8**) pooled supernatant collected on day 5 from SC-islets cultured in a 24 well-plate, (**9-10**) two replicates of supernatant from SC-islets incubated on rOoC collected on day 5. The picture of the gel has been cropped, where Lane 2-6 is not included, however, the picture of the gel is provided in raw format in **SI-5**. (**F**) The ratio of quantifier/qualifier transitions for bovine insulin (squares), human insulin (triangles), somatostatin-14 (diamonds), and glucagon (circle) obtained for calibration standards and QCs (dark grey), and samples (light grey). Both transitions of somatostatin-14 were not detected in any of the examined sample.

4 Concluding remarks

The study was dedicated to combining the determination of multiple peptide hormones with liquid chromatography-mass spectrometry and SC-islets-on-a-chip. It has been shown that liquid chromatography is needed to separate the target peptides from interferences in the sample matrices. However, when the complexity of the samples grows and large amounts of proteins are present, chromatography and mass spectrometry may not be enough for successful peptide determination (e.g. urocortin-3 co-elutes with BSA), pointing to the need for the inclusion of sample preparation steps, e.g. electromembrane extraction of target peptides.

Acknowledgements

Financial support was obtained from the Research Council of Norway through its Centres of Excellence funding scheme, project number 262613 and partly from the UiO:Life Science convergence environment funding scheme. S.R.W. is a member of the National Network of Advanced Proteomics Infrastructure (NAPI), which is funded by the Research Council of Norway INFRASTRUKTUR-program (project number: 295910).

Conflict of interest

The authors declare no conflict of interest.

Data Availability Statement

The data that support the findings of this study are available from the corresponding author upon reasonable request.

5 References

[1] Tang X-Y, Wu S, Wang D, Chu C, Hong Y, Tao M, et al. Human organoids in basic research and clinical applications. Signal Transduction Targeted Ther. 2022;7(1):168.
[2] Kim J, Koo B-K, Knoblich JA. Human organoids: Model systems for human biology and medicine. Nat Rev Mol Cell Biol. 2020;21(10):571-84.
[3] Ingber DE. Human organs-on-chips for disease modelling, drug development and personalized medicine. Nat Rev Genet. 2022;23(8):467-91.
[4] Busek M, Aizenshtadt A, Koch T, Frank A, Delon L, Martinez MA, et al. Pump-less, recirculating organ-on-a-chip (rOoC) platform. Lab Chip. 2023.
[5] Lin A, Sved Skottvoll F, Rayner S, Pedersen-Bjergaard S, Sullivan G, Krauss S, et al. 3D cell culture models and organ-on-a-chip: Meet separation science and mass spectrometry. Electrophoresis. 2020;41(1-2):56-64.
[6] Kogler S, Kømurcu KS, Olsen C, Shoji J-y, Skottvoll FS, Krauss S, et al. Organoids, organ-on-a-chip, separation science and mass spectrometry: An update. TrAC, Trend Anal Chem. 2023:116996.
[7] Cabrera O, Berman DM, Kenyon NS, Ricordi C, Berggren P-O, Caicedo A. The unique cytoarchitecture of human pancreatic islets has implications for islet cell function. Proc Natl Acad Sci U S A. 2006;103(7):2334-9.
[8] Ishihara H, Maechler P, Gjinovci A, Herrera P-L, Wollheim CB. Islet β-cell secretion determines glucagon release from neighbouring α-cells. Nat Cell Biol. 2003;5(4):330-5.
[9] Henquin J-C, Ibrahim MM, Rahier J. Insulin, glucagon and somatostatin stores in the pancreas of subjects with type-2 diabetes and their lean and obese non-diabetic controls. Sci Rep. 2017;7(1):11015.
[10] Rorsman P, Braun M. Regulation of Insulin Secretion in Human Pancreatic Islets. Annu Rev Physiol. 2013;75(1):155-79.
[11] Rorsman P, Huising MO. The somatostatin-secreting pancreatic δ-cell in health and disease. Nat Rev Endocrinol. 2018;14(7):404-14.
[12] Zhang X, Ma Z, Song E, Xu T. Islet organoid as a promising model for diabetes. Protein Cell. 2022;13(4):239-57.
[13] Jiang L, Shen Y, Liu Y, Zhang L, Jiang W. Making human pancreatic islet organoids: Progresses on the cell origins, biomaterials and three-dimensional technologies. Theranostics. 2022;12(4):1537-56.

[14] Bi H, Ye K, Jin S. Proteomic analysis of decellularized pancreatic matrix identifies collagen V as a critical regulator for islet organogenesis from human pluripotent stem cells. Biomaterials. 2020;233:119673.
[15] Heaton ES, Jin S. Importance of multiple endocrine cell types in islet organoids for type 1 diabetes treatment. Transl Res. 2022;250:68-83.
[16] van der Meulen T, Xie R, Kelly OG, Vale WW, Sander M, Huising MO. Urocortin 3 Marks Mature Human Primary and Embryonic Stem Cell-Derived Pancreatic Alpha and Beta Cells. PloS one. 2012;7(12):e52181.
[17] Flisher MF, Shin D, Huising MO. Urocortin3: Local inducer of somatostatin release and bellwether of beta cell maturity. Peptides. 2022;151:170748.
[18] Olsen C, Wang C, Abadpour S, Lundanes E, Hansen AS, Skottvoll FS, et al. Determination of insulin secretion from stem cell-derived islet organoids with liquid chromatography-tandem mass spectrometry. J Chromatogr B. 2023;1215:123577.
[19] Rogeberg M, Malerod H, Roberg-Larsen H, Aass C, Wilson SR. On-line solid phase extraction–liquid chromatography, with emphasis on modern bioanalysis and miniaturized systems. J Pharm Biomed Anal. 2014;87:120-9.
[20] Thomas A, Benzenberg L, Bally L, Thevis M. Facilitated qualitative determination of insulin, its synthetic analogs, and C-peptide in human urine by means of LC–HRMS. Metabolites. 2021;11(5):309.
[21] Yang J, Wilson I, Rainville P. Evaluation of hybrid surface technology for the analysis of the B-group vitamins by LC-ESI-MS/MS. J Chromatogr B. 2022;1204:123336.
[22] van Midwoud PM, Rieux L, Bischoff R, Verpoorte E, Niederländer HAG. Improvement of Recovery and Repeatability in Liquid Chromatography−Mass Spectrometry Analysis of Peptides. J Proteome Res. 2007;6(2):781-91.
[23] Lauber M, Walter T, Gilar M, DeLano M, Boissel C, Smith K, et al. Low adsorption HPLC columns based on MaxPeak high performance surfaces. Waters White Paper 720006930EN. 2020.
[24] Gritti F, Horvath K, Guiochon G. How changing the particle structure can speed up protein mass transfer kinetics in liquid chromatography. J Chromatogr A. 2012;1263:84-98.
[25] Davis JC, Alves TC, Helman A, Chen JC, Kenty JH, Cardone RL, et al. Glucose response by stem cell-derived β cells in vitro is inhibited by a bottleneck in glycolysis. Cell Rep. 2020;31(6):107623.
[26] Barsby T, Otonkoski T. Maturation of beta cells: lessons from in vivo and in vitro models. Diabetologia. 2022;65(6):917-30.
[27] Almeida AM, Castel-Branco MM, Falcão AC. Linear regression for calibration lines revisited: weighting schemes for bioanalytical methods. J Chromatogr B. 2002;774(2):215-22.
[28] Omar-Hmeadi M, Lund P-E, Gandasi NR, Tengholm A, Barg S. Paracrine control of α-cell glucagon exocytosis is compromised in human type-2 diabetes. Nat Commun. 2020;11(1):1896.
[29] Campbell JE, Newgard CB. Mechanisms controlling pancreatic islet cell function in insulin secretion. Nat Rev Mol Cell Biol. 2021;22(2):142-58.
[30] Rosli N, Kwon H-J, Lim J, Yoon YA, Jeong J-S. Measurement comparability of insulin assays using conventional immunoassay kits. J Clin Lab Anal. 2022;36(7):e24521.
[31] Hædersdal S, Andersen A, Knop FK, Vilsbøll T. Revisiting the role of glucagon in health, diabetes mellitus and other metabolic diseases. Nat Rev Endocrinol. 2023.

[32] Kothegala L, Miranda C, Singh M, Krieger J-P, Gandasi NR. Somatostatin containing δ-cell number is reduced in type-2 diabetes. Int J Mol Sci. 2023;24(4):3449.
[33] Farré-Segura J, Fabregat-Cabello N, Calaprice C, Nyssen L, Peeters S, Le Goff C, et al. Development and validation of a fast and reliable method for the quantification of glucagon by liquid chromatography and tandem mass spectrometry. Clin Chim Acta. 2021;512:156-65.
[34] Lenhart AE, Kennedy RT. Monitoring hormone and small molecule secretion dynamics from islets-on-chip. Anal Bioanal Chem. 2023;415(4):533-44.
[35] Quintard C, Tubbs E, Achard J-L, Navarro F, Gidrol X, Fouillet Y. Microfluidic device integrating a network of hyper-elastic valves for automated glucose stimulation and insulin secretion collection from a single pancreatic islet. Biosens Bioelectron. 2022;202:113967.

Supplementary materials for: Simultaneous LC-MS determination of glucose regulatory peptides secreted by stem cell-derived islet organoids

Christine Olsen[1,2], Chencheng Wang[2,3], Aleksandra Aizenshtadt[2], Shadab Abadpour[2,3], Elsa Lundanes[1], Frøydis Sved Skottvoll[4], Alexey Golovin[5], Mathias Busek[2], Stefan Krauss[2], Hanne Scholz[2,3], and Steven Ray Wilson[2,3*]

[1] Department of Chemistry, University of Oslo, Blindern, Oslo, Norway

[2] Hybrid Technology Hub-Centre of Excellence, Institute of Basic Medical Sciences, Faculty of Medicine, University of Oslo, Oslo, Norway

[3] Department of Transplant Medicine and Institute for Surgical Research, Oslo University Hospital, Oslo, Norway

[4] Department of Smart Sensors and Microsystems, SINTEF Digital, Oslo, Norway

[5] Department of Immunology and Transfusion Medicine, Oslo University Hospital, Oslo, Norway

*Correspondence should be addressed to the following author(s):

Prof. Steven Ray Wilson

Department of Chemistry

University of Oslo

Postboks 1033, Blindern 0315 Oslo

s.r.h.wilson@kjemi.uio.no.

1 Significantly increased sensitivity at higher collision gas pressures for insulin and glucagon

The LC-MS method applied in this study, had previously been optimized for human insulin where a collision gas pressure of 2.5 mTorr had been selected based on reduced variance of fragmentation based on direct injection [1]. With the introduction of other peptides, the collision gas pressure was reexamined to see if the obtained peak areas and sensitivity of the method could be increased. The average peak area of human insulin obtained at 4.0 mTorr was 11663 with a RSD of 12% (n = 3), while at 2.5 mTorr the average peak area was 8746 with a RSD of 8% (n = 3). For glucagon the average peak area was 88028 (8 % RSD, n = 3) and 64654 (3% RSD, n = 3) for 4.0 mTorr and 2.5 mTorr, respectively. An independent two sample t-test, at 95% confidence, showed that the peak areas obtained for human insulin and glucagon were significantly higher for 4.0 mTorr collision gas pressure compared to 2.5 mTorr, while the variances at each gas pressure were not significantly different. For somatostatin-14 there was no significant difference depending on applied collision gas pressure; the peak area at 4.0 mTorr was 35886 (12% RSD, n = 3), while the peak area was 33708 (5% RSD, n = 3) at 2.5 mTorr. Based on the increased sensitivity for human insulin and glucagon, a collision gas pressure of 4.0 mTorr was applied in the following experiments.

2 Estimation of gradient delay

During gradient optimization, the gradient delay was examined by running the analysis of the peptides in non-retained conditions, as the elution time of the peptides would help in determining at which %B the target analytes eluted in the original shallow gradient from 1% B to 60% B in 8 min (an increase of 7.4% B/min). The system delay was estimated by analyzing a 20 pg/µL peptide mix (consisting of bovine insulin, human insulin, somatostatin-14, and glucagon) in 0.5% FA in Krebs buffer. A gradient starting at 60% B running up to 90% B was applied, and the obtained peptide peaks co-eluted at approx. 6.5 min (N = 2), see **Figure S1**. With an elution time of 11.3 min for bovine insulin in water, the expected %B at the elution was calculated by: (11.3 min – 6.5 min)*7.4% B = 35.5% B. The gradient was step-wise optimized based on this estimation, to separate the target analytes from the interferences in Krebs buffer and cell medium.

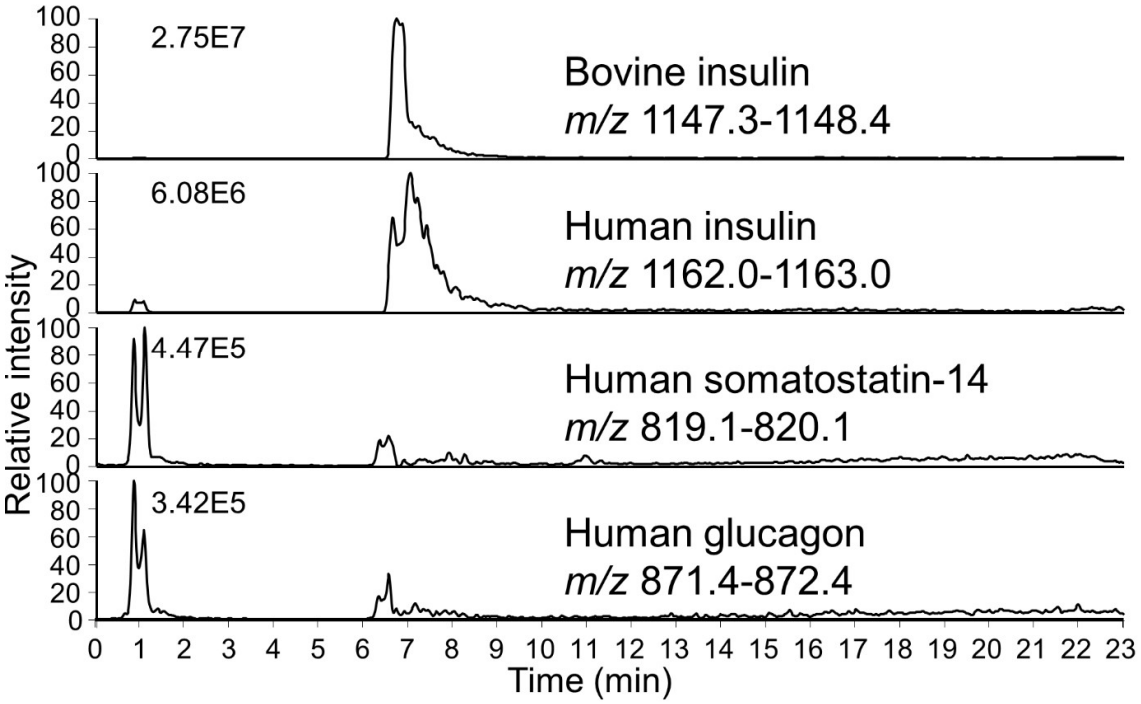

Figure S1: Representative chromatogram obtained in fullscan mode for 20 pg/µL of human insulin, somatostatin-14, glucagon, and 5 pg/µL of bovine insulin in 0.5% FA in Krebs buffer. The peaks co-eluted at 6.5 min when running the chromatography at non-retained conditions by starting the gradient at 60% B.

3 Comments concerning attempted quantification of background secretion of somatostatin-14 and glucagon from SC-islets during cultivation

During cultivation on a well-plate or a rOoC device, the SC-islet organoids are maintained with cell medium containing 5.5 mM glucose. The glucose should stimulate the SC-islets to secrete peptide hormones, including insulin (discussed in main document in Section 3.4), somatostatin-14 and glucagon.

For somatostatin-14, the peak area obtained in supernatant from the well-plate at day 5 was 647 (RSD = 40, n = 3, N = 1), and 786 (RSD = 29, n = 3, N = 1) on day 7 (representative chromatogram in **Figure S2A**), while on the rOoC at day 5 the peak area was 522 (RSD = 30, n = 3, N = 1), and 409 (RSD = 8, n = 3, N = 1) on day 7 (representative chromatogram in **Figure S2B**), which is in the range of the estimated limit of detection. By comparing the peak areas in the samples with the peak area of 701 obtained from 0.1 pg/µL of somatostatin-14 (**Figure S2C**), it is highly probable that the SC-islets do secrete somatostatin-14. However, as seen in the chromatograms, the qualifier transition for somatostatin-14 (*m/z* 819.6 to *m/z* 129.1) was not detected in the samples from the well-plate or the rOoC, meaning the identification could not be confirmed.

Only glucagon was quantified in the secretion from the SC-islet organoids on the well-plate with an average of 0.13 pg/µL of glucagon per SC-islet on day 5 (RSD = 15%, n = 4, N =1) and an average of 0.025 pg/µL of glucagon per SC-islet on day 7 (RSD = 27%, n = 4, N = 1). On the rOoC, the average peak area for glucagon was 4907 at day 5 (RSD = 25%, n = 4, N =1), and 3492 on day 7 (RSD = 21%, n = 4, N =1), which was in the same area as the estimated limit of detection of 0.1 pg/µL glucagon in cell medium, which gave a peak area of 4016, shown Figure 5C.

In conclusion, a combination of better sensitivity and a larger batch of SC-islet organoids is needed to be able to determine glucose stimulated secretion of somatostatin-14 and glucagon from SC-islet organoids.

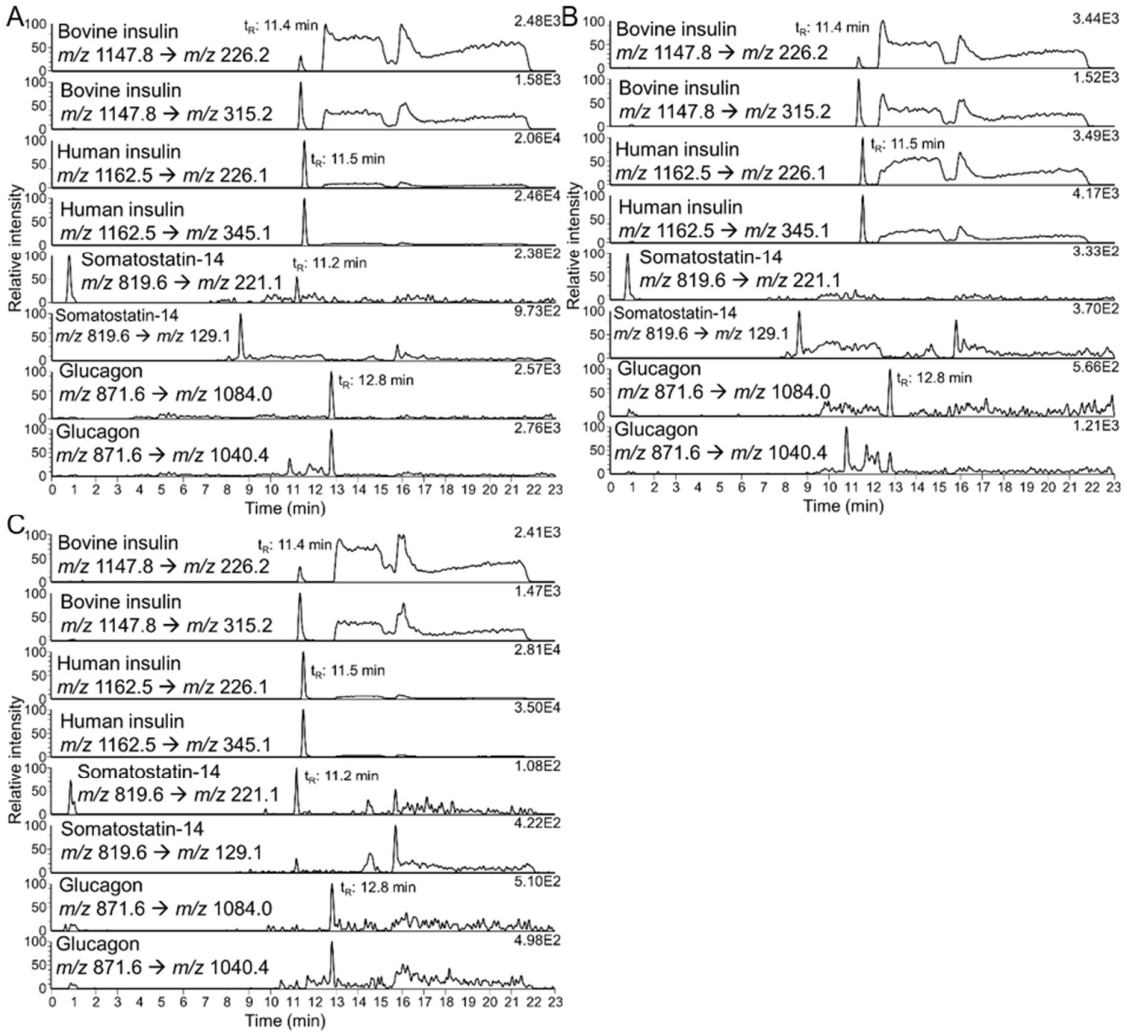

Figure S2: Representative chromatograms obtained in SRM mode of: Supernatant from SC-islet organoids cultivated (**A**) in well-plate and (**B**) on rOoC device, and (**C**) calibration standard with 100 pg/µL human insulin, 0.1 pg/µL somatostatin-14, and 0.1 pg/µL glucagon with 5 pg/µL bovine insulin in 1.0% FA in cell medium. The first transition for each hormone is the quantifier, while the second transtion is the qualifier.

4 Characterization of the cell composition in stem cell-derived islets

The SC-islets were further characterized with flow cytometry and immunofluorescence staining to confirm the presence of somatostatin and glucagon-producing cells. Primary antibodies including human C-peptide (Developmental studies Hybridoma Bank, University of Iowa, IA, USA), glucagon (GCG, Sigma Aldrich, MO, USA), somatostatin (SST, Santa Cruz, CA, USA) and chromogranin A (CHGA, Novus Biologicals, Centennial, CO, USA) represent insulin-producing cells, glucagon-producing cells, somatostatin-producing cells, and pan-endocrine cells in the organoids respectively [2]. Representative flow cytometry quantification shows that > >95% of cells are endocrine cells (Q2 and Q3, **Figure S3A-II**), and >66% of cells are insulin-producing cells (Q1 and Q2, **Figure S3A-II**). While there are >22% of cells are glucagon-producing cells (Q9 and Q10, **Figure S3A-IV**) and >17% somatostatin-producing cells (Q5 and Q6, **Figure S3A-VI**). None of the mentioned cell types were found in negative controls, **Figure S3A-I, III, and V**). SC-islets were fixed with 4% PFA at room temperature for 30 min and embedded for cryosection. Section slides immunofluorescence staining corresponded with flow cytometry results, showing that the majority of the cells are human C-peptide-positive cells, and there is a large presence of somatostatin-positive cells and glucagon-positive cells (**Figure S3B**).

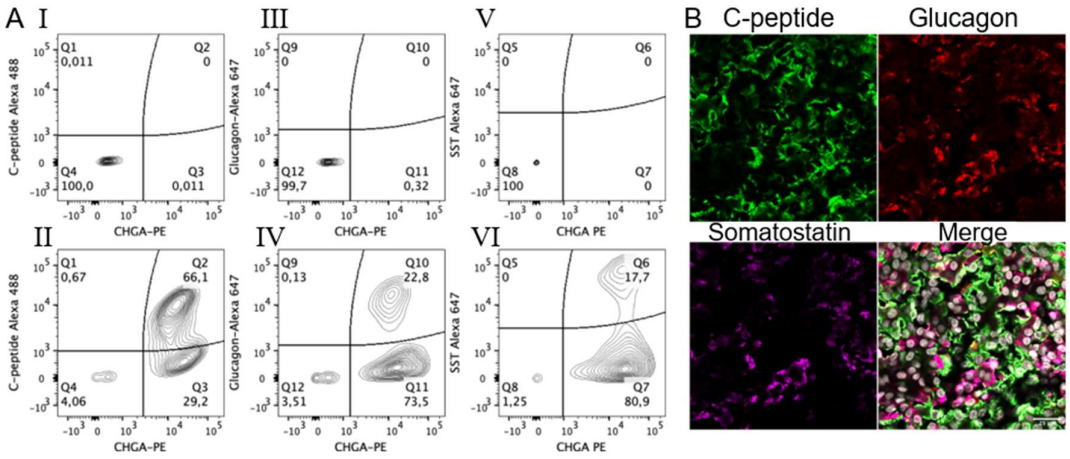

Figure S3: Representative flow cytometry quantification (%) of dispersed SC-islets stained for (I-II) C-peptide and chromogranin A (CHGA), (III-IV) glucagon and CHGA, and (V-VI) somatostatin-14 and CHGA. (I, III, and V) Negative control for flow cytometry quantification. (**C**) Representative immunostaining images of SC-islets stained for C-peptide (green), glucagon (red), somatostatin-14 (magenta), and merge including staining for cell nucleus with Hoechst 333242 (white). Scale bar = 25 µm.

5 Gel electrophoresis

Krebs buffer and cell medium have proved to be difficult matrices to work with for obtaining sufficient sensitivity in the determination of small peptide hormones and separation of the target peptide hormones from interferences found in the matrices. By comparing the obtained protein bands found in Krebs buffer (Lane 2, **Figure S4**), and cell medium (Lane 7), to a water standard containing a mixture of 10 ng/µL of human insulin and 10 ng/µL of bovine serum albumin (Lane 1), there is clearly more proteins present in Krebs buffer and cell medium.

We also examined if there were any changes to Krebs buffer following incubation on a well-plate (Lane 3) and incubation on a rOoC device (two replicates in Lane 4 and Lane 5), however, no changes were detectable with gel electrophoresis and Coomassie blue staining of proteins, see **Figure S4**.

Matrix matching in calibration standards to be applied for determination with LC-MS is of great importance. In this study, calibration standards were prepared from Krebs buffer and cell medium, however, when secreted peptides from stem cell-derived islet (SC-islet) organoids is of interest, we are unable to match the exact composition of the matrix following incubation of SC-islets. In the case of Krebs buffer, the initial composition of Krebs buffer (Lane 2, **Figure S4**) cannot be differentiated by gel electrophoresis from the composition of the supernatant collected after incubation of SC-islets in Krebs buffer with 20 mM glucose and 30 mM KCl (Lane 6). However, for cell medium, there are several other proteins bands visible in the range between the band originating from human insulin and bovine serum album (Lane 1) in supernatant collected from SC-islets incubated on well-plate (Lane 8) and on rOoC device (two replicates Lane 9 and 10), compared to cell medium (Lane 7) which has not been incubated with SC-islets.

The protein amount, and subsequently the need for separation of target hormone peptides from potential interferences is much larger in Krebs buffer compared to water, and even more important for cell medium, and in supernatant collected after incubation of SC-islet organoids.

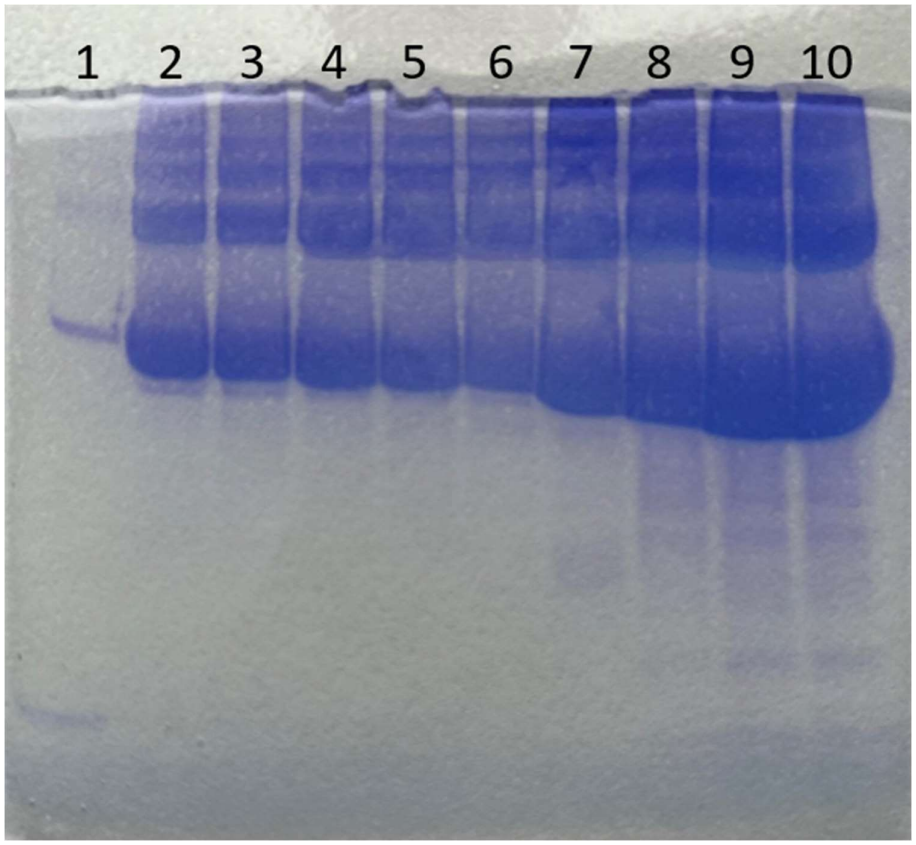

Figure S4: Stained protein band after by gel electrophoresis of the following samples: (**1**) 10 ng/µL og human insulin and 10 ng/µL of bovine serum albumin in water and (**2**) 0.5% formic acid in Krebs buffer. Krebs buffer incubated on: (**3**) well-plate and (**4-5**) two replicates of krebs buffer incubated on rOoC device. (**6**) Supernatant collected from SC-islet organoids incubated in Krebs buffer with 20 mM glucose and 30 mM KCl. (**7**) 1.0% formic acid in cell medium, (**8**) pooled supernatant from SC-islet organoids incubated on well-plate collected on day 5, (**9-10**) two replicates of supernatant from SC-islet organoids incubated on rOoC collected on day 5.

6 Significant loss of insulin in Krebs buffer incubated on a recirculating organ-on-a-chip device compared to static incubation on cell culture well-plates

Prior to analysis of SC-islet organoids on a microfluidic chip, we examined whether the measurements would be affected by non-defined adsorption of the hormones on the applied device. The rOoC device has been shown suitable for long-term cultures of human stem cell-derived liver organoids and is made out of PMMA [3]. Based on previous experience, human insulin displays a varied degree of non-defined adsorption to a large variety of tubing applied on an LC-instrumentation [1]. Therefore, we found it useful to examine if the PMMA surface in the chip would affect the recovery of our target hormones, and human insulin was used as a model analyte.

After 20 h incubation of 2 ng/µL of human insulin in Krebs buffer on the PMMA rOoC, an average of 1.58 ng/µL human insulin (79% recovery, RSD = 4%, n_r = 3 rOoC loops, N = 1) was recovered. In comparison, an average of 2.09 ng/µL human insulin (104% recovery, RSD = 3%, n_w = 3 wells, N = 1) was recovered after static incubation on a well-plate and an average of 2.12 ng/µL human insulin (106% recovery, RSD = 3%, n_a = 3 aliquots, N = 1) was recovered in aliquots stored in the freezer. It should be noted that in a fourth replicate on the rOoC the recovered amount of human insulin was 2.3 ng/µL, however, the replicate was rejected based on Grubbs' test for outliers.

Based on one-way ANOVA, at least one of the recovered concentrations of human insulin was significantly different from the others. It was determined by Fisher's least significant difference test, that there was no significant difference between the recovered concentration of human insulin on the well-plates and the control stored in the freezer. However, the recovered human insulin concentration from the rOoC was significantly different from both the concentrations recovered on the well-plate and in the control.

With a significant loss of 21% of human insulin after incubation on the rOoC in Krebs buffer, the PMMA surface on the rOoC might have to be modified to reduce adsorption of human insulin [4].

7 References in supplementary materials

[1] Olsen C, Wang C, Abadpour S, Lundanes E, Hansen AS, Skottvoll FS, et al. Determination of insulin secretion from stem cell-derived islet organoids with liquid chromatography-tandem mass spectrometry. J Chromatogr B. 2023;1215:123577.
[2] Lukinius A, Wilander E, Eriksson B, Öberg K. A chromogranin peptide is co-stored with insulin in the human pancreatic islet B-cell granules. Histochem J. 1992;24(9):679-84.
[3] Busek M, Aizenshtadt A, Koch T, Frank A, Delon L, Martinez MA, et al. Pump-less, recirculating organ-on-a-chip (rOoC) platform. Lab Chip. 2023.
[4] Liu J, Pan T, Woolley AT, Lee ML. Surface-Modified Poly(methyl methacrylate) Capillary Electrophoresis Microchips for Protein and Peptide Analysis. Anal Chem. 2004;76(23):6948-55.